Abstract

The anteroventral cochlear nucleus (AVCN), located at the first level of the central auditory system, sends major ascending inputs to higher auditory levels, such as the superior olivary complex and the inferior colliculus. However, temporal properties of AVCN neurons that might be useful for complex-sound processing have not been fully explored. This study applied different temporal measures, which were related to different sound features, to neural recordings of the responses of AVCN neurons to tones in broadband noise. The detectability of a tone in noise based on each temporal property was compared to psychophysical detection performance. Possible underlying neural mechanisms to extract the temporal information were also explored. The results provided implications for detection mechanisms used by higher auditory levels and the significance of certain stimulus features for detection. This study also examined the effect of inhibitory inputs on AVCN responses to pure tones and complex sounds by iontophoretically injecting inhibitory receptor antagonists. Blocking inhibition was found to affect both average discharge rates and temporal properties, such as discharge regularity, first-spike latency, and synchronization to the envelope of the sound, for some AVCN neurons. The influence of inhibition differed across neuron types and within types. These findings provide useful information for identifying the functional role and the source of inhibitory inputs, and for future modeling of different types of AVCN neurons. Because possible inhibitory sources include descending inputs from higher auditory levels, results of this study illustrated possible feedback mechanisms at the level of the AVCN.

Temporal Properties of Masked and Unmasked Tone Responses in the Anteroventral Cochlear Nucleus and the Influence of Blocking Inhibition

By

Yan Gai

B.S. Electrical Engineering, South China University of Technology, 1999

M.E. Electrical Engineering, South China University of Technology, 2002

M.S. Bioengineering, Syracuse University, 2004

DISSERTATION

Submitted in partial fulfillment of the requirements for the

degree of Doctor of Philosophy in Bioengineering

in the Graduate School of Syracuse University

June 2007

Approved_____

Professor Laurel H. Carney

Date_____

Table of Contents

List of Figures

Acknowledgements

As an international student, I would like to thank all the American people for creating such a wonderful academic environment for someone like myself to carry on studies and research projects that are interesting to me and beneficial to the human society. The group of people I met in this environment have always been friendly and supportive to me. Their dedication to scientific research and care for other people in the world has earned my highest respect.

My advisor, Laurel Carney, is one of the busiest persons I ever met. Yet she went through all the details with me step by step for every experiment I did, and every document I wrote. I had the courage in dealing with the difficulties and challenges I met during my study and research only because I knew there was someone who could always back me up and help me to solve all the problems at the end. She saw every opportunity that might be beneficial to my development, for not only my present study, but also my future career. She was happy about every improvement I made, even if it was only a grammar issue. With her criticisms, I became stronger in front of other people.

Laurel introduced me to many other nice people in this field. The iontophoretic experiment wouldn't have been possible without the support from Don Caspary at Southern Illinois University. He has generously introduced us every related technique in detail (including sending heavy equipment by mail) and took the burden of troubleshooting for us. Shig Kuwada at University of Connecticut also provided me with great ideas for making electrodes. The way he characterized problems and the manner he dealt with the difficulties made my experiment more enjoyable.

Chapter I

General Introduction

1.1   Background and motivation

In our daily life, our auditory system receives a variety of sounds from the environment and transforms the sounds into information that can be used by our brain. Throughout the ascending auditory pathway, neural responses represent important sound features, such as the frequency spectrum, temporal envelope, and sound level. In addition to sound representation, there are complex neural mechanisms to perform different auditory tasks, such as detecting signals from background noise, locating sound sources, and separating different acoustic streams. For some of these tasks, certain types of neurons have been found to play critical roles. For example, some neurons in the superior olivary complex (SOC) and the inferior colliculus (IC) are sensitive to interaural differences (Kuwada et al., 1979; Caird and Klinke, 1983), which can be useful for sound localization. For other tasks, it is not yet clear what mechanisms or what types of neurons are responsible for the processing.

Detection of signals in noise is one of the most important tasks in our life, since signals, the sounds that we pay attention to, are seldom presented alone without other sounds in the background. Detection of signals that are at or slightly above threshold in background noise is of particular interest for hearing research, since this task is especially difficult for listeners with hearing loss, even with hearing aids (Abel et al., 1990; Nabelek et al., 2004; van Tasell et al., 1988). To date, the inefficiency of hearing aids in helping

listeners with detection at least partly results from our lack of knowledge about what detection mechanisms are used by the auditory system and what stimulus features determine detectability. Psychophysical studies that are designed to answer these questions, e.g., detection of tones in roving-level noise (Kidd et al., 1989) or reproducible noise (Pfafflin and Mathews, 1966, Gilkey et al., 1985; Isabelle and Colburn, 1991; Evilsizer et al., 2002; Davidson et al., 2006), can reveal some knowledge of the general listening strategies for normal hearing listeners, whereas the underlying neural mechanisms must be assessed with physiological approaches.

As stated earlier, it is not clear which part of the auditory system or which type of neuron is most responsible for detection. The present study used physiological approaches to obtain neural responses to tones embedded in noise in the anteroventral cochlear nucleus (AVCN), the lowest level in the central auditory system. The AVCN is one of the three major functionally and anatomically separated parts of the cochlear nucleus (Rose et al., 1959). The motivation of recording from the AVCN was not based on any assumption that the "problem" can be solved at this level; rather, the goal was to find out what kind of information available at this level is most robust for detection, and how feasible it is for higher auditory levels to use this information. Projections from AVCN bushy cells are the major inputs to the medial (MSO) and lateral (LSO) superior olivary nuclei on both sides of the brain (Warr, 1982; Cant and Casseday, 1986). AVCN T-stellate cells project directly to the contralateral IC (Cant, 1982; Oliver, 1987; for review, see Young, 1998). Based on knowledge of tone-in-noise responses in the AVCN, hypotheses of higher-level processing can be created and used as guidelines for

physiological studies at those levels, which are usually more diverse in response to tones in noise (e.g., IC: Rees and Palmer 1988; Ramachandran et al. 1999).

The present study included several temporal analyses of tone-in-noise responses obtained in the gerbil AVCN. It is somehow surprising that after a number of temporal approaches have been applied to different areas of auditory research, such as pitch (e.g., Licklider, 1951; de Cheveigne and Pressnitzer, 2006) and binaural hearing (e.g., Domnitz and Colburn, 1976), the commonly used analysis for tone-in-noise responses is still focused on average discharge rate (Rhode et al., 1978; Geisler and Sinex, 1980; Gibson et al., 1985; Young and Barta, 1986, Rees and Palmer, 1988) or synchronization to tone frequency (Rhode et al., 1978; Costalupes, 1985; Miller et al., 1987). One reason for the average discharge rate to be so popular in tone-in-noise studies probably lies in the similarity between masked and unmasked rate-level functions for most auditory neurons. The masked rate-level function (for tones in noise) is commonly described as a shift of the unmasked rate-level function (for tones alone) to higher tone levels (Young and Barta 1986; Rees and Palmer, 1988; May and Sachs, 1992), although a decreased dynamic range is observed when the masking-noise level is high (Greenwood and Goldberg, 1970; Geisler and Sinex 1980; Gibson et al. 1985; Rhode et al. 1978; Young and Barta 1986). However, the neural coding mechanism can be potentially different when a noise is added to a tone based on the following hypothesis. When a tone is presented alone, sound representation is the major task of the auditory system. The capture of the sound features, such as frequency, duration, and level, provides enough information to the brain to perceive the sound. However, when a masking noise is added, more complex processing mechanisms will be triggered to separate the tone from the noise, as suggested by the

remarkable detectability of signals from noise for normal-hearing listeners. In other words, the system does more than a simple representation of the tone plus the noise. Based on this hypothesis, tone-in-noise responses should be studied more carefully than pure-tone responses with all appropriate rate or temporal approaches.

In addition to the direct analysis of neural responses, modeling of AVCN neurons helps to improve our understanding of the signal-processing mechanisms present at this level. AVCN neurons receive excitatory inputs from auditory-nerve fibers (ANFs) (Fekete et al., 1984; for review, see Brown et al., 1993), and some neurons also receive inhibitory inputs (Oertel, 1983; Wenthold et al., 1988; Wickesberg and Oertel, 1988; Saint Marie et al., 1989; Babalian et al., 2002; Arnott et al., 2004). It is relatively straightforward to simulate the excitatory inputs using computational models (Banks and Sachs, 1991; Rothman et al., 1993), since the response properties of ANFs to a variety of sounds have been intensively studied (e.g., Evans, 1978; Rhode et al., 1978; Winter and Palmer, 1991; Joris and Yin, 1992; Cedolin and Delgutte, 2005), and computational AN models have been established (Giguere and Woodland, 1994; Robert and Eriksson, 1999; Zhang et al., 2001; Zilany and Bruce, 2006). Based on knowledge of the excitatory inputs, some properties of AVCN neurons can be explained with relatively simple processing strategies, e.g., enhanced synchronization to tone frequency (Rothman and Young, 1996; Joris et al., 1994).

However, not all response properties of AVCN neurons can be explained by excitatory inputs. For example, the enhanced synchronization to amplitude modulation found in the AVCN (Frisina et al., 1990; Rhode and Greenberg, 1994) is hypothesized to be caused by the presence of inhibition (Rhode and Greenberg, 1994), which is likely to

be the case since later Backoff et al. (1999) show that inhibition enhances the AM synchrony in the PVCN and the DCN. Previous modeling studies of choppers (Banks and Sachs, 1991; Hewitt and Meddis, 1993) also propose different hypotheses about whether transient responses are related to inhibitory inputs. Using modeling approaches, the inhibitory inputs are difficult to simulate accurately since they can come from multiple sources, including neurons in other parts of the CN (Wickesberg and Oertel, 1988), higher auditory levels (Ostapoff et al., 1997; Thompson and Schofield, 2000), or even the contralateral CN (Wenthold, 1987; Babalian et al., 2002). Ideally, accurate simulations of the inhibitory inputs require creating a large network involving those inhibitory neurons. However, if for a particular type of neuron the effect of inhibition is found to be negligible for a given stimulus, the neural modeling can then focus on only excitatory inputs. If the effect of inhibition indeed matters, knowledge of some basic response properties of the inhibition allows phenomenological simulations of the inputs without knowing the exact function of the inhibitory neuron that projects to the targeted neuron. The iontophoretic technique was used here to study the properties of the inhibitory inputs and their potential effect on detection of tones in noise.

1.2   Applying temporal measures to tone-in-noise responses

In Chapter II (Gai & Carney, 2006), several temporal metrics are described and compared to the average discharge rate in terms of their ability to explain detection performance based on tone-in-noise responses obtained from the AVCN. The average discharge rate based on single-neuron responses failed to predict psychophysical detection thresholds. On the one hand, it is hard to rule out the possibility that some

pooling mechanism can combine average rates across neurons and thereby increase the detectability by reducing the variance (Delgutte, 1996). On the other hand, a pooling strategy will be inefficient if single neurons contain other forms of information (i.e., temporal information) that are more robust for detection and more easily extracted than average rate.

First, a temporal correlation metric was tested to quantify the amount of change available in the temporal responses when a tone was added to a noise. The results showed that sufficient temporal information was contained in the neurons' responses to account for psychophysical detection thresholds. This metric does not indicate what type of information is useful or how feasible it is to extract this information. Therefore, more specific temporal approaches were constructed and tested. As stated earlier, synchronization to tone frequency is the major temporal approach used by previous tone-in-noise studies (Rhode et al., 1978; Costalupes, 1985; Miller et al., 1987). Detection performance explained by synchronization to tone frequency was found to be consistent with previous studies, and was able to predict psychophysical detection thresholds at low and mid frequencies. However, the present study was unable to propose a physiological mechanism to extract this type of fine-structure information.

Envelope-related approaches have not been applied to detection of tones in noise in previous physiological studies. Here an envelope-slope metric adopted from a psychophysical detection study (Richards, 1992) was used to measure the fluctuation in time-varying rate obtained from the post-stimulus time (PST) histogram. Since the addition of a tone to noise reduced the amount of rate variation over time, the tone can be detected based on reduced fluctuation. It was hypothesized that the fluctuation of neural

responses originated from the locking to stimulus envelope. This metric can be realized by changing the parameters of a physiological model for the IC, the same-frequency inhibition and excitation (SFIE) model (Nelson and Carney, 2004). The model transforms the fluctuation coding into rate coding at a level higher than the AVCN, but it is not limited to the IC. Model thresholds based on responses of some AVCN neurons can predict psychophysical detection thresholds. In summary, envelope-related information is robust for detection of tones in noise and can be easily extracted physiologically.

The third temporal metric, temporal reliability, measured the discharge-pattern consistency for tone-in-noise responses. Although reliability is commonly used to characterize neural responses to certain sound stimuli in physiological studies (e.g., Mainen and Sejnowski, 1995; Martin et al. 2004; DeWeese et al., 2005), it has never been considered as a useful coding mechanism for a particular task. However, if a higher-level neuron receives multiple inputs from a lower level, the reliability of input responses will presumably affect the integration across inputs, which determines the discharge of the targeted neuron. In the present study, detection performance based on reliability was tested. In general, this metric was also promising in predicting the psychophysical detection thresholds; however, the present study was unable to propose a physiological mechanism to compute the reliability without being affected by the overall discharge rate.

After the above results were published in Gai and Carney (2006), some other temporal approaches were explored, including the correlation index and the spike-distance metric. As will be discussed in Chapter II, although synchronization to tone frequency has been found to be a robust detection metric at low and mid frequencies, there are difficulties in finding a physiological mechanism to extract this information.

The correlation index (Louage et al., 2004; Joris et al., 2006) measures the coincidence of discharges across different repetitions and can be constructed with a simple physiological mechanism, coincidence detection. For responses to pure tones, the correlation index has been found to represent synchronization to tone frequency. However, the present study showed that for responses to tones in noise, the correlation index is inconsistent with synchronization to tone frequency; instead, it changes with the tone level in a way similar to temporal reliability. Therefore, a physiological mechanism to extract the synchronization to tone frequency is yet to be discovered.

The spike-distance metric (Victor and Purpura, 1996, 1997) quantifies the differences of spike timing with respect to stimulus onset between neural responses. A confusion matrix can be constructed based on the spike-distance metric to allow the calculation of mutual information, which measures the efficiency of the neural responses in coding a set of sound stimuli for different temporal resolutions. It was discovered that absolute spike timing did not contain as much information as the above approaches for detection of tones in noise, at least for mid- and high-CF primary-like units. The present study also questioned the accuracy of deriving the "best temporal resolution" based on this method.

1.3   Application of inhibitory receptor antagonists

Chapters IV and V focus on the iontophoretic study of inhibitory inputs received by AVCN neurons. Although previous studies have tested the effect of inhibition on CN neurons' responses to pure tones (AVCN, Caspary et al, 1994; VCN, Ebert and Ostwald, 1995a, b; AVCN, Kopp-Scheinpflug et al., 2002), amplitude-modulated tones (DCN and

PVCN, Backoff et al., 1999), and tones in noise (VCN, Ebert and Ostwald, 1995b), none of these topics have been fully explored. Average discharge rate is the most commonly used metric to quantify changes in neural responses to pure tones at characteristic frequency (CF) or other frequencies when inhibitory inputs are blocked. Temporal contrast, e.g., peak vs. sustained rates and spontaneous vs. sound-driven activity (Ebert and Ostwald, 1995; Kopp-Scheinpflug et al., 2002), has been studied for pure-tone and tone-in-noise responses. Although more temporal measures have been applied to amplitude-modulated responses, changes in these measures after blocking inhibition have not been associated with other response properties to provide a general description of the characteristics and functions of inhibitory inputs.

In Chapter IV, changes in neural responses to pure tones after blocking inhibition are analyzed. Since a relatively large number of repetitions (100) for CF tones were used in this study, changes in detailed temporal response patterns can be obtained. For AVCN choppers that showed significant changes after blocking inhibition, the discharge regularity decreased, and the largest change occurred at different post-onset time period for neurons with different chopping patterns. A number of primary-like and unusual units showed substantially decreased first-spike latency, indicating the presence of inhibition on response onset that seemed to contradict the general assumption of delayed inhibition.

Chapter V describes iontophoretic results for responses to tones in noise and to two types of amplitude-modulated stimuli. Rate and temporal metrics described in Chapters II and III were applied to neural responses before, during and after the injection of inhibitory receptor antagonists. There were three aims as stated below.

The first aim was to quantify the overall change in each metric caused by blocking inhibition. For example, the average discharge rate was expected to increase for any tone-noise combination after blocking inhibition. The change in the amount of temporal fluctuation was assumed to agree with the change in the synchronization to amplitude-modulated stimuli, if the temporal fluctuation was indeed related to stimulus envelope.

The second aim was to test the effect of inhibition on detection performance based on each metric, that is, to test whether detection thresholds were changed when the inhibition was blocked. If the majority of neurons did not show changes in threshold, it can be concluded that the presence of the inhibition was not to facilitate tone-in-noise detection at the level of the AVCN based on a specific type of information. For the spike-distance metric, the major focus was to examine whether the temporal resolution that yielded the maximal coding efficiency changed after blocking inhibition.

Third, if blocking inhibition showed different effect sizes on tone responses as compared to noise responses, some characteristics of the inhibitory source neuron could be inferred. For example, inhibitory neurons in the CN with glycinergic neurotransmitters are either D-stellate cells in the VCN (Wickesberg and Oertel, 1988; Arnott et al., 2004) or vertical cells in the dorsal cochlear nucleus (Wickesberg and Oertel, 1988, 1990). D-stellate cells respond actively to broadband noise but poorly to tones (Rhode and Greenburg, 1994; Winter and Palmer, 1995), while vertical cells response actively to CF tones but poorly to broadband noise (Gibson et al., 1985; Rhode and Greenburg, 1994). Therefore, the influence of these two cell types on the targeted AVCN neurons is hypothesized to differ for tones versus noise.

1.4   Summary

The present study applied several temporal metrics to tone-in-noise responses of AVCN neurons, including features related to stimulus fine structure, stimulus envelope, and spike-timing consistency. Detection performance based on the most sensitive units for each metrics was quantified and compared to psychophysical detection thresholds. The fine-structure related metric, synchronization to tone frequency, was found to be a reliable cue at low and mid frequencies. The envelope-related metric, PSTH fluctuation, and two spike-timing-consistency related metrics, temporal correlation and correlation index, were found to be reliable cues at all frequencies. Corresponding physiological mechanisms were explored for each metric; however, only the PSTH fluctuation can be easily realized with known neural mechanisms.

The effect of inhibitory inputs on pure-tone and amplitude-modulated responses generally agreed with previous studies. In addition, more detailed analysis of the PSTH provided a better understanding of the characteristics of inhibitory inputs, such as the latency and smoothness. The effect of inhibitory inputs on the temporal metrics for tone-in-noise responses indicated not only how much inhibition affects detection, but also how neural representations of different stimulus features change with inhibition. The results of the iontophoresis studies can help to refine present neural models and to better understand signal processing by AVCN neurons.

Chapter II

Temporal Measures and Neural Strategies for Detection of Tones in Noise Based on Responses in Anteroventral Cochlear Nucleus

Abstract

To examine possible neural strategies for the detection of tones in broadband noise, single-neuron extracellular recordings were obtained from the anteroventral cochlear nucleus (AVCN) in anesthetized gerbils. Detection thresholds determined by average discharge rate and several temporal metrics were compared to previously reported psychophysical detection thresholds in cat (Costalupes 1983). Because of their limited dynamic range, the average discharge rates of single neurons failed to predict psychophysical detection thresholds for relatively high-level noise at all measured characteristic frequencies (CFs). However, temporal responses changed significantly when a tone was added to a noise, even for neurons with flat masked rate-level functions. Three specific temporal analyses were applied to neural responses to tones in noise. First, temporal reliability, a measure of discharge time consistency across stimulus repetitions,

decreased with increasing tone level for most AVCN neurons at all measured CFs. Second, synchronization to the tone frequency, a measure of phase-locking to the tone, increased with tone level for low-CF neurons. Third, rapid fluctuations in the post-stimulus time histograms (PSTHs) decreased with tone level for a number of neurons at all CFs. For each of the three temporal measures, some neurons had detection thresholds at or below psychophysical thresholds. A physiological model of a higher-stage auditory neuron that received simple excitatory and inhibitory inputs from AVCN neurons was able to extract the PSTH fluctuation information in a form of decreased rate with tone level.

2.1 Introduction

Monaural detection of tones in background noise is a fundamental problem in auditory physiology and psychophysics. For auditory-nerve (AN) fibers and most cochlear-nucleus (CN) neurons, average discharge rate increases monotonically with tone level. However, the dynamic range of most AN fibers and CN neurons for rate encoding is significantly reduced by the presence of background noise (Geisler and Sinex 1980; Gibson et al. 1985; Rhode et al. 1978; Young and Barta 1986). This decrease is due to a reduction in maximum rate at high tone levels and to increased rates in response to the noise alone (Gibson et al. 1985).

Neural temporal response patterns change when a tone is added to a noise (Greenwood and Goldberg 1970). The most intensively studied temporal property is the synchronization coefficient of discharges to tone frequency, which has been shown to yield lower detection thresholds than discharge rates in both AN fibers (Rhode et al. 1978) and CN neurons (Miller et al. 1987) at relatively high noise levels. However, neural mechanisms that can extract phase-locking information for tone-in-noise detection are unclear. Moreover, phase locking to high-frequency tones is presumably too weak to be a cue for detection. The present study explored temporal approaches as alternatives to average discharge rate or synchronization to tone frequency, seeking strategies that are physiologically realizable and not restricted to low frequencies.

Extracellular recordings were made from neurons in the anteroventral cochlear nucleus (AVCN) in response to tones in noise, and detection thresholds as determined by the average discharge rate and by several temporal measures of the neural responses were compared to psychophysical detection thresholds. The CN is the first stage of the

auditory central nervous system and receives direct input from AN fibers. The rate-related dynamic-range properties of most AVCN neurons in response to tones in noise are similar to those of AN fibers (Gibson et al. 1985; May and Sachs 1992; Rhode et al. 1978). However, since AVCN neurons can receive convergent AN fiber inputs (Liberman 1991), as well as inhibitory inputs (Caspary et al. 1994; Kopp-Scheinpflug et al. 2002; Wickesberg and Oertel 1990), the detailed temporal information exhibited by AVCN neurons differs from that of AN fibers. For example, a number of AVCN neurons show enhanced synchronization to tones (Joris et al. 1994) and to the envelope of amplitude-modulated stimuli (Frisina et al. 1990) as compared to AN fibers.

Before introducing the temporal measures used here, several issues related to previous studies should be discussed. First, the noise spectrum levels used in most previous physiological studies (AN: Young and Barta 1986; inferior colliculus: Rees and Palmer 1988) were relatively low compared to those used in psychophysical experiments (e.g., Costalupes 1983; Zheng et al. 2002). In the present study the noise levels were chosen to match the levels typically used in psychophysical studies of masked detection.

Second, in previous physiological studies of detection of tones in broadband noise, the temporal-information analysis was mainly focused on the change of synchronization to the tone frequency. Although envelope-based psychophysical models have been used to explain human performance in tone-in-noise detection (Gilkey and Robinson 1986; Richards 1992), possible changes in the neural responses caused by changes in the stimulus envelope have not been investigated for detection, given the absence of a distinct envelope for broadband noise. However, after narrowband filtering in the periphery, the "effective" noise waveform has an envelope with slower

modulations than the original stimulus envelope (Lawson and Uhlenbeck 1950; Louage et al. 2004). It has been shown that in response to tone and noise stimuli, envelope-locked temporal response properties of AN fibers and CN neurons can be separated from fine-structure phase locking by using pre-discharge stimulus ensembles (van Gisbergen et al. 1975) or autocorrelograms (Louage et al. 2004, 2005). In the present study, we measured the change in the fluctuation of the post-stimulus time histograms (PSTHs) caused by the addition of a tone to a noise. It was assumed that the fluctuation was dominated by the envelope, not the fine structure, of the "effective" stimulus.

Third, in the ascending auditory pathway, the discharge of a higher-stage neuron is not a simple summation of its input from lower-stage neurons. Modeling studies have shown that if a neuron receives multiple subthreshold inputs from lower-stage neurons, the relative timing across inputs can affect the discharge of the targeted neuron, even if the inputs are independent (e.g., Banks and Sachs 1991; Rothman et al. 1993). The present study explored several possible neural processing strategies that could be used by higher auditory centers that receive projections from the AVCN.

In order to examine both slow and rapid information in neural responses, temporal analysis windows of different lengths were applied to tone-in-noise responses for each analysis. First, changes in the temporal discharge patterns were quantified by a temporal correlation metric. More specific temporal metrics were then applied to neural responses to extract different types of information, including temporal reliability, synchronization to the tone frequency, and fluctuation of the PSTH. A higher-stage physiological model was tested for its detection performance based on the fluctuations of PSTHs recorded from AVCN neurons. In addition to these temporal metrics computed from the whole or

steady-state responses, changes in the first-spike latencies of AVCN neurons to tones in noise were examined.

2.2   Methods

2.2.1   Animal preparation and recording procedures

Extracellular recordings were obtained in the AVCN of adult Mongolian gerbils (*Meriones unguiculatus*). The animal was anesthetized with an intraperitoneal injection of a mixture of ketamine (170 mg/kg) and xylazine (7 mg/kg). A syringe pump (BSP-99, Braintree Scientific Inc.) was used for continuous subcutaneous injection of 50% ketamine plus xylazine and 50% saline (0.9%), at a rate of 0.05 cc/hr or less. Supplemental intramuscular injections of ketamine and xylazine were administered based on the animal's pedal reflex and respiration rate. The animal was placed in a double-walled soundproof room with an automated heating pad to maintain a constant body temperature of 37.5°C. After a tracheotomy, the left pinna was removed and a hole was made in the bulla. A second hole was made in the temporal bone to expose a small portion of the cerebellum directly above the AVCN. These procedures were approved by the Syracuse University Institutional Animal Care and Use Community (IACUC).

Glass electrodes filled with 3 M NaCl were advanced by a manual micropositioner. Each penetration was constrained within a small range of stereotaxic angles. Occasionally, the location of neurons was verified histologically. Sound stimuli were delivered through a plastic tube coupled to the left auditory meatus. An acoustic calibration was performed with an ER-7C probe microphone (Etymōtic Research) at the beginning of each experiment, and linear compensation of the sound stimulus using the

calibration table was performed for the frequency range of 0.1 to 10 kHz. A programmable Tucker-Davis-Technologies System III was used to generate the stimuli digitally and record the action potential times, under the control of Matlab. Sub-microsecond accuracy was achieved for discharge-time recordings.

A low-level broadband noise (0.1 to 10 kHz, 50-msec duration, repeated every 100 msec) was used as a search stimulus while isolating single neurons. An automated threshold tuning curve was used to identify the threshold (Liberman 1978), CF, and spontaneous rate for each neuron. Responses to a CF tone with a duration of 25 msec, repeated every 100 msec at several levels (e.g., 0 to 80 dB SPL with a 10-dB step size), were used to categorize unit types according to Blackburn and Sachs (1989). For tone-in-noise responses, the frequency of the tone was set equal to the CF of the neuron, and the tone level was varied (e.g., 30 to 80 dB SPL with a 10-dB step size). The Gaussian noise masker had a frequency spectrum from 0.1 to 10 kHz; neurons with CFs outside the range of 0.3 to 8 kHz were not included in the analysis. The noise spectrum level was set at 30 dB SPL for all neurons (the overall level of the noise was 70 dB SPL); 40 dB SPL noise spectrum level was also tested when possible. Noise waveforms were generated randomly for each neuron at each noise level, but were identical (frozen) for all presentations of noise-alone and tone-plus-noise stimuli, due to the requirement of repetitive stimulus presentations by the temporal analyses. Tone and noise tokens were gated simultaneously with 10-msec cosine-squared ramps. The tone-plus-noise stimulus had a duration of 250 msec, and was repeated every 475 msec. Thirty to 50 presentations of each stimulus were obtained for each neuron. In each presentation, the tone level was randomly selected to

avoid sequential effects. After each tone-in-noise presentation, the tone alone was

presented to obtain unmasked rate-level functions.

2.2.2 Average discharge rate

The average discharge rate was defined as the total discharge count in each

stimulus presentation, including both onset and sustained activity, divided by the stimulus

duration. A d' metric based on the mean and the standard deviation of the average

discharge rate was used to quantify the rate change in response to noise-alone and tone-

plus-noise stimuli (MacMillan and Creelman 2005).

$$d' = \frac{M_{tn} - M_n}{\sqrt{(\sigma_n^2 + \sigma_{tn}^2)/2}} \qquad \text{(Eqn. 2-1)}$$

M_n and M_{tn} are the mean average rates across repetitions in response to the noise alone

and a tone plus the noise, respectively. σ_n^2 and σ_{tn}^2 are the estimated variances of the

average rates for the noise alone and the tone plus the noise, respectively. The lowest

tone level that had d' $\geq$ 1 was defined as the detection threshold.

2.2.3 Temporal correlation

A direct measure of the overall change in the temporal discharge pattern when a

tone was added to a frozen noise was the correlation coefficient between the two

responses. A low correlation value indicated a large change in the neural response due to

the addition of the tone. If no significant change occurred, there was not sufficient

temporal information available to detect the tone. However, to provide useful

information, the change caused by the stimulus had to be larger than the variation from trial to trial in response to the same stimulus, i.e., the noise alone. Figure 2-1 shows a neuron's responses to a noise at 30 dB SPL spectrum level and to the noise plus a 65 dB SPL tone. r_b is the correlation coefficient between the PSTHs of even- and odd-numbered presentations of the noise alone. r_a is the correlation coefficient between the PSTHs of Odd-numbered presentations of the noise alone and odd-numbered presentations of the tone plus the noise. The detection threshold based on temporal correlation was defined as the lowest tone level for which r_a was significantly lower than r_b [t-test of two dependent correlations (Blalock 1972), $p < 0.05$].

PSTHs were convolved with a Gaussian smoothing function before the correlation was computed. The standard deviation of the Gaussian smoothing function was referred to as the temporal analysis window, which was varied over a large range (0.2, 0.6, 1.6, 4.5 and 12.8 msec) to examine both slowly and rapidly changing temporal information. The Gaussian function was truncated to 3 standard deviations in length (as in Martin et al. 2004). For each temporal analysis window, the PSTH was convolved with the Gaussian smoothing function, and the bin width of the resulting PSTH was then chosen to match the temporal analysis window.

Note that each correlation was measured between two groups of discharge trains, i.e., even- and odd-numbered presentations, instead of between every pair of individual discharge trains. Measuring the correlation between two PSTHs was more practical because the correlation between two individual discharge trains was very small when the smallest temporal analysis window was applied, due to the sparseness of discharges. Interleaved presentations were chosen for each group to avoid sequential effects.
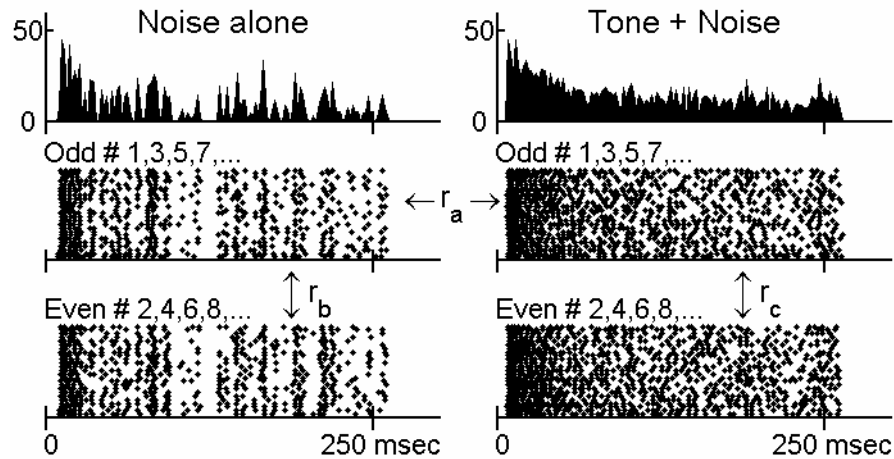
Fig. 2-1 Responses of a chopper unit to a noise at 30 dB SPL spectrum level and the same frozen noise with an added 65 dB SPL tone. Top panels are PSTHs obtained from 50 trials, with 2-msec bin width. Bottom panels are dot rasters of discharge times grouped into odd- and even-numbered trials. r_a is the correlation coefficient between the odd-numbered trials to noise-alone and to tone-plus-noise stimuli. r_b (noise alone) and r_c (tone plus noise) are the correlation coefficients between the odd- and even-numbered trials, respectively. G309u9, CF = 482 Hz, spontaneous rate (SR) = 0 sp/sec, threshold in quiet = 22 dB SPL.

Since each correlation value was obtained from just one comparison between two PSTHs, the temporal correlation appeared to be noisy and was not strictly monotonic for every neuron. In the present study, the detection threshold based on the temporal correlation was defined as the lowest tone level that showed a significant change when all higher tone levels also showed significant changes. This rule also applied to any of the following metrics that were not strictly monotonic.

Temporal correlation measured the amount of change in the neural responses caused by adding a tone to a specific noise waveform. However, this is not a physiologically realistic detection mechanism since a direct comparison between the noise-alone and tone-plus-noise responses is generally not available. In addition, changes in temporal correlation did not indicate how the response changed or potential mechanisms that caused the change. Three more specific temporal strategies are discussed below: temporal reliability, synchrony to tone frequency, and PSTH fluctuation.

2.2.4   Temporal reliability

Due to the stochastic nature of the AN fiber inputs, the discharge times of AVCN neurons varied across presentations of the same stimulus waveform. Reliability measured the consistency of a single neuron's discharges to a number of presentations of the same stimulus (Mainen and Sejnowski 1995; Martin et al. 2004). As illustrated in Fig. 2-1, r_b measured the consistency of discharge times in response to the noise alone and can be thought of as a measure of reliability. Similarly, the correlation coefficient between the PSTHs of even- and odd-numbered presentations of the tone-plus-noise stimulus was

denoted as r_c. As with the temporal correlation measure, discharge trains in each

temporal-analysis window were smoothed before the correlation coefficient was

computed. The presence of a tone was determined if the addition of a tone caused a

significant change in the reliability. The detection threshold was defined as the lowest

tone level that elicited a significant increase or decrease in the reliability for any temporal

analysis window [t-test of two independent correlations (Blalock 1972), $p < 0.05$], as

long as this increase or decrease persisted at all the tone levels higher than the threshold

for that particular temporal analysis window.

2.2.5   Synchrony to the tone frequency

The synchronization coefficient, also called the vector strength (Goldberg and

Brown 1969), of the response to each stimulus presentation was computed at the tone

frequency for tone-plus-noise and noise-alone responses. The onset response (discharges

within 12 msec after the stimulus onset) was not included when computing

synchronization. The discharge trains were not smoothed so as to preserve fine-timing

information for mid- and high-CF neurons. The mean synchronization coefficient for all

presentations at each tone level was tested for significance (Mardia 1972, $p < 0.05$). The

detection threshold was defined as the lowest tone level that elicited significant

synchronization. The criterion for significant synchronization had to account for the

number of discharges (Mardia 1972); the number of discharges used here was the mean

discharge count averaged across stimulus presentations.

2.2.6   Fluctuation of the PSTH

Richards (1992) used the average slope of the stimulus envelope as a decision variable to predict human performance in psychophysical detection experiments. After the extraction of the stimulus envelope, the difference between adjacent points in the envelope was computed and averaged across the stimulus duration. This average slope measured the amount of fluctuation in the stimulus envelope. A similar metric was applied in the present study to the neural response PSTHs with different temporal analysis windows.

Discharge times were smoothed by the Gaussian smoothing function described above and combined across all stimulus presentations to form the PSTH. The discharge count in the previous bin was subtracted from the count in each bin of the PSTH. The absolute values of all the subtracted numbers were then summed. The fluctuation of the PSTH was defined as the sum divided by the number of bins in the PSTH for a given temporal analysis window. The change in fluctuation with changing tone level was measured for each neuron.

In the Results section, a higher-stage physiological model with combined excitatory and inhibitory inputs that was able to extract the PSTH fluctuation is presented. Detection performance based on this model was superior to that based on the computed fluctuation of the PSTH as described above. Therefore, only detection thresholds of the physiological model are presented below.

2.2.7 First-spike latency

It has been shown in previous studies that AVCN neurons have decreased first-spike latencies when the level of a pure CF tone is increased (for review, see Moller 1975). The present study explored first-spike latency changes with tone level when a noise masker was present. The first spikes were identified by using an approach presented by Young et al. (1988), which involved manually placing a cursor at the beginning of the stimulus-driven response to remove spontaneous activity.

2.3 Results

Data presented here describe recordings from 102 isolated AVCN units in 19 gerbils. Responses of all 102 neurons were studied with tones in 30-dB SPL noise, and 57 of them were also studied with tones in 40-dB SPL noise. Neurons were classified into three major categories based on their short-tone-burst responses (Blackburn & Sachs 1989). Fifty-three "primary-like" units included response types associated with bushy cells (e.g., primary-like and primary-like-with-notch). Thirty-five "chopper" units included both transient and sustained chopper response types, since no consistent difference was found between the two types of choppers for any of the analyses. Fourteen "other" units included neurons that could not be classified into the first two categories. Figures 2-2*A*–2-5*A* show examples of short-tone PSTHs for four representative neurons (two primary-like and two chopper units arranged in order of increasing CF). The response properties to tones in noise were analyzed on the basis of the discharge rate and the temporal measures. The detection thresholds for each metric were compared with psychophysical detection thresholds for cat (Costalupes 1983), as behavioral results are

A. Short-tone PSTH
50 dB SPL

B. Noise-alone PSTH

C. Tone-plus-noise PSTH
65 dB SPL

D. Rate-level

G309u9
Chopper, CF: 482 Hz

Noise: 30

Pure tone

E. Temporal correlation

F. Temporal reliability

0.2 msec
0.6 msec
1.6 msec
4.5 msec
13 msec

Tone level (dB SPL)

G. Synchronization

H. Fluctuation of the PSTH

I. SFIE model

Tone level (dB SPL)
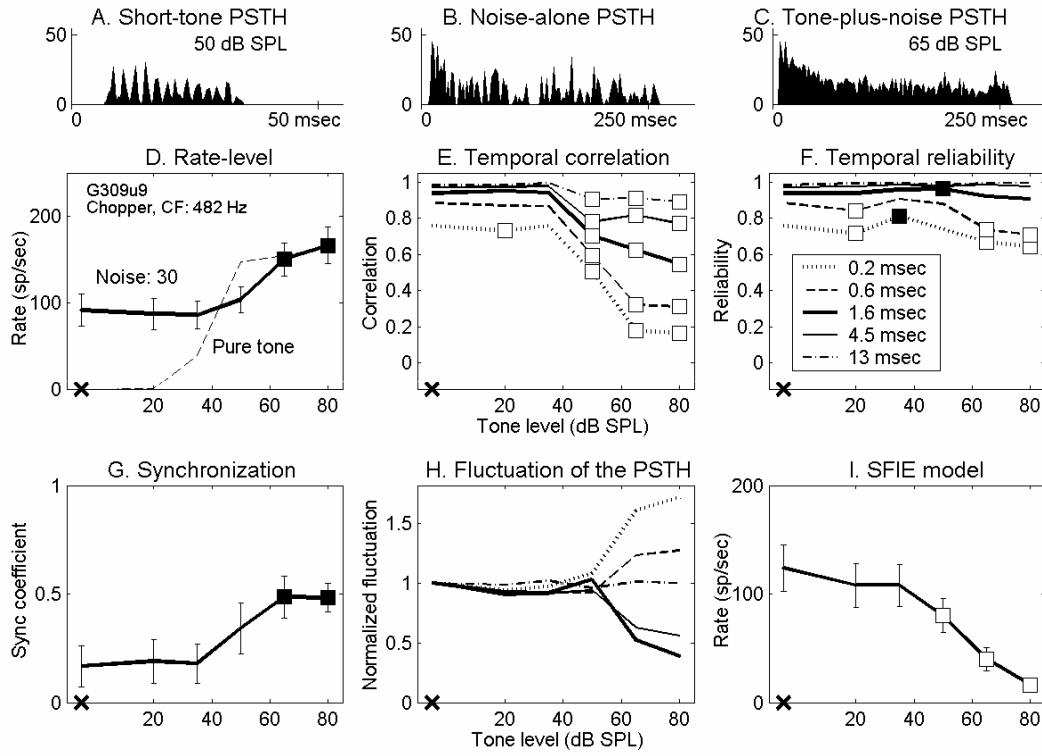
Fig. 2-2 Responses of a chopper unit to a short tone (25 msec, 50 dB SPL), long tones

(250 msec), noise alone (250 msec), or tones plus noise (250 msec). *A*, PSTH for

responses to the short tone at CF. Bin width = 0.5 msec. B-I, Tone-in-noise responses. *B*,

PSTH for noise at 30 dB SPL spectrum level. Bin width = 2 msec. *C*, PSTH for noise in

B plus a 65 dB SPL tone. Bin width = 2 msec. *D*, Masked rate-level functions for a 250-

msec CF tone and for the tone plus the noise. *E*, Temporal correlation measured with

different temporal-analysis windows. *F*, Temporal reliability measured with different

temporal-analysis windows. *G*, Synchronization coefficient to the tone. *H*, PSTH

fluctuation measured with different temporal-analysis windows. *I*, Rate-level function of

the SFIE model. All filled squares indicate significant increases, and all open squares

indicate significant decreases ($p < 0.05$ or d'≥ 1). The x on the abscissa indicates

responses to noise alone. G309u9, CF = 482 Hz, SR = 0 sp/sec. Pure-tone rate threshold

in quiet = 22 dB SPL (same neuron as in Fig. 1). Fifty trials per stimulus condition. Error

bars are standard deviations.

not available for gerbil. In the Costalupes study, the noise was continuously presented, whereas the noise was gated in the present study; therefore, the psychophysical thresholds were corrected with 1- to 3-dB elevations at mid and high frequencies to compensate for the effect of noise duration on detection thresholds (Wier et al. 1977).

2.3.1   Average discharge rate

Figures 2-2*D*–2-5*D* show masked and unmasked rate-level functions for tones at CF of the four representative neurons; the masker noise spectrum level was 30 dB SPL. Figure 2-2*D* and 2-3*D* show that the average discharge rates of a chopper and a primary-like unit increased significantly for the two highest tone levels (filled squares). However, the discharge rates of the other two neurons (Figs. 2-4*D* and 2-5*D*; 1 chopper and 1 primary-like unit) were independent of tone level up to the highest tone level tested (70 or 80 dB SPL). The average rate in response to a pure tone at CF with the same stimulus duration is also shown for comparison (dashed lines, Figs. 2-2*D*–2-5*D*). The dynamic range of each neuron's discharge rate was at least 30 dB SPL for pure tones but was usually reduced in the presence of the noise (e.g., Figs. 2-3D–2-5D, but not for Fig. 2-2D). For all neurons recorded, this reduction of dynamic range was mainly the effect of increased activity at low tone levels caused by the addition of masking noise. For some neurons, it was also an effect of reduced maximum responses at high tone levels caused by the presence of the masking noise (Figs. 2-4D and 2-5D). These observations agreed with those of Gibson et al. (1985).

Figure 2-6A shows the detection thresholds for all neurons based on average rate. The symbols in the shaded area represent neurons with unchanged rate-level functions up
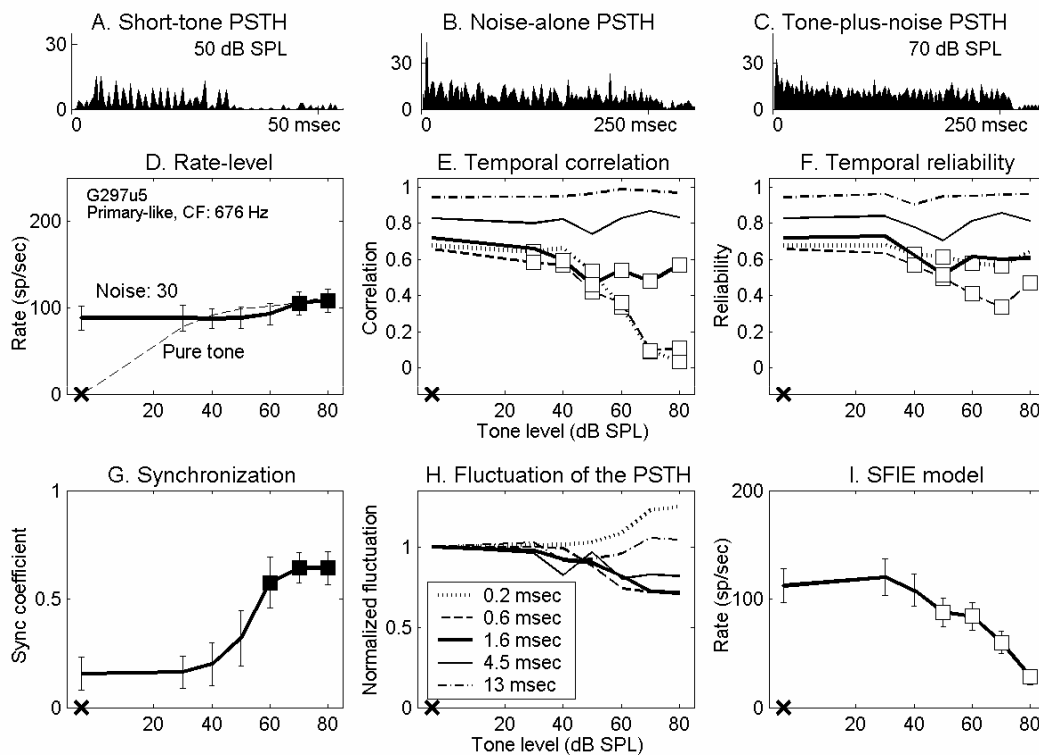
Fig. 2-3 Responses of a primary-like unit. Same format as Fig. 2-2. Tone level in *C* is 70 dB SPL. Fifty tone-in-noise trials. G297u5, CF = 676 Hz, SR = 49 sp/sec, pure-tone rate threshold in quiet = 20 dB SPL. The pure-tone PSTH in panel *A* showed clear phase locking to the tone.
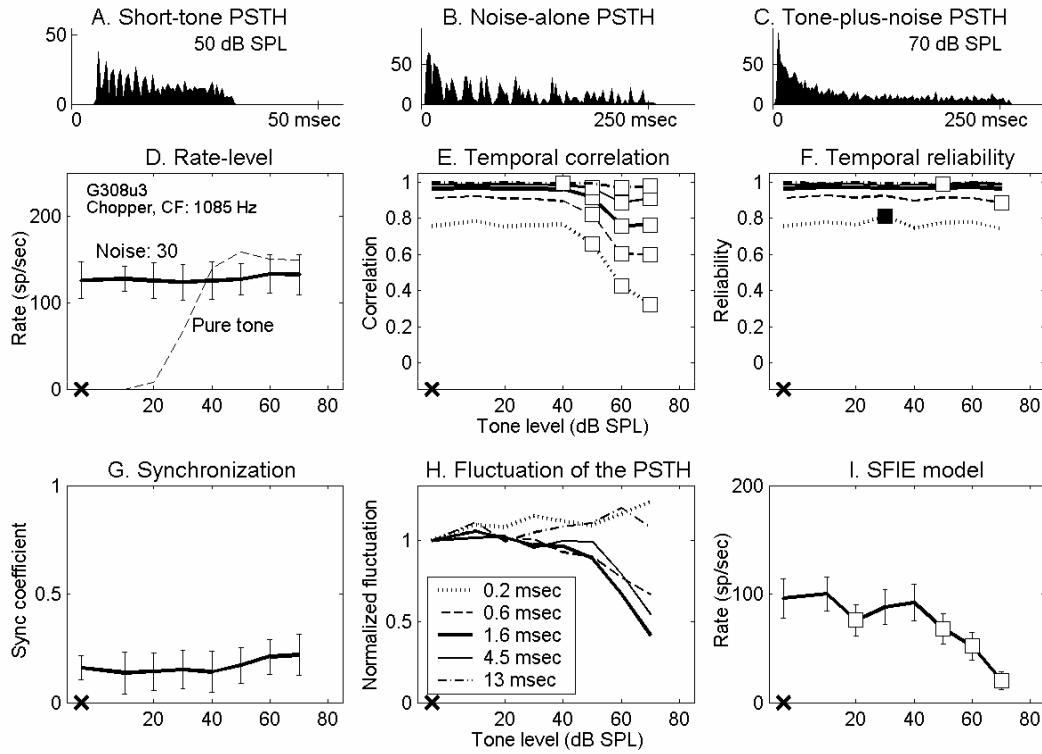
Fig. 2-4 Responses of a chopper unit. Same format as Fig. 2-2. Tone level in *C* is 70 dB SPL. Fifty tone-in-noise trials. G308u3, CF = 1085 Hz, SR = 0 sp/sec, pure-tone rate threshold in quiet = 21 dB SPL.
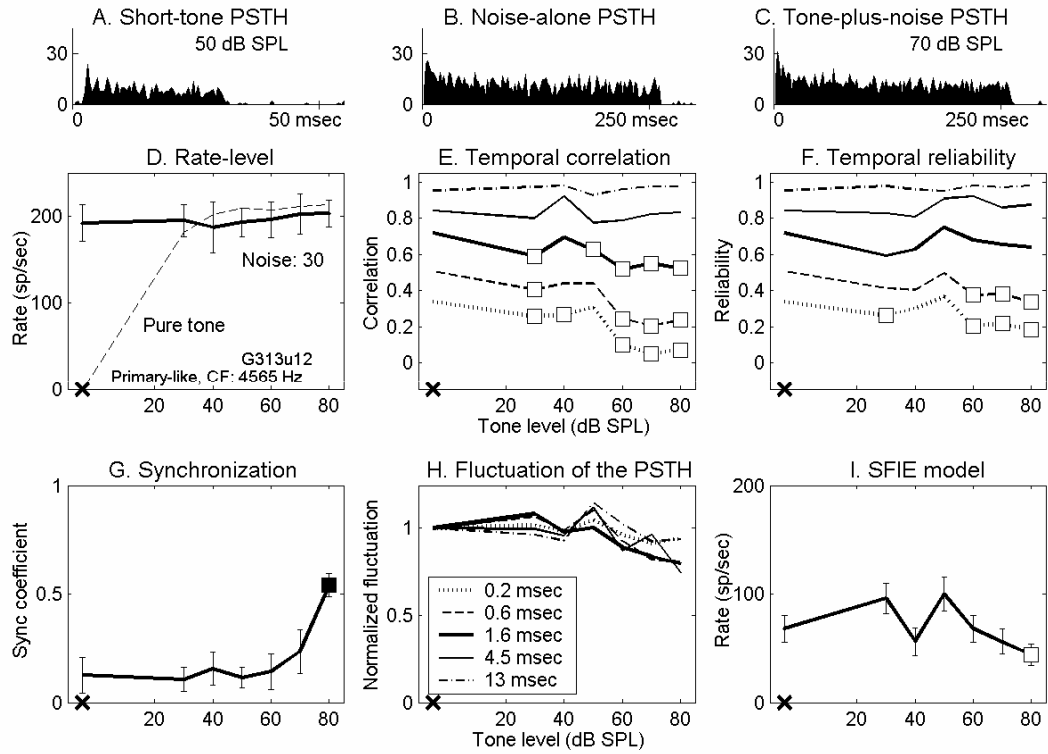
Fig. 2-5 Responses of a primary-like unit. Same format as Fig. 2-2. Tone level in *C* is 70 dB SPL. Thirty tone-in-noise trials. G313u12, CF = 4565 Hz, SR = 38 sp/sec, pure-tone rate threshold in quiet = 12 dB SPL.

to the highest tone level tested (70 or 80 dB SPL). When the noise spectrum level was 30

dB SPL (Fig. 2-6A, left panel), 45% of neurons had flat rate-level functions. Even among

the 55% of neurons with measurable thresholds, the neural thresholds were higher than

psychophysical detection thresholds (solid lines). The percentage of neurons with flat

rate-level functions was even higher when the noise spectrum level was 40 dB SPL (Fig.

2-6A, middle panel). In general, chopper units had lower rate thresholds than did

primary-like units at similar CFs. At a noise spectrum level of 40 dB SPL, no primary-

like unit at mid and high frequencies showed a significant change in average rate at any

tone level (Fig. 2-6A, middle panel). The right panel of Fig. 2-6A will be discussed later

with the results of other analyses.

2.3.2   Temporal correlation and first-spike latency

Values of temporal correlations for the four representative neurons are shown in

Figs. 2-2E–2-5E. Detection performance based on the temporal correlation of chopper

units was approximately invariant with window size. For example, the detection

threshold of the chopper unit shown in Fig. 2-2E was 50 dB SPL for every temporal

analysis window. (The significant point at 20 dB SPL using the smallest temporal

analysis window was discarded based on the rule described in the Methods section.) For

the chopper unit shown in Fig. 2-4E, the detection threshold was invariant with all

temporal analysis windows except the largest one. In contrast, at a noise spectrum level

of 30 dB SPL, approximately 68% of the primary-like units had lower detection

thresholds when the temporal analysis windows were smaller. For example, the two

primary-like units shown in Figs. 2-3E and 2-5E had detection thresholds that were
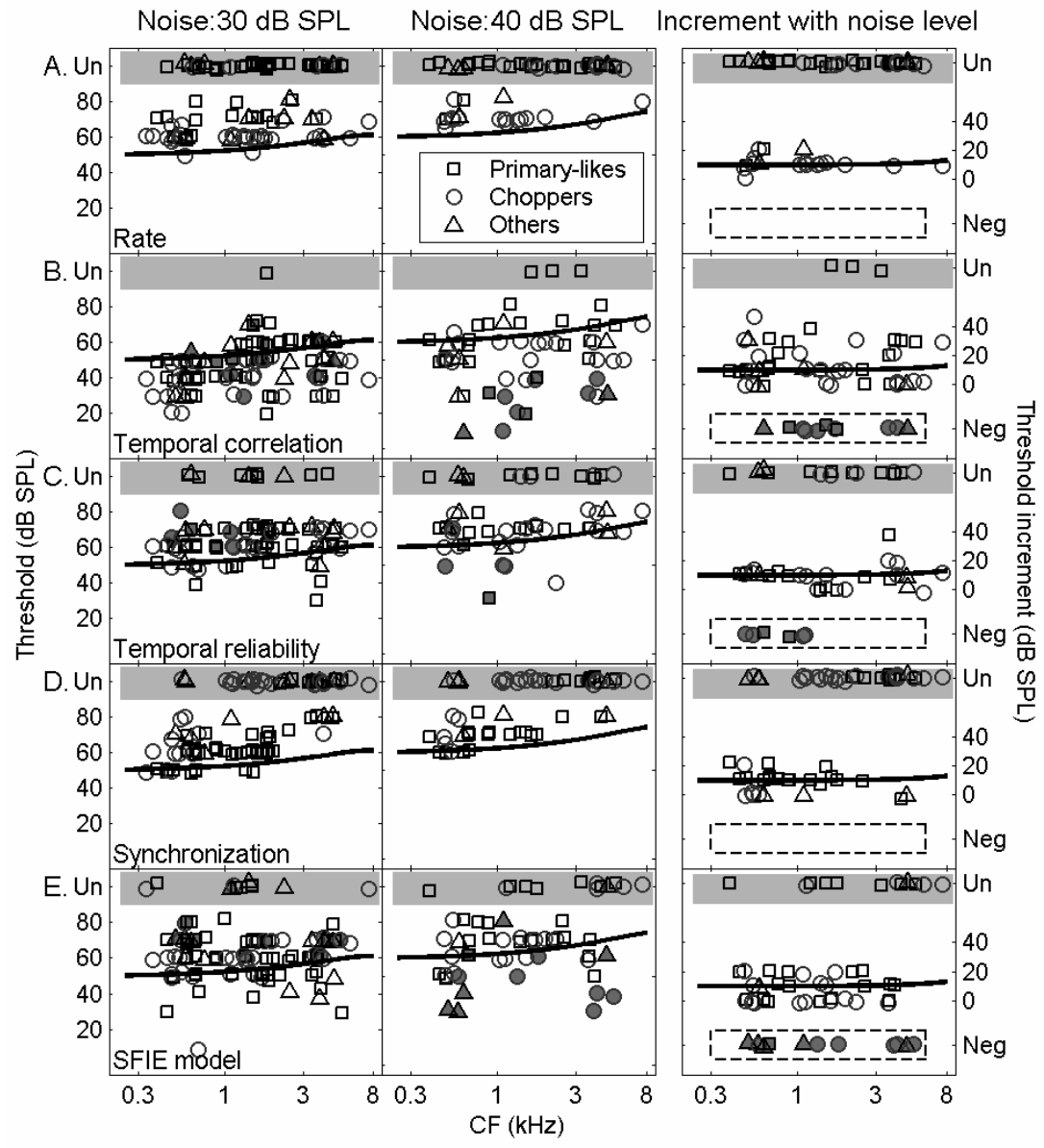
Fig. 2-6 Left and middle columns, detection thresholds based on (*A*) average discharge rate of the neuron, (*B*) temporal correlation, (*C*) temporal reliability, (*D*) synchronization to the tone, and (*E*) SFIE model discharge rate at noise spectrum levels of 30 (*left*) and 40 (*middle*) dB SPL. The shaded areas, labeled *Un*, indicate no measurable detection threshold up to the highest tone level tested (45%, 1%, 12%, 39% and 11% of neurons for 30-dB SPL noise, and 67%, 5%, 27%, 56% and 23% of neurons for 40-dB SPL noise, based on the measures of *A* to *E*, respectively). The solid lines represent psychophysical detection thresholds of cat (Costalupes 1983) corrected for noise duration (Wier et al. 1977). Right column, the increase of the detection threshold for each neuron when the noise spectrum level increased from 30 to 40 dB SPL, for neurons that were tested at both noise levels. The shaded areas, labeled *Un*, indicate neurons with unmeasurable thresholds at 40 dB SPL noise spectrum level. The shaded symbols circled by the dashed lines, labeled *Neg*, indicate neurons with lower thresholds at 40 dB SPL, including those neurons that had unmeasurable thresholds at 30 dB SPL but measurable thresholds at 40 dB SPL noise spectrum level (these neurons are also marked in the left and middle panels as shaded symbols). The solid lines in the right panels represent the increase in the psychophysical detection threshold when the noise level was increased by 10 dB. For the purpose of illustration, small jitters drawn from a Gaussian distribution with standard deviation of 1 dB SPL were added to each threshold value to avoid completely overlapping symbols.

relatively low for the three smallest temporal analysis windows, while the two largest temporal analysis windows exhibited no significant change up to the highest tone level tested.

Figure 2-6B shows detection thresholds as determined by temporal correlation. For neurons with detection performance that varied across different temporal analysis windows, the lowest threshold was selected. Compared to the rate thresholds in Fig. 2-6A, the detection thresholds of most neurons were lower than the psychophysical thresholds, including neurons that had flat masked rate-level functions. No significant difference was found in the detection thresholds of different neuron types.

The correlation coefficient measured the discharge similarity between neural responses to noise-alone and tone-plus-noise stimuli. A low correlation can result from different discharge patterns, or from the same pattern shifted in time. To examine the possibility of a shift in latency, we measured the maximum value of the normalized cross-correlation function between noise-alone and tone-plus-noise responses, which was essentially the maximum correlation coefficient between the two responses with different delays introduced. The detection threshold of a neuron as determined by temporal correlation did not change when a latency shift was taken into account, although sometimes the maximum correlation was slightly higher than when the correlation coefficient had no relative delay (results not shown here).

For some AVCN neurons, the first-spike latency decreased monotonically with increasing tone level when a masking noise was present (63% and 24% of neurons when the noise spectrum level was 30 and 40 dB SPL, respectively). Figure 2-7 shows the mean and the standard deviation of the first-spike latency for the four representative
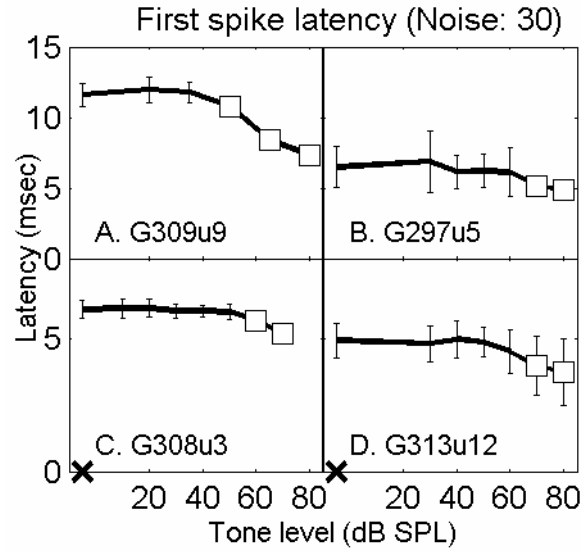
Fig. 2-7 First-spike latencies of the four representative neurons in response to tones in noise. *A*, *B*, *C*, and *D* correspond to the four neurons in Figs. 2-2 – 2-5, respectively. The noise spectrum level was 30 dB SPL. The open squares indicate significant decrease in the first-spike latency to the tone-plus-noise condition compared to noise-alone condition ($d' \geq 1$). The x on the abscissa indicates responses to noise alone.

neurons. Each open symbol indicates a significant decrease ($d' \geq 1$) in the first-spike latency at a certain tone level compared to the latency for noise alone. In general, the lowest tone level associated with a significant change in first-spike latency agreed with the average rate threshold, such as the neuron in Fig. 2-7B. For the 30 dB SPL noise spectrum level, 25% of neurons had lower detection thresholds when based on the first-spike latency than when determined by average rate, such as the neurons in Fig. 2-7, A, C and D; yet 24% of neurons had lower rate thresholds. Since first-spike latency did not yield significantly better detection performance than did average rate, it was not further explored in this study.

2.3.3 Temporal reliability

Temporal reliability measures a single neuron's consistency when responding to multiple presentations of the same stimulus. Values of temporal reliability based on tone-in-noise responses of the four representative neurons are shown in Figs. 2-2F–2-5F. Note that for the noise-alone condition, the temporal reliability was equal to the temporal correlation. Before discussing how reliability changed with different sound stimuli for each neuron, it should be noted that the reliability across neurons was quite diverse. It was commonly observed that low-CF neurons were more reliable than high-CF neurons for both noise-alone and tone-plus-noise stimuli. For example, the primary-like unit with a CF of 676 Hz in Fig. 2-3F had higher reliability values than the primary-like unit with a CF of 4565 Hz in Fig. 2-5F, especially for smaller temporal analysis windows. Also, chopper units were typically more reliable than primary-like units, except at very low CFs.

The reliability of a number of neurons changed significantly when a tone was added to the noise. The two primary-like units in Figs. 2-3F and 2-5F showed a clear decrease in temporal reliability with increasing tone level when relatively small temporal analysis windows were used. However, the chopper unit in Fig. 2-4F did not show a systematic change in reliability with increasing tone level. For small temporal analysis windows, approximately 75% and 65% of AVCN neurons showed decreased reliability with increasing tone level for 30 and 40 dB SPL noise spectrum level, respectively, while the rest showed unchanged or increased reliability with increasing tone level. For large temporal analysis windows, fewer neurons showed systematic changes.

The left and middle panels of Fig. 2-6C show the detection thresholds based on temporal reliability for the two noise levels tested. For a number of neurons, the thresholds determined by temporal reliability were at or below the psychophysical thresholds, but more neurons had thresholds higher than the psychophysical thresholds. No significant difference was found in the detection thresholds across different neuron types.

2.3.4   Synchrony to the tone frequency

Figures 2-2G–2-5G show the synchronization coefficients of the four representative neurons computed at the tone frequency, which was set equal to CF. In general, low-CF neurons had higher synchronization than high-CF neurons (Figs. 2-3G and 2-5G), and primary-like neurons had higher synchronization than chopper neurons with similar CFs (Figs. 2-2G and 2-3G). These properties were consistent with previous

descriptions of AVCN neurons' synchronization to pure CF tones (e.g., Blackburn and Sachs 1989).

Figure 2-6D shows the detection thresholds based on the synchronization coefficient for all neurons. A small number of neurons, mainly primary-like units, had detection thresholds equal to or lower than the psychophysical thresholds at low CFs. The majority of chopper units had detection thresholds higher than the psychophysical thresholds.

2.3.5   Fluctuation of the PSTH

Figure 2-1 shows the dot rasters and PSTHs of a chopper unit in response to a 30-dB SPL noise (left panels) and to the noise plus a 65 dB SPL tone (right panels). Certain temporal discharge patterns, resulting from consistent discharge timing across trials, can be easily visualized in the dot rasters of the noise-alone responses (middle and bottom left). These discharge patterns are also apparent in the fluctuations of the PSTHs (upper left). However, discharge patterns are weaker in the tone-plus-noise response (middle and bottom right), which results in relatively flat PSTHs (upper right). As stated earlier, after passing the broadband noise through peripheral auditory filters, the envelope of the effective stimulus has more low-frequency energy and thus fluctuates more visibly than the envelope of the original waveform (Lawson and Uhlenbeck 1950; Louage et al. 2004). Adding a tone to the noise flattened the envelope of the stimulus, resulting in a more evenly distributed PSTH of the neural response. Figures 2-2H–2-5H show values of the PSTH fluctuation for the four representative neurons using different temporal analysis windows. For each temporal analysis window (represented by each line), the values of

PSTH fluctuation at different tone levels were normalized by the corresponding value of the fluctuation with noise–alone stimuli for the purpose of illustration. For the first three neurons (Figs. 2-2–2-4), the tone-plus-noise PSTHs were significantly flattened as compared to the noise-alone PSTHs when the temporal analysis resolution was chosen to approximately match the PSTH fluctuations. For the high-CF primary-like neuron in Fig. 2-5, the fluctuation of the PSTH did not change as much as for the other three neurons. Approximately 56% and 37% of all neurons tested showed decreased fluctuation for at least one temporal analysis window for noise spectrum levels of 30 and 40 dB SPL, respectively. For neurons that showed decreased fluctuation, approximately 90% of them showed the most significant decrease when using a 1.6-msec temporal analysis window (thick lines, Figs. 2-2H–2-5H) among the five windows tested.

The fluctuation was computed as the difference between adjacent discharge counts averaged over the stimulus duration. If the shape of the PSTH did not change and only the discharge rate increased, the computed fluctuation increased. As seen in Fig. 2-2H, the reduction of fluctuation at high tone levels dominated the increased rate when a 1.6-msec temporal analysis window was used. However, for the smallest (0.2 msec) and largest (13 msec) temporal analysis windows, the measured fluctuation increased at high tone levels, which may have been affected by the increased rate or a stronger onset response. Since the measured fluctuation using these two temporal analysis windows was less consistent across neurons as compared to the decrease measured using the 1.6-msec window, the increase in fluctuation was not considered to be a reliable cue for tone-in-noise detection.

2.3.6   Same-frequency inhibition and excitation (SFIE) model

The temporal strategies described above require a higher-stage auditory center to process the temporal information in CN neural responses for tone-in-noise detection. In the Discussion section we will address the difficulty of finding physiological substrates for calculating the temporal correlation, temporal reliability, and synchronization to the tone frequency. Here we present a physiological model for extracting the information contained in the fluctuation of the PSTH. Modeling methods will be presented first, followed by the model results.

a. Modeling methods

The fluctuation of the PSTH was reflected in the difference of discharge counts in adjacent bins. A physiological mechanism that uses this information therefore must have access to both present and previous discharge activity to make a comparison. A natural way to provide this comparison is a delayed inhibition. Nelson and Carney (2004) proposed a phenomenological model to account for the response properties of inferior-colliculus (IC) neurons to amplitude modulation, the same-frequency inhibition and excitation (SFIE) model (Fig. 2-8A). As will be addressed later, the PSTH fluctuations were assumed to be dominated by locking to stimulus envelope. Since the model shows rate tuning to the frequency of fluctuations of stimulus envelopes and receives delayed inhibitory inputs, it simulates a physiological mechanism that can extract PSTH fluctuations obtained from AVCN neurons in order to detect the presence of the tone.

The model receives on-CF excitatory inputs and delayed on-CF inhibitory inputs. When the reversal potential of inhibitory post-synaptic potentials (IPSPs) is close to the
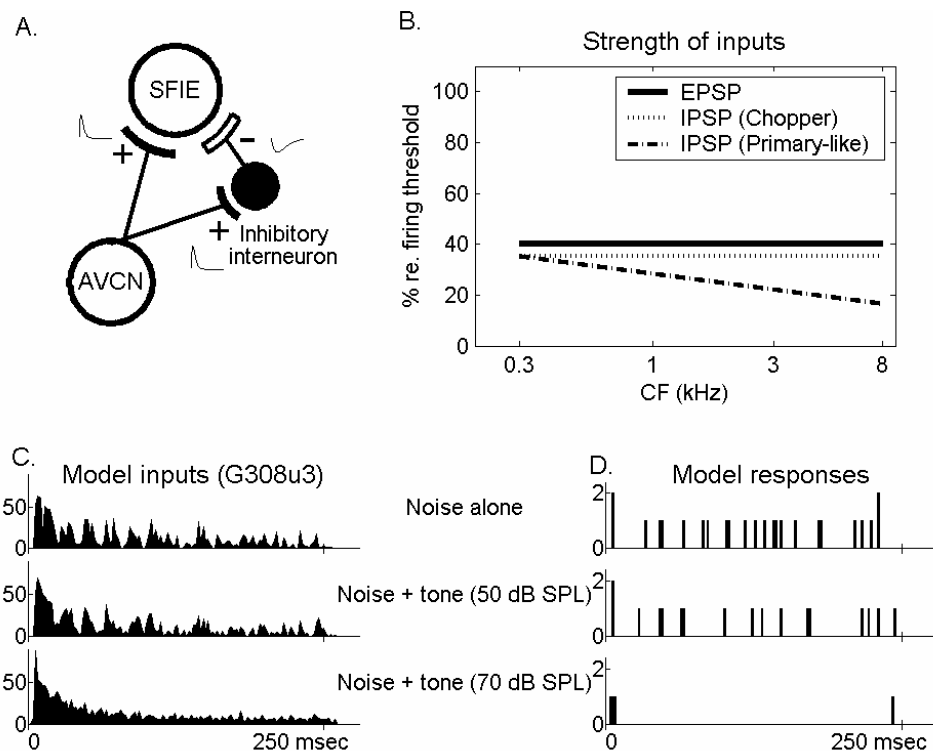
Fig. 2-8 *A*, schematic diagram of the same-frequency inhibition and excitation (SFIE) model. *B*, The strength of EPSPs and IPSPs (the value 100% was equivalent to the excitatory strength of a single input action potential that just caused the membrane potential to reach the discharge threshold). *C*, PSTHs of a chopper neuron (the unit shown in Fig. 2-4) describing the inputs to the model. *D*, Model responses. In *C* and *D*, the top panels correspond to a noise at 30 dB SPL spectrum level; the middle and bottom panels correspond to the same frozen noise plus a 50 (middle) or 70 (bottom) dB SPL tone. Bin width = 2 msec. + and - signs indicate excitatory and inhibitory inputs, respectively, and illustrative EPSPs and IPSPs are plotted beside the + and - signs.

resting potential of the cellular membrane, this type of inhibition is called a shunting inhibition (for review, see Koch 1999). The effect of a shunting inhibition on the discharge rate is subtractive when the inhibitory inputs terminate on the cell body, and divisive when they terminate on distal dendrites (Koch 1999). The neuron model used here had a single compartment and the inhibitory effects were thus mainly subtractive. A leaky integrate-and-fire model with time-varying conductances was used to simulate the SFIE model neuron (see Appendix). The model inputs were discharge times in 30 to 50 repetitions obtained from a single AVCN neuron. No temporal analysis window was used since the smoothness of the inputs was determined by the time constants of the excitatory post-synaptic potentials (EPSPs) and IPSPs.

The time constants of the EPSPs and the IPSPs were 0.5 msec and 2 msec, respectively. These relatively fast time constants were required by the model in order to extract the rapidly changing PSTH fluctuation. The inhibitory inputs were delayed by 1 msec to simulate the synaptic delay associated with an inhibitory interneuron. The strength of excitatory and inhibitory inputs used for different CFs is shown in Fig. 2-8B; a value of 100% was equivalent to the strength of one input discharge that just caused the membrane potential to reach the discharge threshold. The strength of inhibition was kept constant for model cells that had inputs from chopper units, but linearly decreased with CF for model cells that had inputs from primary-like units. This configuration was chosen to maintain a reasonable discharge rate (e.g., greater than 20 spikes/sec in response to noise alone) for model neurons with high-CF primary-like inputs, which would otherwise have had rates too low to contain any reliable information. Among all model parameters,

the strength of excitatory and inhibitory inputs was most critical for determining the

model's detection threshold.

The SFIE model required multiple input discharge trains to detect the fluctuations

of the PSTHs. Here the responses of a single AVCN neuron to 50 stimulus repetitions

were used as the multiple inputs to provide one repetition of the model discharge count.

The variance of the model discharge count was added based on the variance of the input

(i.e., the variance over the mean of the model discharge count was set equal to the

variance over the mean of the input discharge count). The model detection threshold was

the lowest tone level that had d' $\geq$ 1. Note that a decrease of model rate was used in the

calculation of d'.

b. Modeling results

Figure 2-8D illustrates the responses of a model cell that received input from the

chopper unit shown in Fig. 2-4 (re-plotted in Fig. 2-8C). For noise alone, the model

neuron received excitatory inputs that fluctuated with time (Fig. 2-8C, top). Although the

strength of the inhibitory inputs was as strong as that of the excitatory inputs, the

membrane potential still reached the discharge threshold frequently. Hence the model

showed sustained activity to noise alone or when a low-level tone was added to the noise.

Yet when a high-level tone was added to the noise, the model received fewer fluctuating

excitatory inputs from the chopper unit (Fig. 2-8C, middle and bottom). Meanwhile, the

inhibitory inputs were more constant and thus more effective in preventing the membrane

potential from depolarizing. The model thus yielded mainly subthreshold activity and low

discharge rates in response to high-level tone-in-noise stimuli, and a significant decrease

in the model rate indicated the presence of a tone.

Figures 2-2I–2-5I show the rate-level function of the SFIE model with the discharge times of the four representative neurons as inputs. The first two neurons (Figs. 2-2I and 2-3I) had monotonically decreasing model rates with increasing tone level. The third neuron (Fig. 2-4I) had a clear trend of decreased model rate, although there was a dip at 20 dB SPL (the detection threshold of this neuron was defined as 50 dB SPL). The model discharge rate with inputs from the fourth neuron (Fig. 2-5I) was noisier. Note that only responses from 30 trials were obtained for the neuron in Fig. 2-5, whereas 50 trials were obtained for the other three representative neurons.

Figure 2-6E shows the detection thresholds as determined by the model rate with inputs from recorded AVCN neurons. Some of the model thresholds were equal to or lower than the psychophysical thresholds. Here the model rate included both onset and sustained activity; performance did not change significantly when only sustained activity was analyzed. No significant difference was found in the detection thresholds across different neuron types.

Although the rate-level functions of the SFIE model qualitatively represented the fluctuation of the PSTH, it was commonly observed that the model rate changed significantly at a lower tone level than did thresholds based on fluctuation of the PSTH. For example, the fluctuation of the PSTH of the chopper unit with a temporal analysis window of 1.6 msec (Fig. 2-2H) did not show a significant decrease at 50 dB SPL, whereas the SFIE model did (Fig. 2-2I). There were cases for which no systematic change was observed in PSTH fluctuation up to the highest tone level tested, but the rate of the SFIE model decreased monotonically with tone level. The better performance of the model was partly the result of the nonlinear behavior of a neuron model that

generated discharges only if the membrane potential exceeded a discharge threshold. When the input neural response had a flat PSTH due to the addition of a tone, it was more likely to cause subthreshold activity that was not reflected in the number of model discharges. An extreme example is shown in the bottom panels of Fig. 2-8, C and D, for a noise plus a 70-dB SPL tone. Except at the onset and offset, the model input only caused subthreshold activity and led to no sustained model responses. However, when calculating PSTH fluctuation, the subtraction between adjacent counts still left some sustained activity that contributed to the values shown in Fig. 2-4H. Hence the spiking model was more sensitive to the reduction of fluctuation in the envelope and less affected by the absolute input rate than non-spiking models were.

2.3.7   Comparisons of the detection performance between different measures

Direct comparison of detection thresholds among the approaches presented here was complicated by several issues. First, the measures of rate, correlation, and synchronization required different statistical methods to test for significant changes. Second, the detection thresholds of the average rate and the synchronization were based on neural responses for individual trials, while the other temporal approaches required combinations of discharge times across trials. Third, the detection thresholds of the temporal correlation and the temporal reliability for each neuron were chosen as the best performance across all temporal analysis windows, whereas the measures of average rate and synchronization did not involve different temporal resolutions. The SFIE model can also be thought of as using one temporal resolution, since the time constants and inhibitory delays of the model were fixed for all neurons.

The ability to predict psychophysical detection thresholds based on the performance of each cue (Fig. 2-6, left and middle panels) was described above for two noise levels. Another way to test a detection cue was to measure how detection performance based on this cue changed with noise level compared to the psychophysical thresholds, which are approximately 10 dB higher for 40-dB SPL noise than for 30-dB SPL noise (Costalupes 1983). The right column in Fig. 2-6 shows the increment of threshold for neurons tested at both noise levels. The increment in the psychophysical detection thresholds, indicated by the solid lines (Fig. 2-6, right panels), was 10 dB SPL for low and mid frequencies, and gradually increased to 13 dB SPL at the highest frequencies (Costalupes 1983). For each detection cue, a certain number of neurons had thresholds that were increased by a similar amount as compared to the psychophysical thresholds. For example, 54% of primary-like neurons showed a 10-dB increment in threshold based on synchronization to the tone frequency (Fig. 2-6D, right panel), although some of these neurons had higher detection thresholds than the psychophysical thresholds at both noise levels (Fig. 2-6D, left and middle panels). Since the tone level was usually measured with a 10-dB step, some of the neurons that showed a 0 or 20 dB SPL increment in their thresholds might actually have had smaller or larger increments in threshold if a higher resolution of tone level steps had been used. For the temporal correlation, temporal reliability, and SFIE model, there were neurons that showed decreased detection threshold with increased noise level (enclosed by dashed lines in the right column of Fig. 2-6), which was contradictory to the psychophysical observation. The detection performance of these neurons as determined by that particular detection cue should be evaluated with caution (Fig. 2-6, left and right columns, symbols with a dot

in the center). Nevertheless, these neurons may still contribute to the detection task if a population of neurons are combined to predict the psychophysical detection thresholds at different noise levels.

2.4   Discussion

The present study showed that the average discharge rate of individual anteroventral cochlear nucleus (AVCN) neurons was incapable of predicting psychophysical tone-in-noise detection performance, while the temporal correlation measure indicated that abundant temporal information was available. Three temporal cues—reliability, synchronization to the tone frequency, and fluctuation of the post-stimulus time histograms (PSTH)—were shown to yield detection thresholds in some neurons that were comparable to psychophysical results. The same-frequency inhibition and excitation (SFIE) model provided a specific, physiologically realistic mechanism for the extraction of temporal envelope fluctuation and transformation into a representation in terms of discharge rate.

2.4.1   Average discharge rate

A reduction in the dynamic range of the discharge rate caused by a broadband noise was found in most of the neurons in the present study and showed trends similar to previous studies of auditory-nerve (AN) fibers and VCN neurons (AN: Geisler and Sinex 1980; Rhode et al. 1978; Young and Barta 1986; CN: Gibson et al. 1985). It has been reported that a small number of AN fibers with low- and mid-spontaneous rates have rate thresholds comparable to behavioral detection thresholds (Young and Barta 1986). Since

the dynamic range of the average discharge rate of CN neurons is similar to AN fibers (Gibson et al. 1985), it would be expected that the rate coding of some CN neurons should be sufficient to account for psychophysical detection thresholds. However, the highest noise spectrum level in Young and Barta's study was 30 dB SPL. The present study showed that detection performance based on discharge rate was even worse for the 40 dB SPL noise spectrum level.

One limitation of this study was that the animals were anesthetized with ketamine during the recordings. May and Sachs (1992) suggested that VCN neurons in awake cats may exhibit larger dynamic ranges in rate than neurons in anesthetized or decerebrate cats. Another limitation was that the rate coding discussed thus far was based on single neurons. It is likely that the rate information in an optimally weighted population of independent neurons would predict lower detection thresholds than the most sensitive individual neuron. Theoretically, combining the average discharge rate across identical but independent neurons can reduce the variance of the rate. For example, the detection threshold based on the average rate of the chopper neuron in Fig. 2-2 was 65 dB SPL, but might be reduced to 50 dB SPL if the estimated variance of the rate was reduced by combining 10 statistically identical and independent neurons, although the absolute rate change was small at 50 dB SPL. In other words, in order to achieve lower detection thresholds than the single-neuron thresholds, small rate changes in a precise system are critical.

A mechanism that could combine the average rates across a population of neurons to reduce the variance is not clear. Discharges of higher-stage auditory neurons that receive multiple inputs from AVCN neurons are affected by refractoriness and by the

relative timing differences between individual inputs. Since the majority of AVCN neurons showed decreased temporal reliability with increasing tone level, the reduction of the coincidence across neurons upon addition of the tone would act against the increased average rate for any higher-stage neurons with subthreshold inputs.

2.4.2   Temporal reliability

Martin et al. (2004) calculated the coefficient of reliability as the mean cross-correlation coefficient of every pair of smoothed discharge trains for all possible combinations of trials. They found that the discharge pattern of auditory thalamic neurons in response to tones was scrambled when broadband noise was added, which was reasonable since the noise in each stimulus presentation was not identical (frozen). In the present study, the temporal reliability measure focused on discharge-timing similarity across identical neurons to the same stimulus; thus the noise was frozen to maintain consistent response patterns, as seen in Fig. 2-1.

Most of the AVCN neurons exhibited decreased reliability when a CF tone was added to broadband noise, especially for relatively small temporal analysis windows. The exact factors that determined the temporal reliability for AVCN neurons are not clear from the results obtained here. Nevertheless, some similarities between current results and a previous study of neocortical neurons (Mainen and Sejnowski 1995) may provide some insight. In that study, the reliability of discharge timing was shown to be significantly higher in response to fluctuating current pulses than to a DC current, although the average discharge count did not vary much across trials for either stimulus. In the present study, of the neurons that had decreased reliability for at least one temporal

analysis window, 92% and 71% also had decreased PSTH fluctuation at noise levels of 30 and 40 dB SPL, respectively, although the detection thresholds based on the two metrics were not always the same. Therefore, one possible factor contributing to the observed temporal reliability is the presence of temporal features contained in the stimulus waveform that cause synchronization in the neural responses. This hypothesis implies an association between the temporal reliability and the envelope of the effective stimulus. However, as shown by the chopper unit in Fig. 2-4, which had large changes in the PSTH fluctuation but small changes in the reliability when a high-level tone was added to the noise, the relationship between the stimulus envelope and the temporal reliability is not as direct as the relationship between the stimulus envelope and the PSTH fluctuation.

The two primary-like units in Figs. 2-3 and 2-5 showed decreasing temporal reliability for relatively small temporal analysis windows. This decreased reliability might seem to contradict the increased synchronization to the tone frequency. Although the higher reliability of low-CF neurons as compared to high-CF neurons was presumably due to the stronger phase locking at low frequencies, a higher synchronization coefficient caused by the addition of a tone did not necessarily correspond to higher response reliability across presentations or to a higher coincidence of discharge times across identical neurons. For the two primary-like units (Figs. 2-3C and 2-5C), the increased synchronization with the tone level indicated that discharges appeared at a more precise phase in each tone cycle; however, since the neuron did not discharge in every tone cycle, the reduction of the PSTH fluctuation suggested that the activity was spread out over more tone cycles. If the fluctuation of PSTHs was mainly determined by the envelope of

the effective stimulus, as will be discussed next, it is reasonable to conclude that the neural response to stimulus envelope played a more important role in determining the temporal reliability than did the synchronization to the tone frequency.

2.4.3   Fine timing vs. envelope

We hypothesized that PSTH fluctuation was caused mainly by the stimulus envelope because AVCN neurons have been shown to discharge in synchrony to the envelope of amplitude-modulated stimuli (Frisina et al. 1990; Rhode and Greenberg 1994). In the present study, the envelope that was assumed to be responsible for the PSTH fluctuation was the envelope of the effective stimulus after peripheral filtering (Louage et al. 2004), which differs from the envelope achieved by the Hilbert transform of the original waveform. The fluctuation of the PSTH might also be affected by the neuron's intrinsic properties and its inputs.

It is difficult to discriminate fine-timing and envelope-related cues because they are not clearly delineated by response properties analyzed with different temporal resolutions. For the majority of neurons, the 1.6-msec analysis window was found to provide the best resolution for measuring PSTH fluctuation among the five windows tested. Although this 1.6-msec window was smaller than the period of a CF tone for low-frequency neurons, fluctuations measured on this time scale were classified as envelope-related for two reasons. First, this resolution value was fixed for all neurons and was independent of their CFs. As long as the temporal resolution did not match the CF exactly, the fluctuation was associated with factors other than phase locking to the tone. Second, stronger synchronization to the tone at higher tone levels caused more precise

timing in each tone cycle, which should have resulted in more peaky PSTHs, as opposed to the observed flattened PSTHs using the 1.6-msec analysis window, as shown in Figs. 2-2–2-4.

By using different temporal analysis windows that ranged from sub-millisecond to tens of milliseconds, the best resolution for processing the temporal information quantified by each metric was examined. There were three major conclusions related to temporal resolution. First, performance based on the temporal correlation of chopper units was less affected by the choice of temporal analysis window, while most primary-like units showed lower thresholds with relatively small window sizes. This difference implies that temporal information carried by these primary-like units would not be useful for detection if higher-stage auditory pathways were not sufficiently fast or accurate. Second, the temporal reliability for most of the neurons predicted better detection performance when using relatively small temporal analysis windows. Third, the decrease in PSTH fluctuation with tone level was most significant with a temporal analysis window of 1.6 msec for most AVCN neurons.

Louage et al. (2005) measured the intrinsic oscillations of AVCN neurons in response to broadband noise with the shuffled autocorrelogram (SAC). They found the dominance of synchronization transitioned from the tone frequency to envelope-locking at CFs of approximately 4 kHz. The present study showed that the rapid fluctuation of PSTHs, presumably caused by the rapidly changing stimulus envelope, contained information for detection for both low and high CFs. In fact, the detection thresholds based on the PSTH fluctuations of low-CF neurons were lower than high-CF neurons, which agreed with the psychophysical detection thresholds. There are two reasons for this

apparent discrepancy between the study of Louage et al. and the present study. First, synchronization to fine structure and to envelope can be independent of each other (van Gisbergen et al. 1975). Synchronization to the tone frequency only relies on the discharge phase in each tone cycle and does not incorporate the cycle in which a discharge falls. Therefore, a low-CF neuron can synchronize to both the envelope and the fine structure (Rhode and Greenberg 1994). Second, Louage et al. focused on the relative importance of fine-timing and envelope synchronization in determining the overall neural response, while the present study focused on determining which cue was more sensitive to the addition of a tone to noise.

Comparisons between Fig. 2-6 D and E indicated that the envelope-related cue was able to predict the psychophysical thresholds at both low and high CFs, while synchronization to the tone frequency was only able to predict the psychophysical thresholds at low CFs. In addition, it has been discussed earlier that the change of temporal reliability when a tone was added to noise was dominated by the stimulus envelope. Therefore, we conclude that envelope-related cues may be critical for tone-in-noise detection at both low and high frequencies.

2.4.4   SFIE model

The SFIE model (Nelson and Carney 2004) was originally developed to predict the responses to amplitude-modulated stimuli of inferior colliculus (IC) neurons, which have an average firing rate that is tuned to modulation frequency. The present study showed that with inputs from a number of AVCN neurons, a decrease in the discharge rate of the model can indicate the presence of a tone in background noise. The model

provided a fundamental detection strategy that separated the tone from the noise without cross-frequency integration. The result indicated that single-neuron responses elicited by fluctuations in the stimulus envelope may contain useful information for detection of tones in noise, though in reality the physiological mechanism probably involves more complicated arrangements than simple combinations of excitatory and inhibitory inputs with matched CFs.

In the central nucleus of the IC (ICC), the frequency tuning of the inhibitory inputs was found to match to that of the excitatory inputs for most neurons (Palombi and Caspary 1996); stimulating the lateral lemniscus can cause EPSPs and delayed IPSPs in the same ICC neuron (for review, see Wu et al. 2004). These observations are consistent with the assumptions of the SFIE model. A study of ICC neurons in decerebrate cats (Ramachandran et al. 1999) showed that the majority of neurons responded to broadband noise with diverse shapes in the rate-level functions and discharge rates to tones and to noise. However, Rees and Palmer (1988) mainly reported weak responses of ICC neurons to broadband noise in anesthetized guinea pigs. It is unclear whether decreased neural responses with increasing tone level were ever observed in that study. In addition to ICC neurons, there are neurons at other levels of the auditory system that receive combined excitatory and inhibitory inputs. For example, the lateral and medial superior olivary nuclei (LSO and MSO) receive ipsilateral and contralateral inhibitory inputs, as well as excitatory inputs (LSO: Brownell et al. 1970; Wu and Kelly 1994; MSO: Cant and Hyson 1992; Grothe and Sanes 1993). These neurons are also physiological candidates for the SFIE model as tone-in-noise detectors.

The time constants used in the model simulation were relatively short in order to follow the rapidly changing PSTH fluctuations. One study of ICC neurons showed EPSP time constants of several milliseconds (Wu et al. 2004), which were several times longer than the values used here. The EPSP time constants of LSO and MSO neurons are closer to the values used here (Smith et al. 2000; Wu and Kelly 1994). Note that the relatively low temperature used in those *in vitro* studies might have led to slower measured time constants (Smith et al. 2000) than what could have been obtained at the animals' body temperature.

2.4.5   Possible physiological mechanisms for the temporal approaches

The next step beyond the exploration of the types of information that are potentially useful for detection is to understand what physiological mechanisms can process the information from AVCN neurons. As mentioned earlier, the temporal correlation metric indicated change in the neural responses, but such change cannot be easily represented by any feasible physiological strategy. Thus, only the other three temporal metrics are discussed below.

Temporal reliability was used to measure the consistency of the discharge pattern of a neuron across trials; we hypothesize that it also reflects the coincidence of discharge timing across a population of neurons. A neuron that requires the temporal convergence of multiple excitatory subthreshold inputs to reach its discharge threshold functions as a coincidence detector. When a tone is added to a noise, the discharge rate of the coincidence-detection neuron is decreased if the reliability of its input is reduced with approximately a constant number of input discharges; however, if the number of input

discharges is higher for the tone, the target neuron is more likely to increase its discharge rate, counteracting the reliability cue. Simulations of a coincidence-detection neuron with inputs from AVCN recordings revealed that the input rate had a stronger effect than the reliability did (result not shown here). Therefore, not all AVCN neurons could use a simple coincidence-detection mechanism to extract the information in the temporal reliability measure.

Changes in the fluctuation of PSTHs can be detected by the SFIE model, as discussed above. For the chopper unit in Fig. 2-4, another way to detect the fluctuation is to set a high discharge threshold for the membrane potential of the post-synaptic neuron that receives multiple excitatory inputs from AVCN neurons and no inhibitory inputs. For example, based on the PSTHs shown in Fig. 2-4 B and C for a noise alone and for a 70-dB SPL tone plus noise, a discharge threshold set just under the peak values of the noise-alone PSTH and above the sustained activity of the tone-plus-noise PSTH would result in a decreased discharge rate of the post-synaptic neuron upon addition of the tone to the noise. This thresholding mechanism can be realized by the coincidence-detection neuron described above by increasing the discharge threshold. However, similar to the problem with the coincidence-detection mechanism, the thresholding mechanism would fail to detect the tone if the input rate increased with tone level.

The fine-timing information for tone-in-noise detection was quantified with the synchronization coefficient in the present study and previous studies (Miller et al. 1987; Rhode et al. 1978). The computation of the synchronization to the tone frequency requires knowledge of the tone frequency and an "internal clock" (Joris et al. 2005; Louage et al. 2004) to mark the phase of each discharge in a tone cycle. Before

discussing possible mechanisms that do not involve an internal clock, it should be noted that simple coincidence detection across identical and independent neurons, although it seems intuitive, does not reliably detect increased synchronization to the tone with increasing tone level due to the decreased temporal reliability and more uniformly spread discharge activity.

One way to avoid the requirement of an internal clock is to have accurate delay lines that are proportional to the neuron's CF. These delay lines can be used by a first-order autocorrelation model that increases its rate when the coincidence between non-delayed inputs and delayed inputs is higher when a tone is added. To date, direct physiological evidence for delay lines have not been identified. Another way to avoid using an internal clock and the knowledge of tone frequency is to construct a shuffled autocorrelogram (Louage et al. 2004, 2005). However, the physiological mechanism for constructing an autocorrelogram is still unclear (Cariani and Delgutte 1996).

In addition to synchronization to the tone frequency, phase changes across AN fibers with different CFs are used by the phase-opponency model (Carney et al. 2002) for tone-in-noise detection as an alternative fine-timing cue. The detection thresholds of this model were shown to match to human psychophysical detection thresholds at low frequencies (Kidd et al. 1989). The physiological evidence for this model is still under exploration.

2.4.6   Future studies

The temporal approaches used here were based on the responses of on-CF neurons. The possibility that detection performance would improve by including off-CF

neurons in those analyses was not explored. Lewis and Henry (1995) showed responses of a high-CF AN fiber to a low-CF tone and the tone plus a broadband noise (their Fig. 2-8). This fiber had only onset and offset responses to the tone-alone stimulus but a sustained response to the tone-plus-noise stimulus that was phase-locked to the off-CF tone. It is possible that some AVCN neurons also have such properties, which may provide useful phase-locking information for tone-in-noise detection. The role of off-CF neurons should be considered in further studies of the temporal metrics presented here.

The present study found that the rapidly changing fluctuation of the PSTH contained useful information for detection, which was presumably determined by the effective stimulus envelope. It was unclear whether the best temporal resolution, 1.6 msec, was general for detection of tones in noise with any bandwidth or was unique to broadband noise. In a reliability study of neocortical neurons (Mainen and Sejnowski 1995), the best timescale for precise discharge timing was found to be 1 to 2 msec, even when the current pulses used to stimulate the neurons fluctuated at a much slower rate. It is possible that the rapid fluctuation of AVCN responses to tones in sub-critical-band noise still contain useful information for detection. Nevertheless, contributions of the slow-changing envelope to the detection of a tone in narrowband noise cannot be ruled out until further experiments are conducted. Such studies would be of interest for comparison to psychophysical studies of detection with different masker bandwidths.

2.5   Appendix

A single-compartment leaky integrate-and-fire model with time- and voltage-dependent conductances (Cook et al. 2003) was used.

The neuron model used to simulate the SFIE model can be expressed as

$$C_m \frac{dV(t)}{dt} = -G_m V(t) + G_E \exp(-\frac{t-t_E}{\tau_E})(V(t)-V_E) + G_I \exp(-\frac{t-t_I}{\tau_I})(V(t)-V_I)$$

Parameter descriptions and values are listed in Table 2-1. The model inputs are arrival times of incoming excitatory or inhibitory discharges, t_E and t_I, respectively. When the membrane potential, $V(t)$, exceeds a discharge threshold, θ, an action potential is marked in time as the model output. A dead time of 0.7 msec is used to simulate the absolute refractory period after each action potential.

Table 2-1 Parameter values for the SFIE model

Parameters	Description	Value
C_m/G_m	Ratio of membrane capacitance to membrane conductance for leakage	0.5 msec
G_E, G_I	Maximum membrane conductances for excitatory and inhibitory postsynaptic currents (EPSCs and IPSCs, respectively)	Adjusted to yield the strength of EPSPs and IPSPs as described in Fig. 2-8B
τ_E, τ_I	Time constants of EPSCs and IPSCs, respectively	Adjusted so that the decay time constants of evoked EPSPs and IPSPs were 0.5 msec and 2 msec
θ	Discharge threshold	15 mV above the membrane's resting potential
V_E	Reversal potentials for EPSCs	55 mV above the resting potential
V_I	Reversal potentials for IPSCs	Set equal to resting potential

Chapter III

More Analyses of Tone-in-noise Responses: Correlation Index and Spike-distance Metric

3.1   Introduction

In Chapter II, detection performance based on the responses of AVCN neurons to tone-in-noise stimuli using average rate and several temporal analyses was described. Two additional temporal analyses were tested with the same set of physiological data after the publication of the above results in Gai and Carney (2006). The results of these analyses will be presented in this chapter.

When a neuron responds to a sound, information carried by inter-spike intervals is presumably easy for the brain to use since it does not require knowledge of the stimulus. An autocorrelogram based on all-order inter-spike intervals has been used in various studies, such as modeling studies for pitch (Licklider, 1951; Meddis and Hewitt, 1991). The shuffled autocorrelogram (SAC), constructed by including the intervals across repetitions but excluding the intervals within each spike train, was shown to be a better measure of temporal information carried by inter-spike intervals since it is not constrained by the refractoriness after each discharge (Louage et al., 2004). In general, the SAC is a relatively simple method to examine fine-structure or envelope-related information for both periodic and aperiodic stimuli (Louage et al., 2004, 2005), although a mechanism for computing the inter-spike intervals that it requires is still unclear.

The correlation index is the peak value of the SAC, which measures the occurrence of simultaneous discharges across repetitions. The correlation index can be realized with a simple coincidence-detection mechanism (Louage et al., 2005; Joris et al., 2006); that is, no interval computation is required. In Louage et al. (2005) and Joris et al. (2006), the correlation index is applied to neural responses to pure tones, sinusoidally amplitude-modulated (SAM) tones, and noise. For pure-tone responses, the correlation index measures synchronization to tone frequency in a similar way as the vector strength (Joris et al., 2006), but it does not have the drawback of compressing high-synchrony values. For SAM responses, the correlation index measures synchronization to modulation frequency, and for noise responses, synchronization to the noise envelope. However, the correlation index has not been applied to tone-in-noise responses. It is unclear how the correlation index changes with a mixture of synchronization to tone frequency and to envelope.

As pointed out in Chapter II, for low-CF neurons that are partially synchronized to both fine structure and envelope, increasing the level of a tone added to noise causes increased synchronization to tone frequency and decreased fluctuations in time-varying rate due to the flattening of the stimulus envelope. Therefore, the correlation index is affected by two counter-acting cues and does not represent either fine-structure alone or envelope-related cues alone. In fact, the correlation index was expected to change in a way similar to temporal reliability, since both measure across-repetition consistency of discharge times. As shown in Chapter II, the dominance of envelope over fine structure caused a decrease in the temporal reliability with increasing tone level. A similar change was expected to occur in the correlation index.

The correlation index and the other temporal metrics described in Chapter II can be divided into two categories based on their dependence on spike-time precision. Synchronization to tone frequency and PSTH fluctuation reflect response features that are not directly related to spike timing with respect to stimulus onset, but rather are related to relative spike timing (e.g. intervals, or fluctuations in rate over time). For example, two spike trains that were locked to different phases of the same stimulus do not have the same absolute spike timing but could have the same synchronization coefficient. More generally, two different spike trains in response to two different stimuli can have the same synchronization coefficient. On the other hand, those metrics that involve correlation or coincidence detection (i.e., temporal correlation, temporal reliability, and correlation index) rely on the absolute spike times with respect to stimulus onset. Victor and Purpura (1996, 1997) develop a distance metric that can be applied to absolute spike times to quantify the dissimilarity across spike trains over varying time scales. If absolute spike times are critical for coding a certain set of stimuli, then the spike-timing distance should be larger for responses to different stimuli in the set than for responses to different repetitions of the same stimulus.

To study detection of a tone in noise, the spike-distance metric was applied to responses to noise-alone stimuli and to noise with tones at different levels. In the category that relies on absolute spike timing, this metric is most similar to temporal correlation, since both directly compare noise-alone and tone-plus-noise responses, while temporal reliability and correlation index measure the similarity of responses to different repetitions of the same stimulus. In general, comparisons of detection performance between the two categories of temporal measures indicate whether the temporal

information critical for detection of tones in noise is carried by absolute or relative spike times.

3.2   Methods

3.2.1   Animal preparation, stimulus generation and recording procedures

The experimental procedures were the same as described previously. Briefly, the gerbil was anesthetized with ketamine and xylazine. Single-neuron extracellular recordings in the AVCN were obtained with a single-barrel glass electrode through an opening in the temporal bone and the bulla (Frisina et al., 1990). Sound stimulus was a white noise (30 or 40 dB SPL spectrum level from 0.1 to 10 kHz) or the noise plus a simultaneously gated CF tone that varied in level. Each stimulus was presented 30 to 50 times, had a duration of 250 msec, and was repeated every 475 msec. The noise waveform was randomly generated and kept frozen for each dataset. Both amplitude and phase were digitally compensated for each stimulus using a calibration table obtained at the beginning of each experiment.

3.2.2   Correlation index (CI)

The correlation index (CI) is basically a measure of the degree of similarity of discharges in response to different repetitions of a stimulus. The calculation was the same as that described in Joris et al. (2006). For each pair of spike trains, the total number of coincidences of spike times across repetitions was counted. For M repetitions, there were $M(M-1)/2$ different pairs of spike trains. In order to match the calculation of SAC in

Joris et al. (2006), in which the order of the two spike trains matters (e.g., spike train #1

vs. spike train #2 yields different results from spike train #2 vs. spike train #1),

$M(M-1)$ pairs of spike trains were counted, so that half of the CI values were duplicates

of the other half. The total number of coincidences across all paired combinations is

denoted as N_c. CI was computed as

$$CI = \frac{N_c}{M(M-1)r^2\omega D} \qquad \text{(Eqn. 3-1)}$$

where r is the average discharge rate, ω is the temporal analysis window (i.e.,

coincidence window), and D is the stimulus duration (250 msec).

The temporal analysis window determines the window during which two spikes

are considered coincident. In the Chapter II, five arbitrarily selected windows, 0.2, 0.56,

1.6, 4.5, and 12.8 msec, were applied to some of the temporal metrics. However, only the

smallest 2 windows could be applied to the CI, since the larger windows allowed more

than 1 spike to fall into the same window. No Gaussian smoothing function was applied

since values of spike trains had to be either 1's or 0's for coincidence detection.

To determine a detection threshold based on the CI, the lowest tone level that

yielded a significantly different CI compared to that of the noise alone was identified. A

bootstrapping algorithm (Moore et al., 2002) was used to test the significance of the

difference in CI between responses to noise-alone (M repetitions) and noise-plus-tone (M

repetitions) stimuli; the difference was denoted as ΔCI_0. Basically, spike trains in

response to both noise-alone and noise-plus-tone stimuli were mixed together and

regrouped randomly into two new groups (M spike trains each), and the difference in CI

between the two new groups, denoted as ΔCI, was computed. A distribution of ΔCI

using 500 different random groups was formed. By comparing the ΔCI_0 and ΔCI for the mixed distribution the statistical significance was obtained. In fact, since more than 80% of neurons showed decreased CI with tone level (see Results) at both noise levels, only significant decreases in CI derived using the above method were considered. The detection threshold was the lowest tone level that had a significantly lower CI than that for noise alone for any temporal-analysis window, as long as the decrease in CI remained significant for all higher tone levels for that particular window.

3.2.3   Spike-distance metric and mutual information

The dissimilarity of two spike trains, as measured by the spike distance metric, can be interpreted as how much effort is required, or how costly it is, to transform one spike train into the other with a certain degree of temporal freedom (Victor and Purpura, 1997). More specifically, one spike train can always be created from another spike train by adding (cost = 1) and deleting (cost = 1) spikes, or by shifting the timing of spikes (cost = $q|\Delta t|$; $|\Delta t|$ is the time difference between the two spikes). The action is determined by minimizing the total cost of transferring one spike train into the other. When $|\Delta t| < 2/q$, the cost of shifting the spike is lower than adding and deleting spikes, and vice versa. Therefore, q determines the temporal resolution. When $q = 0$, the spike distance is equal to the difference between spike counts of the two spike trains. When $q = \infty$, the spike distance is the sum of the total number of spikes of the two trains excluding coincident spikes.

When there are several sets of spike trains in response to several stimuli, a confusion matrix can be created to indicate the discharge consistency within each stimulus and across different stimuli. The mutual information derived from the confusion matrix indicates the efficiency of the responses in coding the stimuli. A detailed illustration of the procedure can be found in Chase and Young (2006). In the present study, a confusion matrix was created based on spike distances in the responses to noise-alone and the noise-plus-tone stimuli with different tone levels. High mutual information suggests that the tone-in-noise responses were highly "separated" in a metric space, regardless of the monotonicity of the underlying changes. For example, when $q = 0$, the spike distance metric is equal to average discharge rate. High mutual information can be achieved even if the rate change is nonmonotonic with tone level as long as the rates are different in response to different stimuli. In general, the average rate and several of the temporal metrics presented in Chapter II are monotonic with tone level; however, some nonmonotonicity can be observed for two adjacent tone levels due to variability in the responses. Therefore, only responses to three tone levels were included in computing the spike distance metric: noise alone, noise plus the highest-level tone (70 or 80 dB SPL), and noise plus the third-highest-level tone (50 or 60 dB SPL), to provide potentially large distances between the responses.

Values of q were logarithmically spaced between 10 and 17,783 with 4 values per decade, which was shown to yield a smooth change of mutual information based on spike distances for AVCN neural responses. $q = 0$ was also included to test average-rate coding. The computations of the confusion matrix and mutual information were the same as described in Chase and Young (2006). Note that a detection threshold was not

obtained based on the mutual information; rather, the goal was to compare rate coding

and spike-timing coding for each neuron.

3.3   Results

Tone-in-noise responses of the same 102 units presented in Chapter II were re-

analyzed here with the correlation index and spike distance metrics. Four representative

neurons (from Figs. 2-2 to 2-5, 2 primary-like and 2 chopper units) will be presented first,

followed by population results.

3.3.1   Correlation index

Figure 3-1*A* shows the change of CI with increasing tone level for two temporal-

analysis windows, 0.2 and 0.6 msec. A common trend was that the CI decreased with

tone level. As shown in Chapter II, the synchronization to tone frequency for 3 out of 4

neurons increased significantly with tone level (Figs. 2-2*D*, 2-3*D*, and 2-5*D*). Therefore,

the CI did not represent synchronization to tone frequency in the presence of background

noise, as it did for pure tones. In fact, the change of CI with tone level was similar to that

of temporal reliability (Figs. 2-2*F* to 2-5*F*). For easier comparison, the temporal

reliability (computed as the correlation coefficient between the PSTHs constructed with

even-numbered and odd-numbered repetitions) of the 4 neurons is re-plotted in Fig. 3-1*B*.

The detection thresholds based on CI and temporal reliability were the same for neurons *c*

and *d*, but different for neurons *a* and *b*. For example, the lowest tone level that showed a

significant decrease ($p < 0.05$, bootstrapping; see Methods) of CI for neuron b was 60 dB

A. Correlation Index (Noise: 30)

a. G309u9
b. G297u5
d. G313u12
0.2 msec
0.6 msec
c. G308u3

CI
Tone level (dB SPL)
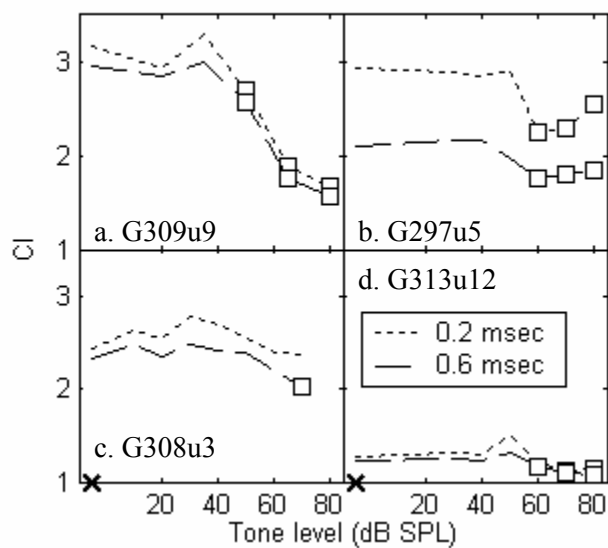
B. Temporal reliability (Noise: 30)

Reliability

0.2 msec
0.6 msec
1.6 msec
4.5 msec
13 msec

a.
b.
c.
d.

Tone level (dB SPL)
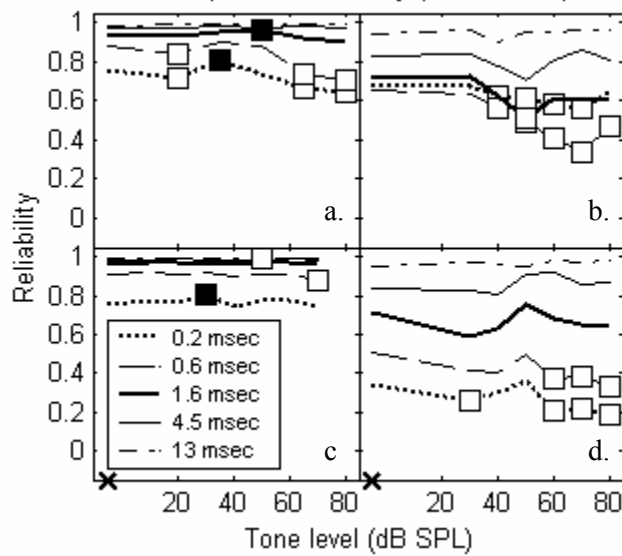
Fig. 3-1 Correlation index (*A*) and temporal reliability (*B*, re-plotted from Figs. 2-2*F* to 2-5*F*) for the four representative neurons at different temporal resolutions. Panels *a* and *c* show two choppers, and panels *b* and *d* show two primary-likes. The CF was 482, 676, 1085, and 4565 Hz, for neurons in *a*, *b*, c and *d*, respectively. Open (filled) squares indicate significant decrease (increase) at a certain tone level compared to that of noise alone. X on the abscissa marks the noise alone. The noise spectrum level was 30 dB SPL.

SPL, while the lowest tone level that showed a significant decrease of temporal reliability for neuron b was 40 dB SPL.

Figure 3-2 shows detection thresholds based on CI for noise spectrum levels of 30 (*left*) and 40 (*middle*) dB SPL. These thresholds were comparable with detection thresholds based on temporal reliability (Fig. 2-6*C, left and middle*). A small number of neurons showed detection thresholds equal to or lower than psychophysical detection threshold in cat (solid lines; Costalupes, 1983, corrected for noise duration based on Wier et al., 1977). In the right panel, most neurons showed increased thresholds with noise level that were close to the psychophysical threshold increments (solid line) but more variable than the threshold increments based on temporal reliability (Fig. 2-6*C, right*).

In Joris et al. (2006), 0.05 msec was chosen as a standard window based on the effect of the coincidence window size on the CI. Applying the CI with 0.05-msec temporal window on AVCN responses (not shown here) yielded worse detection performance in general compared to the result using the above two temporal windows (0.2 and 0.6 msec). As stated in the Methods, windows larger than these two were not included either, since no more than 1 spike was allowed to fall in the same window.

3.3.2   Spike-distance metric and mutual information

a. Best temporal resolution

Figure 3-3 shows the mutual information (MI) based on spike-time distances for the four representative neurons (solid lines). The x-axis is the cost, q, which corresponds to a temporal resolution of $1/q$ (Victor and Purpura, 1997). $q = 0$ represents average rate
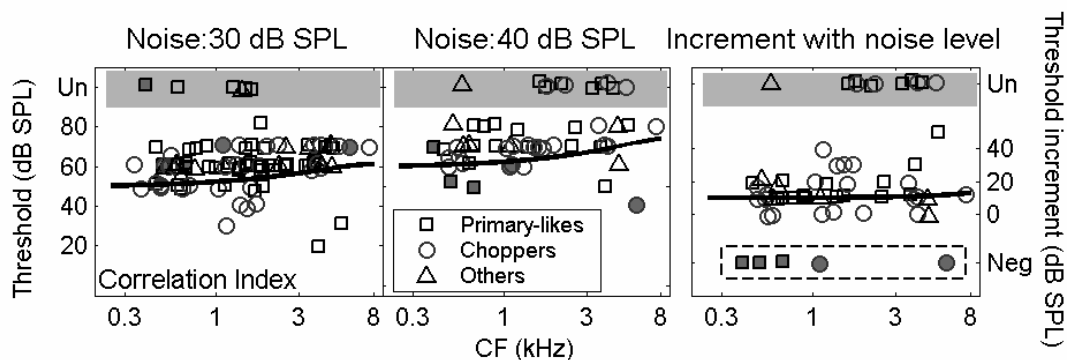
Fig. 3-2 *Left* and *middle* panels: Detection thresholds based on correlation index (CI) plotted in the same format as Fig 2-6 for noise spectrum level of 30 (*left*) and 40 (*middle*) dB SPL. Solid lines indicate psychophysical thresholds in cat (Costalupes, 1983). Shaded areas, labeled Un, indicate unmeasurable thresholds (no significant change occurred up to the highest tone level tested). *Right* panel shows threshold increments when noise level increased from 30 to 40 dB SPL. The solid line indicates psychophysical threshold increments. Shaded areas, labeled Un, indicate unmeasureble thresholds at 40 dB SPL noise level. Filled symbols in *right* panel, labeled Neg, indicate decreased thresholds with increasing noise level (these neurons are also marked with filled symbols in *left* and *middle* panels).

coding. For neurons *c* (primary-like) and *d* (chopper), the MI at q = 0 was close to 0,

consistent with the fact that these two neurons had flat masked rate-level functions (Figs.

2-4*D* and 2-5*D*). For these two neurons, the MI peaked at relatively high values of q,

indicating that temporal coding for detection based on absolute spike times was most

efficient with relatively high spike-timing precision (1/q = 1.8 and 0.6 msec, for neurons
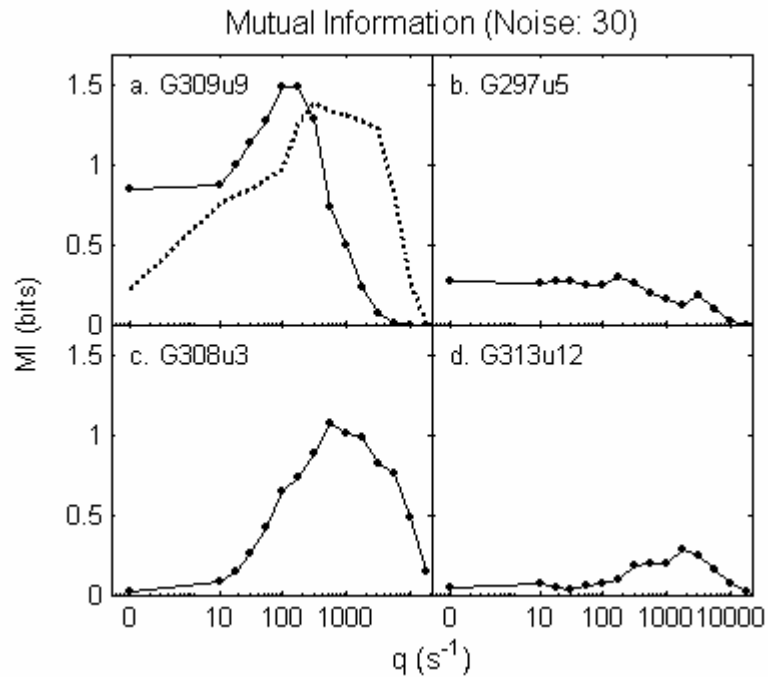
Fig. 3-3 Mutual information (MI) based on spike-time distances of tone-in-noise

responses with varying q for the four representative neurons. Solid lines, mutual

information based on all spike times. Note that the mutual information of the two

choppers (*a* and *c*) was substantially larger than that of the two primary-like units (*b* and

d). The dotted line in panel *a* is the MI with reduced average-rate information. For every

spike train in response to noise-alone or tone-plus-noise stimuli, no more than the first 23

spikes (the mean discharge count for responses to noise–alone stimuli), beginning at the

stimulus onset, were included.

c and *d*, respectively). Neuron *a* (chopper) had a relatively high value of MI at q = 0,

since its average discharge rate showed a significant change with tone level (Fig. 2-2*D*).

However, the best coding for detection was achieved at a resolution of 10 msec. This is a

relatively large time scale that did not support any of the temporal measures presented in

Chapter II. The implication of the large time scale will be discussed later with population

results. Neuron *b* (primary-like) was even more interesting in that including spike-timing

information did not improve the detection efficiency compared to average-rate coding,

even though this neuron showed better detection performance using any of the previously

tested temporal metrics than using rate coding (Fig. 2-3). This example suggested that the

spike-time distance metric was not related to the other temporal metrics that were based

on either absolute or relative spike times.

To describe population results, the MI as a function of q was categorized into

symmetrical band-pass shaped (neurons *c* and *d*), low-pass shaped (neuron *b*), and

asymmetrical band-pass shaped (neuron *a*). The symmetrical band-pass shape described

MI functions with no average-rate information. The low-pass shape described MI

functions with the maximum information contained in average rate. The asymmetrical

band-pass shape describes MI functions with substantial rate information, but the

maximum information was obtained when spike timing information was included. Fig. 3-

4 shows the MI based on spike-time distance for all recorded neurons grouped by

response types (primary-like, chopper, and unusual). A common trend in the best

temporal resolution was that those neurons with symmetrical band-pass shaped functions

showed consistently higher values of best q compared to neurons with asymmetrical

A. Type: Primary-likes

B. Type: Chopper
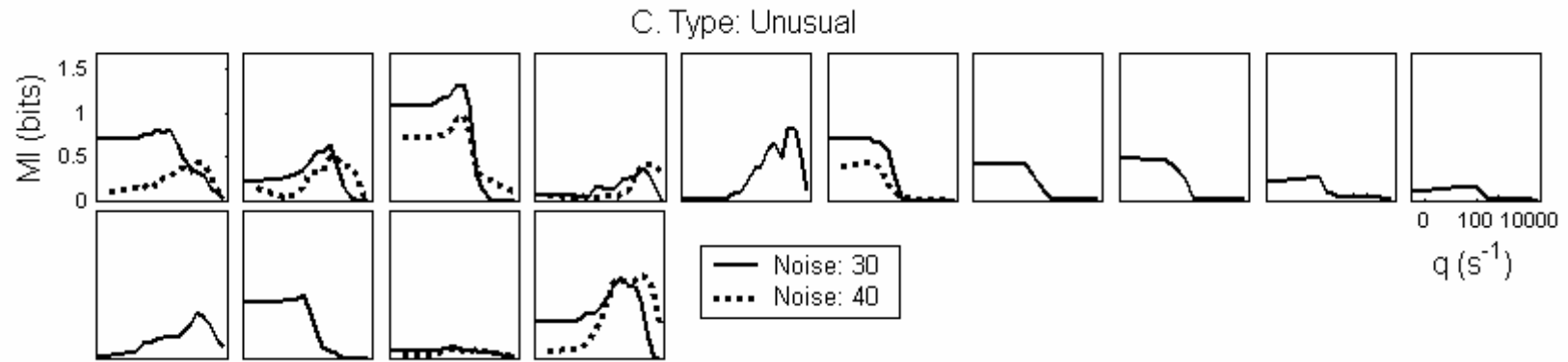
Fig. 3-4 Mutual information (MI) based on spike-time distances of tone-in-noise responses with varying q for all primary-like (*A*),

chopper (*B*), and unusual (*C*) units. In each group, neurons are arranged with increasing CF from left to right, top to bottom. Solid

lines, 30 dB SPL spectrum level noise. Dotted lines, 40 dB SPL spectrum level noise.

band-pass shaped functions. However, the best temporal resolution derived in this manner can be hard to interpret for the following two reasons.

First, as q increases, the number of spikes required for sampling the space also increases (Victor ad Purpura, 1997). Due to limited data samples, however, the same number of spikes was used for different q values. Therefore, the best q can be underestimated. Second, it is likely that the presence of average-rate information at q = 0 biased the best q toward lower values for the asymmetrical band-pass shaped functions. To examine this possibility, the MI with varying q values for neuron *a* was re-computed with artificially reduced rate information by including only the first 23 spikes (the mean discharge count for noise alone) from the stimulus onset for each noise-alone or tone-in-noise response. The resulted MI was plotted in Fig. 3-3*a* (dotted line). In comparison to the original MI that was computed with all recorded spikes, the curve shifted to the right (towards higher q values).

The bias toward smaller q values with the presence of rate change can also cause changes in best q at different noise levels. Figure 3-5*A* re-plotted the MI of a chopper at 30 and 40 dB SPL noise spectrum level from the population results (Fig. 3-4*B*, third row, fourth column). The best temporal resolution was higher at 40 dB SPL than at 30 dB SPL noise spectrum level. However, when the same strategy was used to reduce the rate information, as shown in Fig. 3-5*B*, the best temporal resolution did not vary across noise level. Therefore, the best temporal resolution will not be a focus for further exploration in this study.
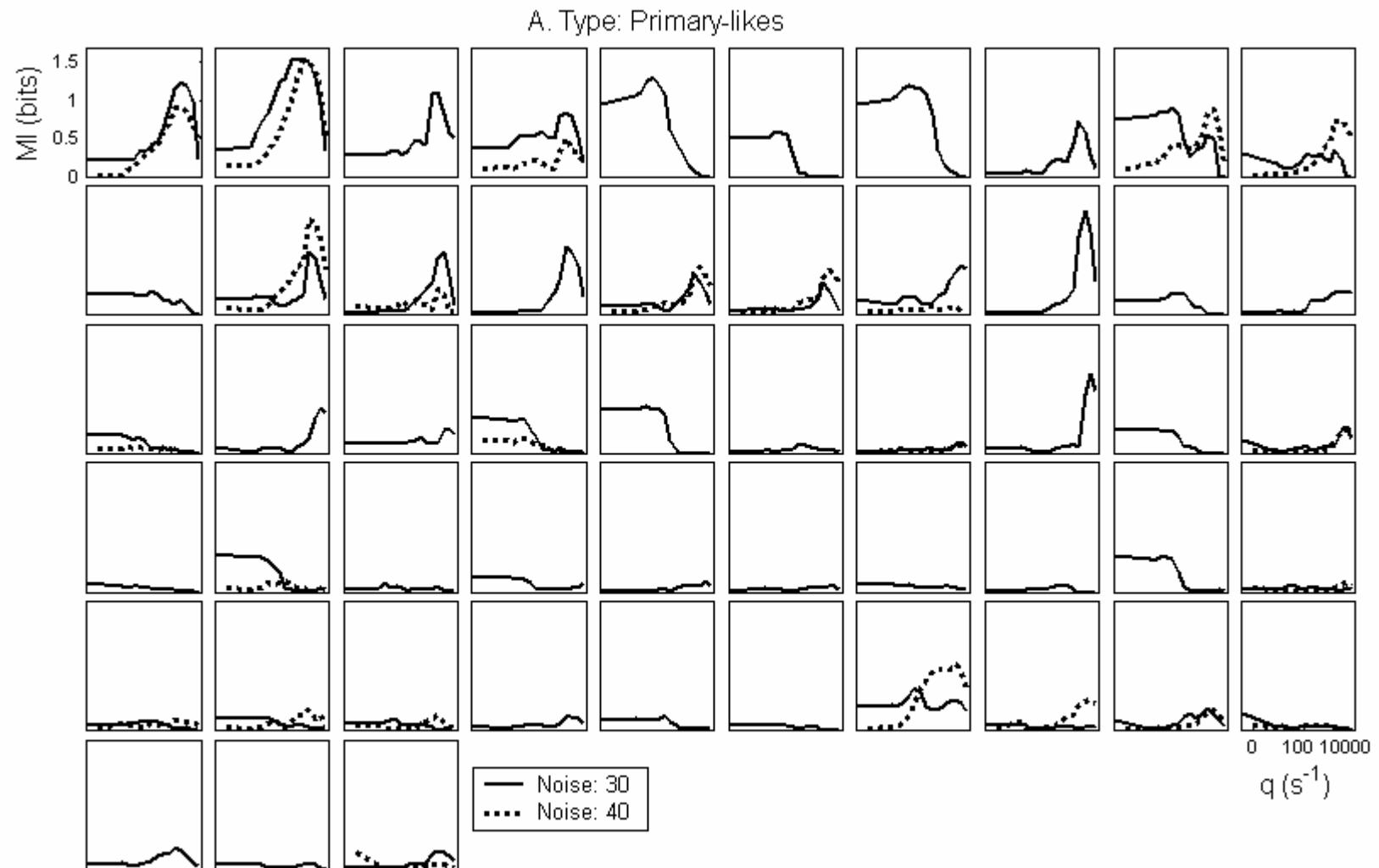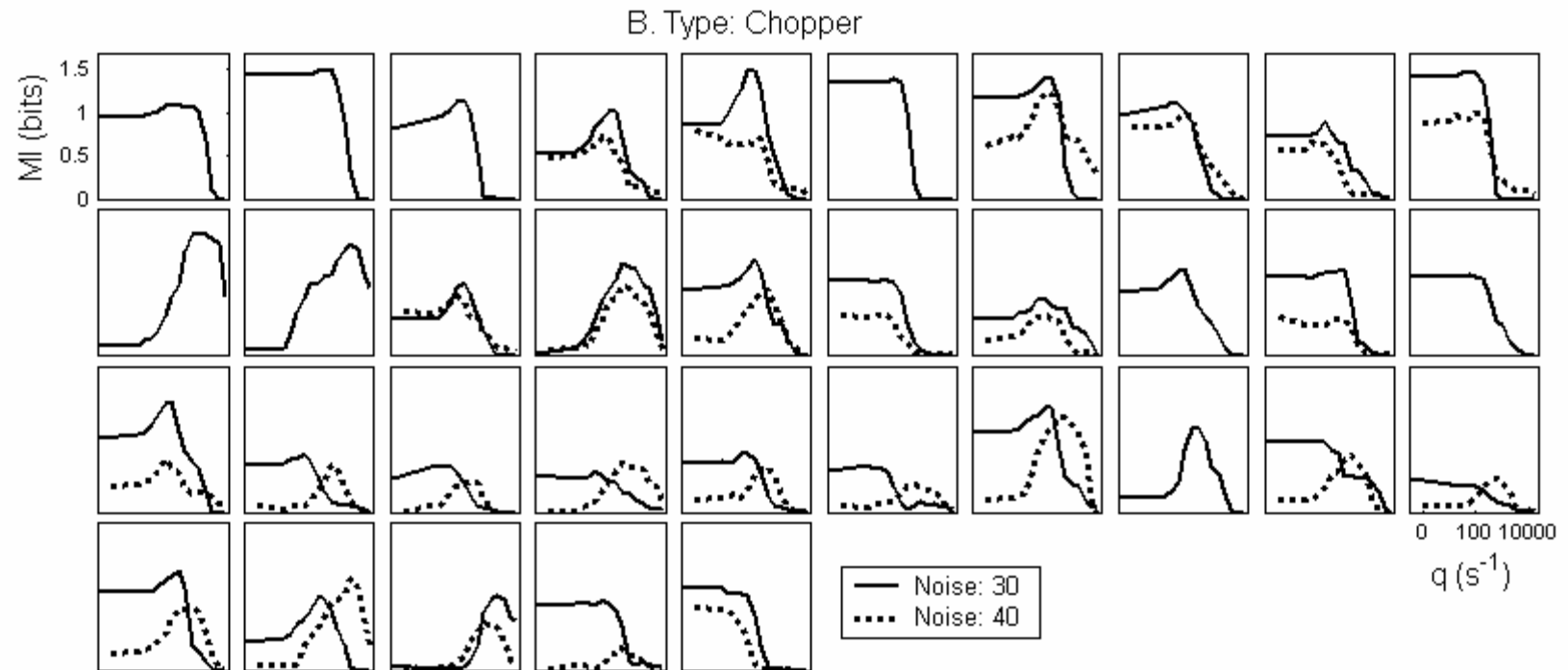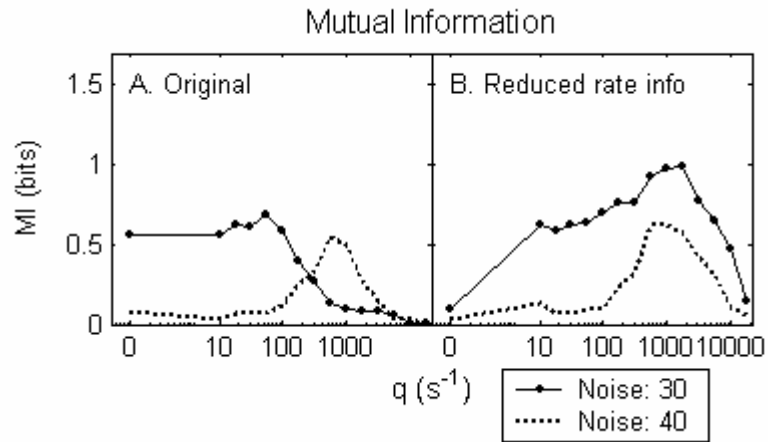
Fig. 3-5 Mutual information (MI) based on spike-time distances of tone-in-noise responses with varying q at different noise spectrum levels. *A*, MI based on all spikes recorded. *B*, MI with reduced average-rate information (the number of spikes in each repetition for noise alone and noise plus tones was no more than the mean number of spikes for noise alone). Solid lines, 30 dB SPL spectrum level noise. Dotted lines, 40 dB SPL spectrum level noise. G315u20. CF = 1579 Hz. Chopper.

b. Maximum mutual information

In Fig. 3-4 (population results), neurons are arranged with increasing CF for each response type. In general, the maximum MI decreased substantially with CF for primary-likes (Fig. 3-4*A*), but only slightly for choppers (Fig. 3-4*B*). This trend can be better visualized in Fig. 3-6, where the peak MI is plotted as a function of CF. The maximum MI for choppers was generally higher than that of primary-likes and unusual neurons at all measured CFs. Victor and Purpura (1996) illustrated that discharge regularity, measured by the coefficient of variation (CV), can have a large effect on coding efficiency based on either average rate or absolute spike times. In other words, the absolute spike times are more meaningful when inter-spike intervals vary less. Figure 3-7 shows the CV for each neuron in response to noise alone (CV is the standard deviation divided by the mean of inter-spike intervals). Although some choppers and unusual neurons showed lower CV (higher regularity) than primary likes, which was consistent with larger MI, the discharge regularity was generally uncorrelated to the maximum MI. This observation also held when the CV was calculated using tone-plus-noise responses.

Chapter II showed that detection performance based on synchronization to tone frequency was worse at mid and high CFs. Figure 3-8 shows the MI based on synchronization to tone frequency vs. CF. The decreased MI based on synchronization indeed seemed to resemble the maximum MI based on spike-time distance. However, when individual neurons were considered, a significant correlation was not found between these two measures. Figure 3-9 shows the maximum MI plotted against the MI based on synchronization. In fact, the MI based on synchronization was higher than the maximum MI based on spike-time distance for 72% and 63% of primary-likes at 30 and
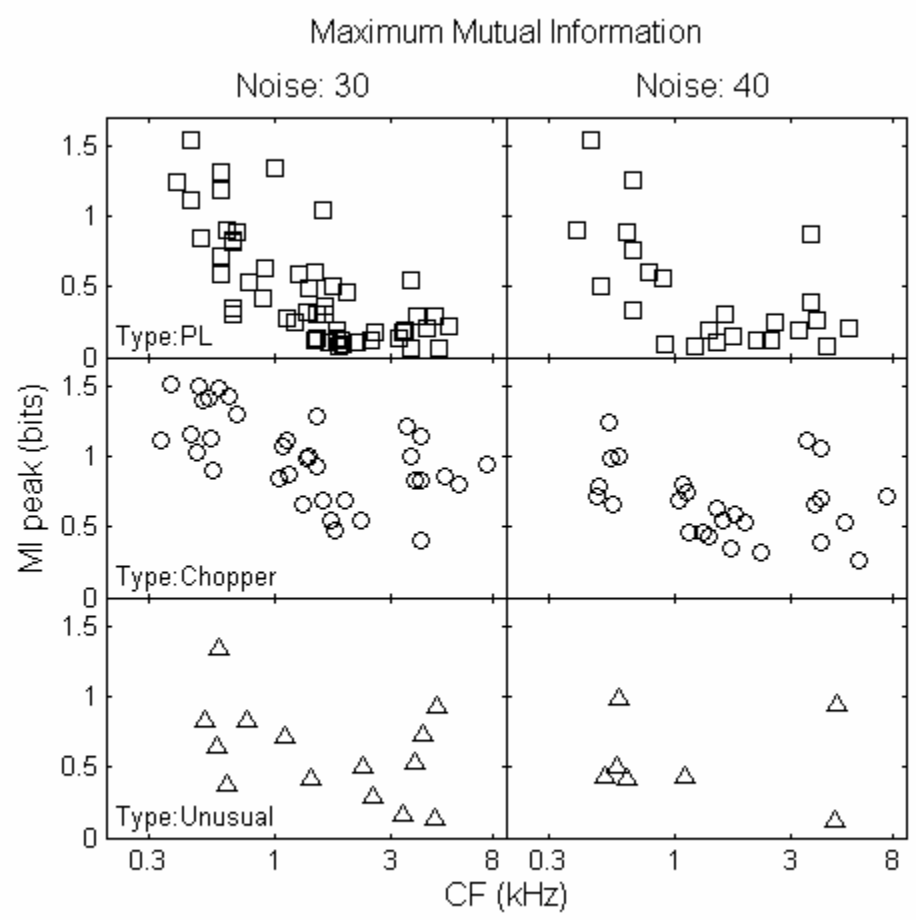
Fig. 3-6 Maximum mutual information (MI) based on spike-time distances of tone-in-noise responses vs. neuron CF. *Left* columns, 30 dB SPL spectrum level noise. *Right* columns, 40 dB SPL spectrum level noise.
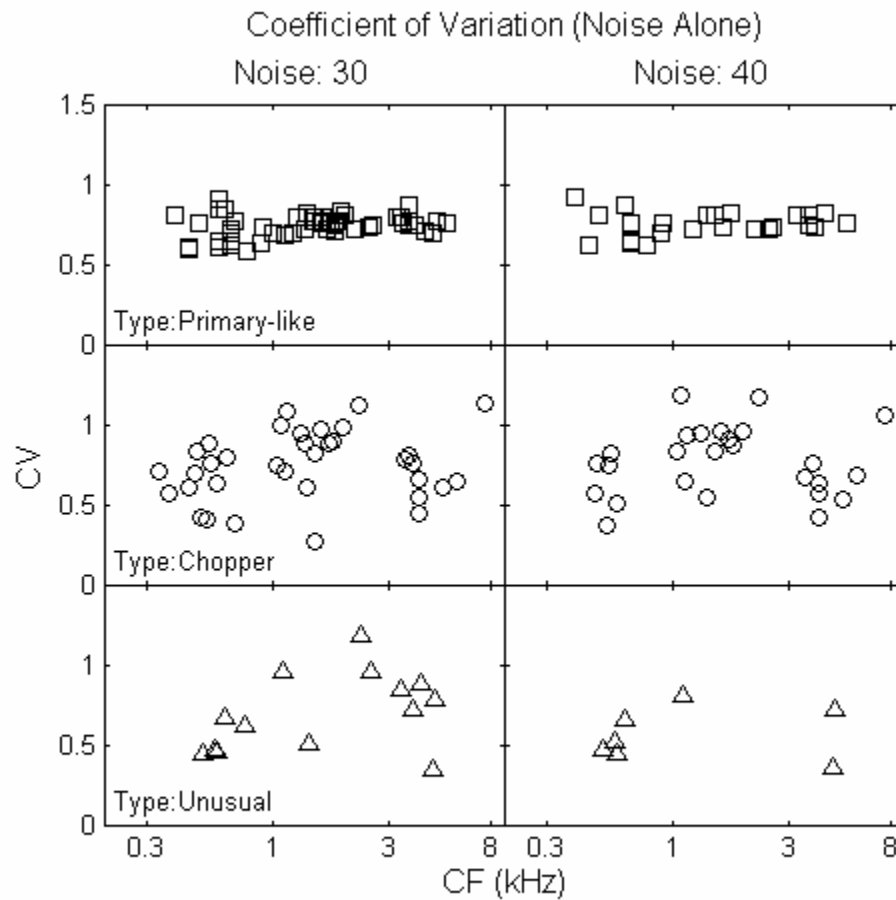
Fig. 3-7 Coefficient of variation (CV) calculated from noise-alone responses vs. neuron

CF. *Left* columns, 30 dB SPL spectrum level noise. *Right* columns, 40 dB SPL spectrum

level noise.
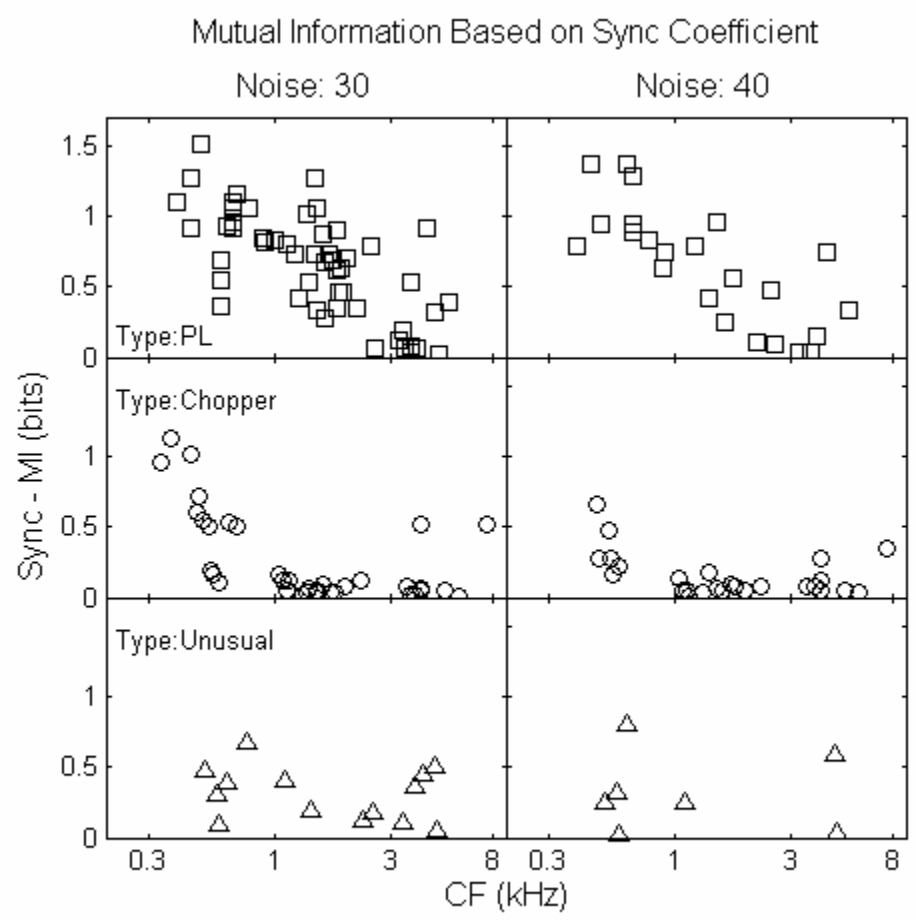
Fig. 3-8 Mutual information (MI) based on synchronization to tone frequency vs. neuron CF. To match the computation of MI based on spike-time distance, the synchronization was also computed based on 3 sets of neural responses (to noise-alone stimuli, the third highest tone level in tone-plus-noise stimuli, and the highest tone level in tone-plus-noise stimuli).
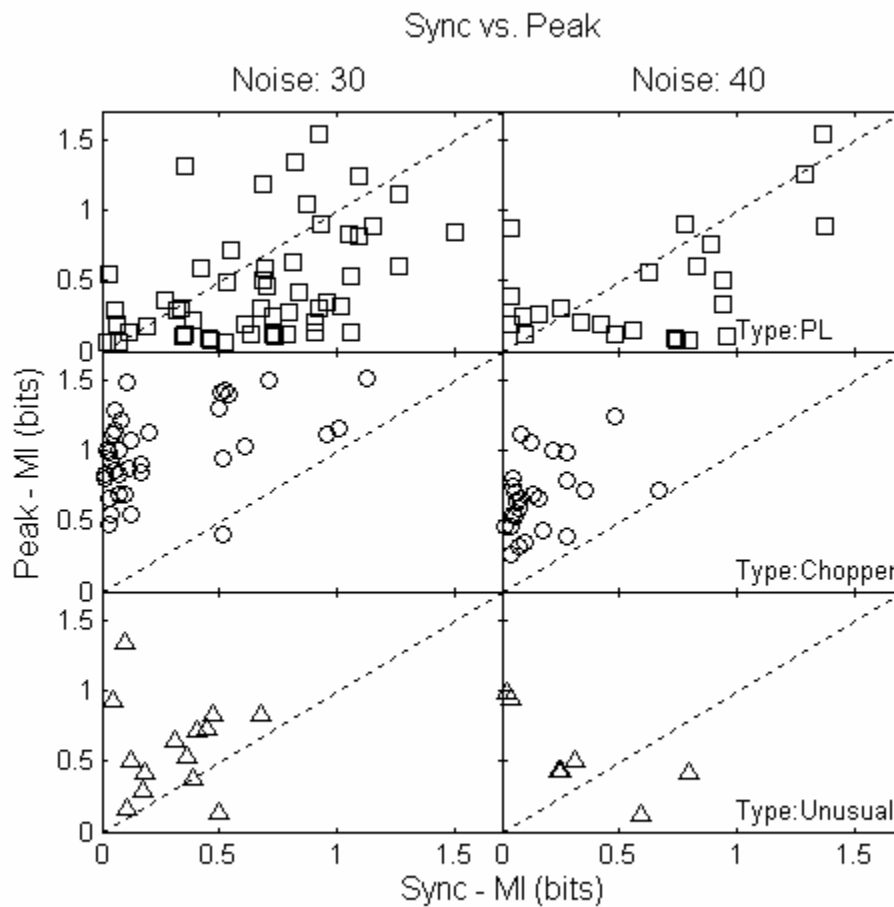
Fig. 3-9 Maximum mutual information (MI) based on spike-time distances vs. MI based on synchronization to tone frequency. *Left* columns, 30 dB SPL spectrum level noise. *Right* columns, 40 dB SPL spectrum level noise.

40 dB SPL noise spectrum level, respectively (the maximum MI was sometimes achieved with average rate information; if only timing information was considered, the maximum MI would be even lower).

In summary, absolute spike times of choppers carried more useful information for detection of tones in noise than primary-likes, and the spike-distance metric was found to be generally unrelated to other types of temporal information.

c. Average rate vs. timing

Figure 3-4 shows that for each type of AVCN neuron, some carried average-rate information (low-pass shaped), some carried spike-timing information (symmetrical band-pass shaped), and some carried both (asymmetrical band-pass shaped). Note that when the noise spectrum level increased from 30 (solid lines) to 40 (dotted lines) dB SPL, declined rate performance and improved spike-timing performance as the MI change from low-pass or asymmetrical band-pass shape into symmetrical band-pass shape was observed for 36% of units. Figure 3-10 plots the maximum MI against the MI based on average rate. Symbols on the diagonals indicated that the best coding for detection of tones in noise was average-rate coding, and symbols above the diagonals indicated that the best coding for detection of tones in noise was spike-timing coding. When noise level increased, the symbols generally moved away from the diagonals. This observation suggested that when the average rate was saturated by high-level noise, detection information was more likely to be carried by absolute spike times.
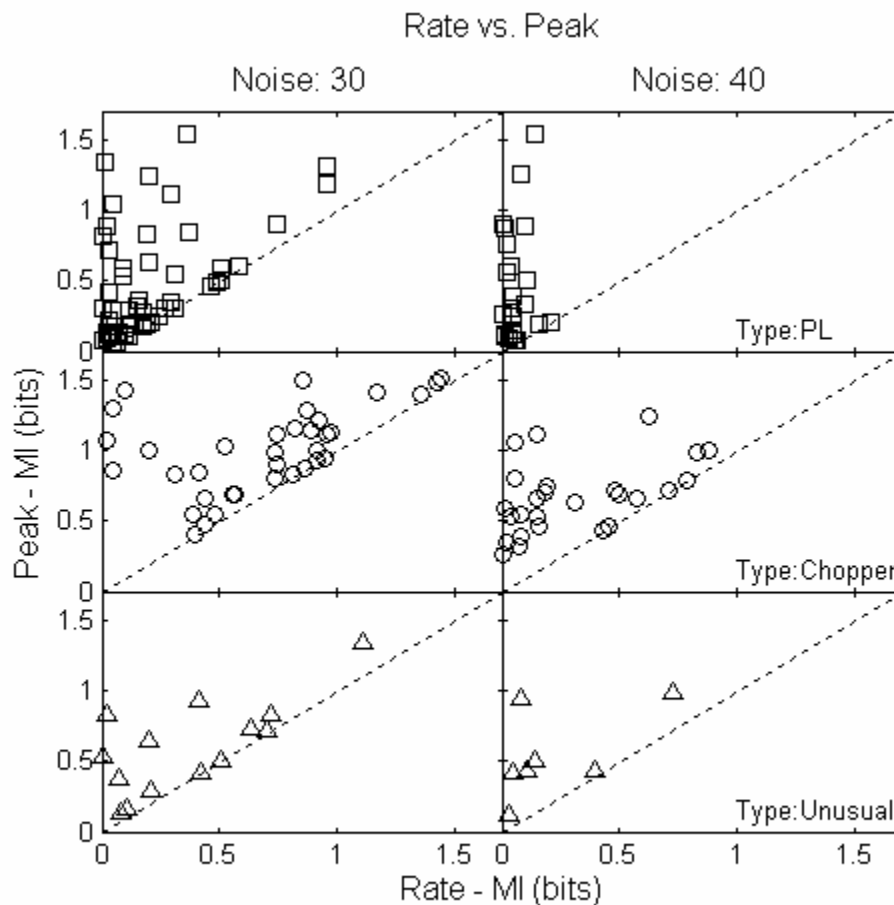
Fig. 3-10 Maximum mutual information (MI) based on spike-time distances vs. MI for average-rate coding (MI at q = 0). *Left* columns, 30 dB SPL spectrum level noise. *Right* columns, 40 dB SPL spectrum level noise.

3.4   Discussion

3.4.1   Correlation index

As stated in Chapter II, to date no physiological mechanism has been discovered to use the information carried by phase locking to tones. Joris et al. (1995) shows that the correlation index, which can be implemented by relatively simple neural mechanisms, represented the synchronization to tone frequency for neural responses to pure tones. However, this study showed that in the presence of broadband noise, the correlation index decreased with tone level for the majority of AVCN neurons, even when synchronization to tone frequency increased with tone level for some neurons.

This study showed that the correlation index changed with tone level in a way similar to the temporal correlation metric. The detection-performance difference between the correlation index and temporal reliability was not surprising, considering the different computational methods and statistical tests used for these two metrics. The correlation index is more feasible than temporal reliability, since coincidence detection is a simpler neural mechanism than correlation. Nevertheless, it is still unclear what mechanism could be used to normalize the coincidence count by average discharge rate (Eqn. 3-1). This normalization is critical for detection of tones in noise because simulations without the normalization showed that coincidence detection was more sensitive to the change in average rate than to spike-timing coincidence (Chapter II, Discussion).

3.4.2   Spike-distance metric vs. other temporal metrics

Temporal information carried by spike times can exist in different formats. This study divided all the tested temporal metrics for detection of tones in noise into two categories, a relative-spike-time category and an absolute-spike-time category. Note that the "absolute" spike time does not necessarily refer to "precise" spike time; different temporal resolutions can be achieved by temporal smoothing, binning or varying the cost factor for moving spikes. Rather, by absolute spike timing we refer to the timing of spikes with respect to stimulus onset.

The first category included the synchronization to tone frequency and PSTH fluctuation metrics. We hypothesized that PSTH fluctuation was mainly caused by locking to the stimulus envelope. Strictly speaking, however, when the stimulus envelope changes with time, an accurate measure of locking to the envelope will be related to absolute spike times, which is not simply the PSTH fluctuation (spike timing in response to two stimuli with completely different envelopes may have the same PSTH fluctuation). Therefore, it should be noted that the first category should not be interpreted as synchronization to fine structure and envelope.

The second category included temporal correlation, temporal reliability, correlation index, and spike-distance metric. The degree of the dependence on absolute spike times of each of these metrics varies. The spike-distance metric is mostly strongly related to absolute spike times, since spike trains are directly compared to each other, both in response to the same stimulus and across different stimuli. Temporal correlation is less dependent on absolute spike times for two reasons. First, comparison is made between PSTHs, rather than individual spike trains. Second, only variation to noise-alone

stimuli was included as a baseline to determine significant changes caused by addition of tones to the noise, and variation in responses to tone-plus-noise stimuli was not considered. Temporal reliability and correlation index only depend on absolute spike times in response to the same stimulus. How absolute spike times change across stimuli was not included in these metrics.

No direct relationship was found between the results for the spike-distance metric and for the other temporal metrics in either category. Different types of neurons carry different amounts of temporal information with absolute spike times. This study showed that information carried by spike times and average rate decreased dramatically with increasing CF for primary-likes, but only slightly for other types of neurons. This decreasing trend with CF for primary-likes was not observed for any of the other temporal metrics (Fig. 2-6) except synchronization to tone frequency, while a closer examination of the relationship between spike-time distance and synchronization to tone frequency showed no significant correlation for individual neurons. In fact, most primary-like neurons showed better detection performance based on synchronization to tone frequency than on the spike-distance metric.

3.4.3 Best temporal resolution

The present study showed that the best temporal resolution, determined by q, can be biased to low values by variations in average rate. The bias was reduced by including only a constant number of spikes beginning at stimulus onset. However, this approach resulted in a loss of information carried by the spikes that were removed. More importantly, the spike trains were effectively responses to stimuli with different

durations. The alternative strategy of equalizing rates by keeping stimulus duration the same and selectively removing spikes throughout the duration of the response would impair the temporal information. Therefore, to study the best temporal resolution based on absolute spike times, a better strategy to normalize the rate change must be designed.

3.4.4   Spike-distance metric vs. template

Templates with particular temporal features have been used in previous detection models (Dau et al., 1996; Breebaart et al., 2001). In these models, a temporal representation derived from neural responses for a single trial is compared to a template to make a decision, such as whether a tone is present or not. These methods involving comparisons to templates typically rely on absolute stimulus features or absolute spike times (based on instantaneous rate functions), depending on how the comparisons are made. Results based on the spike-distance metric in this study suggested that the use of a template method for a certain task may be appropriate for some types of neurons but not others. For example, a strategy for detection of tones in noise using a template is unlikely to yield a satisfactory result for primary-like neurons in the AVCN.

In summary, the spike-distance metric based on spike-timing precision is not an optimal metric for evaluating temporal information. For AVCN neurons, information useful for detection is more likely to be carried by features that are not anchored in time or by other forms of information that are less strictly dependent on absolute spike times (i.e., temporal reliability and correlation index). Future studies should examine these issues for neurons at other auditory levels and for other types of auditory tasks.

Chapter IV

Influence of Inhibitory Inputs: I. Responses to Pure Tones

Abstract

Anatomical and physiological studies have shown that AVCN neurons receive glycinergic and GABAergic inhibitory inputs, which primarily affect on-CF responses. The effects of inhibition on the temporal responses of target neurons have not been fully tested, which limits the understanding of the functional role of inhibition. In this chapter, changes in responses to pure tones of AVCN neurons by blocking glycinergic and GABAergic inhibition are analyzed in both the frequency and temporal domains for different types of neuron and compared to previous iontophoretic and modeling studies. Sustained and slowly adapting choppers showed increased regularity throughout the response duration after blocking inhibition, whereas most transient choppers showed increased regularity in the early part of the response. The first-spike latency decreased for the majority of AVCN neurons. This decrease was more than 0.8 msec for 34% of primary-likes and unusual neurons.

4.1   Introduction

4.1.1   General introduction

The CN sends major inputs to higher auditory levels; therefore, understanding the response properties and information-processing mechanisms of CN neurons can play a critical role in exploring higher-level neurons. The understanding of CN neurons would be straightforward if these neurons only received excitatory inputs from auditory nerve fibers (ANFs), because the characteristics of ANFs have been extensively studied. Established models of ANFs (Giguere and Woodland, 1994; Robert and Eriksson, 1999; Zhang et al., 2001; Zilany and Bruce, 2006) provide useful tools to simulate responses of CN neurons caused by excitatory ANF inputs by varying different parameters, such as the number of fiber inputs, the CF and spontaneous rate of each input, and the strength of each input with respect to the discharge threshold of the postsynaptic model neuron (Bank and Sachs, 1991; Hewitt et al., 1991; Rothman et al., 1993). However, it is difficult to simulate inhibitory inputs to CN cells because the source of inhibition remains unclear for specific neurons or neuron types in the CN, although anatomical studies have demonstrated particular inhibitory projections from one area to another (see below).

If a neuron receives inhibitory inputs that are strong enough to alter its response characteristics, these inputs can be particularly meaningful and powerful since they may convey information from neurons at the same level or from higher levels, which allows local circuits or descending mechanisms. Therefore, various anatomical and physiological studies have been done to identify the source of inhibitory inputs and to study the characteristics of inhibitory inputs and how they affect the target neuron's responses, directly or indirectly.

4.1.2   Anatomical studies

Early anatomical evidence of the presence of inhibitory inputs received by AVCN neurons was the finding of synaptic terminals that contain flattened or pleomorphic vesicles (Cant and Morest, 1979; Cant, 1981), in contrast with the spherical vesicles associated with ANF endings (Lenn and Reese, 1966). The flattened vesicles are associated with glycinergic inhibition in the AVCN (Altschuler et al., 1986; Wenthold et al., 1988). The pleomorphic vesicles are associated with GABAergic inhibition for bushy cells (Cant and Morest, 1979; Saint Marie et al., 1989), and are associated with glycinergic inhibition for some PVCN stellate cells. All principle cell types in the AVCN are stained with glycine (Wenthold et al., 1988) and GABA (Saint Marie et al., 1989), although the distribution on cell bodies vs. dendrites and the density of the endings vary across neuron types. Note that the GABAergic inhibition described here only refers to $GABA_A$ receptor mediated inhibition, not $GABA_B$, although both are present in the VCN (Altschuler et al., 1993). Ebert and Ostwald (1995a) report that injecting $GABA_A$ receptor antagonist muscimol had significant effects on neurons that responded to GABA injection, while injecting $GABA_B$-receptor antagonist baclofen on the same neurons showed small effects that were not consistent with the GABA effect.

By making horseradish peroxidase (HRP) injections in the AVCN, Wickesberg and Oertel (1988) found frequency-specific connections from the dorsal cochlear nucleus (DCN) to the AVCN and also a local circuit within the AVCN. The DCN interneurons were confirmed to be tuberculoventral/vertical neurons (Wickesberg and Oertel, 1990; for review, see Oertel and Wickesberg, 1993). D-stellate neurons, located in the

posteroventral cochlear nucleus (PVCN) and AVCN, project glycinergic inputs to the AVCN, PVCN and DCN (Smith and Rhode, 1989; Arnott et al., 2004). Yet there is no anatomical evidence showing that D-stellate cells project to a specific cell type in the AVCN.

A third source of glycinergic inhibition that has not raised as much attention as the above two sources is the descending input from the superior olivary complex (SOC). The lack of attention to this input may be partly due to the difficulty of studying these inputs in brain-slice preparations. A study in guinea pig using retrograde labelling combined with immunocytochemistry reports glycinergic projections from the lateral (LNTB) and ventral (VNTB) nuclei of the trapezoid body and the dorsal periolivary nucleus (DPO) to the CN, and most of the glycinergic projections are ipsilateral (Ostapoff et al., 1997). A particularly interesting finding of that study is the reciprocal connection between the CN and the posteroventral periolivary nucleus (PVPO). The only known input to the PVPO is an ascending projection from the CN, and the only known output of the PVPO is the descending projection to the same area of the CN (guinea pig: Thompson and Schofield, 2000).

There are also commissural glycinergic projections from the contralateral CN to the ipsilateral CN identified by anatomical (Wenthold, 1987) and physiological (Babalian et al., 2002) studies. Using the whole-brain preparation, Babalian et al. (2002) show that 63% of recorded CN neurons, including bushy and stellate cells, received commissural inhibition. In the present study, the commissural inhibition was not considered to be a major source of glycinergic inhibitory activity since no sound was delivered to the contralateral ear in these experiments. If an inhibitory neuron were spontaneously active,

it could provide tonic inhibition. However, Wenthold (1987) shows that neurons in the contralateral CN with commissural projections are large stellate cells, which usually have low or medium spontaneous activity (Blackburn and Sachs, 1989; Smith and Rhode, 1989).

Compared to glycinergic inhibition, sources of GABAergic inhibition to the AVCN are less clear. Although there are GABAergic inhibitory interneurons located in the DCN, no connections between these neurons and the VCN have been found. Golgi cells in the superficial granule cell domain are GABAergic (Kolston et al., 1992). These cells do not project to the VCN (but rather to regions overlying the VCN); however, it is likely that some AVCN neurons, such as T-stellate cells, send distal dendrites that receive inputs from these cells (Ferragamo et al., 1998). However, the effect of inhibition is not expected to be strong when the inputs synapse on the distal dendrites of the target neurons, which is confirmed by the fact that GABAergic inhibitory post-synaptic potentials (IPSPs) are insignificant during brain-slice recording (Oertel, 1983; Ferragamo et al., 1998), in which the GABAergic inputs from outside the CN are absent.

The major source of GABAergic inhibition is presumably the descending projection from the SOC. Most of these GABAergic neurons are bilaterally located in the VNTB (Ostapoff et al., 1997). Since neurons that project bilaterally to the CN also receive descending inputs from the inferior colliculus (IC), descending pathways from high auditory levels to the CN can be formed (Schofield and Cant, 1999). Some of these bilateral inputs from the SOC may also be glycinergic (Schofield and Cant, 1999).

4.1.3   *In vitro* physiological studies

In vitro intracellular studies use the presence of IPSPs created by electrical or chemical stimulation of ANFs or other parts of the CN as evidence of inhibitory inputs. Note that in these brain-slice preparations inhibitory sources from outside the CN are removed. In Oertel (1983), IPSPs were observed with delays of 1.2 msec or longer for both bushy and stellate cells (the latency of EPSPs was approximately 0.7 msec). These late IPSPs were further confirmed to be mediated by glycinergic inhibition (Wu and Oertel, 1986; Wickesberg and Oertel, 1990), rather than GABAergic inhibition. Using strong electrical stimulation, trains of glycinergic late IPSPs caused by intrinsic inputs within the VCN are observed for VCN T-stellate cells (Ferragamo et al., 1998). These intrinsic inputs are believed to come from D-stellate cells, which respond to strong electrical stimulation with trains of EPSPs. Direct evidence of glycinergic projections from DCN tuberculoventral neurons to the AVCN was obtained by stimulating the DCN with glutamate to create IPSPs for AVCN bushy and stellate cells (Wickesberg and Oertel, 1990) and blocking the inhibition with glycine receptor antagonists. Because inhibitory sources from outside the CN are typically removed in the CN brain slice preparation, GABAergic inhibition from SOC cannot be studied with that approach.

4.1.4   *In vivo* physiological studies

Lateral inhibition is a basic mechanism found in visual (e.g., Ganz, 1964) and somatosensory (Von Bekesy, 1967) research, thus efforts have been made to identify "side-band" inhibition received by auditory neurons using off-CF tones. Due to the low spontaneous activity found for many AVCN neurons, some baseline activity has to be

created to exhibit side-band suppression. Martin and Dickson (1983) iontophoretically inject excitatory amino acid to generate some baseline activity, and then detect side-band inhibition with off-CF tones. Rhode and Greenberg (1994) use masked response areas to reveal the presence of inhibition when adding an off-CF tone to broadband noise decreases the neural responses. These findings support the idea of lateral suppression and inhibition. However, results derived by tone suppression are not direct measures of the frequency response of inhibition. In the presence of strong excitation at CF, the effect of on-CF inhibition may not be clear. Moreover, some inhibitory interneurons (such as onset choppers) respond more strongly to broadband noise than to pure tones, which complicates the interpretation of masked response areas. (These methods might be more appropriate in studying neurons that are known to have non-overlapping excitatory and inhibitory areas.)

Paolini et al. (2005) use intracellular recording to examine the presence of IPSPs as evidence of inhibitory inputs for VCN choppers. The results suggested that the different degree of discharge regularity for transient and sustained choppers might originate from different amounts of overlap between excitatory and inhibitory areas. More specifically, transient choppers have inhibitory response areas that closely match excitatory areas, and this match results in declined firing rate and regularity compared to sustained choppers. Sustained choppers have more lateral inhibition that is less effective in altering the firing rate and regularity in response to CF tones (Paolini et al., 2005).

Compared to *in vitro* studies, *in vivo* intracellular recording allows the examination of inhibition from outside the CN in response to sound stimuli. However, due to the dominance of excitatory post-synaptic potentials (EPSPs) in response to sound

stimuli, the presence of IPSPs is hard to detect except after the tone offset. Moreover, for shunting inhibition that has a reversal potential close to the resting potential, IPSPs might not be detectible. This technique also cannot discriminate glycinergic from GABAergic inhibition.

In comparison to the above methods, iontophoretically applying inhibitory receptor agonists or antagonists is a more direct test of the effect of inhibition. Caspary et al. (1979) test the effect of glycinergic and GABAergic inhibition on average rate and PSTHs of AVCN and DCN neurons; they injected the inhibitory receptor agonists, glycine and GABA, most frequently; the glycine receptor antagonist, strychnine, was also injected for a number of neurons. The major finding of Caspary et al. (1979) is that more neurons respond to glycine rather than GABA, and the spontaneous activity is more affected by inhibition than is the tone-evoked activity. A more detailed iontophoretic study using inhibitory receptor antagonists (Caspary et al., 1994) examined the effect of glycinergic and GABAergic inhibition on the frequency response area for AVCN choppers and primary-likes (including phase-locked units). The results agreed with findings in the PVCN (Palombi and Caspary, 1992) and the IC (Palombi and Caspary, 1996) that in contrast to the lateral inhibition found in visual and somatosensory systems, inhibition alters the maximum response or near-CF response for the majority of AVCN neurons. This finding is contradictory to the results based on masked response areas (Rhode and Greenberg, 1994). Because sustained choppers were not differentiated from transient choppers in Caspary et al. (1994), it is not clear whether this finding agrees or disagrees with Paolini's (2005) finding that sustained choppers receive lateral inhibition.

Besides the changes in the frequency response area during iontophoresis, changes in temporal responses to CF tones have also been studied. Ebert and Ostwald (1995a, b) iontophoretically apply GABA to VCN neurons. In general, they find that onset response is emphasized as inhibition reduces more of the sustained activity and even more of the spontaneous activity (the latter agrees with Caspary et al., 1979). They also observe changes in the chopping discharge pattern for 15 PVCN choppers and 4 AVCN choppers. The regularity of sustained choppers decreases the most during the later part of responses, and the regularity of transient choppers decreases the most during the early part of responses.

In addition to applying inhibitory receptor antagonists, Kopp-Scheinpflug et al. (2002) also record prepotentials to study pre-synaptic activity for AVCN neurons that receive large endbulb synaptic endings. The difference between post-synaptic and pre-synaptic responses decreases after blocking inhibition. Inhibition also accounts for the non-monoticity of the post-synaptic rate-level functions. Similar to the finding of Ebert and Ostwald (1995a), sustained activity is more affected by inhibition than onset activity, as measured by the "peak-to-sustained" ratio.

If onset activity were not effectively changed by inhibitory inputs, one would expect that the change in first-spike latency after blocking inhibition would be relatively small. In fact, the average value and variability of the first-spike latency is reduced after application of bicuculline (GABA receptor antagonist) for PVCN neurons (Palombi and Caspary, 1992).

In summary, extracellular experiments using the iontophoretic technique provide more details about the inhibitory inputs than intracellular recordings of IPSPs. However,

the intracellular study does have some advantages over the extracellular iontophoretic technique. The presence of IPSPs is direct evidence of inhibition, whereas in iontophoretic experiments there is always some uncertainty in determining whether an observed change of response is due to a drug effect or other factors (such as current effects).

4.1.5   The present study

The initial motivation for choosing the AVCN as the study focus was to perform a relatively complete test on the temporal responses of AVCN bushy cells, which are major ascending inputs to the binaural nuclei. At low and mid CFs, AVCN bushy cells generally show enhanced synchronization to tone frequency (Joris et al., 1994), which is reasonable since fine-timing information is critical for binaural localization and possibly for binaural masked detection. Most of the known inhibitory neurons, such as D-stellate cells and vertical cells, do not shown significant synchronization to tone frequency. Therefore, the presence of inhibitory inputs for bushy cells indicates that the function of bushy cells may not be solely to provide a faithful representation of stimulus fine structure.

As described above, some of the iontophoretic studies use inhibitory receptor agonists. Although the change of neural responses with enhanced inhibition does indicate some function of the inhibition, applying inhibitory receptor antagonists might generate more "meaningful" responses, i.e., the behavior of a neuron with only excitatory inputs. As pointed out by Ebert and Ostwald (1995b), the steady injection of agonists actually creates a source of tonic inhibition, which can be qualitatively different from sound-

evoked inhibition received by the target neuron. In contrast, applying inhibitory receptor antagonists removes the effect of inhibition only when the inhibition is active. Another reason to focus on inhibitory receptor antagonists was the observation of decreased activity for some neurons during iontophoretic injections, presumably caused by non-drug effects (e.g., a current effect). These effects make it difficult to interpret decreases in activity during iontophoresis. In contrast, increased neural activity elicited by inhibitory receptor antagonists appears to be more reliable for indicating drug effects.

4.2   Methods

4.2.1   Sound stimuli

Sound stimuli were created digitally with Matlab, and converted to analog signals with a programmable Tucker Davis System (TDT) III. A plastic tube was coupled to the left ear meatus to deliver sound stimuli. Linear compensation of levels for frequencies from 70 Hz to 10 kHz was performed for each sound stimulus, based on a calibration table generated at the beginning of each experiment with an ER-7C probe microphone (Etymōtic Research). Units with CFs outside the range of 0.3 to 9 kHz were not studied.

Rate-level functions of short tones at CF (25-msec duration, repeated every 100 msec at several levels with a 10- or 15-dB step size) were most frequently used to monitor the iontophoretic effect on neural responses. One hundred repetitions were obtained at each tone level for the categorization of response types according to Blackburn and Sachs (1989) and for the study of temporal response details. The frequency response area was studied by varying the frequency and level of the 25-msec tones for 10 repetitions. For each repetition, the tone level increased with a 15- or 20-dB

step size; at each tone level, the tone frequency swept from below CF to above CF (e.g., 2 octaves below and 1 octaves above) in half-octave steps unless limited by the frequency range of the calibration. Three or 4 tone levels were obtained for each unit, with 1 level slightly above threshold, 1 level at 70 or 80 dB SPL, and 1 or 2 intermediate levels. Both on-CF and off-CF tones described above had 5-msec cosine-squared ramps.

4.2.2   Recording and iontophoresis

Electrical signals were amplified by an AC Preamplifier (GRASS P55) through a High Impedance Input Module (GRASS HZP). A voltage-crossing criterion was used to discriminate spikes from background noise, and the times of the peaks of spikes were marked as spike times. Sub-microsecond accuracy was achieved for discharge-time recordings. Single-neuron extracellular recordings and iontophoresis were obtained with 6-barrel piggyback electrodes (Havey and Caspary, 1980). The recording electrode (15 – 50 MΩ) protruded 10–25 μm from the injecting barrels. The tip of the injecting multi-barrel electrode was 10–20 μm in diameter. Each injecting barrel contained one of the following chemicals: strychnine-HCl (10–20 mM, PH = 3–3.5), glycine receptor antagonist; bicuculline methiodide (10 mM, pH = 3–3.5), GABA$_A$ receptor antagonist; gabazine (3–5 mM, pH = 3–3.5), GABA$_A$ receptor antagonist; glycine (500 mM, pH = 3.5–4); γ-aminobutyric acid (GABA, 500 mM, pH = 4–4.5). Injecting currents (20–35 nA per barrel; one or two barrels with the same chemical were used at a time) were generated and monitored by a 4-channel current generator (NeuroPhore BH-2, Harvard Apparatus); otherwise, a negative holding current (-15 nA) was maintained for each barrel. (Lower holding currents were used when the barrel was partially plugged as indicated by

impedance measurements.) To avoid the building up of net charges, a balancing barrel (the center barrel of the piggyback electrode) continuously injected a current that was equal to the sum of the currents in all the other barrels with inverse polarity. The balancing barrel and the attached recording barrel were filled with 1 M sodium acetate (Kopp-Scheinflug et al., 2002). The use of sodium was to be consistent with extracellular ionic concentrations; the use of acetate was to reduce diffusion and transport number during application of hyperpolarizing currents (Muller, 1992). Occasionally, one of the injecting barrels was filled with 1 M sodium acetate as a control barrel to test the possible effect of electrical current alone.

The multi-barrel electrode was advanced by a manual micropositioner through the dura and cerebellum to the AVCN. Each penetration was constrained within a small range of stereotaxic angles, which was determined previously when collecting data for Chapter II. After recording from a unit, the electrode was moved by at least 150 μm and no recording was made from another neuron until at least 30 min after a previous injection.

4.2.3   Data analysis

Neuron response types were categorized based on Blackburn and Sachs (1989). To simplify the results, three basic classes were used, including primary-likes and primary-like-with-notches, choppers (including different chopping types), and

unusual/onset units[1], unless differences were observed within a class. More detailed

classification was used when necessary. For the classification of choppers, the first and

second "spike per peak" values were 0.95 – 1.05 and 0.92 – 1.05, respectively (value 1.0

means one spike in each chopping peak for every repetition). Neurons that showed clear

chopping patterns but failed this criterion were classified as unusual cells. However, the

single-neuron extracellular recordings cannot guarantee recordings of every spike,

especially at high tone levels (70 or 80 dB SPL) that usually caused decreased spike

amplitudes. The above criterion was slightly broadened for 3 units at high tone levels as

long as these units had spike-per-peak values within the rigid criterion at mid tone levels.

Spontaneous rate (SR) and threshold were computed by an automated threshold

tuning curve program (Liberman, 1978), as described in Chapter II. The SR of some units

was found to change substantially during the experiment; however, since the effect of

inhibition on SR was not a major focus of this study, the threshold tuning curve was not

monitored during iontophoretic injections, as was the rate-level function. Therefore, the

SR was computed based on spikes during 50 to 100 msec after stimulus onset (the sound-

evoked response was always shorter than 40 msec) from responses collected at the lowest

tone level (this level was always below threshold) for the rate-level function. The SR

computed this way basically agreed with the SR computed from the tuning curve

program.

First-spike latency (FSL) was difficult to measure due to the existence of

spontaneous activity. Young et al. (1988) set a cursor by hand at the beginning of sound-

---

[1] Some studies use "phase-locked" as a neuron type for low frequency units that cannot be clearly classified as primary-likes or choppers due to the strong phase locking to tone frequency. Here this class was not included since most units had CFs around 1 to 2 kHz.

evoked activity by examining the post-stimulus time histogram (PSTH) for each response and discard all activity before the cursor. Chase (2007) provides a binless algorithm that was used here; this algorithm determines the starting time of the sound-evoked activity by computing the probability of an instantaneous firing rate that can or cannot be generated by spontaneous activity. Specifically, first the algorithm searches for the time when at least 5 spikes (combined across all stimulus repetitions) have occurred. Then the probability of generating a number of spikes in a certain time interval by spontaneous firing is calculated for a set of intervals between the present spike and each previous spike --- the shortest interval includes the previous 5 spikes, and the longest interval includes all previous spikes. When the minimum probability across different lengths of intervals is below a certain criterion (i.e., 10^{-6}), the starting time of tone-evoked activity is marked; otherwise, the time point moves to the next spike. The probability of observing at least n spikes in an interval of t_n is computed as

$$P_{t_n}(\geq n) = 1 - \sum_{m=0}^{n-1} \frac{(N\lambda t_n)^m e^{-N\lambda t_n}}{m!}$$ (Eqn. 4-1)

(Chase, 2007). λ is the spontaneous rate. N is the number of repetitions (N = 100 in the present study).

The starting time of sound-evoked activity derived from this algorithm is not strictly a minimum latency, since the accumulation of first spikes from several trials are required to detect a change of probability. Nor is it the mean FSL. In this study, the starting point was used to exclude spontaneous spikes that occurred before the sound-evoked response and the mean FSL was then computed based on the remaining spikes. It should be noted that some early spikes (the 5 earliest spikes across all repetitions) were always excluded, and thus a few sound-evoked spikes may be missed by this technique.

Although not a study focus, the response area was tested to provide a description of the inhibitory frequency tuning and for comparison to a previous study (Caspary et al., 1994). That study uses a z-score method to determine whether inhibition is on-CF vs. off-CF. Here a similar method was used by computing the d' using mean and standard deviations of firing rate at each frequency.

$$d' = \frac{M_1 - M_0}{\sqrt{(\sigma_1^2 + \sigma_0^2)/2}} \qquad \text{(Eqn. 4-2)}$$

M_1 and M_0 are the mean average rates across 10 repetitions at a certain frequency and sound level for injection and control, respectively. σ_1^2 and σ_0^2 are the estimated variances of the average rates for injection and control, respectively. The d' measures the significance of a rate increase caused by blocking inhibition. For a given sound level, the d' at the frequency with the maximum response (usually at CF, but sometimes shifted to frequencies lower than CF at high tone levels) was compared to the d' away from CF.

4.2.4 Drug-effect analysis

In the following text, "positive effect" (Caspary et al., 1994) will be used to refer to consistently increased neural responses to CF tones, based on the rate-level function that was frequently recorded during iontophoresis. "Drug effect" (Caspary et al., 1994) will be used to refer to an effect on neural responses that was presumably caused by the inhibitory receptor antagonists or agonists, rather than by other unknown factors (e.g., current injection, mechanical effects of the electrode on the neuron, or change in the pH).

A microscope with x100 amplification was used to examine the proximity of the injecting and recording barrels after recording. [This microscope was available after 9

positive-effect neurons (from experiments g340 – g 354) had already been studied.]

Before the introduction of the microscope, units without a positive effect were excluded

from this study unless the same penetration yielded other positive-effect neurons. In other

words, a unit that showed no change in rate was included only if a given electrode was

known to work properly. After the introduction of the microscope, units that showed

unchanged rate were counted as negative-effect units if one of the two following

conditions was met --- 1) the injecting and recording tips of the electrode remained close

to each other after the recording session, and 2) during the same penetration there were

other positive-effect units. If none of the two conditions was met, the unit was not

included in the results presented here.

In this study, a unit was considered to be a positive-effect unit only when it passed

the following two criteria. The first criterion was a significant increase of average rate (t

test, $p < 0.05$) for at least one super-threshold level (at lest 10 dB above threshold). In

other words, a significant rate increase for tone-evoked activity was required (issues with

the spontaneous rate will be discussed later). The second criterion was that the increase of

rate remained significant until the end of the injection and did not disappear immediately

after the injection was ended (it was common that the maximum effect occurred

sometime after the injection current was ended). Some units showed significantly

increased rate occasionally during the injection but the increase disappeared before or

right after the injection was ended; these units were considered to be negative-effect

units.

Recovery was indicated when the average discharge rate consistently decreased

by at least 10% of the maximum rate after the injection was ended. The recovery process

was highly variable across units and across inhibitory receptor antagonists. Possible

factors for this variability included the structure of the electrode (the distance between the

recording and injecting barrels), the location of the electrode with respect to the neuron,

the morphology of the neuron (especially the distribution of inhibitory input endings),

and the concentration of the drug. For units that did not show signs of recovery within the

holding time (between 3- min to 4 hr), the positive effects were still considered drug

effects as long as the above two criteria were met. Sometimes the positive effect

happened quickly after the beginning of injection, presumably due to a short distance

between the neuron and the injecting barrels. However, the positive effect was

maintained for a time period after the termination of injection (between tens of minutes to

several hours) except for one unit.

A *t*-test was used to test the significance of rate change in response to CF tones

after blocking inhibition, and the *t* values were compared across neuron types.

$$t = \frac{M_1 - M_0}{\sqrt{s_1^2 / N + s_0^2 / N}} \qquad \text{(Eqn. 4-3)}$$

M_1 and M_0 are the mean average rates across 100 repetitions in response to a CF tone at a

certain sound level for injection and control, respectively. s_1^2 and s_0^2 are the estimated

variances of the average rates for injection and control, respectively. N is the number of

repetitions (N = 100).

4.3   Results

4.3.1   General descriptions of positive effects and the recovery process

Data presented here were responses from 89 units in 38 gerbils. Table 4-1 gives a summary of units that showed positive or negative effects to inhibitory receptor antagonists, based on changes in the average discharge rate in response to CF tones after inhibitory receptor antagonists were injected. In general, 52 out of 89 neurons showed positive effects to inhibitory receptor antagonists for either glycine (21/59) or GABA (34/73) inhibition. There were 2 units (1 sustained chopper and 1 unusual) out of 12 units that showed positive effects to both types of inhibitory receptor antagonists. Here the 12 units referred to units that showed positive-effects and full recovery to one type of inhibitory receptor antagonist (glycinergic/GABAergic) and were then tested with another type of antagonist (GABAergic/glycinergic). Thirty out of 37 negative-effect units were tested with both types of inhibitory receptor antagonists, and the other 7 negative-effect units were only tested with one type of antagonist.

There were 29% to 47% of positive-effect units that showed recovery for different inhibitory receptor antagonists (Table 4-1). Although the percentage of neurons that showed full or partial recovery did not differ substantially for different antagonists (Table 4-1), it was commonly observed that bicuculline injection had a relatively quick and complete recovery process as compared to the other two antagonists.

As stated earlier, negative-effect units can also show significantly increased rate temporarily; however, the increased rate either disappeared before the injection was ended or immediately after the injection was ended (it will be shown below that the amount of rate increase for negative-effect units was smaller than that observed for

Table 4-1 Summary of positive and negative effect for all recorded neurons

	Cell Type	PL	PLN	Chp-S	Chp-T	Chp-SA	Unusual	Onset	Overall
Strychnine	N	25	3	8	5	8	9	1	59
	Positive Effect	**7**	**3**	**2**	**2**	**1**	**6**	**0**	**21 (35%)**
	>10% Recovery	**2**	**0**	**1**	**1**	**1**	**2**	**0**	**7 (33%)**
	↓ High Level (neg)	6	0	4	2	3	1	1	17 (28%)
	↑ High Level (neg)	8	0	1	1	5	2	0	17 (28%)
Bicuculline	N	15	0	3	3	3	2	1	27
	Positive Effect	**7**		**3**	**3**	**2**	**1**	**1**	**17 (63%)**
	>10% Recovery	**3**		**2**	**0**	**2**	**1**	**0**	**8 (47%)**
	↓ High Level (neg)	4		0	0	0	0	0	4 (15%)
	↑ High Level (neg)	3		0	0	1	0	0	4 (15%)
Gabazine	N	14	0	10	4	8	8	2	46
	Positive Effect	**4**		**3**	**1**	**2**	**5**	**2**	**17 (37%)**
	>10% Recovery	**2**		**1**	**1**	**1**	**0**	**0**	**5 (29%)**
	↓ High Level (neg)	4		3	1	2	5	1	16 (35%)
	↑ High Level (neg)	4		1	2	0	1	0	8 (17%)

↓ High Level (neg), negative-effect units with average rate decreased significantly at any levels 20 dB above threshold. ↑ High Level (neg), negative effect units with average rate increased significantly at any levels 20 dB above threshold.

positive-effect units). Among the 38 units that did not show a positive effect to strychnine, 17 showed significantly increased rate (but the increase was not persistent over time), and 17 showed significantly decreased rate (Table 4-1). Among the 39 units that did not show a positive effect to bicuculline or gabazine, 12 showed significantly increased rate (but the increase was not persistent over time), and 20 showed significantly decreased rate (Table 4-1).

For units that showed significantly decreased rate, it was unclear whether the cause was drug or non-drug effect (current effect, pH effect, etc). This decreased rate was observed in the same electrode penetration with units that showed positive effects for 14 units after blocking glycinergic inhibition and for 17 units after blocking GABAergic inhibition. Sometimes decreased rates were observed with electrodes that were found to have separated tips (the recording barrel tip was detached from the injecting barrels) under the microscope after the penetration; these units were excluded from the present study. To test the non-drug effects, currents were injected from the balancing barrel or one of the barrels filled with only sodium acetate (pH = 7) for 7 units. Two of the 7 units showed a rapid increase of rate after turning on the current. One unit recovered after the termination of injection, but another unit did not recover. Current was also injected from barrels filled with sodium acetate (pH = 3) for 1 unit, and the rate decreased significantly. In summary, the cause of decreased rates was uncertain.

Glycine and GABA (inhibitory receptor agonists) were only injected for 2 and 3 units, respectively. A chopper that showed a positive effect to bicuculline did not show changes to glycine (a strychnine injection was not available for this unit). An unusual unit that showed different positive effects to strychnine and bicuculline showed decreased rate

to glycine (this unit will be described in detail below). One primary-like and one chopper showed positive effects to bicuculline but negative effects to GABA. The last unit, a primary-like, did not show a change to strychnine, bicuculline or GABA.

4.3.2 Basic results for different neuron types

a. Primary-likes and primary-like-with-notches

Figures 4-1 and 4-2 show positive effects of two PLs to bicuculline and strychnine, respectively. The left three columns are responses to 100 repetitions of the 25-msec CF tones (rate-level functions, PSTHs, and inter-spike intervals vs. time). The PSTHs and interval plots were obtained at the highest tone level (70 or 80 dB SPL). The first unit showed a maximum change 61 min after the 15-min injection of bicuculline was ended, and the positive effect was highly reduced 166 min after the injection was ended. For the second unit, the maximum change occurred 108 min after the 54-min injection of strychnine. The unit became unavailable for recording soon after.

The rightmost column was the response area measured with 10 repetitions of 25-msec tones at different frequencies. The dark area represents positive change (rate increase after blocking inhibition). The inhibitory inputs had a broader response area than the excitatory inputs. Note that the SR also increased together with sound-evoked activity (Fig. 4-1, first column). To eliminate the effect of the change in SR on the response area, the SR was subtracted out from the sound-evoked responses (result not shown). These response areas based on driven rate were still broader with the inhibitory inputs. However, it was unclear whether the inhibitory inputs consisted of one source of responses with broad frequency tuning or several sources with slightly off-CF tuning but

Response to Bicuculline: PL
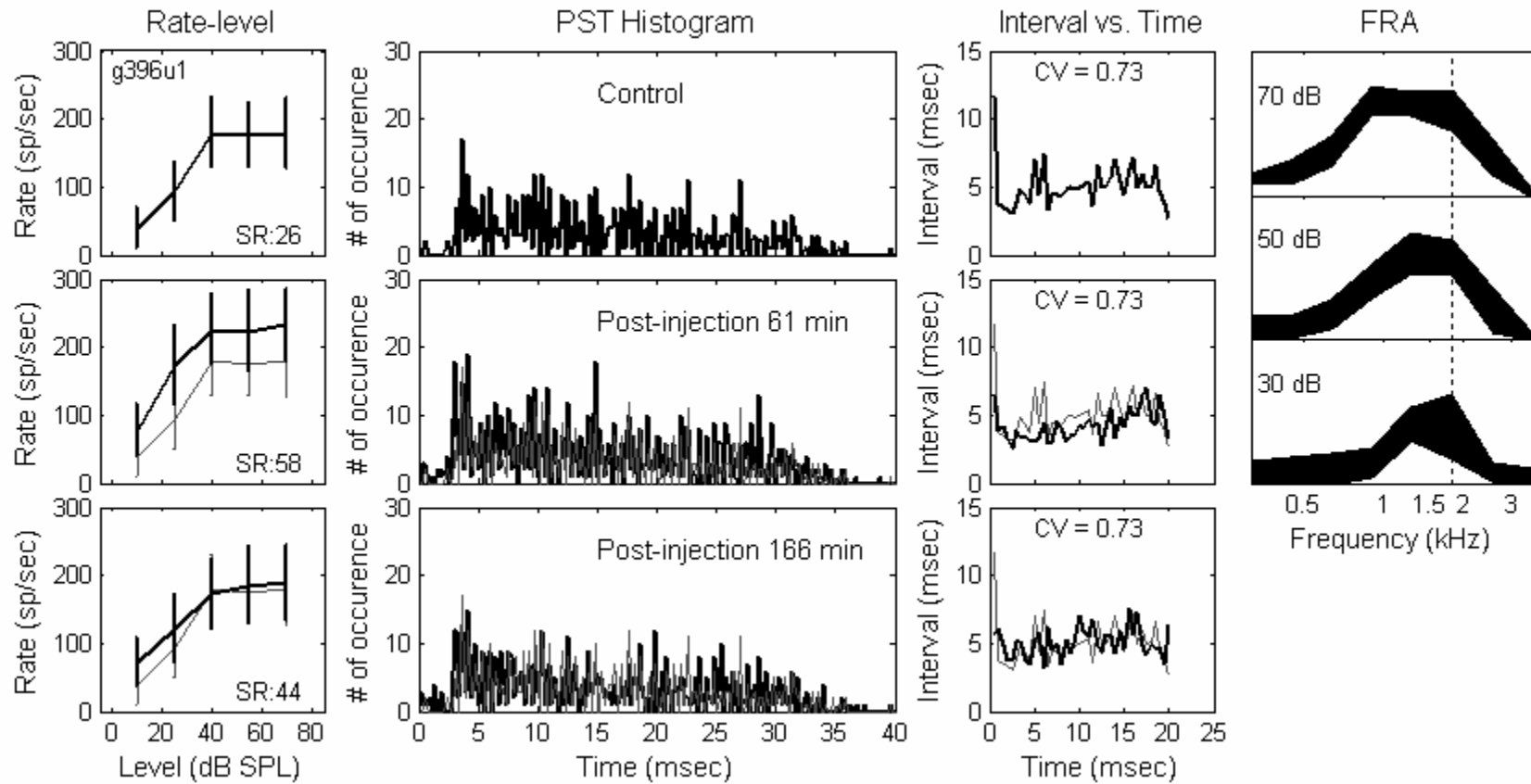
Fig. 4-1 Pure-tone responses of a PL unit (g396u1) before and after injection of bicuculline. Total duration of bicuculline injection was 15 min. First column, rate-level functions for CF tones (CF = 1808 Hz). The spontaneous rate (SR) was computed by averaging the discharge rate between 50 to 100 msec after stimulus onset. Second and third columns, PSTHs and mean inter-spike intervals over time in response to a 70 dB SPL tone at CF. In the first three columns, the first row plots responses before injection. The second and third rows plot responses after injection (thick lines), as well as responses before injection (thin lines) for comparison. Fourth column, frequency response area obtained with short tones at different frequencies and levels. The vertical dotted line marked the CF. Shaded areas indicate maximum average-rate increase during and after injection. CV, coefficient variation (Blackburn and Sachs, 1989).

Fig. 4-2 Same format as Fig. 4-1. PL, g342u4, total duration of strychnine injection was 54 min. CF = 1103 Hz.
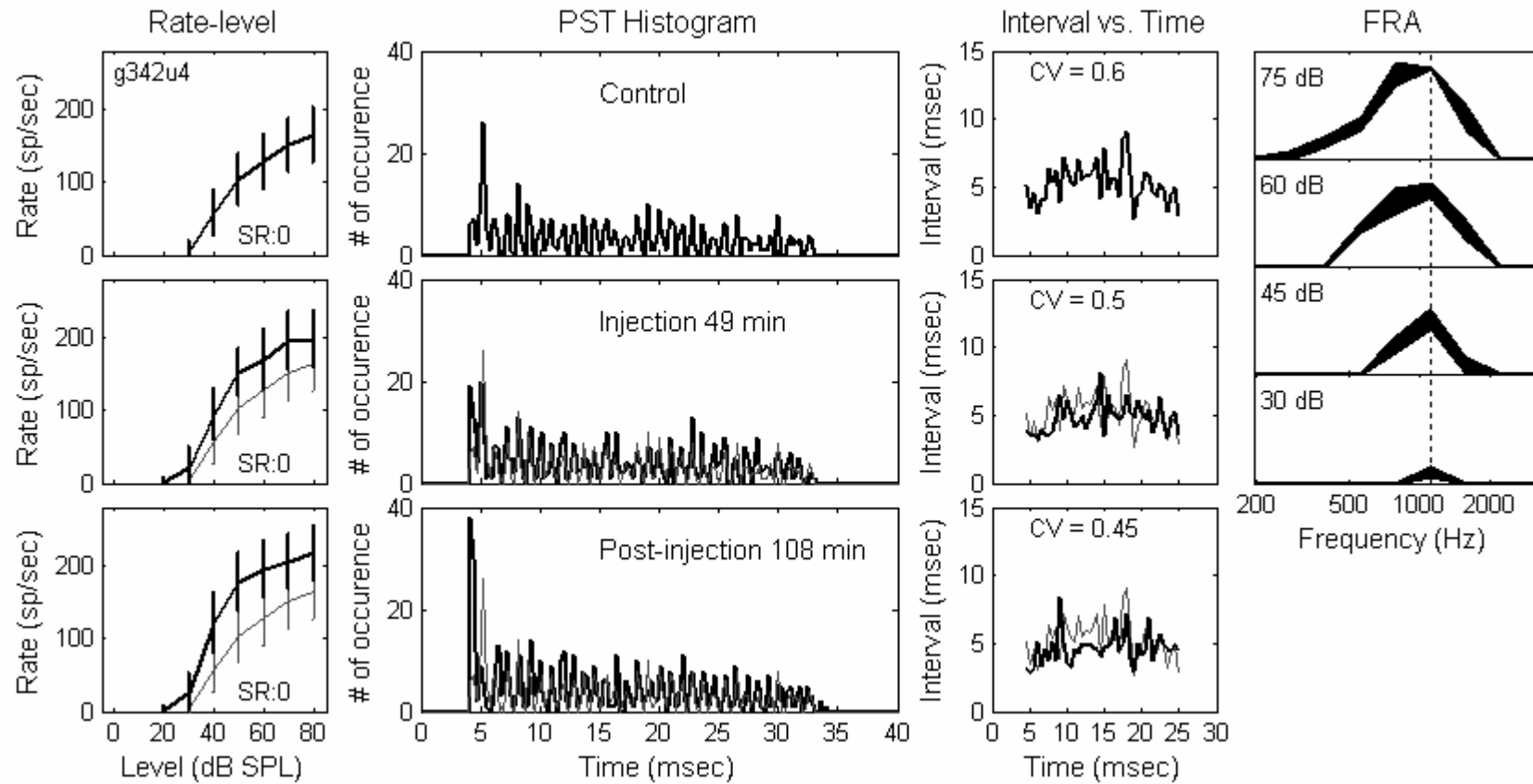
overlapping the excitatory area (Caspary et al., 1994). The second PL unit (Fig. 4-2) did

not show a change in SR. The response area indicated off-CF inhibition at the highest

tone level, though the off-CF inhibition became less significant at lower tone levels.

The first PL (Fig. 4-1) did not show a change in the shape of PSTH, which was

the case for most PLs. The second PL (Fig. 4-2) gradually showed an earlier and sharper

onset with increased average rate. There were other units that also showed this "early

peak" during or after injection. This phenomenon will be presented in more detail below.

Since both PLs had CFs between 1 and 2 kHz, they phase locked to the tone

frequency. No change in the synchronization coefficient was observed with drug

injection. In general, blocking inhibition did not vary the synchronization to tone

frequency or the phase of the synchronized response. Figure 4-3 shows rate-level

functions and PSTHs for all 18 PL and 3 primary-like-with-notch (PLN) units. Diverse

effects of inhibition were observed. For example, the shape of the rate-level function and

the first-spike latency changed in different ways across units.

As shown in Table 4-1, all three PLN units responded to blocking glycinergic

inhibition but not to blocking GABAergic inhibition. The sample size was too small to

make any conclusion; few of these response types were seen, presumably because the

recording sites were anterior and globular bushy cells (that have PLN responses) are

more posterior in the AVCN (Cant and Morest, 1979; Smith and Rhode, 1987).

Nevertheless, this finding agreed with an immunocytochemical study (Saint Marie et al.,

1989) which reports that fewer GABAergic endings are located on globular bushy
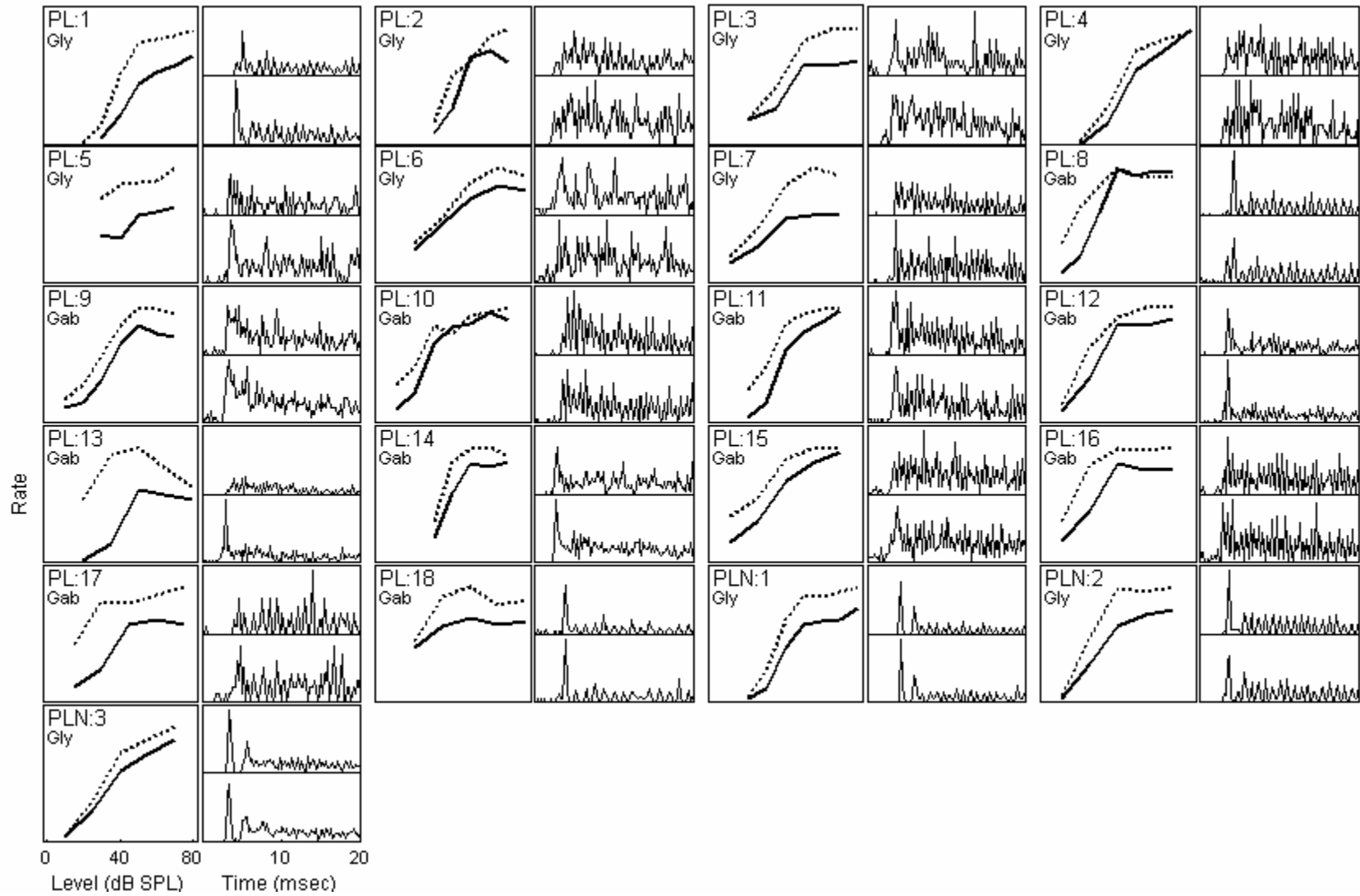
Fig. 4-3 Rate-level functions and PSTHs in response to CF tones for all PL and PLN units. In the rate-level plots, solid lines are average rates before injection, and dotted lines are maximum average rates during or after injection. In the PSTH plots, top panels are PSTHs before injection, and bottom panels are PSTHs when maximum average rates during or after injection were obtained. All PSTHs are responses to the highest-level CF tones.

cells compared to spherical bushy cells (that have PL responses, Rhode et al., 1983).

b. Choppers

Figure 4-4 shows changes in tone responses after gabazine injection for a transient chopper (Chp-T). Apart from the increase of average discharge rate, a systematic change in the PSTH was observed. Before the injection of gabazine, 3 clear chopping cycles could be identified (Fig. 4-4, top row, 2nd column). During the injection, a clear 4th peak was observed (middle row, 2nd column). The unit showed full recovery 18 min post-injection (bottom row, 2nd column); average rate decreased and the 4th peak disappeared. The 3rd column shows the mean inter-spike intervals over time that were used to classify chopper types. The intervals were only plotted up to 20 msec to avoid the end effects (Young et al., 1988; Blackburn and Sachs, 1989). This unit was classified as a transient chopper (also called transiently adapting chopper) since the intervals increased abruptly over the early part of the response and then slightly decreased later (Fig. 4-3, top row, 3rd column). During the injection of gabazine the abrupt increase of intervals at the beginning of the response disappeared. The response area indicated that the inhibitory inputs had frequency tuning similar to that of the excitatory inputs, or on-CF inhibition. This unit did not show a positive effect after strychnine injection.

Figures 4-5 and 4-6 show changes to GABA receptor antagonists for two slowly adapting choppers (Chp-SA). These examples, one for gabazine and the other for bicuculline, are presented to show that some basic observations obtained with these two types of GABA receptor antagonists were generally agreeable, except that the recovery process was usually faster with bicuculline. These two units were classified as Chp-SAs
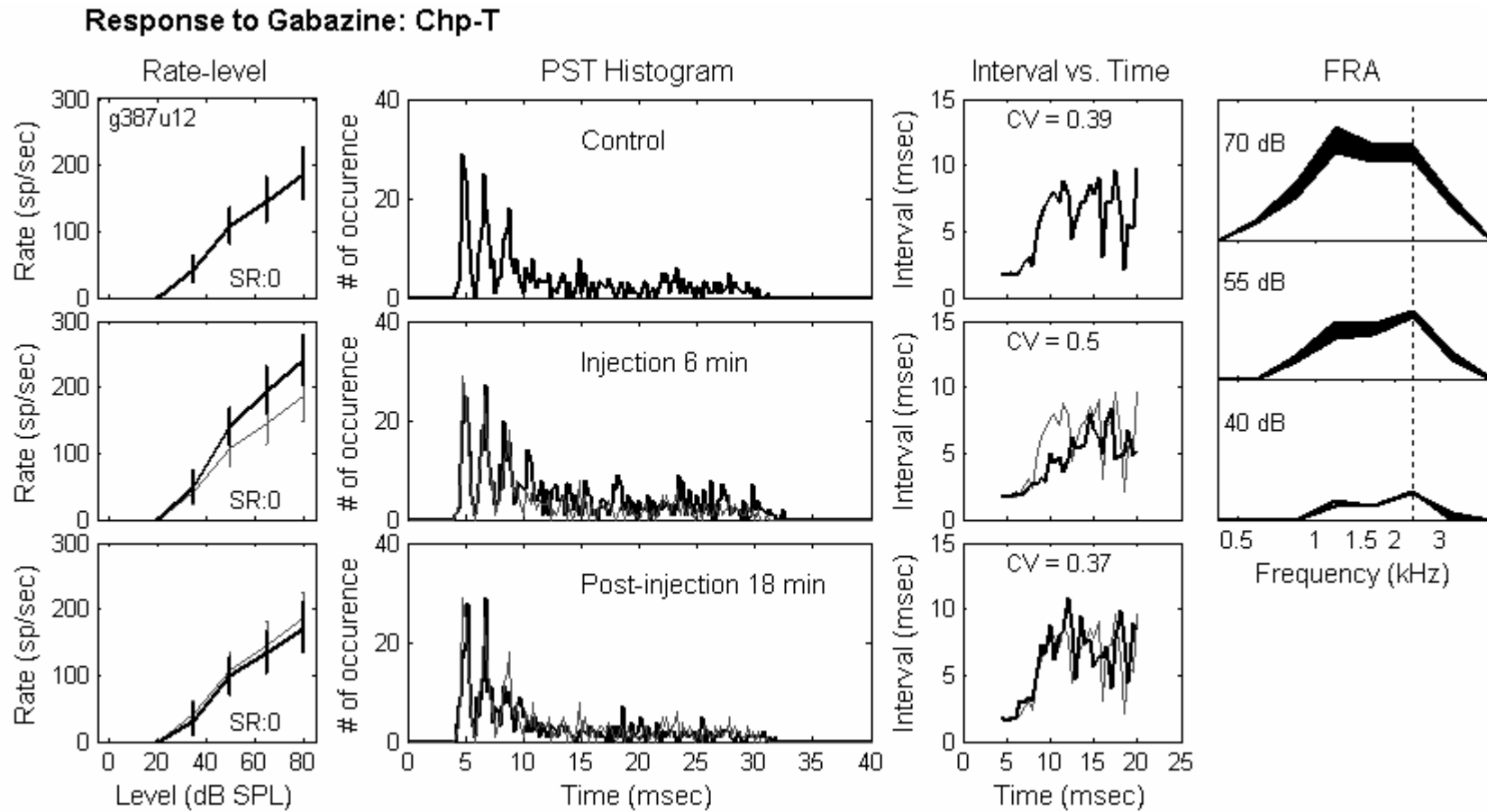
Fig. 4-4 Same format as Fig. 4-1. Chp-T, g387u12, total duration of gabazine injection was 11 min. CF = 2362 Hz.
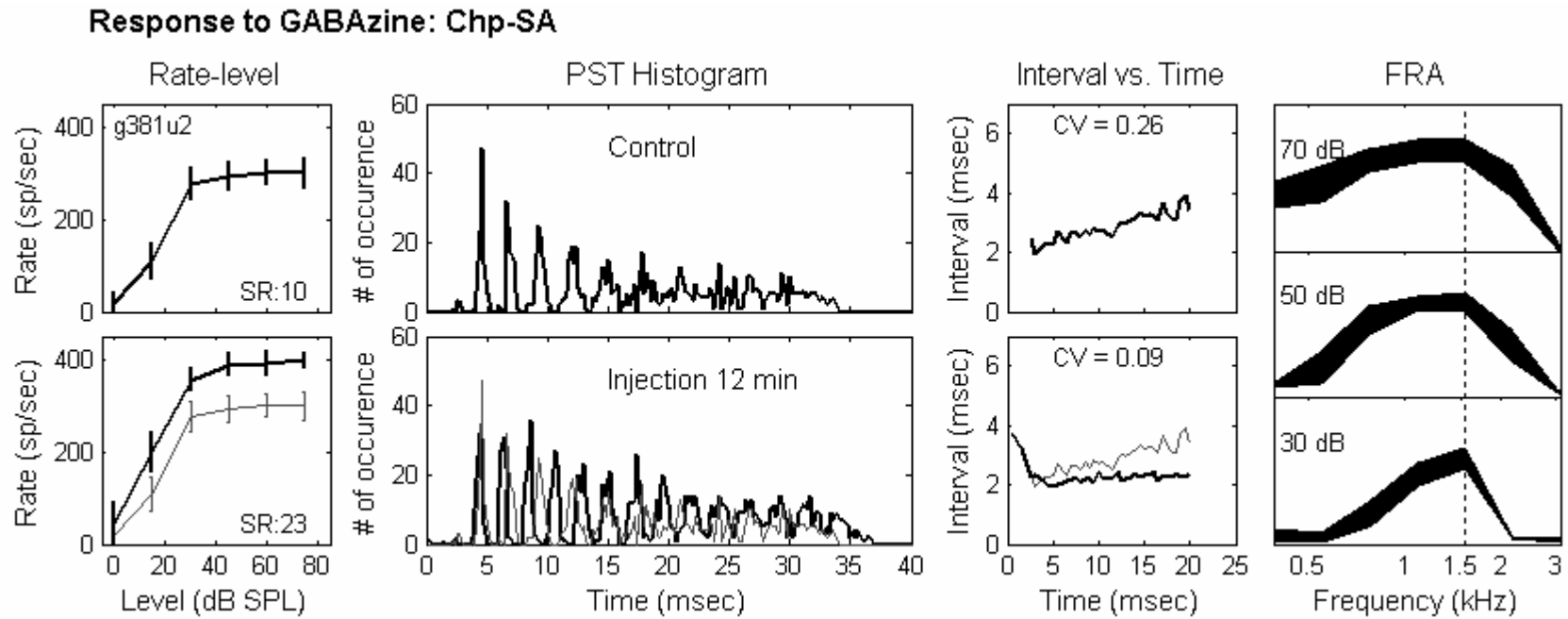
Fig. 4-5 Same format as Fig. 4-1. Chp-SA, g381u2, total duration of gabazine injection was 12 min. CF = 1547 Hz.
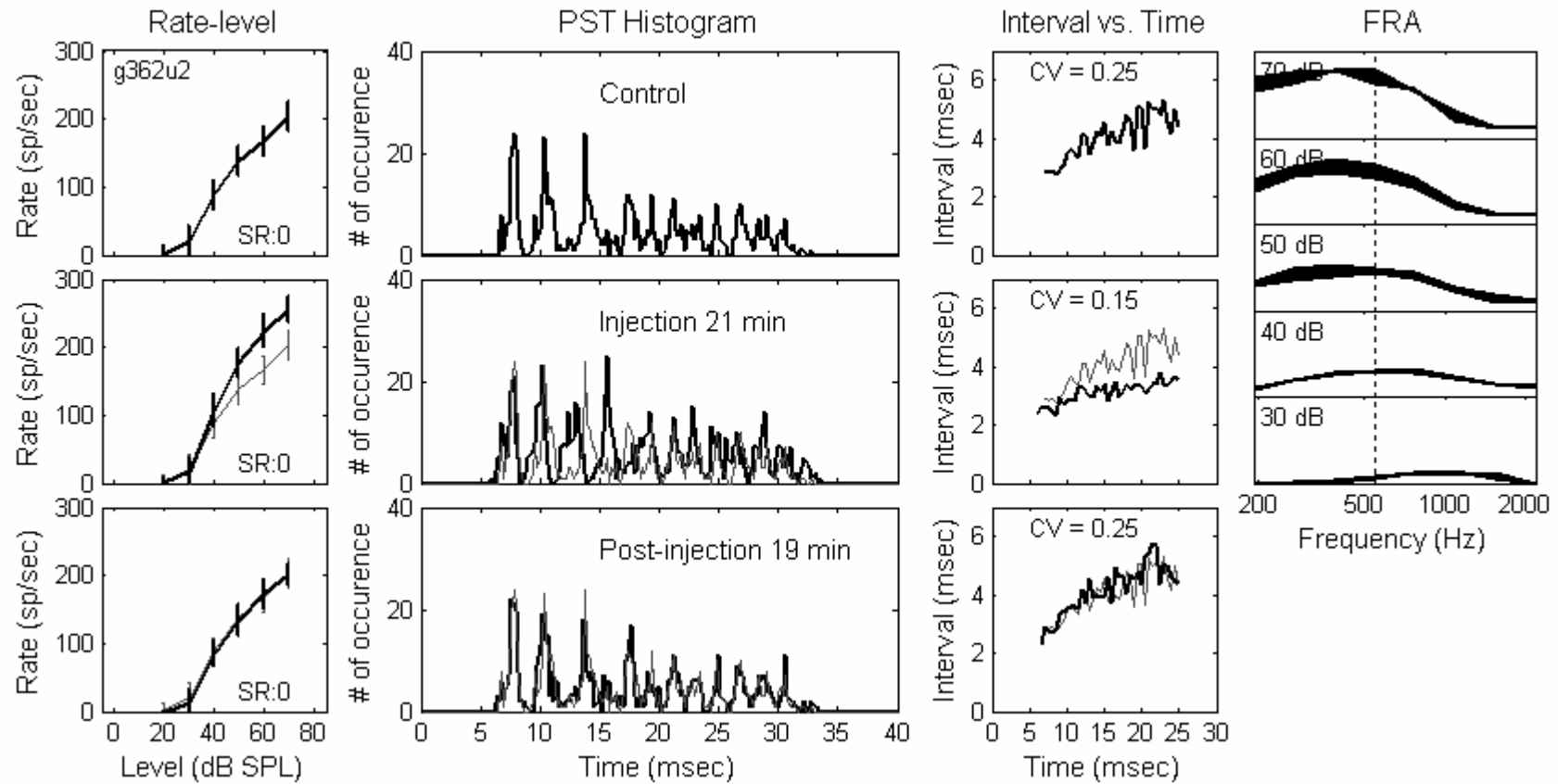
Fig. 4-6 Same format as Fig. 4-1. Chp-SA, g362u2, total duration of bicuculline injection was 23 min. CF = 543 Hz.

since their inter-spike intervals increased with time up to 20 msec. However, when GABA receptor antagonists were injected, the inter-spike intervals became relatively constant with time so that the two slowly adapting choppers indeed became sustained choppers. The CV decreased from 0.26 to 0.09, and from 0.25 to 0.15 for the two choppers, respectively. The change of regularity can also be observed from the PSTHs (2nd columns) as a larger number of distinct chopping cycles appeared during drug injection. The chopping cycles also decreased correspondingly. The response areas of the two units indicated that the frequency tuning of the inhibitory inputs was broad. The second Chp-SA did not show a positive effect after strychnine injection (no strychnine was injected for the first Chp-SA due to time limitation).

Figure 4-7 shows changes after bicuculline injection for a sustained chopper (Chp-S). Sustained choppers have inter-spike intervals that are nearly constant over time (Blackburn and Sachs, 1991). In this study various degrees of change to the sustained properties were observed. In the inter-spike interval plots (Fig. 4-6, top row, 3rd column), before blocking inhibition, a slight increase in intervals as a function of time was observed. Nevertheless, this unit was classified as a Chp-S since the increase was substantially smaller than for Chp-SA units (in this study, all Chp-S units had CVs ≤ 0.2 and Chp-SA units had CVs > 0.2). After bicuculline was injected, the intervals became more invariant over time. As for Chp-SA units, more chopping cycles with a faster chopping rate were observed in the PSTH (Fig. 4-6, 2nd column) of the Chp-S unit. The frequency tuning of the inhibitory inputs was also broad (Fig. 4-6, 4th column). This unit did not show a positive effect after strychnine injection.
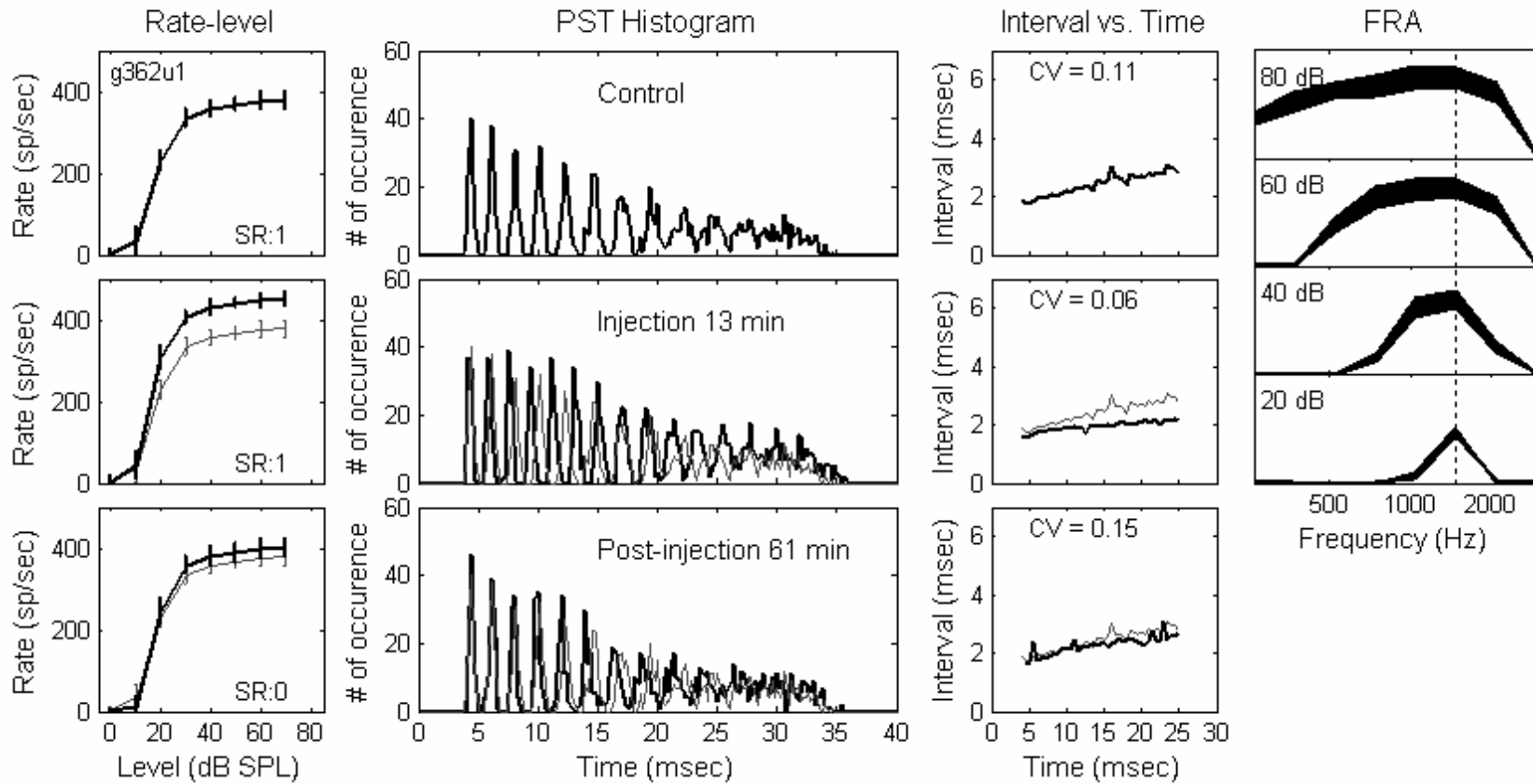
Fig. 4-7 Same format as Fig. 4-1. Chp-S, g362u1, total duration of bicuculline injection was 16 min. CF = 1476 Hz.

Figure 4-8 shows the population results for all choppers that had positive effects. The top 8 responses are obtained from Chp-S units. In general, the change of discharge rate in response to on-CF (and off-CF) tones after the injection of inhibitory receptor
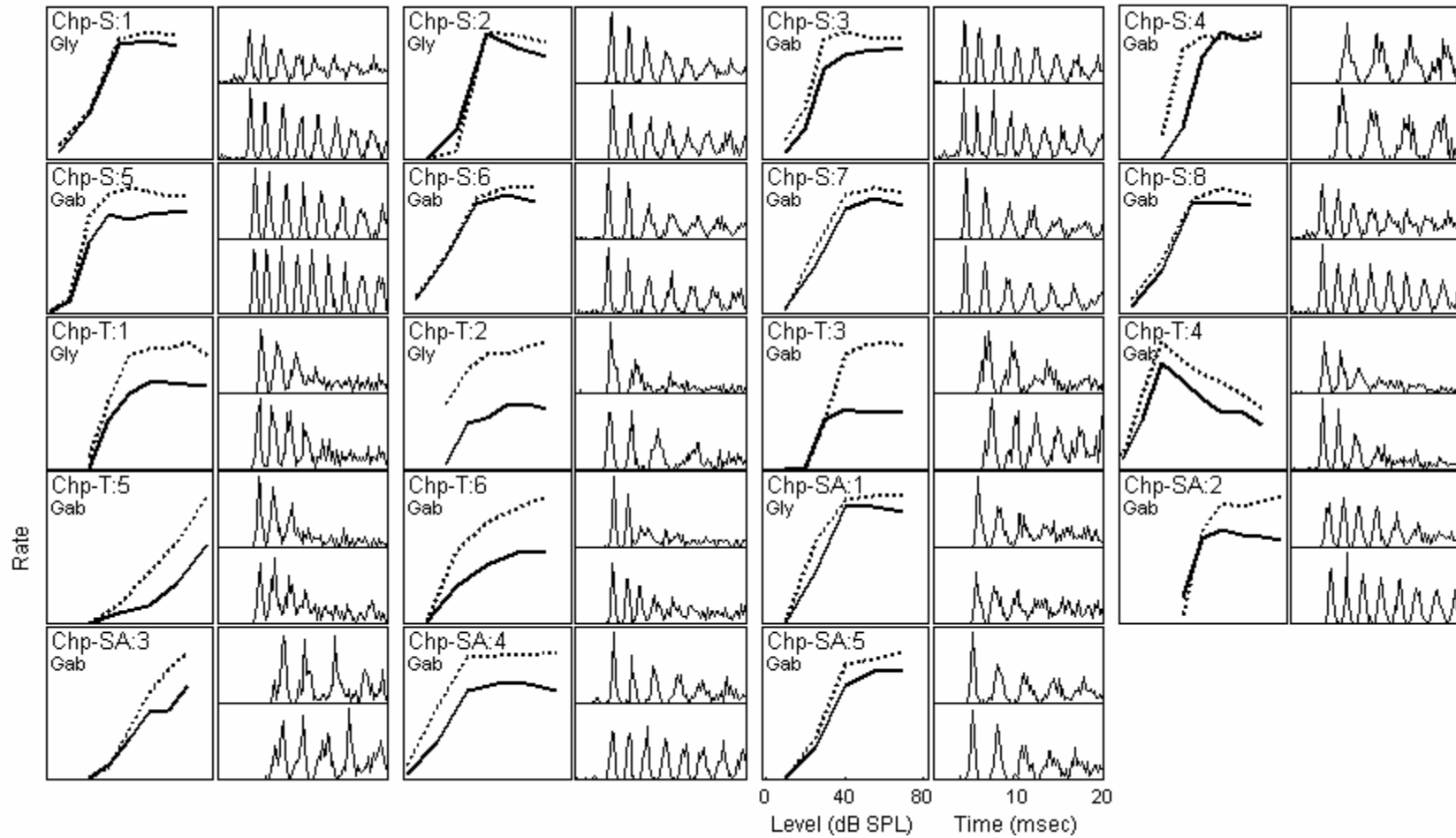
Fig. 4-8 Rate-level functions and PSTHs in response to CF tones for all chopper units (chp-S, Chp-T and Chp-SA). Same format as Fig. 4-3.

antagonists was smaller for Chp-S units than for Chp-SA and Chp-T units. Previous

studies also suggested that Chp-S units may not receive strong inhibition (Banks and

Sachs, 1991; Hewitt and Meddis, 1993) or that Chp-S units mainly receive off-CF

inhibition (Paolini et al., 2005). However, since Chp-S units had more regular discharges,

the variance of the rate was smaller (confirmed by this study), and hence the same

amount of rate change can be more meaningful as compared to the other two chopper

types. Figure 4-9 shows the maximum t values across tone levels for each unit with

injection of glycine (top) or GABA (bottom) antagonists. All the values are above the

significance level (horizontal solid line). Chp-S units showed t values comparable to the

values of other cell types. Therefore, it was concluded that inhibitory inputs received by

Chp-S units affected responses to CF tones. In addition, larger changes of rate were

observed after blocking GABAergic inhibition than after blocking glycinergic inhibition.

As shown by the two Chp-SA and one Chp-S units, the regularity of choppers

could be affected by inhibitory inputs. Figure 4-10 shows the CV values before and after

the injection of inhibitory receptor antagonists for all choppers that showed positive

effects (small CV values indicate regular discharges). The CV is traditionally computed

based on discharges in the time window of 12 to 20 msec (Blackburn and Sachs, 1989),

as shown in Fig. 4-10 top. Chp-SA units (plus symbols) showed the largest change of CV

by blocking inhibition (3 out of 5 units actually became sustained choppers). Six out of 8

Chp-S units (right triangles) also showed decreased CV.

Although one Chp-T became a Chp-S after injection of GABAergic antagonists,

no systematic change of regularity was observed for the other 5 Chp-T units (Fig. 4-4,

downward triangles). However, as illustrated by the Chp-T in Fig. 4-4, the change of
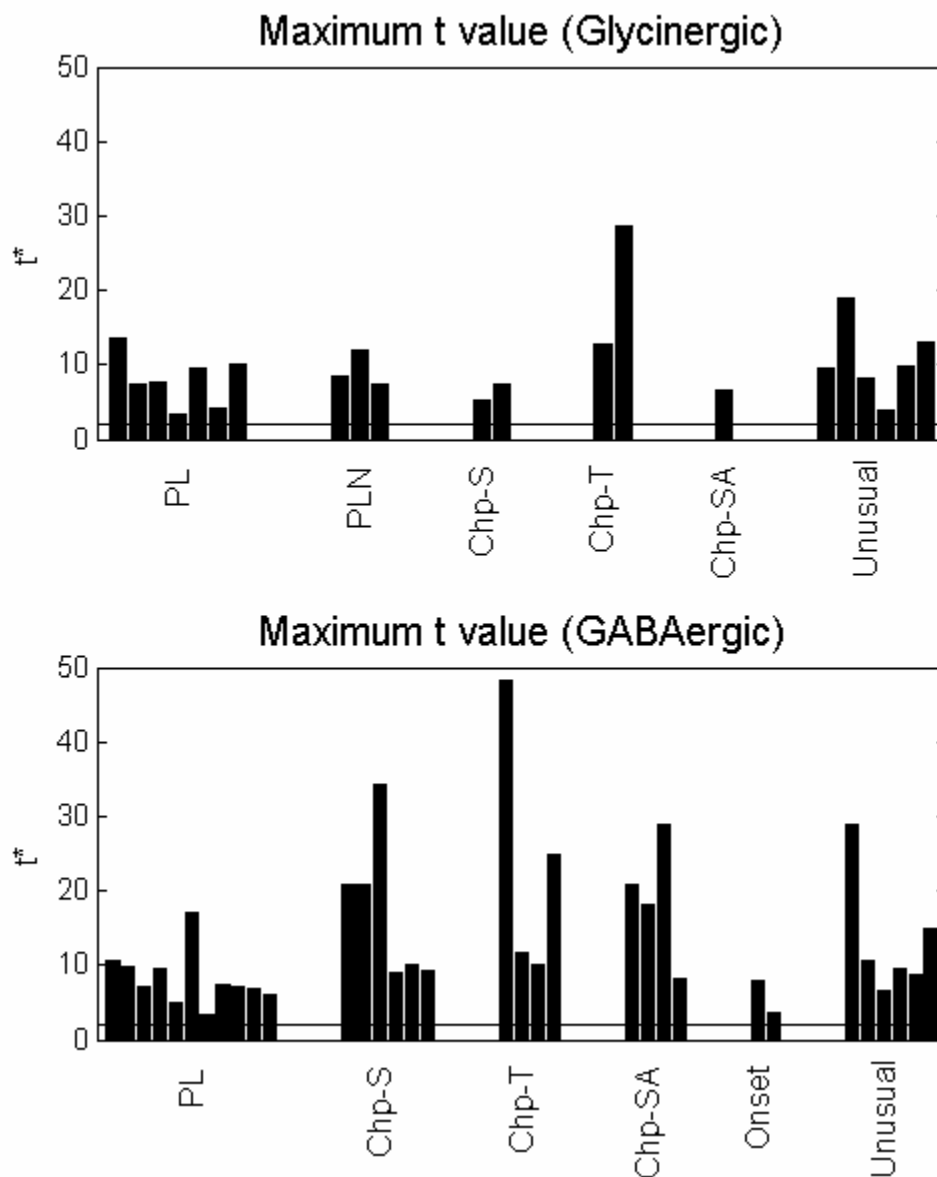
Fig. 4-9 Maximum t values based on changes of average rate at super-threshold levels during or after blocking inhibition for each type of units. Horizontal solid line indicates statistical significance level for *t* values (p < 0.05).
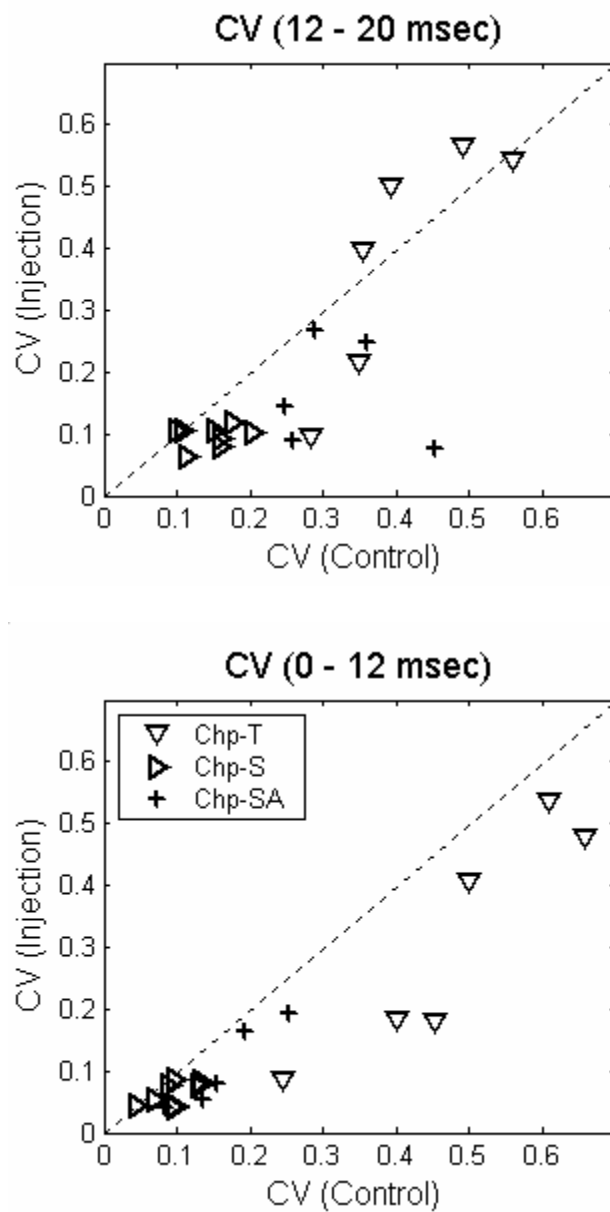
Fig. 4-10 Coefficient variations (CVs) computed based on activity in different time windows for choppers before (x axis) and after (y axis) blocking inhibition. Responses to both glycinergic and GABAergic inhibitions are included.

inter-spike intervals primarily occurred before 12 msec, which was excluded by the traditional CV time window (12 to 20 msec). Fig. 4-10 (bottom panels) shows the CV based on discharges occurred between 0 and 12 msec after stimulus onset. All Chp-T units showed decreased regularity within this time window.

In general, irregular chopping patterns can be generated from regular chopping patterns by inhibitory inputs; however, inhibitory inputs do not necessarily account for all irregular chopping patterns.

c. Unusual/onset response types

The final class of response types, 2 onset and 12 unusual types, will be described here; these units represent all of the neurons studied that did not belong to the major two response types, PLs (and PLNs) or choppers. A higher percentage of these units showed positive effects compared to the two major types (Table 4-1). Four unusual units showed chopper-like or multimodel patterns, although they did not pass the criterion to be characterized as choppers (based on the spike-per-peak ratio; Blackburn and Sachs, 1989).

Figure 4-11 shows responses of an unusual unit to bicuculline (Part A), strychnine (Part B), and glycine (Part C), respectively. In response to CF tones, this unit had a relatively broad peak at the beginning, followed by low activity that built up in time (Fig. 4-11, part A, top row, 2nd column). After injecting bicuculline, both onset and sustained activity increased (middle row, 2nd column), and inter-spike intervals decreased (middle row, 3rd column). The increase of activity was maximal for the late part of the response, and minimal right after the onset. This unit recovered by 64 min post-injection. Similar to

Response to Bicuculline: Unusual (Part A)

Rate-level · PST Histogram · Interval vs. Time · FRA

g368u2
SR:0

Control

CV = 0.36

80 dB

70 dB

SR:0

Injection 22 min

CV = 0.34

60 dB

50 dB

SR:0

Post-injection 64 min

CV = 0.24

Frequency (kHz)

Level (dB SPL)

Time (msec)

Time (msec)
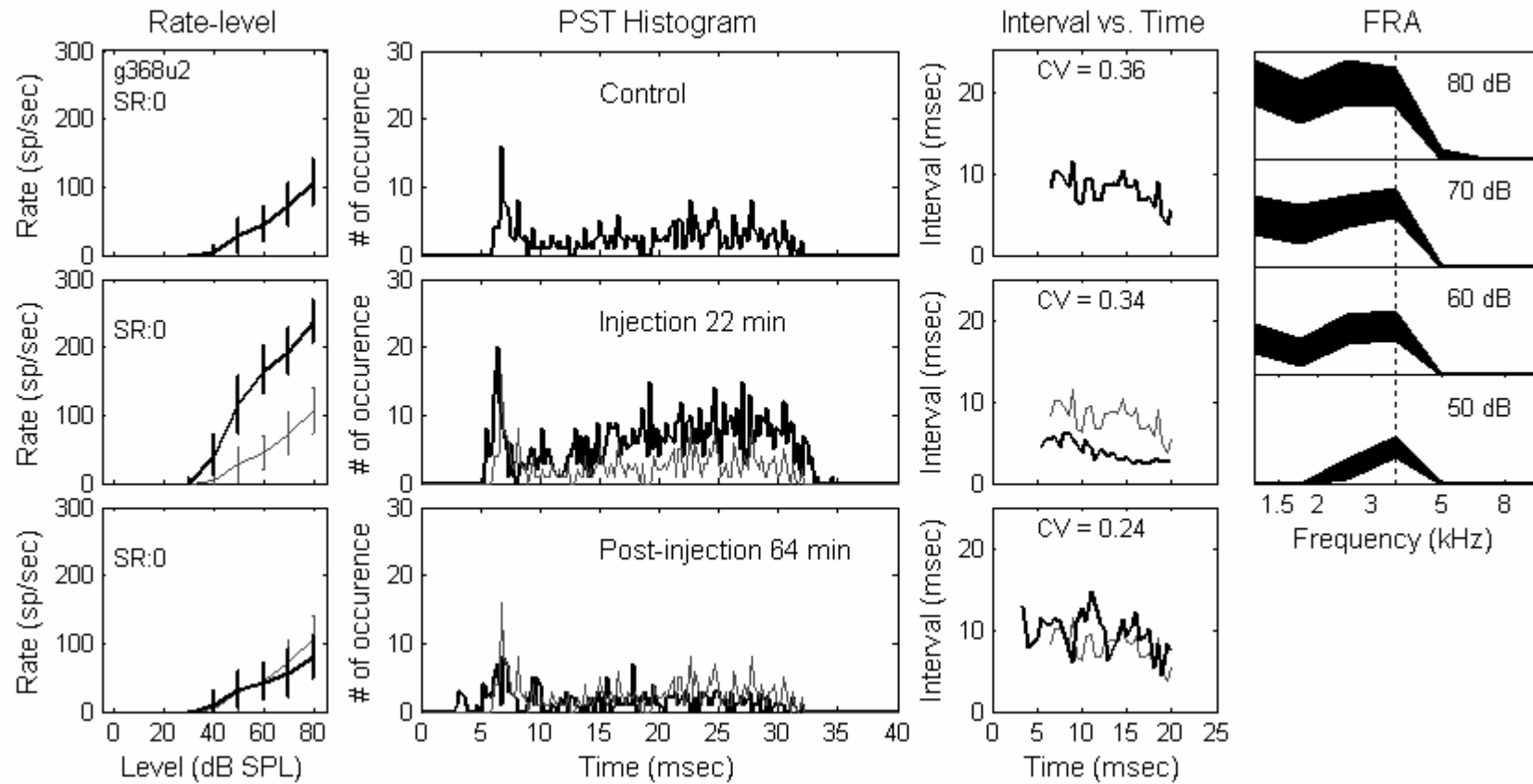
Response to Strychnine: Unusual (Part B)

Rate-level — PST Histogram — Interval vs. Time — FRA
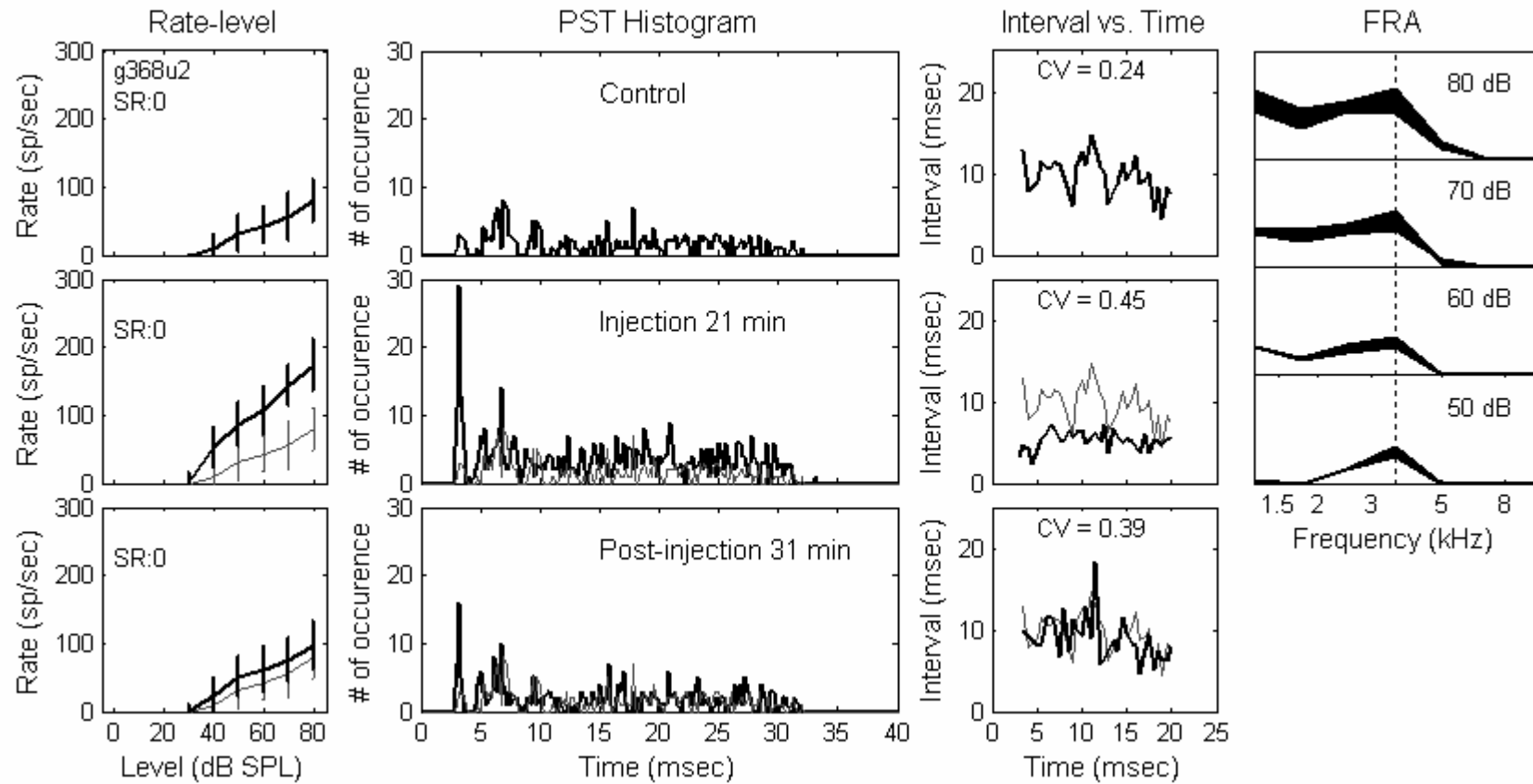
Fig. 4-11 Same format as Fig. 4-1. Unusual, g368u2, total duration of drug injection was 23 min, 60 and 7 min for bicuculline (part A), strychnine (part B) and glycine (part C), respectively. CF = 3544 Hz.

the Chp-T unit (Fig. 4-4), the recovered average rate was slightly lower than the control rate at high tone levels (Fig. 4-11, part A, bottom row, 1st column). This "over-recovery" was reflected in the PSTHs as a less distinct onset and lower activity at the end of the response. The response area indicated that the inhibitory inputs were strong both at and below the unit's CF (Fig. 4-11, part A, 4th column).

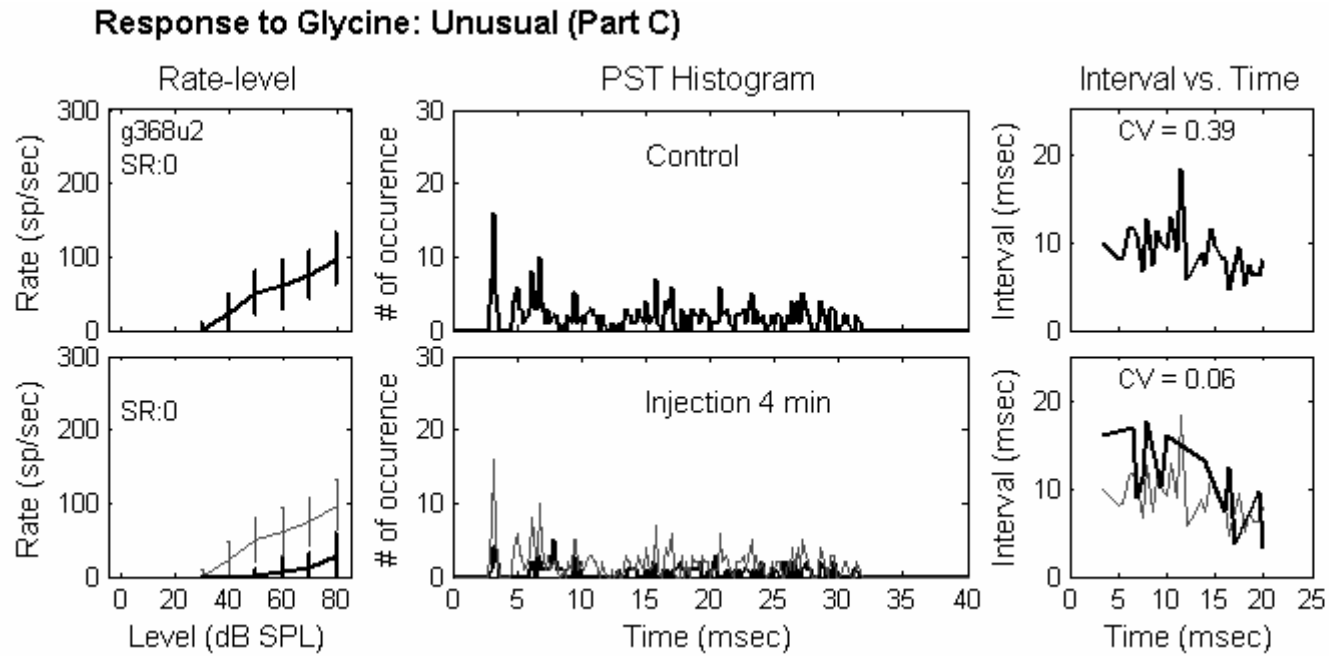Part B (Fig. 4-11) shows the unit's response with injection of strychnine. The recovered response from bicuculline was used as the new control. The most interesting change was the appearance of a precisely timed early peak (middle row, 2nd column). This peak was 4.7 msec earlier than the broad peak seen in the original response (part A, top row, 2nd column). There was also a 1 – 1.5 msec notch after the early peak. The sustained activity showed less increase and was constant over time. The average rate recovered 31 minutes post-injection (part B, bottom row, 1st column). The early peak decreased by half, but did not totally disappear (bottom row, 2nd column). The response area showed a weaker glycinergic inhibitory effect (part B, 4th column) as compared to the GABAergic inhibitory effect (part A, 4th column). Part C (Fig. 4-11) shows the response of this unit after injection with glycine. Both the early peak and sustained activity decreased drastically, confirming the presence of glycinergic inhibition.

Figure 4-12 shows the responses of 12 unusual units (panels 2 and 7 are the same unusual unit shown above in Fig. 4-11) and 2 onset units. The effects of inhibition can be divided into three groups: early inhibition, timed inhibition, and persistent inhibition. The 5 units in panels 2, 4, 8, 10 and 12 showed relatively early inhibition (this early inhibition will be described later in more detail). Units in panels 2 and 10 showed highly isolated early peaks at times when no discharges were present in the control responses.
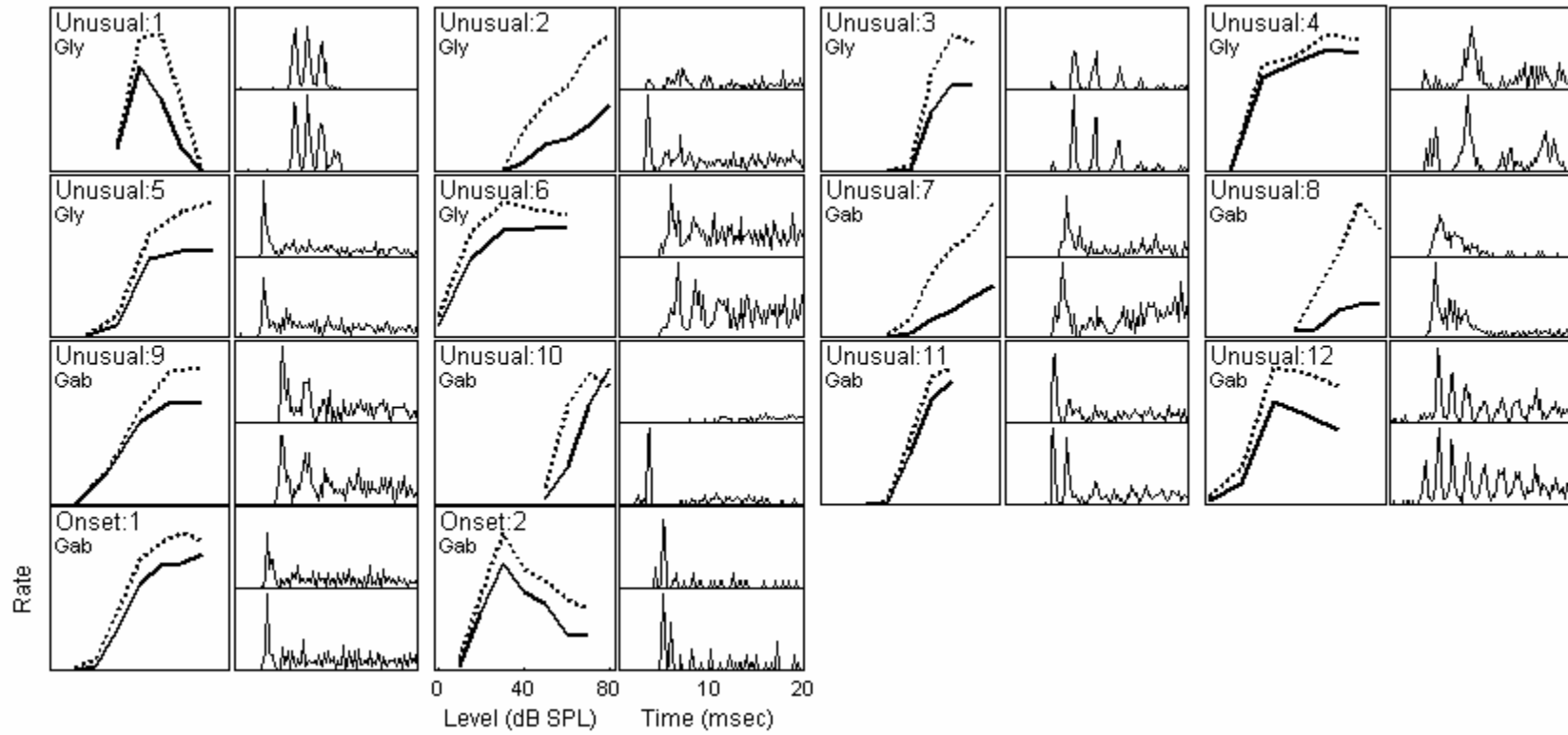
Fig. 4-12 Rate-level functions and PSTHs in response to CF tones for unusual/onset units. Same format as Fig. 4-3.

Units in panels 4 and 8 showed enhanced onsets as compared to the control responses.

The unit in panel 12 had multiple peaks similar to a chopper's (this unit was not

characterized as a chopper since it failed the spike-per-peak criterion). After blocking

inhibition, the timing of these peaks did not change, but an early peak appeared, and the

interval between this extra peak and the second peak was approximately the same as the

later intervals. On the other hand, the 2 units in panels 1 and 11 showed a distinct extra

chopping peak *after* the primary chopping peaks without much change in other parts of

the response. This type of inhibition was called timed inhibition. The other units seemed

to receive inhibition that was relatively persistent throughout the responses.

4.3.3   More about sound-evoked rate and spontaneous rate

As described above, Fig. 4-9 shows average rate changes in terms of t values for

different types of units. Within each unit type, some units showed a positive effect, while

others did not. Since a positive effect was always associated with an increased discharge

rate, it was possible that units with inhibitory inputs had relatively lower rates than units

without inhibitory inputs. Figure 4-13 shows the maximum discharge rates before and

after blocking inhibition for both positive-effect (filled symbols) and negative-effect

(open symbols) units. A large range of discharge rates (approximately 50 to 600 sp/sec)

was observed. It was true that the 5 choppers that had the highest rates (more than 450

spike/sec) did not show positive effects to either glycine or GABA receptor antagonists.

However, for units that had average rates lower than these choppers, positive effects were

observed for both high- and low-rate units. It can thus be concluded that variations in

excitatory inputs determined the range of discharge rate across neurons, and inhibitory

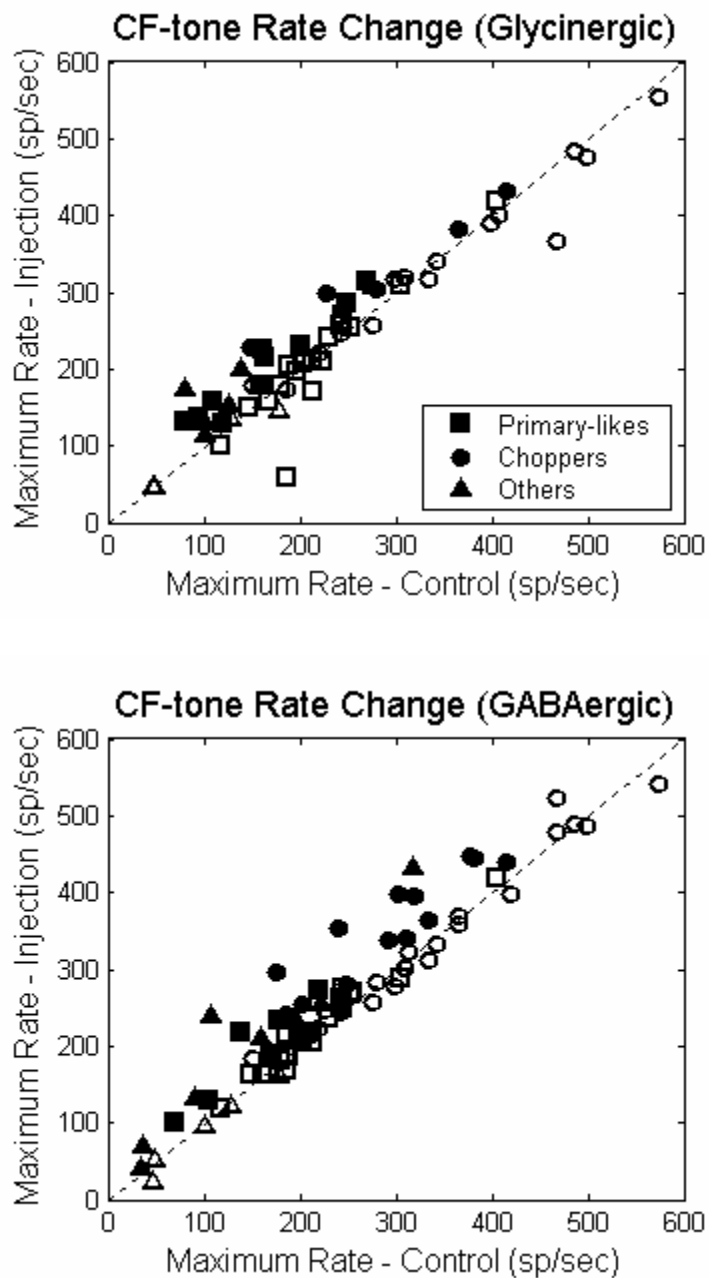inputs only modulated the rate within a limited range.

Fig. 4-13 Maximum rate across level in response to CF tones before and after blocking inhibition. Filled symbols indicate units with positive effect. Open symbols indicate units without positive effect.

During the experiment, 55% of the positive-effect units showed an increase in SR. Figure 4-14*A* shows the *t* values based on changes in SR vs. *t* values based on changes in tone-evoked rate by blocking glycinergic or GABAergic inhibition. Filled symbols indicate positive-effect units, and open symbols indicate negative-effect units. It should be noted that although Table 4-1 shows that 29 negative-effect units showed significantly increased tone-evoked rate, the *t* values of these units (open symbols on the right of the vertical dotted line) are much lower than the *t* values of positive-effect units in general. Recall that these neurons were categorized as negative-effect neurons because the changes in rate were inconsistent over the course of the injection and/or disappeared either before or immediately after the end of the injection period. Both positive-effect and negative-effect units showed insignificant changes in SR. The largest changes in SR were observed with positive-effect units (8 PLs and 3 choppers on the top of Fig. 4-14*A*); however, no *t* values were above the significance criterion (1.96), due to the large variance of the SR.

Previous studies that compare changes in SR with changes in sound-evoked rates have not considered the variance (Caspary et al., 1979; Ebert and Ostwald, 1995a). Ebert and Ostwald (1995a) computed the ratio of sound-evoked rate to SR. To make the present study comparable to that study, Fig. 4-14*B* shows changes in SR and sound-evoked rate in terms of percentage of increase (based on mean rates, without including variance) after injection of glycine or GABA receptor antagonists (one unit that showed an increase in SR from 0 to 40 sp/sec is not included in the plot for graphical reasons). The percentage of change in SR was larger than that of sound-evoked rate for 49% of units. In general, the observed changes in SR were consistent with reports from earlier studies;

A. Rate vs. Spont

B. Rate vs. Spont (Percent of Change)

C. Spont

D. Recovery
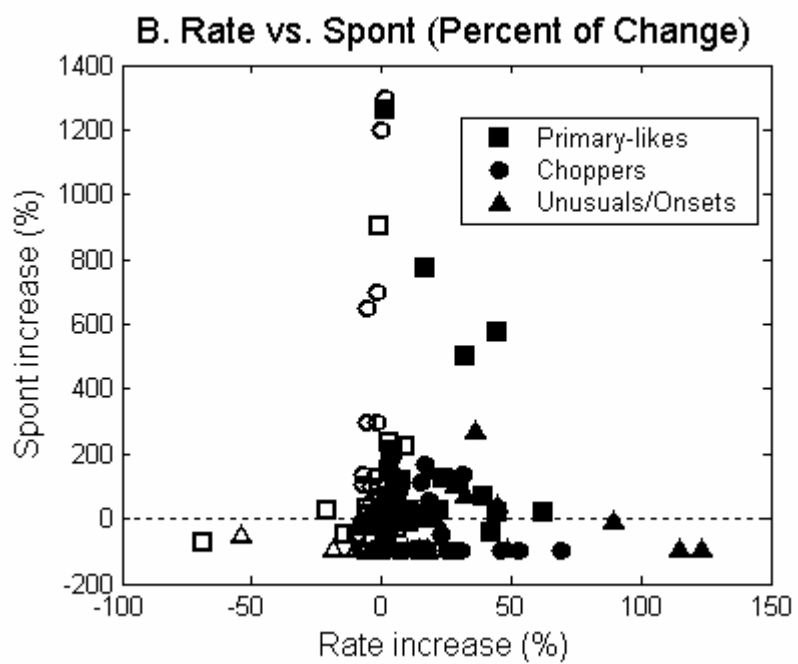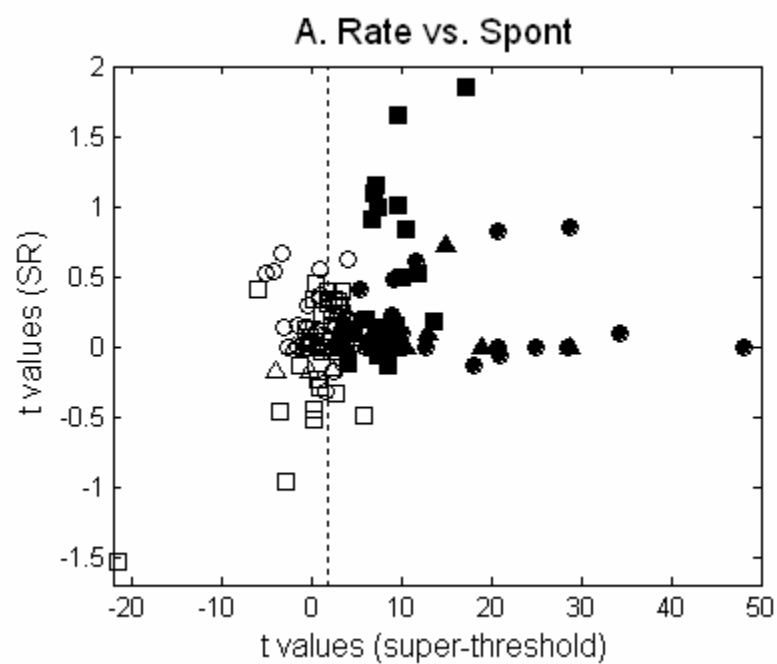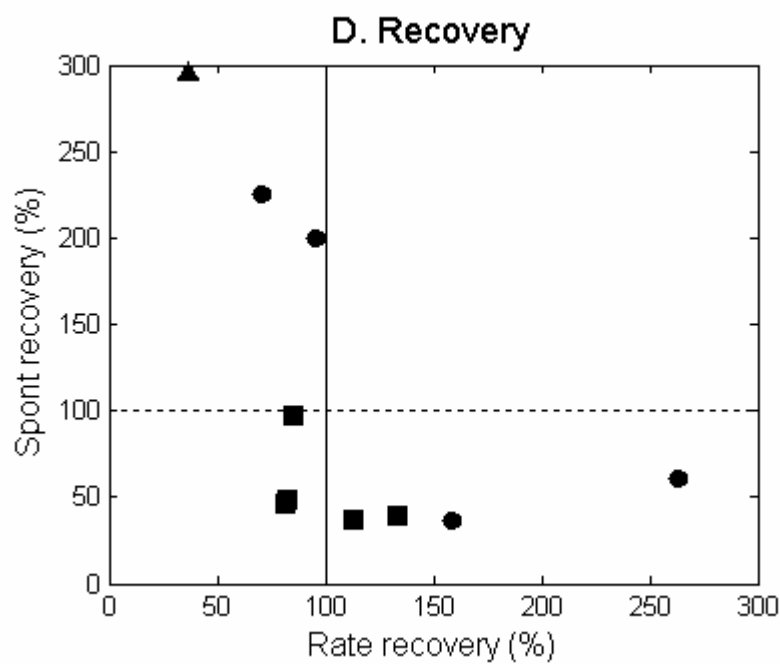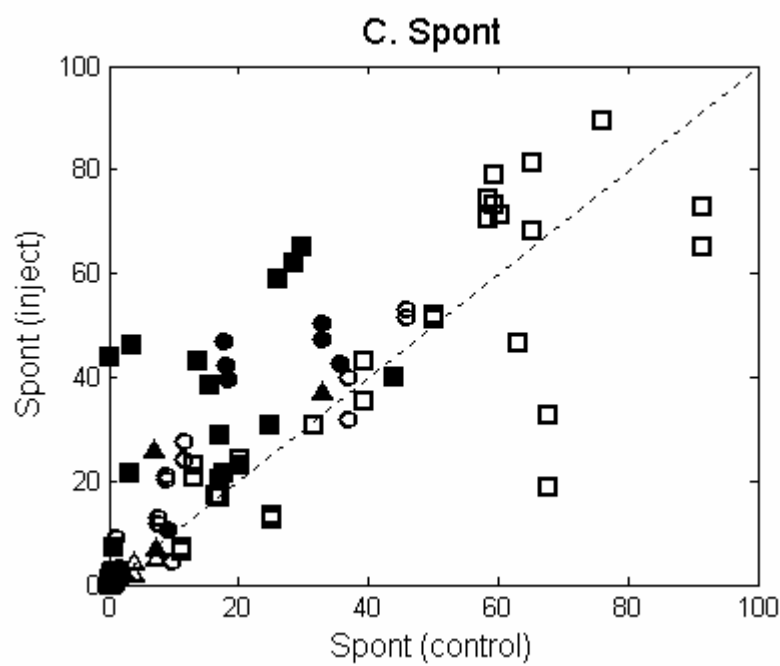
Fig. 4-14 *A*, Change of spontaneous rate compared to change of sound-evoked rate after blocking glycinergic or GABAergic inhibition in terms of *t* values. The vertical dotted line indicates the significant *t* value ($p < 0.05$) for changes in the sound-evoked rate. *B*, change of spontaneous rate compared to change of sound-evoked rate after blocking glycinergic or GABAergic inhibition. *C*, spontaneous rate before and after blocking glycinergic or GABAergic inhibition. Dotted lines indicated no change of spontaneous rate. *D*, recovery of sound-evoked rate vs. recovery of spontaneous rate. Open (filled) symbols indicate units without (with) positive effect. Vertical and horizontal lines indicate 100% recovery. Note that 1 unit which had a spontaneous increase from 0 to 40 sp/sec is not plotted in *A* (spont increase = 40000%), and another unit which did not recover was not plotted in *C* (Spont recovery = -5200%).

however, statistical evaluations of the changes in SR revealed that these changes were not significant.

Figure 4-14*C* shows the mean values of SR before and after blocking inhibition. One interesting observation was that units with original SR greater than 45 sp/sec, which were all PLs or PLNs, never showed positive effects in terms of an increase of sound-evoked rate. The group of 11 units that showed large t values based on the SR (Fig. 4-14*A*) all had low or medium SRs and also had relatively large (but insignificant) changes in the mean SR as compared to other units (Fig. 4-14*C*, *upper left*).

However, one must be cautious when evaluating the drug effect on the spontaneous activity for three reasons. First, as shown in Fig. 4-14*A*, *B*, and *C*, although the largest increase in SR (both as *t* values and as absolute changes; e.g., $t > 1.7$) was observed with positive-effect units, the SRs of negative-effect units also varied in a certain range (t between -1.5 to 0.75). Second, it was observed (for at least 3 positive-effect units) that even before the injection of inhibitory receptor antagonists, the SR already increased substantially (we did monitor the SR frequently before the injection). Third, the recovery of SR did not correlate with the recovery of sound-evoked rate. Figure 4-14*C* shows the percentage of SR recovery vs. the percentage of (sound-evoked) rate recovery for positive-effect units that showed both increased rate and increased SR after blocking inhibition.

4.3.4   First-spike latency and early inhibition

Figure 4-15 shows values of mean (*A* and *B*) and standard deviation (*C* and *D*) of the FSL for all types of units before and after blocking inhibition (glycinergic and

A. Change of mean FSL (all)

B. Change of mean FSL (focused)

C. Change of std FSL (all)

D. Change of std FSL (focused)
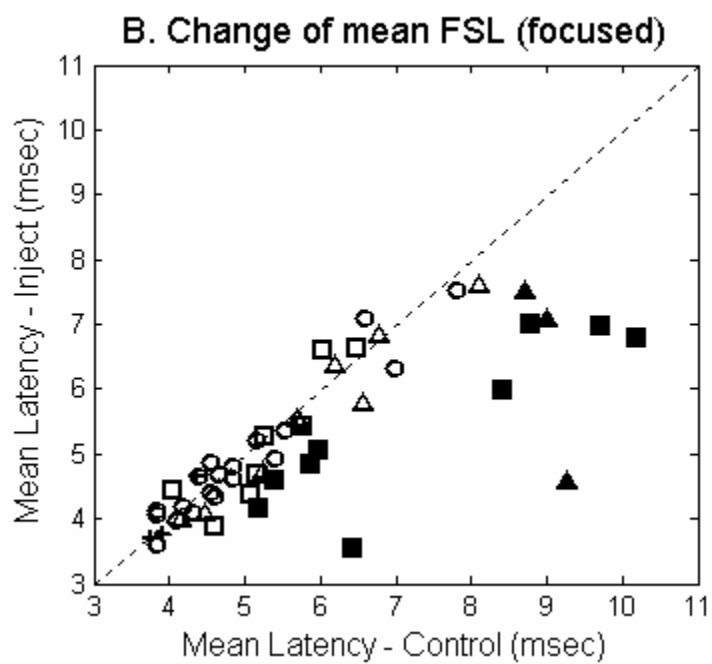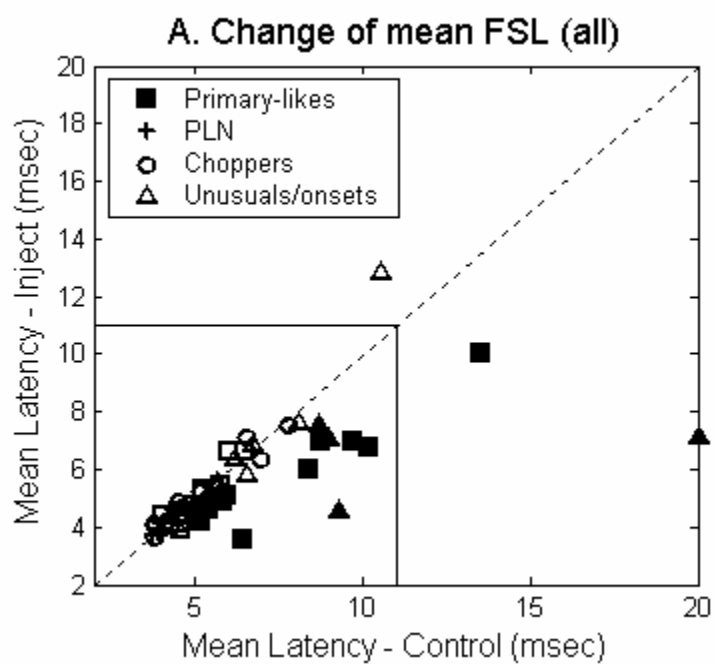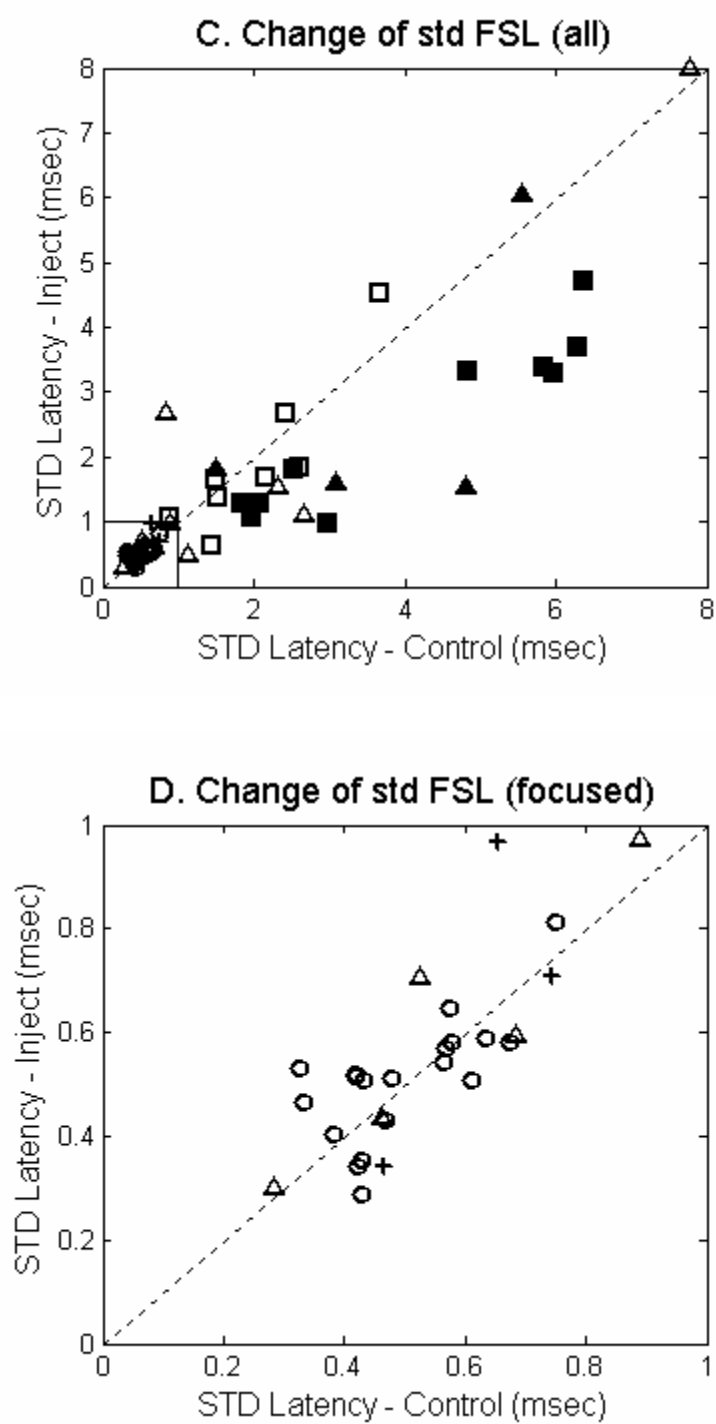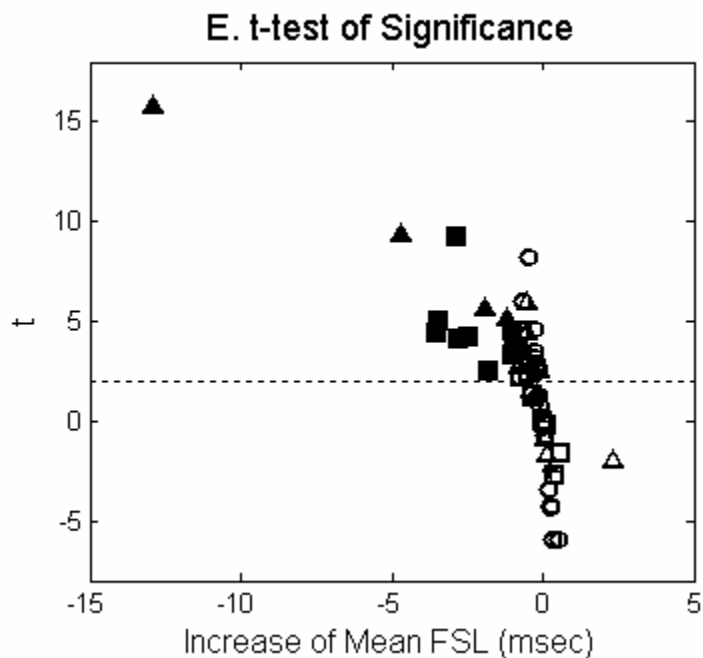
Fig. 4-15 Mean (*A* and *B*) and standard deviation (*C* and *D*) of first spike latency (FSL) before and after blocking glycinergic or GABAergic inhibition. *A* and *C* show all the units; *B* and *D* show the units within the left-bottom rectangular area of *A* and *C*, respectively. Filled symbols are units that had decreased mean FSL for more than 0.8 msec after blocking inhibition. *E*, t-test of significance of the change of FSL. Negative values of the x axis indicate decreased FSL. The horizontal dashed line indicates statistical significance (*t* test, $p < 0.05$).

GABAergic inhibitions are not differentiated in the plots since no difference in trends was observed between the two types of inhibition). Note that the PLN units were separated from PLs here, since the FSLs of the former were shorter and less variable than those of the latter. The FSL was computed based on responses to the highest tone level tested (60 – 80 dB SPL). The mean FSL of 31 units decreased significantly ($p < 0.05$), of 8 units increased significantly ($p < 0.05$), and of 15 units remained unaffected (Fig. 4-15*A*). Figure 4-15*B* amplifies the bottom-left corner of Fig. 4-15*A* to provide a better view of units with short FSLs. These two plots clearly showed that the mean FSLs of choppers (circles) did not vary substantially after blocking inhibition. The filled symbols in these two plots are 14 units that had FSLs that decreased by more than 0.8 msec after blocking inhibition, and all of them were PLs or unusual/onset units. These units accounted for 34% of PLs and unusual/onset types.

Figure 4-15 *C* and *D* show standard deviations of FSL, as a measure of how peaky the onset was. All but two of the units that had FSLs that decreased by more than 0.8 msec (filled symbols) also had decreased standard deviations (Fig. 4-15*C*). Choppers and PLNs all had standard deviations of FSL that were smaller than 0.8 msec (Fig. 4-15*C*, bottom left corner). PLs all had standard deviations of FSL that were larger than 0.8 msec. Figure 4-15*E* shows the *t*-test of significance of the change in FSL. Since choppers had small standard deviations, the FSLs of 14 out of 19 choppers changed significantly (above the horizontal dashed line). Negative values on the abscissa indicate decreased FSLs after blocking inhibition. The decreases of FSL were all above the significance level for units that had FSLs decreased by more than 0.8 msec (filled symbols).

The inhibition associated with units that showed decreases in FSL of more than 0.8 msec after injecting inhibitory receptor antagonists was called early inhibition. Note that the 0.8-msec criterion was arbitrarily chosen since no clear boundary existed between early inhibition and later inhibition (Fig. 4-15 *A* and *B*). As mentioned before, the PL plotted in Fig. 4-2 showed clear early inhibition (0.9 msec change in FSL) that was revealed gradually over the time of the injection. The unusual unit plotted in Fig. 4-11 showed a 1.9-msec decrease of mean FSL after blocking GABAergic inhibition, and 4.7-msec decrease after blocking glycinergic inhibition. Figure 4-16 gives two more examples of early inhibition. The mean FSL decreased by 1.8 and 12.7 msec after blocking GABAergic and glycinergic inhibition for the two units, respectively.

As shown in the mean FSL figure (Fig. 4-15 *A* and *B*), there were different degrees of early inhibition. The mean FSLs of some units were shortened by approximately 0.8 msec, whereas much larger time changes were observed for others. It was unclear whether a single underlying mechanism accounted for the large range of FSL shifts. Four out of 12 units that showed early inhibition required more than 30 min post-injection time to show the maximum effect, and only 1 unit showed recovery during the holding time. It should also be pointed out that blocking glycinergic and GABAergic inhibitions both caused large changes in FSLs, although the sources of these two types of inhibitions are presumably different.

4.3.5   Frequency response areas

The response area was used to evaluate whether the frequency tuning of inhibitory inputs was aligned with that of excitatory inputs. Here a d' metric was used to compare
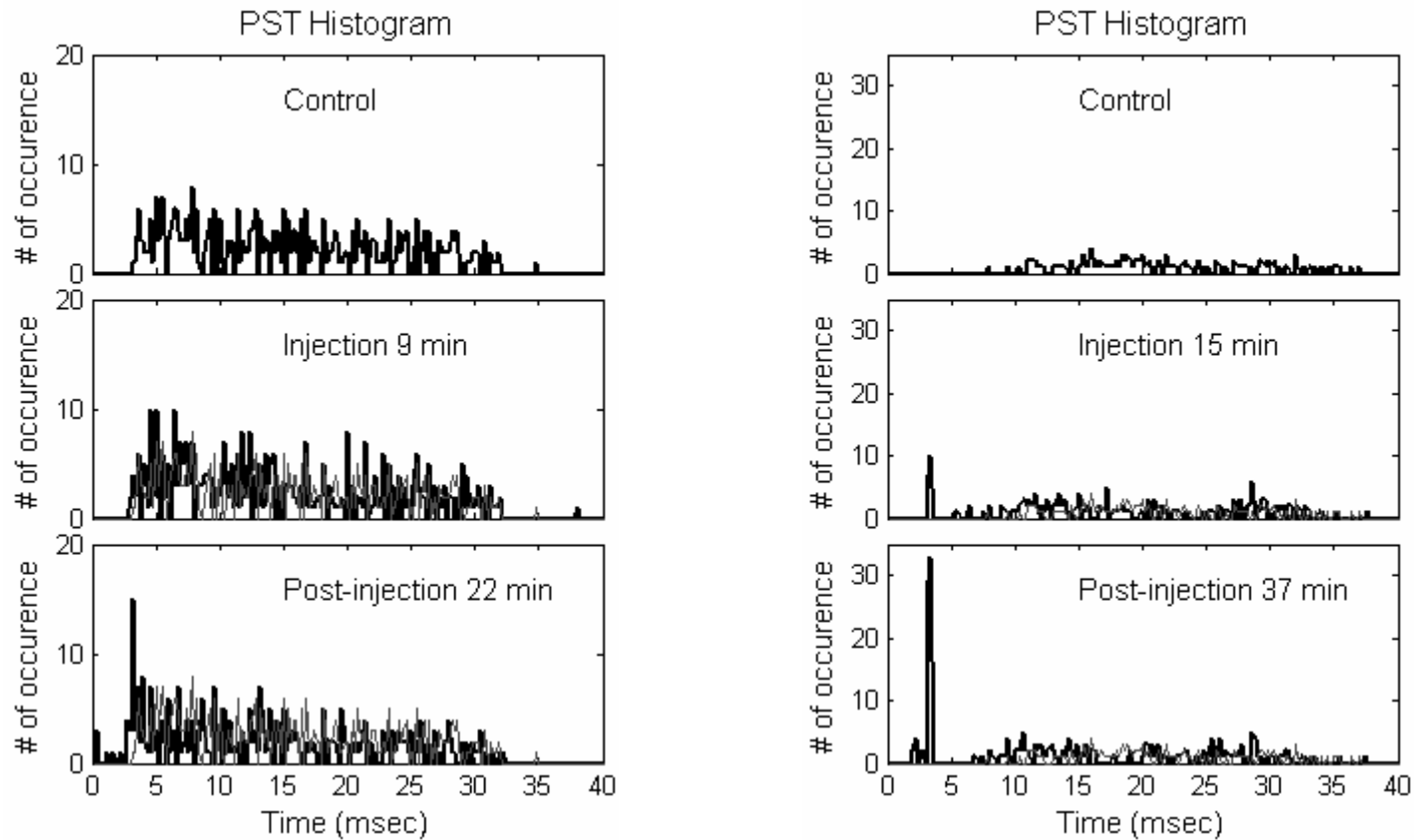
Fig. 4-16 Examples of units with early inhibition in the same format of the 2nd column in Fig. 4-1. *Left*, PL, g383u4, total duration of strychnine injection was 12 min. CF = 3544 Hz. *Right*, unusual, g381u5, total duration of gabazine injection was 16 min, CF = 2211 Hz.

the change at CF with that at other frequencies. At relatively low sound levels, such as 15

to 20 dB above threshold, frequency responses were mostly limited to frequencies near

CF, which made it difficult to determine whether inhibition was on-CF vs. off-CF.

However, when the sound level increased, the maximum firing rate shifted to lower

frequencies, and it was assumed that the responses of inhibitory interneurons also shifted.

The determination of on-CF vs. off-CF inhibition had to combine responses at different

tone levels and consider the frequency shift. A final decision was made based on

responses to either the mid or the high tone level, whichever yielded a more distinct

pattern. For units that showed small changes in the response areas, as well as units that

showed mostly decreased rates after blocking inhibition[2], no description of the response

area was made (marked as N/A). Figure 4-17 shows the change of response areas (left-

hand panel in each pair) after blocking glycinergic (*A*) and GABAergic (*B*) inhibition at

the highest tone level tested. The d' is also shown beside each response area. Four types

of inhibition based on frequency tuning were observed, indicated as "On" (near or at CF),

"Off" (both below and above CF), "Broad" (broad frequency range including CF), and

"Low" (below CF). Table 4-2 summarizes the number of units found in each category.

The 3rd unit in the 4th row of Fig. 4-17*B* showed typical on-CF inhibition,

although the maximum response shifted to frequencies lower than CF (vertical dashed

line). "Broad" inhibition was primarily observed for choppers (79% of choppers showed

---

[2] Occasionally the increase of response during the process of blocking inhibition was unstable,

presumably determined by drug flow. Since the rate-level function was constantly repeated, it

was possible to choose a relatively large increase of response for comparison with the control.

However, the response area was tested only a few times with small number (10) of repetitions. A

decrease of rate in the response area sometimes occurred that was not in line with the general

increase in rate.

A. Glycinergic
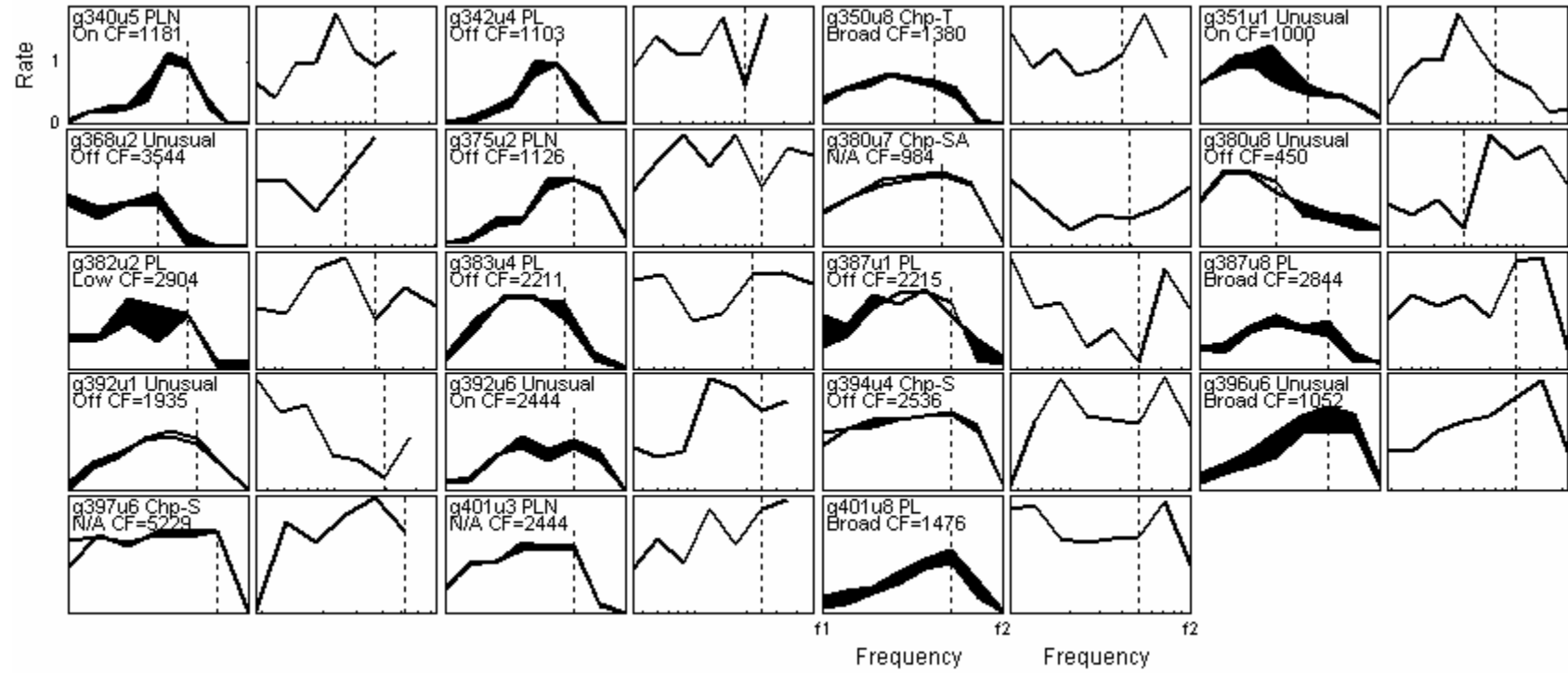
B. GABAergic
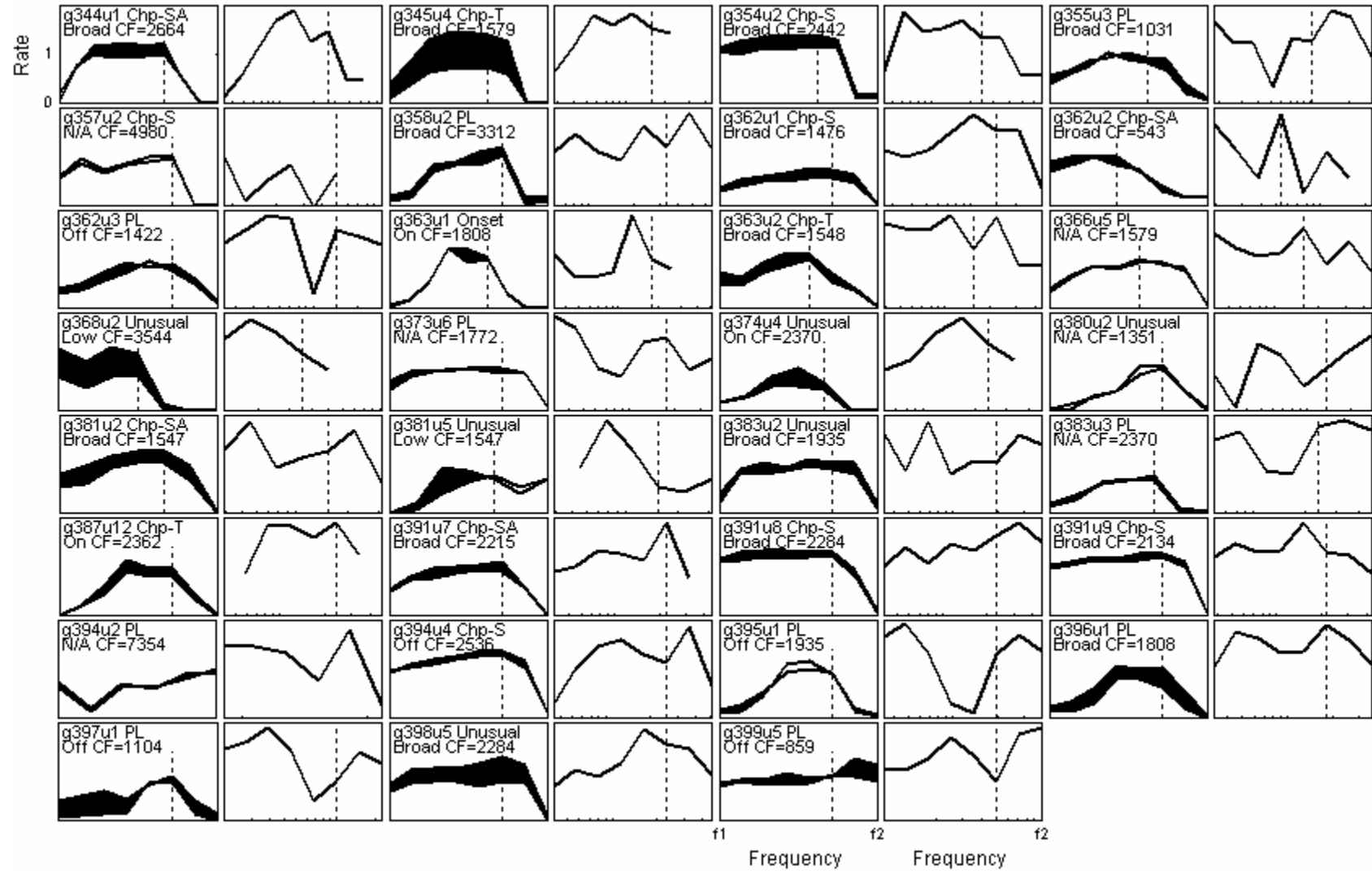
Fig. 4-17 Change of the frequency response area after blocking glycinergic (*A*) or GABAergic (*B*) inhibition. The left-hand panel in each pair shows the response area based on average rate at each frequency (normalized by the maximum control rate) at the highest tone level tested. Shaded areas indicate the increase in rate after blocking inhibition, and unfilled areas indicate decreases in rate. The right-hand panel in each pair shows corresponding d' values at each frequency. For both *A* and *B*, the x axis was the tone frequency, and vertical dashed lines indicate unit CFs. f1, minimum tested frequency (usually –2.5 octave below CF); f2, maximum tested frequency (usually 1.5 octave below CF).

Table 4-2 Summary of the type of inhibition based on changes in the frequency response area.

Cell Type	# of units	On	Broad	Off	Low
PL	13	0	5	7	1
PLN	2	1	0	1	0
Chp-S	6	0	4	2	0
Chp-T	4	1	3	0	0
Chp-SA	4	0	4	0	0
Unusual	11	3	3	3	2
Onset	1	1	0	0	0
Overall	41	6	19	13	3

"Broad" inhibition). Note that choppers tended to show active responses to frequencies that were well below CF and quickly decreased responses to frequencies just above CF, especially for Chp-S units (all Chp-S units showed this low-pass shaped response areas), which limited the examination of inhibitory effects on the high-frequency side.

Sometimes it was difficult to discriminate "On" and "Broad" inhibition, since both types showed a relatively large effect of inhibition around CF. Some of the 5 PLs marked as "Broad" could have been marked as "On" inhibition if our criterion had been slightly different. These two types of inhibition accounted for 63% of total responses (units marked as N/A were excluded). Seven out of 13 "Off"-inhibition units were PLs, and only 2 of 13 "Off"-inhibition units were choppers. "Low" inhibition was less frequently observed, and "High" inhibition was not observed here (the right-most unit in the 2nd row of Fig. 4-17*A* shows inhibition on the high frequency side, but at a lower level it became "Off" inhibition).

4.4   Discussion

4.4.1   Average-discharge rate at CF

Although all positive-effect units showed significant increases in average rate for at least one sound level, blocking GABAergic inhibition had a larger effect on the average rate than blocking glycinergic inhibition (Fig. 4-9). Whether or not a unit received inhibitory inputs was not related to its maximum tone-evoked rate (Fig. 4-13), which was similar to findings in the IC (Beau et al., 1996). The presence or absence of inhibition was more related to the original SR (Fig. 4-14*B*); units that had original SR > 45 sp/sec, which were all PLs, never showed changes in rate after blocking inhibition.

Although rate saturation was frequently observed for primary-like response types (Fig. 4-3), all the control rate-level functions monotonically increased with tone level, whereas Kopp-Scheinpflug et al. (2002) report non-monotonic rate-level functions for half of their pre-potential units (5 of 10 units). After blocking inhibition, the previous study reports that rate-level functions for 2 of the 5 units became monotonic, whereas the others remained non-monotonic. In the present study, the shape of rate-level functions for primary-like response types did not change as dramatically as observed in the previous study. It is possible that the difference between the two studies is mainly caused by different tone durations. The tone duration was 100 msec in the previous study, and 25 msec in the present study. In the next chapter, tone durations of 250 msec were also used; however, the difference in duration was not found to be a factor. The difference between studies could also have been caused by different recording sites. All recorded units in Kopp-Scheinpflug et al. (2002) have pre-potentials, while no pre-potentials were observed in the present study.

As stated earlier, a "positive effect" referred to a significantly increased rate at CF after blocking inhibition. In general, the percentage of units that showed positive effects was smaller in this study than in previous studies in the VCN (Caspary et al., 1979, 1994; Ebert and Ostwald, 1995a). One possible reason for the relatively low percentage of positive-effect units in the present study was the limited range of recording sites and angles (most recorded units had CFs around 1 to 2 kHz). It was possible that units within this area of the AVCN had relatively fewer inhibitory inputs. Another possible reason was the criterion used here for negative-effect units. In Ebert and Ostwald (1995a), units in penetrations that never had a positive effect were discarded (this is also the criterion

used by Beau et al., 1996). Using that criterion, the present study would have had 45%, 74% and 44% of units that showed positive effects after injection of strychnine, bicuculline, and gabazine, respectively.

4.4.2   Frequency response areas

Caspary et al. (1994) find that for both primary-likes and choppers there are more units with on-CF inhibition than off-CF inhibition. The present study also observed more on-CF inhibition (including broad inhibition) than off-CF inhibition, in general (25 on-CF or broad as compared to 16 off-CF). A unique finding here was that most of the off-CF inhibition was exhibited by PLs or PLNs (9 units), and the majority of choppers (12/14) showed on-CF (especially broad) inhibition. The hypothesis in Paolini's study (2005) that sustained choppers receive lateral inhibition and transient choppers receive on-CF inhibition was not supported by the present study.

Note that for most of the off-CF-inhibition units, the rate-level functions did show changes in rate for high sound levels at CF. This was presumably due to the frequency shift of the maximal response with sound level, i.e., at high sound levels, the "no-inhibition" frequency range actually shifted to frequencies lower than CF.

4.4.3   Temporal responses to CF tones for choppers

Changes in the temporal response patterns reflected in the PSTH after blocking inhibition were observed for each AVCN neuron type, and generally agreed with the findings in VCN choppers after injecting GABA (Ebert and Ostwald, 1995b). For

example, the presence of inhibition reduced the number of chopping cycles and slows down the chopping frequency. The previous study reported results for 50-msec tone bursts, including the regularity for the first 20 msec and the last 20 msec. The regularity of sustained choppers decreases most during the last 20 msec, and the sustained choppers become more similar to transient choppers. The regularity of transient choppers, whose chopping patterns only exist within the first 20 msec, decreases most during the first 20 msec. That is, transient choppers become more transient. Therefore, the previous study concludes that (delayed) inhibitory inputs might be responsible for creating the transient pattern, which supports the hypothesis by a chopper modeling study (Banks and Sachs, 1991).

However, as briefly mentioned in the Introduction, using inhibitory receptor agonists to study inhibitory inputs might have some shortcomings. Besides the fact that the injected constant (tonic) inhibition can be different from the actual inhibition received by the neuron, the function of the "excessive" inhibition can be different from the actual inhibition. For example, the modeling study by Hewitt et al. (1993) shows that by varying the parameters of excitatory synapses (e.g., location and strength), transient chopping patterns can be created without inhibitory inputs. Therefore, although adding more inhibition to transient choppers can further reduce the chopping regularity at the early part of the response, we cannot rule out the possibility that the later part of the irregular response was created by excitatory inputs. Results from the present study showed that for all but one transient chopper blocking inhibition only extended the chopping for several millisecond. For these units, excitatory inputs were presumably responsible for creating the transient pattern. For the one exception, the transient chopper became a sustained

chopper after blocking inhibition. There were 3 out of 5 slowly adapting choppers that became sustained choppers after blocking inhibition. However, it should be noted that for each chopper type, a number of units did not show positive effects at all after applying inhibitory receptor antagonists, some of which were recorded in the same penetrations as positive-effect units. Therefore, it was concluded that inhibitory inputs were able to convert chopping response types, but excitatory inputs dominated the determination of chopping types.

Changes of mean FSL for choppers was small (< 0.8 msec), although sometimes this change was significant due to the small variation of FSL for choppers. Palombi and Caspary (1992) report 75% of PVCN units (mostly choppers) that have decreased FSL (they report an average change of 0.5 msec) after blocking GABAergic inhibition. In the IC, a small number of sustained and unclassified units also show reduction of FSL (Beau et al., 1996). The present study found both increased and decreased FSL for choppers after blocking inhibition (Fig. 4-15). For choppers, the FSL indicates the integration time across a large number of inputs (van Gisbergen et al., 1975; Young et al., 1988). The presence of inhibition can only delay the integration time; therefore, the variation of FSL by inhibition is limited. Nevertheless, to account for the decreased FSL by blocking inhibition, the inhibition had to arrive at the same time or earlier than the excitation, which was somehow counterintuitive since, in previous brain-slice studies (e.g., Oertel, 1983; Ferragamo et al., 1998), electrically shocking ANFs always caused delayed IPSPs. It was likely that some source of spontaneously active inhibition was present for the *in vivo* experiments, such as inputs from outside the CN.

4.4.4 Temporal responses to CF tones for primary-likes and unusual/onset types

More diverse changes in the PSTHs were observed for primary-likes and unusual/onset types after blocking inhibition. Some units exhibited relatively constant inhibition over time, and others showed more dramatic changes at certain time points. Labeling studies have shown that both glycinergic and GABAergic endings tend to be located on the dendrites of the stellate cells (Wenthold et al., 1988; Saint Marie et al., 1989), and on the somas of bushy cells. Correspondingly, as stated above, the effect of inhibition on chopper responses was expected to be smooth as a function of time. Prolonged chopping cycles in the presence of inhibition indicated that the temporal summation of a number of small EPSPs to reach the discharge threshold was delayed by a relatively constant hyperpolarization. This hyperpolarization might become stronger over time to change sustained choppers into slowly adapting choppers.

For neurons that have relatively fewer excitatory and inhibitory inputs on the soma and also that have membrane properties that prevent temporal summation (such as spherical bushy cells; Oertel, 1983; Manis and Marx, 1991), the effect of inhibition was less similar to a smooth hyperpolarization. As mentioned earlier, when units exhibited phase locking to tone frequency, blocking inhibition did not cause significant change in the phase of the response. Therefore, the temporal summation must be minimal in these neurons, and inhibition was more likely to remove individual post-synaptic spikes, rather than to delay their timing.

Here units that showed a decrease of FSL of more than 0.8-msec were referred to as units with early inhibition (filled symbols, Fig. 4-15). Blocking inhibition revealed a precisely timed early onset that was not present in the control response for some units. A

strong, constant (tonic) inhibition was not likely to account for this phenomenon because it would have also blocked most of the later responses. These units seemed to receive precisely timed inhibition at the onset. The underlying mechanism for the early inhibition remains a puzzle.

4.4.5 Spontaneous activity

The present study showed insignificant changes in SR for all units after blocking inhibition. The percentage of increase of SR was much higher than that of the sound-evoked rate. However, when the variance was considered (t values), the change in SR was insignificant, and t-values were lower for SR changes than for sound-evoked rate. Most previous studies (Caspary et al., 1979; Ebert and Ostwald, 1995a) report that injecting inhibitory receptor agonists or antagonists has a bigger effect on SR than on the sound-evoked rate for VCN neurons (the variance of SR was not considered), although for neurons in the IC no significant change of SR is observed (Beau et al., 1996).

4.4.6 Other related issues

The present study used both bicuculline and gabazine as GABA receptor antagonists, since bicuculline has been found to have side effects that are not related to GABAergic inhibition (Kurt et al., 2006). The present study did not do a direct comparison between the two chemicals. Some basic properties, such as changes in the chopping patterns, were observed in responses studied after injection of both chemicals.

As discussed in the Results section, some units that showed decreased rate after blocking inhibition were considered to be negative-effect units (if they met one of the two criteria). In other words, in this study decreases in rate were considered to be caused by artifacts. However, if complex neural circuitry existed, such as the local circuit in the CN proposed by Ferragamo et al. (1998, their Fig. 15) including both excitatory interneurons and inhibitory interneurons, or the feedback loop between VCN and PVPO (Thompson and Schofield, 2000), complicated changes in the discharge rate after blocking inhibition would be possible.

In summary, diverse changes in average rate and temporal responses after blocking inhibition were observed in this study. In the future, more control experiments need to be done to address some of the ambiguous results. For example, long-time single-barrel recordings from individual units should be obtained to examine whether the spontaneous activity can vary substantially without injections of any chemical or current.

Chapter V

Influence of Inhibitory Inputs: II. Responses to Complex Sounds

Abstract

This chapter examines the effect of inhibition on responses of AVCN neurons to amplitude-modulated sounds and tones in noise. Some properties of the inhibition, such as whether it was tonic or phasic, delayed or advanced, were analyzed in detail. Rate and temporal metrics described in Chapters II and III were applied to the tone-in-noise responses before and after blocking inhibition. In general, consistent changes in threshold for detection of tone in wideband noise were not found based on any of the metrics. The temporal reliability and the correlation index showed the largest change in thresholds among all the metrics; however, both increased and decreased changes were observed, and the two metrics did not always agree for changes in thresholds of individual units. For the average discharge rate and PSTH fluctuation, blocking inhibition caused significant changes in the values of the metrics, but the changes were similar in size for responses to noise-alone and tone-plus-noise stimuli. For other metrics (synchronization to tone frequency, spike-distance metric), significant effects were not observed.

5.1   Introduction

In the previous chapter, the effect of inhibition on neural responses to pure tones and on spontaneous activity was studied. The results provided some insights about the characteristics of inhibitory inputs received by AVCN neurons. In our daily life, pure tones are seldom presented alone. More often, we hear complex sounds with multiple frequency components. The complex sounds tested in this study, amplitude-modulated stimuli and masked tones, were still simplified sounds compared to music or speech. Nevertheless, if response properties related to certain sound features were always enhanced, weakened, or unaffected by inhibition, the observations may be generalized to more complex sounds.

As described in the previous chapter, the idea of lateral inhibition that enhances frequency contrast is not supported by the majority of AVCN neurons. A focus of previous studies with tones and noise was whether inhibitory inputs enhance temporal contrast, in terms of suppressing spontaneous or background-noise activity more than tone-evoked activity (Ebert and Ostwald, 1995a). The temporal contrast can also refer to more suppression in the sustained activity than in the onset responses (Kopp-Scheinflug, 2002). Caspary et al. (1993) compare broadband-noise responses at different noise levels to CF-tone responses at different tone levels for spherical bushy cells using inhibitory receptor antagonists and agonists. They report that inhibition has similar effects on noise responses and pure-tone responses, which did not support the idea of inhibition enhancing temporal contrast (tone-in-noise stimuli were not used in that study). Ebert and Ostwald (1995a) inject GABA in the PVCN and AVCN and report stronger inhibitory effects on background-noise activity than on tone- or tone-plus-noise-evoked activity,

which supports the temporal-contrast hypothesis. It was unclear whether the disagreement of the two studies was due to different recording sites, different drug applications, or other factors. As mentioned in the previous chapter, applying inhibitory receptor agonists creates a source of constant inhibition, which presumably differs from the actual inhibition received by neurons. For example, if an inhibitory interneuron does not respond actively to noise, no suppression of background-noise activity of the target neuron should be observed. Moreover, the level of the background noise used by Ebert and Ostwald was relatively low (the tone level was approximately 25 dB above discharge threshold; the overall noise level was 10 dB below the tone level, e.g., 0 to 10 dB SPL spectrum level; the noise bandwidth was approximately 20 kHz). The present study applied inhibitory receptor antagonists to AVCN neurons for tone-in-noise responses. The noise level was high (30 dB SPL spectrum level), and the tone levels were close to psychophysical detection thresholds.

Changes in the responses to tones in noise by blocking inhibition can also help to identify the source of the inhibitory inputs. Glycinergic inhibitory neurons in the CN that may project to the AVCN are vertical cells and D-stellate cells (Wickesberg and Oertel, 1988, 1990). Vertical cells respond actively to CF tones, and weakly to broadband noise (Gibson et al., 1985). On the contrary, D-stellate cells respond weakly to CF tones, but actively to broadband noise (Rhode and Greenburg, 1994). Therefore, the difference in the effect of inhibition on tones and noise might provide clues about the type of inhibitory neurons. Responses properties of other inhibitory interneurons, especially those located in the SOC, are unclear.

The influence of inhibition on the temporal measures discussed in Chapters II and III was examined in this chapter. Since fewer tone levels and repetitions were used here due to time limitations during the experiments, detection performance of these temporal measures was not compared to psychophysical thresholds. Rather, the focus was to examine whether detection performance changed after blocking inhibition. These detailed temporal measures have not been analyzed in previous iontophoretic studies of AVCN neurons.

Apart from tone and noise stimuli, responses to sinusoidally amplitude-modulated (SAM) tones have also been studied for neurons in the PVCN and DCN while blocking or enhancing inhibition (Backoff et al., 1999). Inhibition enhances the synchronization to the stimulus envelope, especially at low and mid modulation frequencies. The present study tested changes in neural responses to SAM tones in the AVCN after blocking inhibition. For units that showed decreased synchronization to amplitude modulation after blocking inhibition, more detailed analysis was made to identify tonic vs. phasic inhibition.

5.2   Methods

The experimental design was the same as used in the previous chapter, and the data was obtained together with the pure-tone responses described in the previous chapter (from 38 animals). Here complex sounds, two amplitude-modulated stimuli (sinusoidally amplitude-modulated tones and two-tone stimuli) and the tone-in-noise stimuli, were applied before, during and after the iontophoretic injection of glycine or GABA receptor antagonists. Among the 89 units tested with CF tones, only units that showed positive

effects (52 units) were further tested with the three complex stimuli (48 units were tested

with sinusoidally amplitude-modulated tones, 35 were tested with two-tone stimuli, and

47 were tested with tones in noise).

5.2.1   Sound stimuli

Two types of amplitude-modulated stimuli were used. One was the sinusoidally

amplitude-modulated (SAM) tone with carrier frequency equal to the neuron's CF and

modulation depth equal to 100%. The level of the carrier was 20 dB above the neuron's

pure-tone threshold. Another amplitude-modulated stimulus was created by adding two

equal-amplitude tones with frequencies symmetrically placed above and below CF on a

logarithmic scale[3]. The levels of both tone components were 20 dB above the neuron's

pure-tone threshold. Both amplitude-modulated stimuli had 5-msec cosine-squared ramps

and durations of 600 msec, repeated every 1 sec, for 6 to 8 trials. In each trial, several

modulation frequencies were arranged from low to high (e.g., from 16 Hz to 1024 Hz)

with 1-octave steps. Modulation transfer functions based on average rate and synchrony

for both amplitude-modulated stimuli were obtained.

The tone-in-noise stimulus was similar to that used in Chapter II, except that only

a noise spectrum level of 30 dB SPL was used and fewer tone levels were tested here.

The noise was randomly created and frozen for each dataset, and thus varied across tests

(and before and after blocking inhibition).

---

[3] The second type of amplitude-modulated stimulus was called a two-tone stimulus here. It should
be pointed out that the traditional "two-tone stimulus" used in studies related to two-tone
suppression or lateral inhibition usually has one tone at CF; the frequency of the other tone is
varied to map out suppressive or inhibitory sideband regions.

5.2.2   Same-frequency inhibition and excitation (SFIE) model

Chapter II provides the details of the SFIE model (Nelson & Carney, 2005), a model of neurons at auditory levels higher than the AVCN. Here the model was tested with input spikes that were recorded from AVCN cells before and after iontophoretic injections. Briefly, the model received excitatory and delayed inhibitory inputs from the same AVCN neuron. Spike times from 30 to 50 repetitions for each AVCN neuron in response to noise-alone or tone-plus-noise stimuli were used as both excitatory and inhibitory inputs for the model. The neuron model was a conductance-based integrate-and-fire model (see details in Chapter II). The average discharge rate of the model cell generally represented the PSTH fluctuation of the input AVCN neuron.

5.3   Results

5.3.1   Responses to sinusoidally amplitude-modulated (SAM) tones

Forty-eight positive-effect (based on pure-tone responses) units were further tested with SAM-tone stimuli (19 and 30 units for glycine and GABA receptor antagonists, respectively). Figures 5-1 to 5-3 show changes in the rate (r-MTF) and sync (s-MTF) modulation-transfer functions after blocking inhibition for different types of units. Primary-like response types generally showed flat r-MTFs and relatively flat s-MTFs (Fig. 5-2). Choppers showed low-pass (9 units), high-pass (6 units), band-pass (2 units) shaped or flat (1 unit) r-MTFs. Of course, these shapes can be dependent on the range of modulation frequency tested with respect to the unit's individual characteristics (the choice of the range of modulation frequency was limited by frequency boundary in the calibration table). Half of the choppers showed band-pass shaped, and the other half

394u4 Chp-S Gly

397u6 Chp-S Gly

354u2 Chp-S Gab

357u2 Chp-S Gab

362u1 Chp-S Gab

391u8 Chp-S Gab

391u9 Chp-S Gab

394u4 Chp-S Gab

343u5 Chp-T Gly

350u8 Chp-T Gly

345u4 Chp-T Gab

363u2 Chp-T Gab

387u12 Chp-T Gab

380u7 Chp-SA Gly

344u1 Chp-SA Gab

362u2 Chp-SA Gab

381u2 Chp-SA Gab

391u7 Chp-SA Gab

Rate

Sync

16   512   16   512

Mod freq (Hz)   Mod freq (Hz)

Fig. 5-1 Rate (odd-numbered columns) and synchrony (even-numbered columns) modulation-transfer function (MTF) for choppers.

For rate MTFs, shaded areas indicate increased average rate after blocking inhibition. For sync MTFs, shaded areas indicate decreased

synchronization to modulation frequency after blocking inhibition. The y-axis of the synchrony plots is from 0 to 1. The y-axis of the

rate plots was from 0 to a value slightly larger than the maximum rate. Gly, blocking glycinergic inhibition. Gab, blocking

GABAergic inhibition.

Fig. 5-2 Rate (odd-numbered columns) and synchrony (even-numbered columns) modulation-transfer function (MTF) for PLs and PLNs with the same format as Fig. 5-1.
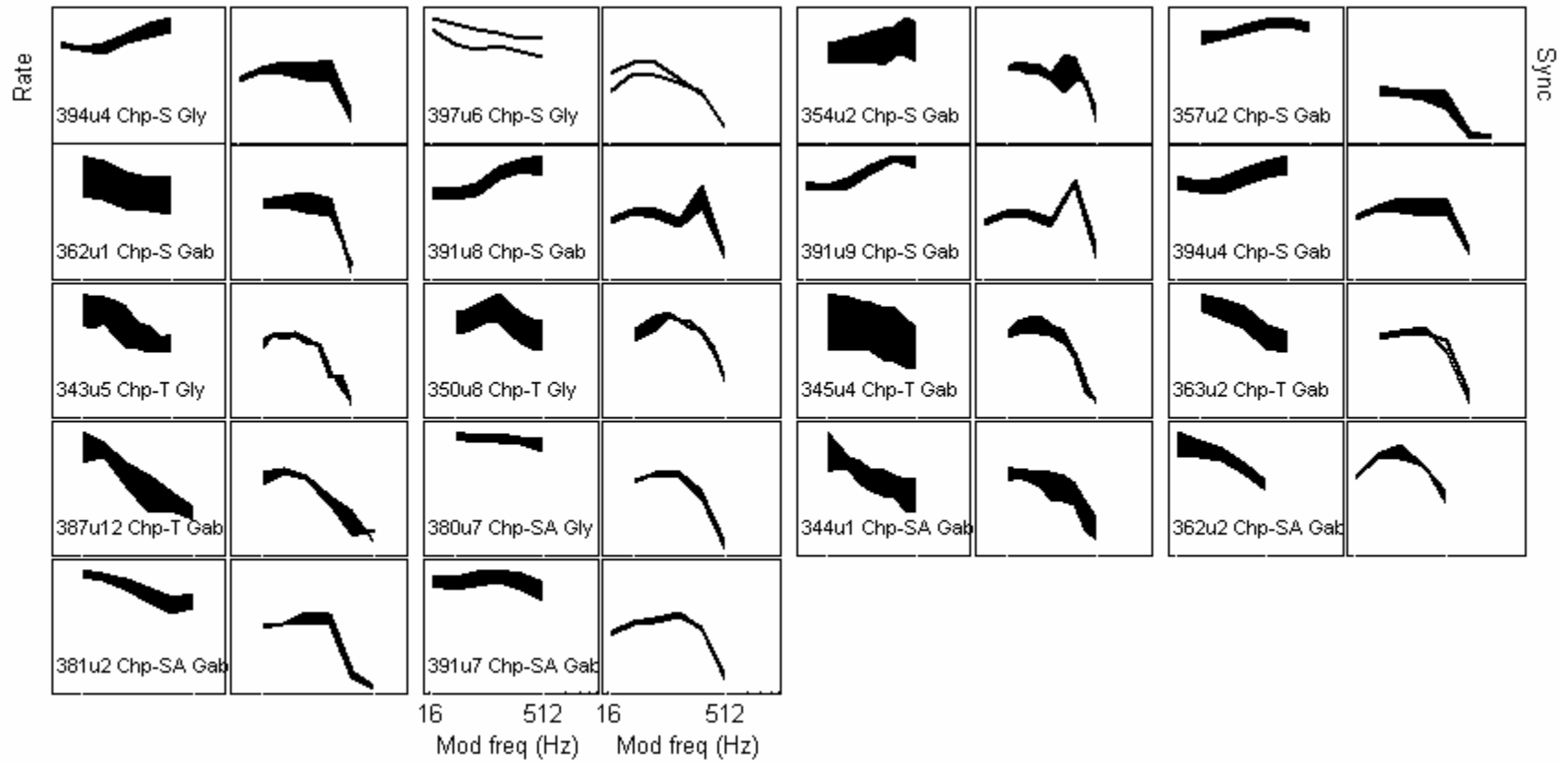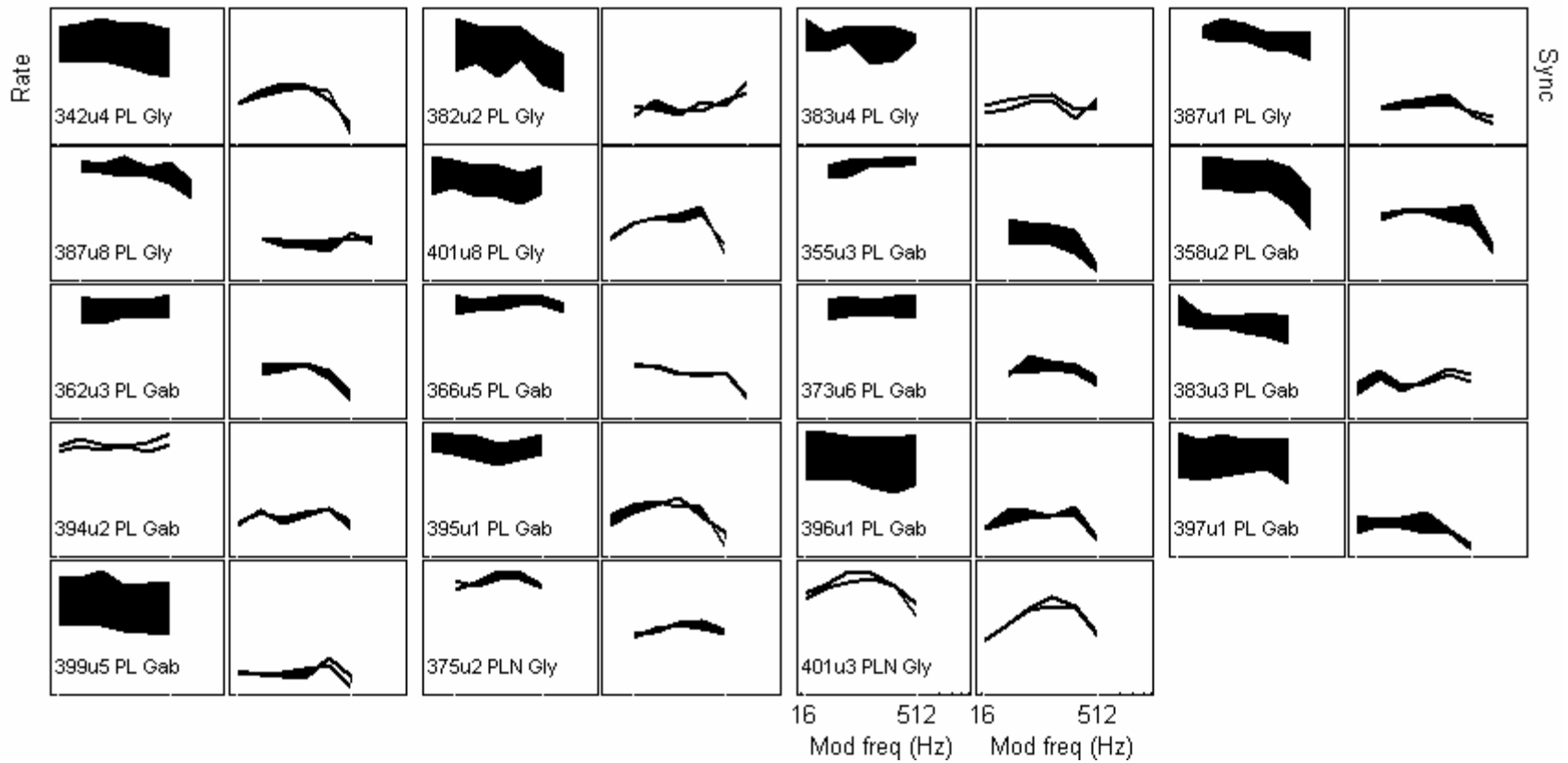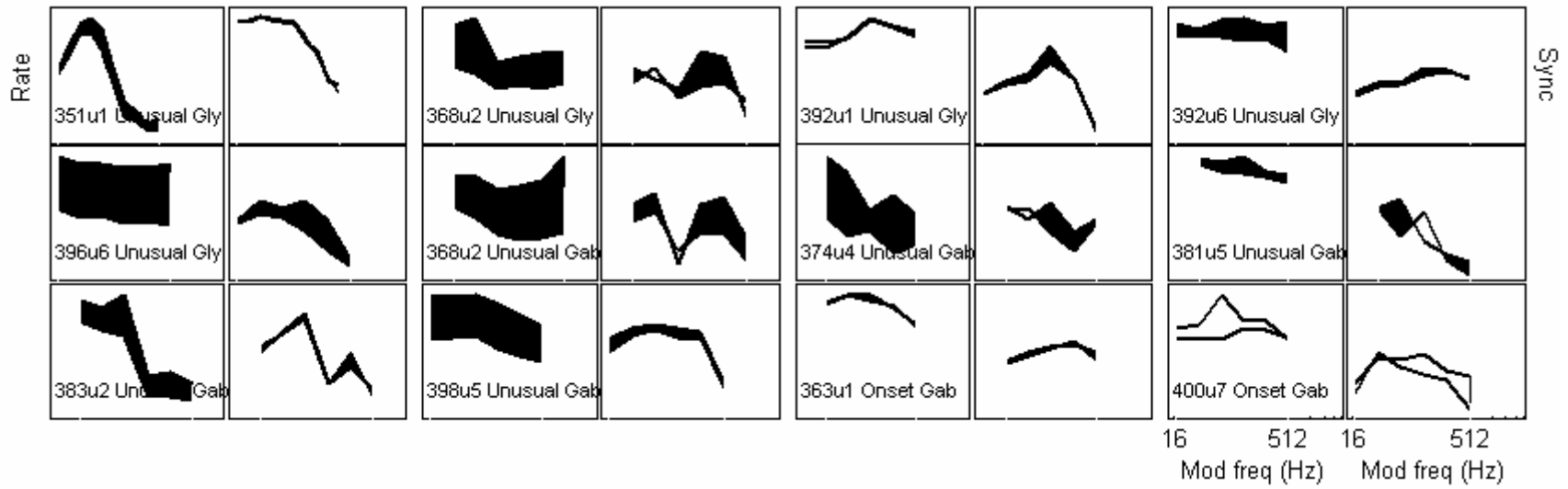
Fig. 5-3 Rate (odd-numbered columns) and synchrony (even-numbered columns) modulation-transfer function (MTF) for unusual/onset units with the same format as Fig. 5-1.

showed low-pass shaped s-MTFs (Fig. 5-1), with maximum synchronies higher than those of primary-likes. The r-MTFs and s-MTFs of unusual/onset response types had more diverse shapes than the basic shapes described above (Fig. 5-3).

After blocking glycinergic and GABAergic inhibition, 14 out of 20 and 26 out of 31 units showed significantly increased rate ($p < 0.05$; Figs. 5-1 to 5-3, shaded areas in r-MTFs). Different degrees of synchrony reduction were observed (Figs. 5-1 to 5-3, shaded areas in s-MTFs; since it was difficult to test the significance of synchrony reduction, units were not classified into decreased or unchanged synchrony groups; the amount of reduction will be presented later). A direct correlation between the amount of rate change and synchrony change did not exist for all response types: for the 18 choppers, the correlation coefficient between maximum rate increase and maximum synchrony decrease was significant (0.70, $p < 0.05$); for the 19 primary-likes and the 12 unusual/onset response types, the correlation was insignificant (0.16 and 0.27, respectively). Figure 5-4 shows two examples of SAM-tone responses. The PL (top) had a rate increase but no change of synchrony. The chopper (bottom) had increased rate and decreased synchrony. Figure 5-5 shows the population changes of synchrony (decrease) and rate (increase). The x-axis is the maximum t values across modulation frequencies (the t values were computed in the same way as Eqn. 4-3 except that the tone level was replaced by modulation frequency). The vertical line indicates the criterion for t to be significant ($p < 0.05$). With similar amounts of rate increase measured by t values, different units showed various amounts of decrease in synchrony. A general observation was that blocking GABAergic inhibition (open symbols) had a larger effect on synchrony than blocking glycinergic inhibition (filled symbols).
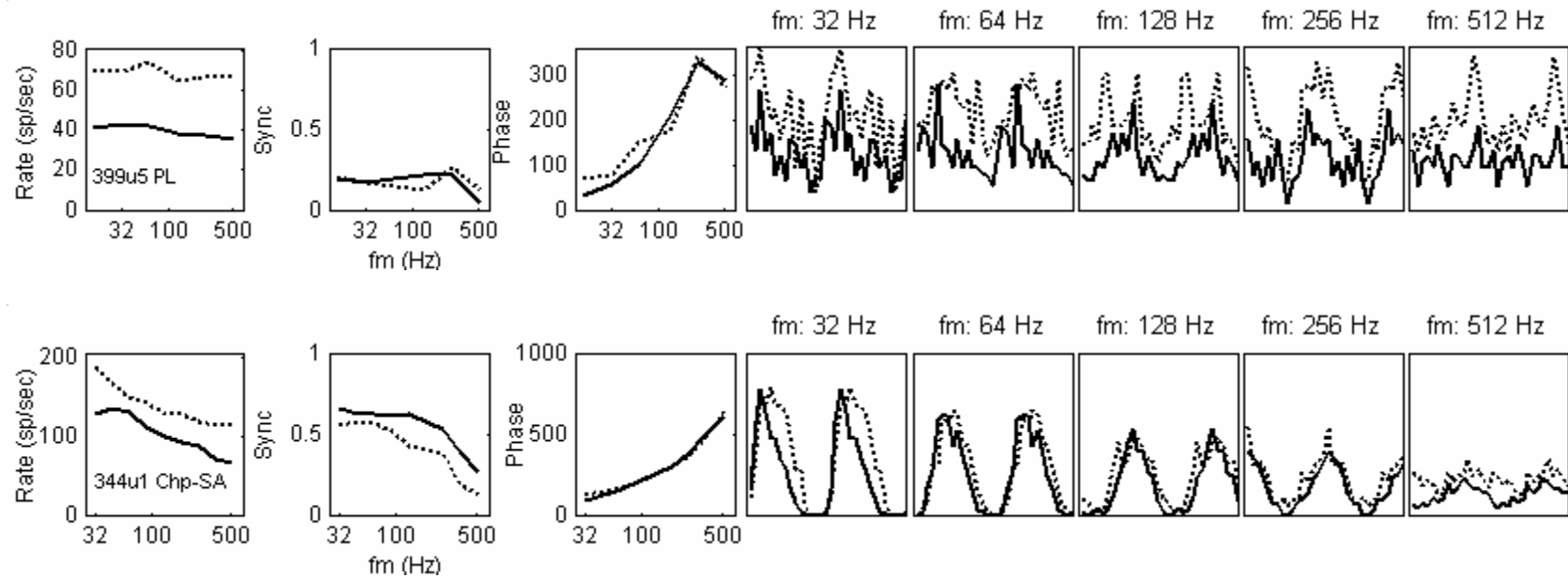
Fig. 5-4 SAM-tone responses of a primary-like (top) and a chopper (bottom) before and after blocking GABAergic inhibition. The left-most two columns plot r-MTF and s-MTF, respectively. The 3rd column plots the phase in degree. Period histograms at different modulation frequencies are plotted on the right (two identical cycles are shown for each fm to provide a better view). Solid (dotted) lines are responses before (after) blocking inhibition.

Fig. 5-5 Synchrony decrease vs. rate increase (in terms of t values) for SAM-tone responses. The x-axis is the maximum t values across modulation frequencies. The y-axis is the maximum decrease of synchrony. Filled symbols indicate units with application of glycine antagonists. Open symbols indicate units with application of GABA antagonists. The vertical line indicates the criterion for t to be significant ($p < 0.05$).

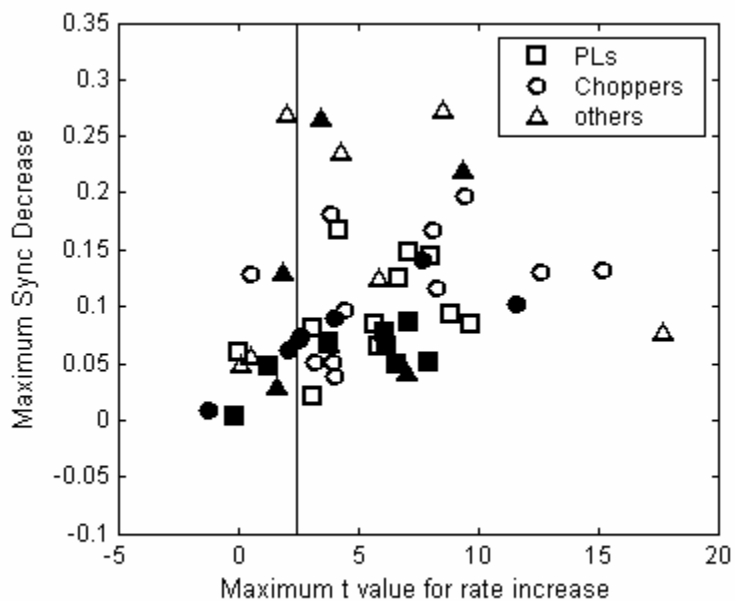Figure 5-4 (3rd column) also shows the change in phase to the amplitude modulation. In general, the largest change in phase occurred at low modulation frequencies. Figure 5-6A shows the change in phase at fm = 32 Hz, a relatively low modulation frequency, for all recorded units. Units that showed increased phase after blocking inhibition (above the dotted line) received inhibition that affected the later part of the response more than the early part of the response in each cycle for fm = 32 Hz. All 13 choppers showed increased phase after blocking GABAergic inhibition (open circles); the rest of the units showed mixtures of increased and decreased phase.

For the 14 units that showed early inhibition (Chapter IV, Fig. 4-15), 12 of them were tested with SAM tones. To examine whether units with early inhibition showed decreased phase (i.e., whether early inhibition had more effect on the early part of the response in each cycle), Fig. 5-6*B* marks the phase changes for units with early inhibition with filled symbols (glycinergic and GABAergic inhibition were not differentiated here). Eight out of 12 early-inhibition units showed decreased phase after blocking inhibition. Thus, for these units, the inhibition generally discharged earlier than the excitation throughout the response. Four early-inhibition units showed invariant or increased phase. For these units, the inhibition was mainly early at the onset responses.

5.3.2   Tonic vs. phasic inhibition

Based on the period histograms of the second example in Fig. 5-4, for fm = 32 Hz blocking inhibition changed the shape of the histogram. In other words, within a modulation cycle, inhibition was stronger at certain stimulus phases. This type of inhibition is referred to as phasic inhibition. Inhibition that was relatively constant across

A.
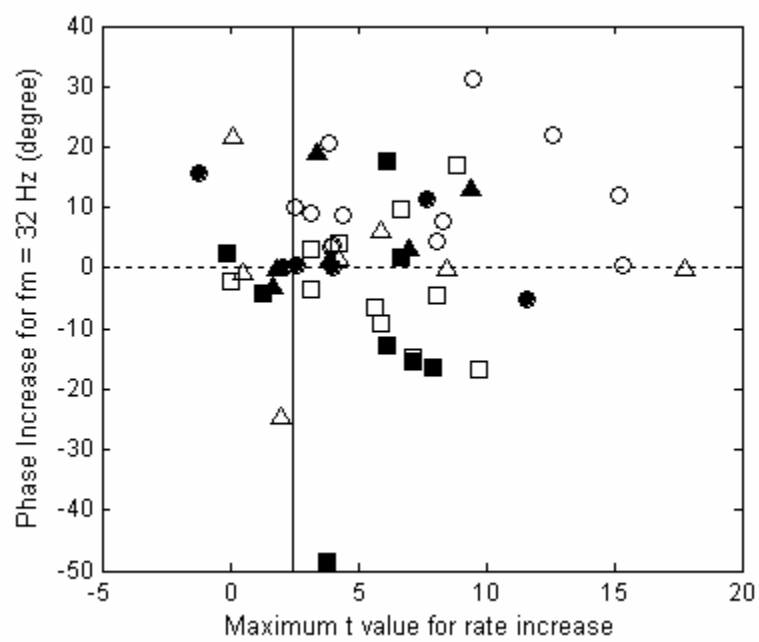
B.
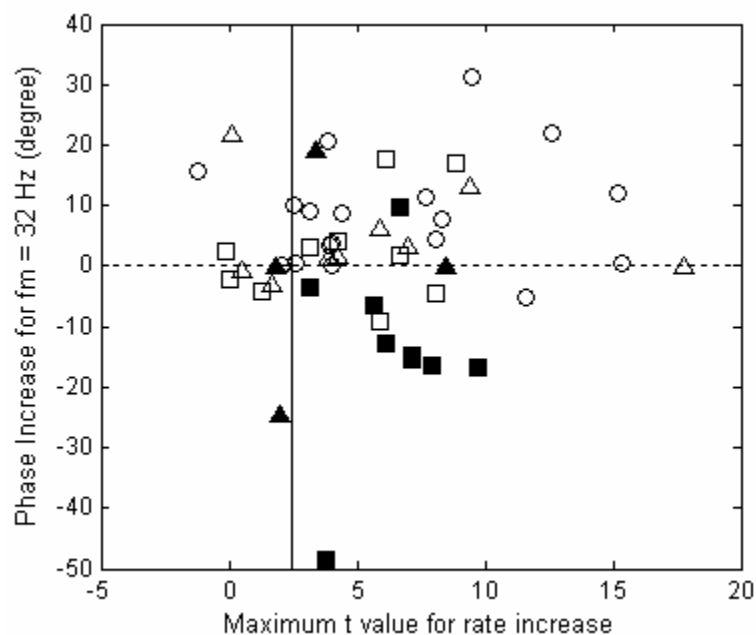
Fig. 5-6 Change of phase vs. change of rate for fm = 32 Hz. The x-axis is the maximum *t* values across modulation frequencies. The y-axis is the increase of phase in degree. In *A*, filled symbols indicate units with application of glycine antagonists. Open symbols indicate units with application of GABA antagonists. In *B*, filled symbols indicate units with early inhibition (see Fig. 4-15). The vertical line indicates the criterion for *t* to be significant (*p* < 0.05).

time is referred to as tonic inhibition. Note that tonic inhibition did not necessarily mean that the inhibitory interneuron discharged constantly all the time. The neuron was likely to be tuned and phase-locked to modulation frequency, since at low modulation frequencies (e.g., fm = 32 Hz) approximately 85% units showed change in phase (Fig. 5-6*A*); however, after possible filtering effect by the dendrites of the target neuron, the locking of the inhibitory neuron's response to the envelope of the modulated stimulus can be too smooth to observe.

To test whether the inhibition was tonic or phasic, simulated tonic inhibition was added to the SAM-tone responses recorded after blocking inhibition. Specifically, a constant value was subtracted from a period histogram so that the remaining number of spikes was equal to the number of spikes before blocking inhibition for a particular modulation frequency. Because the increase of rate by blocking inhibition can be different for different modulation frequencies, the subtracted constant value was varied with modulation frequency, based on the assumption that the tonic inhibition was tuned to modulation frequency. Figure 5-7*A* (top) shows the SAM-tone responses of a primary-like unit before and after blocking GABAergic inhibition. After subtracting out a simulated tonic inhibition, the rate difference disappeared, whereas the synchrony difference remained (Fig. 5-7*A*, bottom). For this unit, a constant inhibition was not capable of predicting the observed change in synchrony. On the contrary, in Fig. 5-7*B*, a constant inhibition predicted most of the difference in synchrony except at high modulation frequencies. Of course, this manipulation can also create an increase in synchrony (8 units), as shown in Fig. 5-7*C*; the increase in synchrony was also an effect of phasic inhibition.

A. Control and blocking GABAergic inhibition
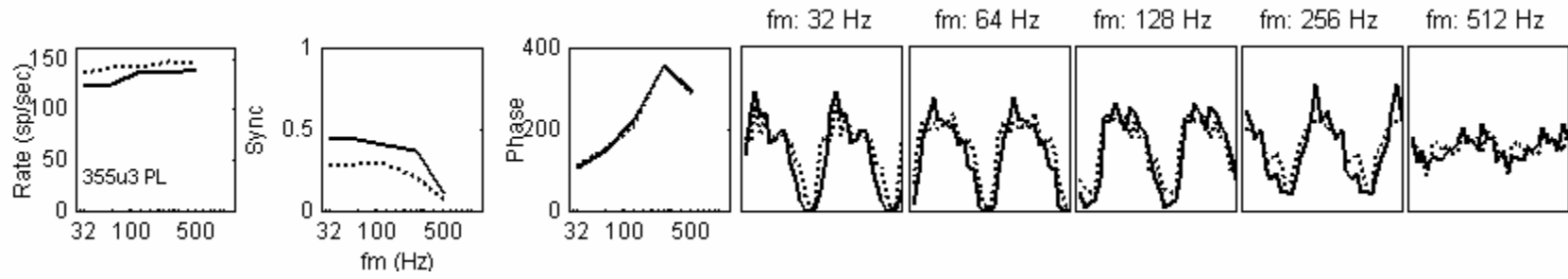
Control and blocking GABAergic inhibition (with simulated tonic inhibition)
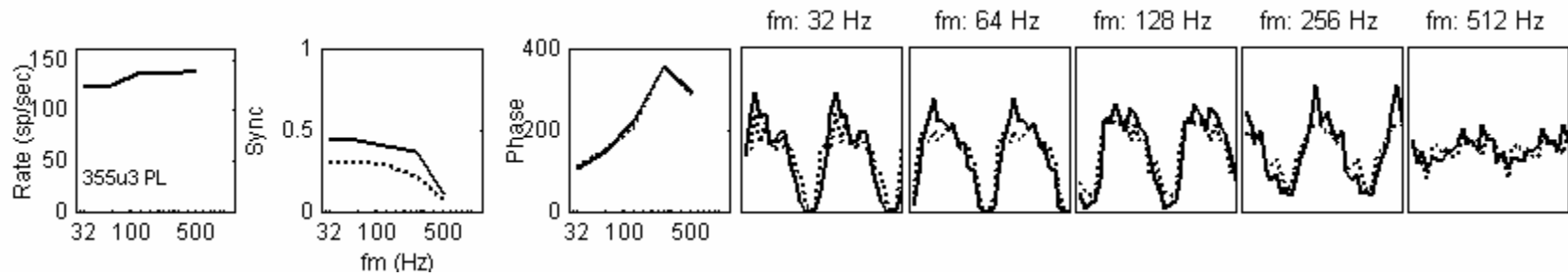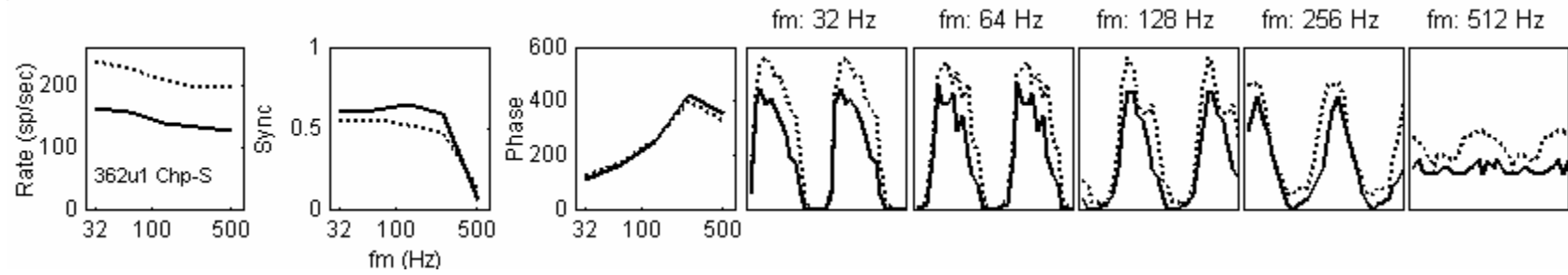
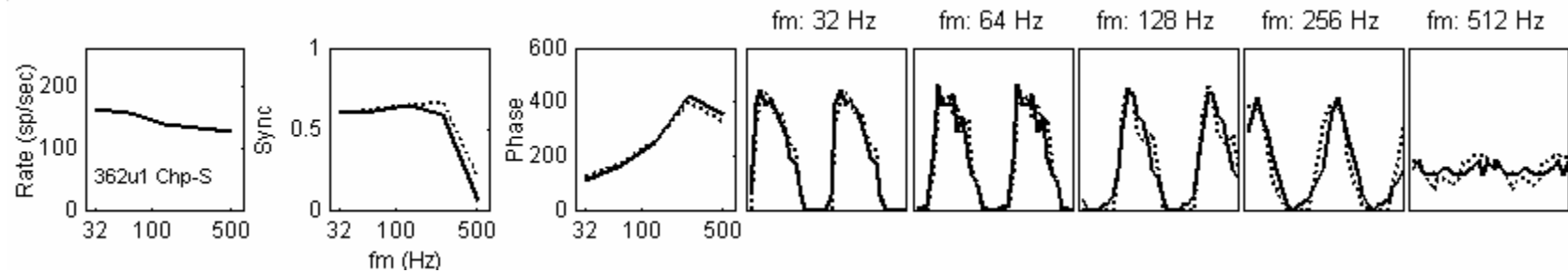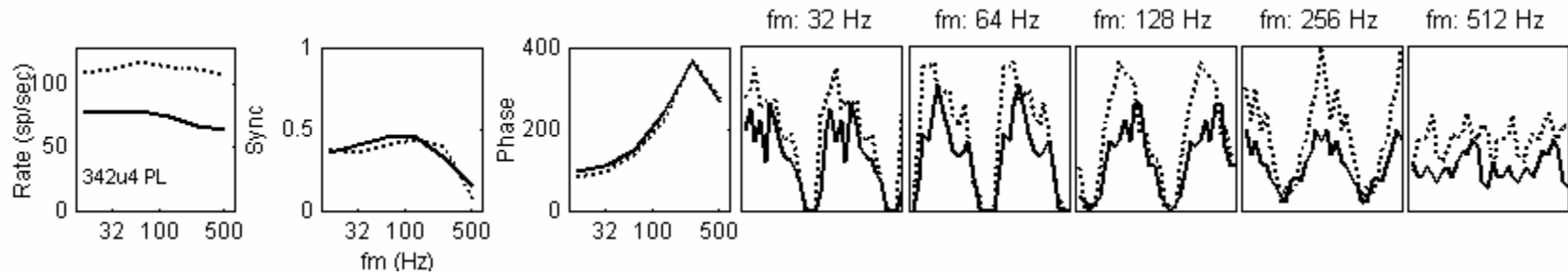## B. Control and blocking GABAergic inhibition

Control and blocking GABAergic inhibition (with simulated tonic inhibition)

C. Control and blocking glycinergic inhibition

Control and blocking glycinergic inhibition (with simulated tonic inhibition)
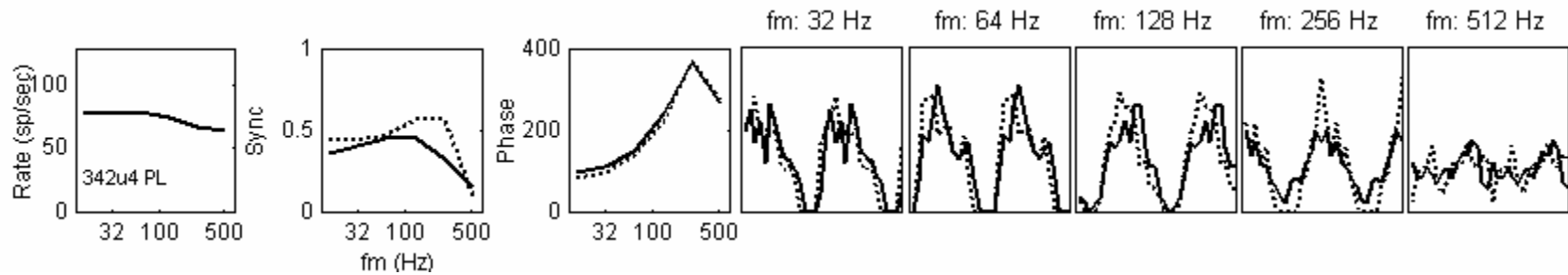
Fig. 5-7 Applying simulated tonic inhibition on 3 units. *A*, a primary-like. *B*, a sustained chopper, C, a primary-like.

Figure 5-5 shows the maximum synchrony change for each unit studied with SAM tones; the maximum change could occur at either low or high modulation frequencies. As mentioned above, distinct phasic inhibition usually occurred only at low modulation frequencies. To test tonic vs. phasic inhibition, the maximum synchrony change can bias the result depending on the corresponding modulation frequency (fm^0). Therefore, changes occurred at all modulation frequencies lower than fm^0 were considered. Figure 5-8 shows the effect of adding simulated tonic inhibition on the average difference of synchrony between control responses and responses after blocking inhibition. For all but 1 chopper, the difference of synchrony between control and blocking inhibition can be more or less accounted for by subtracting constant activity, especially for choppers injected with GABA receptor antagonists (open circles). Combining the results from Fig 5-8 with Fig. 5-6*A*, which shows increased phase at fm = 32 Hz for all choppers after blocking GABAergic inhibition, the following conclusion can be made. The GABAergic inhibition received by choppers were highly smoothed, and probably delayed[4]. At very low modulation frequencies, phasic properties can be observed. At mid and high modulation frequencies, the inhibition appeared to be tonic. This conclusion agrees with the hypothesis in Chapter IV, which was also consistent with in vitro studies (Wenthold et al., 1988; Saint Marie et al., 1989) (see Discussion, 4.4.4). It was unclear about the effect of glycinergic inhibition on choppers, since the sample size was small (6 units) and the observation varied.

---

[4] The "delay" can either be a synaptic delay or a smoothing effect.
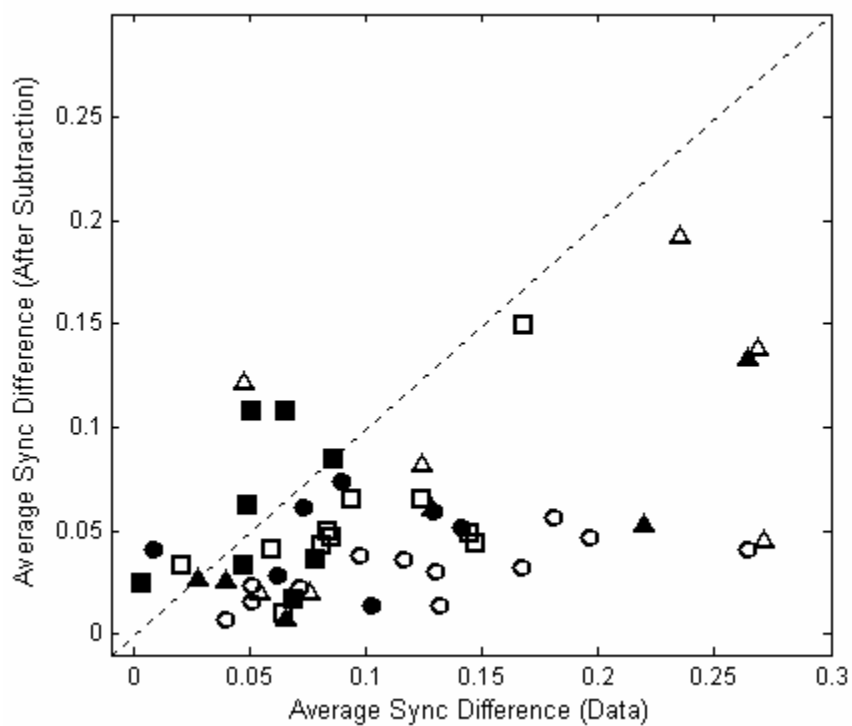
Fig. 5-8 Synchrony difference with simulated tonic inhibition vs. synchrony difference after blocking inhibition. First, the modulation frequency that had maximum synchrony decrease with blocking inhibition (fm^0) was identified. Then the average change of synchrony at all modulation frequencies lower than and equal to fm^0 was computed. Filled symbols indicate units with application of glycine antagonists. Open symbols indicate units with application of GABA antagonists.

5.3.3 Responses to two tones

Thirty-five positive-effect (based on pure-tone responses) units were further

tested with two-tone stimuli (10 and 26 units for glycine and GABA receptor antagonists,

respectively). The two-tone stimuli were similar to the SAM tones except that they

lacked a carrier frequency at CF. Fig. 5-9 shows the two-tone responses of the two units

for which SAM-tone responses were shown in Fig. 5-4. The changes in rate and

synchrony after blocking GABAergic inhibition were generally similar for responses to

both types of amplitude-modulated stimuli[5]. A major difference was that the decrease of

synchrony after blocking inhibition was generally smaller for two-tone responses than for

SAM-tone responses. Figure 5-10 compares the effect of inhibition on synchrony for

these two types of amplitude-modulated stimuli for all recorded units. No units showed

decreases in synchrony of more than 0.2 for two-tone stimuli (Fig. 5-10 right), while 5

unusual and 1 chopper unit showed reduction in synchrony of more than 0.2 for SAM-

tone stimuli (Fig. 5-10 left).

5.3.4 Tone-in-noise: average discharge rate

Forty-seven positive-effect (based on pure-tone responses) units were further

tested with tone-in-noise stimuli (20 and 31 units for glycine and GABA receptor

antagonists, respectively). The example shown in Fig. 5-11*B* represented the observations

---

[5] The maximum synchrony to two-tone stimuli was always lower than the maximum synchrony to
SAM-tone stimuli because the two-tone envelope was broader than the SAM-tone envelope
within each modulation cycle.
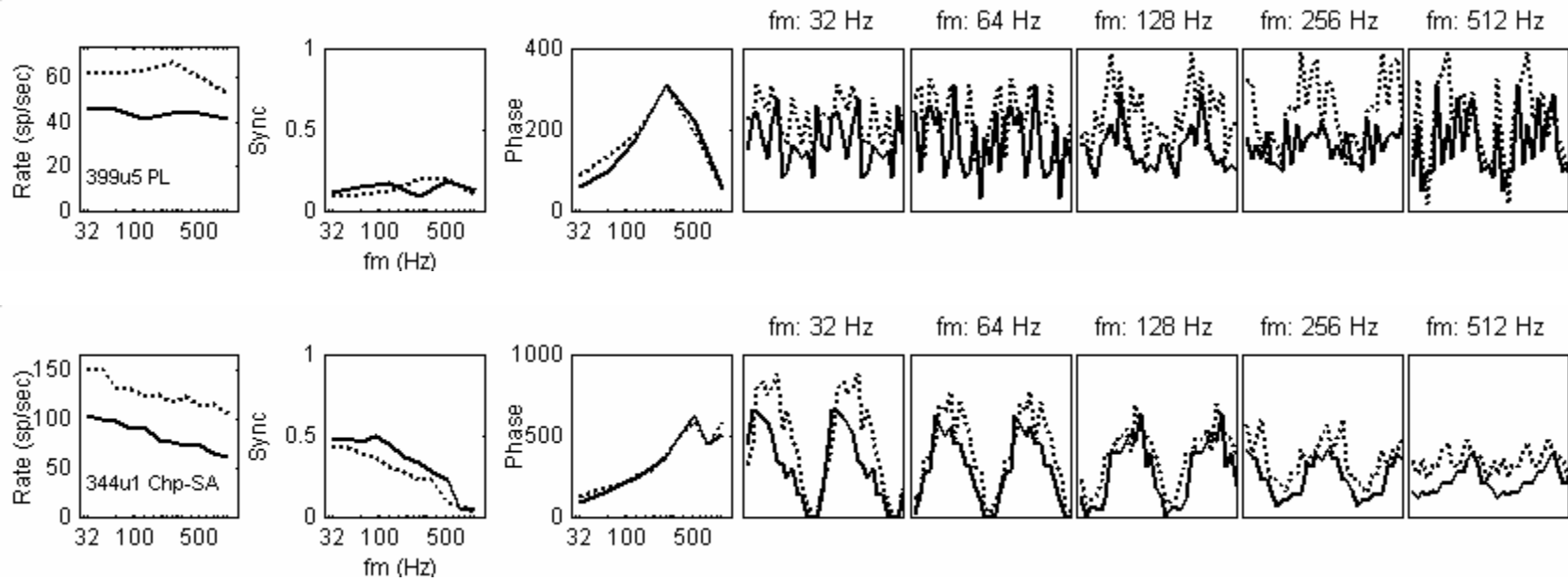
Fig. 5-9 Two-tone responses of a primary-like (top) and a chopper (bottom) before and after blocking GABAergic inhibition. The SAM-tone responses of these two units are plotted in Fig. 5-4.
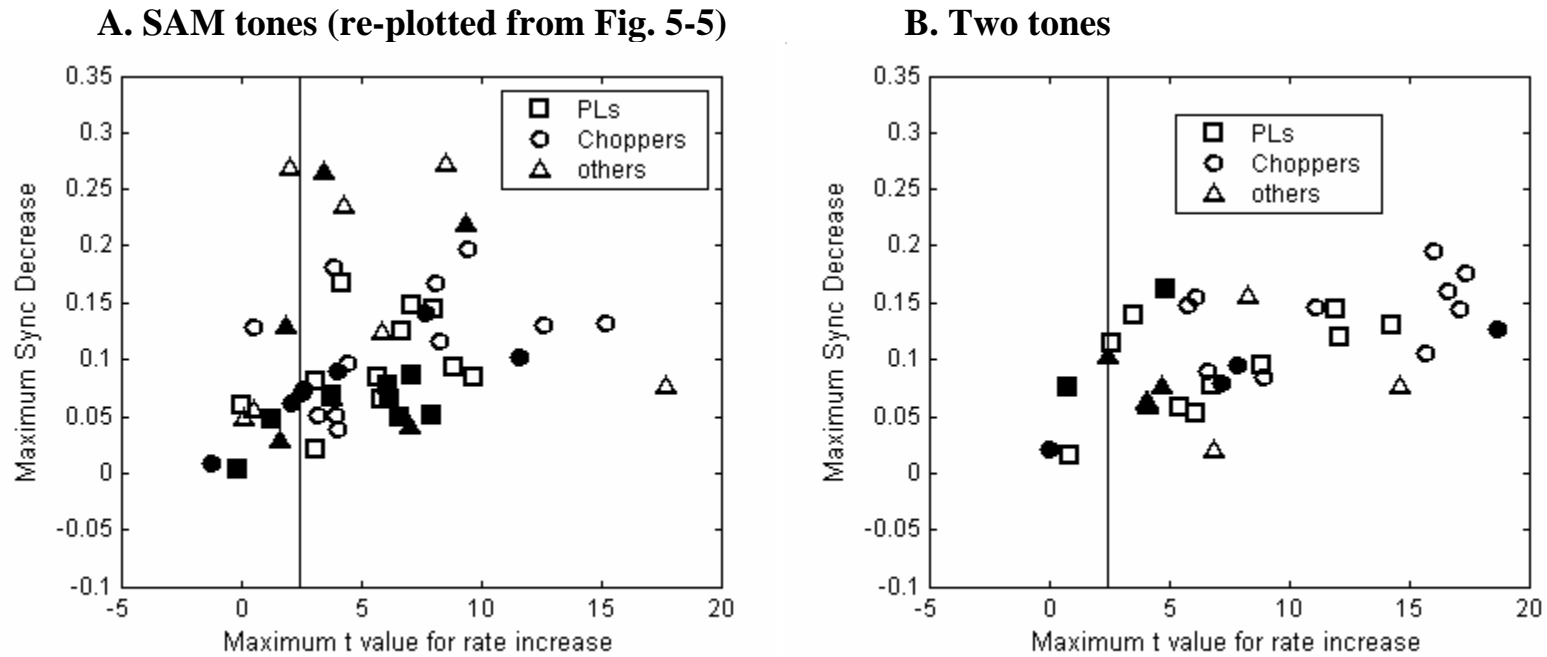
Fig. 5-10 Synchrony decrease vs. rate increase for SAM-tone responses (left) and two-tone responses (right) in the same format of Fig. 5-5. Filled symbols indicate units with application of glycine antagonists. Open symbols indicate units with application of GABA antagonists.

A.
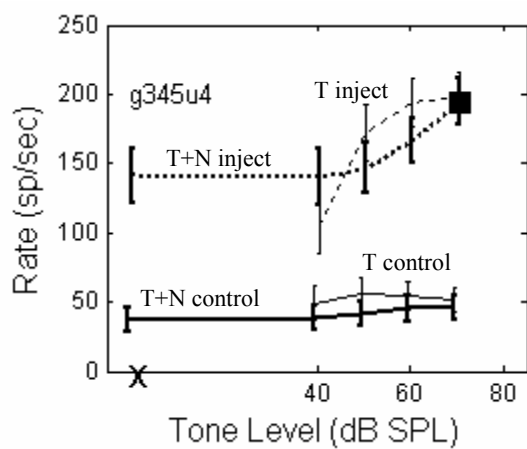
B.
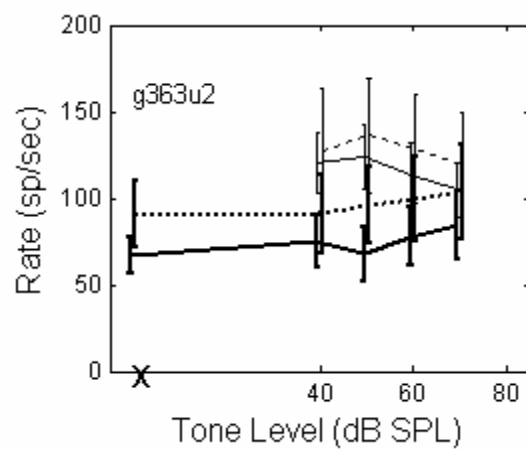
C.
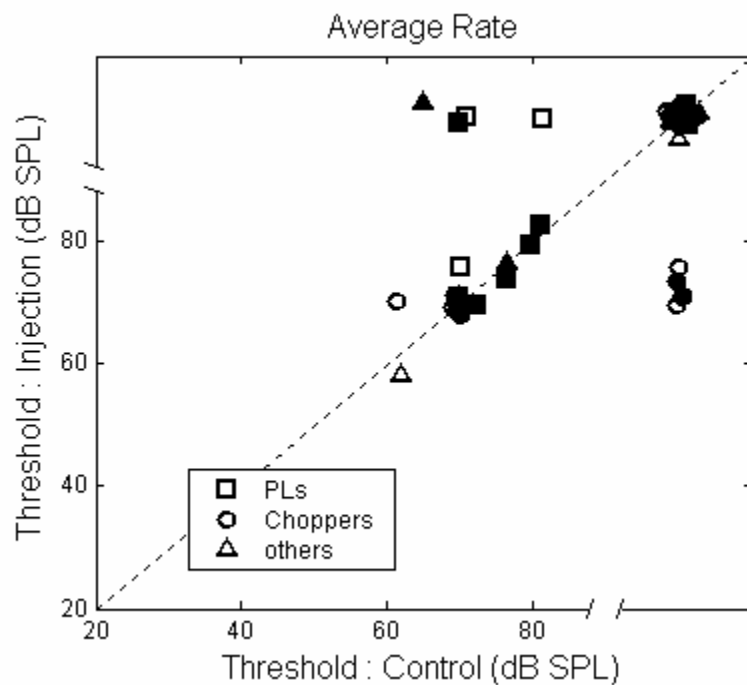
Fig. 5-11 *A* and *B*, Average discharge rates for tones in noise (T+N) and same-duration

tones (T) before and after blocking GABAergic inhibition for two choppers. Small jitters

are added in the tone levels to avoid overlapping of errorbars. *C*, detection thresholds

based on average rate before and after blocking inhibition for all units. Broken points on

axes mark the boundaries between measurable and un-measurable thresholds. For the

purpose of illustration, small jitters drawn from a Gaussian distribution with standard

deviation of 1 dB SPL were added to each threshold. Filled symbols indicate units with

application of glycine antagonists. Open symbols indicate units with application of

GABA antagonists.

of most AVCN neurons that the average rate increased by similar amount at different

tone levels when there was a 30-dB-SPL (spectrum level) noise after blocking inhibition

(thick lines). This kind of change was called "parallel change" (Caspary et al., 1993).

Occasionally, the detection threshold based on average rate changed, as shown in Fig. 5-

11*A*. Detection thresholds based on average rate for all units are plotted in Fig. 5-11*C*.

Ten out of 53 units showed threshold change[6], with 1 unit showing a 10-dB increase and

the other 9 units difficult to quantify since either before or after blocking inhibition the

thresholds were unmeasurable (when the thresholds were measurable, they were at the

highest sound level tested). Specifically, after blocking inhibition, 4 out of 31 primary-

likes or unusual/onset response types showed threshold increases from the highest level

tested to unmeasurable thresholds, 5 out of 22 choppers showed thresholds decrease from

the unmeasurable thresholds to the highest level tested, and 1 out of 22 chopper showed a

threshold increase from 60 to 70 dB SPL. Because of the small sample size of units with

changed thresholds, it was not possible to determine whether the difference in direction

of the response changes for different response types would be generally true.

Figure 5-11 *A* and *B* also show the average rate in response to long-duration pure

tones (250 msec; longer than the tones tested in the previous chapter, but same as the

duration of the tone-plus-nose stimuli; thin lines). If an inhibitory interneuron responded

actively to broadband noise but weakly to tones (as expected for D-stellate cells; Rhode

and Greenburg, 1994), blocking inhibition should increase responses to noise more than

to tones. On the contrary, if an inhibitory interneuron responded weakly to broadband

---

[6] There was one PL that showed threshold increase from 70 to 75 dB SPL. This was not

considered to be a real threshold increase, since the testing tone levels were mistakenly offset by

5 dB after blocking inhibition.

noise but actively to tones (as expected for vertical cells, Gibson et al., 1985), blocking inhibition should increase responses to tones more than to noise. Because tone responses were recorded at different tone levels, the maximum response was used for comparison to noise-alone responses. Figure 5-12 shows rate increases to noise-alone vs. to tone-alone stimuli after blocking glycinergic (filled symbols) or GABAergic inhibition (open symbols). Given that a 10% (arbitrarily selected) higher rate increase in either noise or tone responses was used as an indication of a stronger response to one of the two stimuli, 24 units (47%) showed stronger responses to noise (above the diagonal), 5 units (10%) showed stronger responses to tones (below the diagonal), and the other 22 units (43%) showed less than 10% rate increase for either stimulus (close to the diagonal). No obvious difference was observed for different types of antagonists.

5.3.5 Tone-in-noise: temporal measures

a. Synchronization to tone frequency

Synchronization to tone frequency was generally unaffected after blocking inhibition, as shown by the example in Fig. 5-13. The small decrease of synchronization after blocking inhibition was presumably due to increased baseline activity. Only 2 (PLs) out of 53 units showed changes in detection thresholds (a 10-dB decrease) after blocking inhibition based on synchrony to the tone frequency.

b. PSTH fluctuation

After blocking inhibition, 88% of AVCN units showed more than 10% decrease of PSTH fluctuation (a significance test was unavailable since no variance was obtained
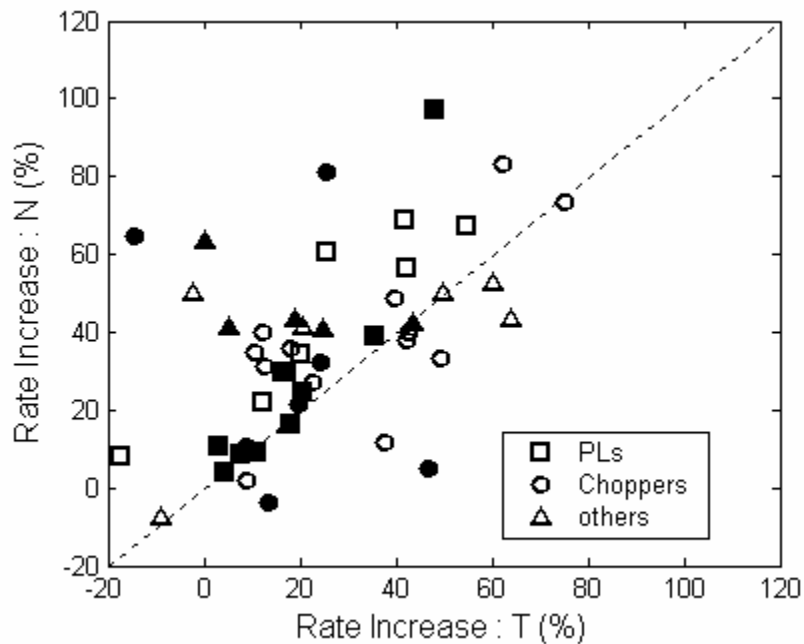
Fig. 5-12 Percentage of rate increase for the maximum tone-alone responses across tone

level (T) vs. percentage of rate increase for noise alone (N). Filled symbols indicate units

with application of glycine antagonists. Open symbols indicate units with application of

GABA antagonists.
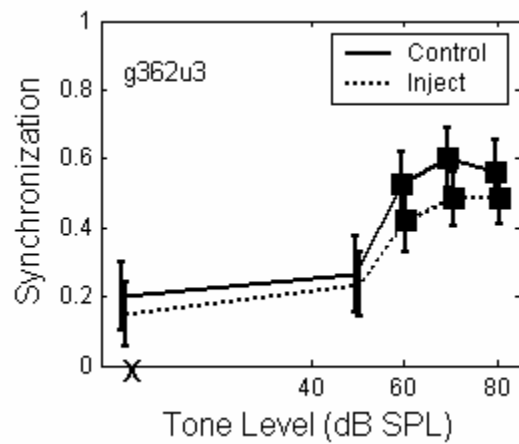
Fig. 5-13 Synchronization to tone frequency for tones in noise (T+N) before and after blocking GABAergic inhibition for a primary-like. Small jitters are added in the tone levels to avoid overlapping of errorbars.

for the PSTH fluctuation). Figure 5-14 *A* and *B* show two examples, both of which showed a decrease in PSTH fluctuation (left column) of a relatively constant amount across tone levels, except at the highest level for the second unit (*B*). Figure 5-14*C* shows the PSTHs of the second unit's noise-alone responses before (top) and after (bottom) blocking GABAergic inhibition. There were more spikes after blocking inhibition, and the fluctuation in the PSTH was also less obvious after blocking inhibition.

As in Chapter II, no detection threshold was defined for the PSTH fluctuation; instead, detection thresholds were measured with the SFIE model. The average rate of the model, which decreased with increasing tone level, was similar to the PSTH fluctuation. However, since no normalization of input rate was included in the model as it was in the measures of PSTH fluctuation (see Chapter II), the model rate was sometimes affected by the input rate. For example, the first chopper (Fig. 5-14*A*) showed an increase in rate from approximately 20 sp/sec to 80 sp/sec in response to noise alone after blocking inhibition. Consequently, when these responses were used as inputs to the SFIE model, the model rate was actually higher after blocking inhibition, even though the PSTH fluctuation was reduced. Nevertheless, the model still showed a decrease in rate with increasing tone level.

Detection thresholds based on SFIE model rate are plotted in Fig. 5-14*D*. After blocking inhibition, 42% of units showed increased or decreased thresholds (no obvious difference was observed with different types of antagonists). As described above, changes in model detection thresholds did not necessarily reflect threshold changes based purely on changes in PSTH fluctuation, which changed in a parallel manner for tone-in-

A.
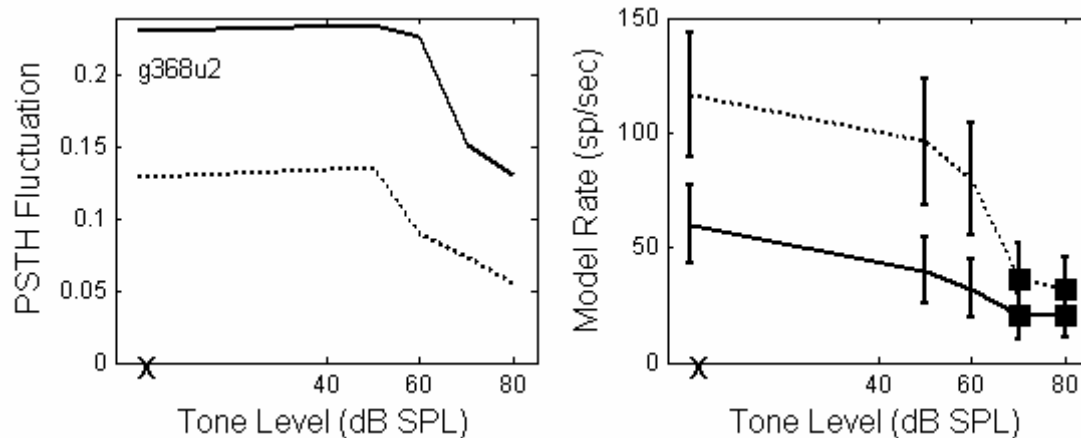
B.
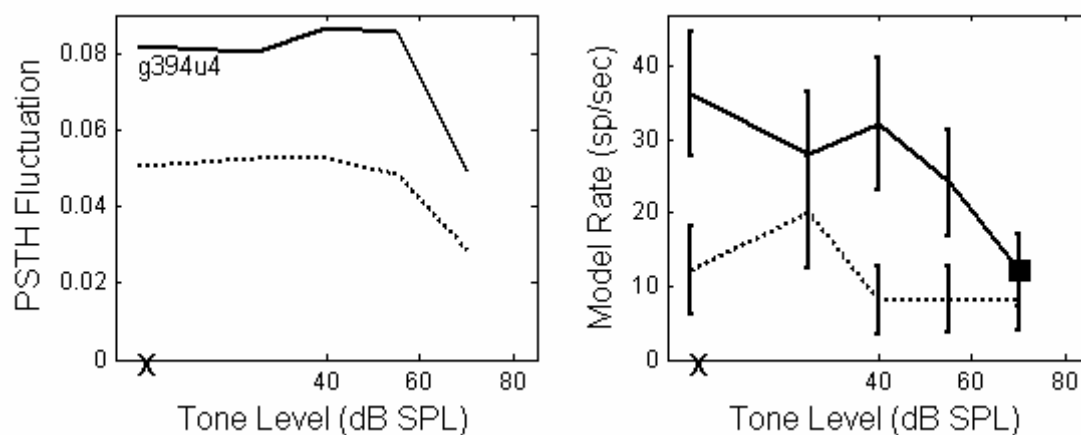
C.
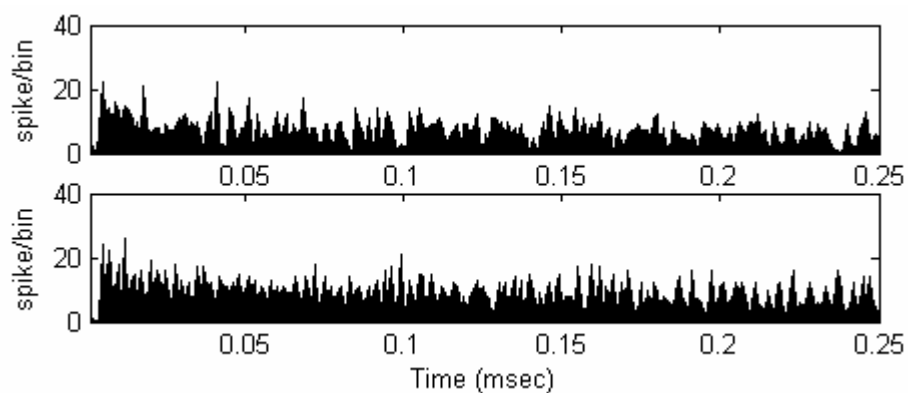
D.
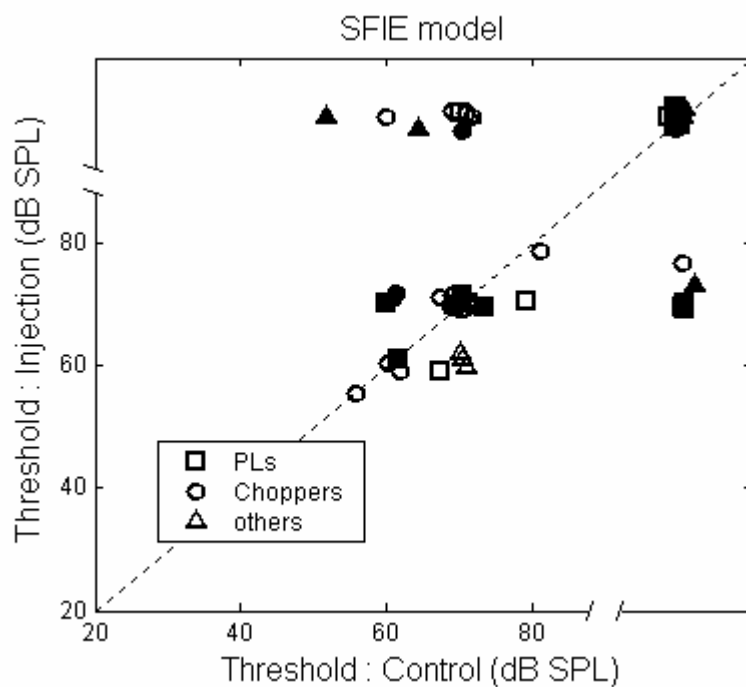
Fig. 5-14 *A* and *B*, PSTH fluctuation (left) and SFIE model rate (right) for tones in noise before and after blocking GABAergic inhibition for two choppers. *C*, PSTHs of the unit shown in *B* in response to noise alone before (top) and after (bottom) blocking inhibition. Resolution = 1 msec. *D*, detection thresholds based on SFIE model rate before and after blocking inhibition for all units, in the same format as Fig. 5-11*C*.

noise and noise-alone stimuli. The discharge rate of the SFIE model was also affected by changes in average rate.

The fluctuation of PSTHs is presumably caused by locking to the envelope of the "effective stimulus" (Louage et al. 2004; see Chapter II). The finding that inhibition enhances PSTH fluctuation seemed to agree with the enhancement of synchronization to amplitude modulation described earlier in this chapter. However, there was no significant correlation between the amount of reduction in PSTH fluctuation and in modulation synchronization (the correlation coefficients between the maximum decrease of envelope slope across tone levels and the maximum decrease of synchrony to SAM tones were 0.02 and 0.40 after blocking glycinergic (16 units) and GABAergic inhibition (28 units), respectively.

c. Temporal reliability and correlation index

Temporal reliability (Chapter II) and correlation index (Chapter III) measured the consistency of discharges across repetitions of a stimulus, and both metrics decreased with tone level. Although they generally agreed with each other, predicted detection thresholds based on the two metrics can be different. Fig. 5-15 shows the change of temporal reliability (top two) and correlation index[7] (bottom) for a primary-like response type after blocking glycinergic inhibition. The detection threshold based on temporal reliability decreased from 70 to 60 dB SPL, whereas the detection threshold based on

---

[7] In Chapter 3, two temporal resolutions, 0.2 and 0.6 msec, were used for the correlation index. Since the detection performance was similar using these two resolutions, in this chapter only 0.6 msec was used.
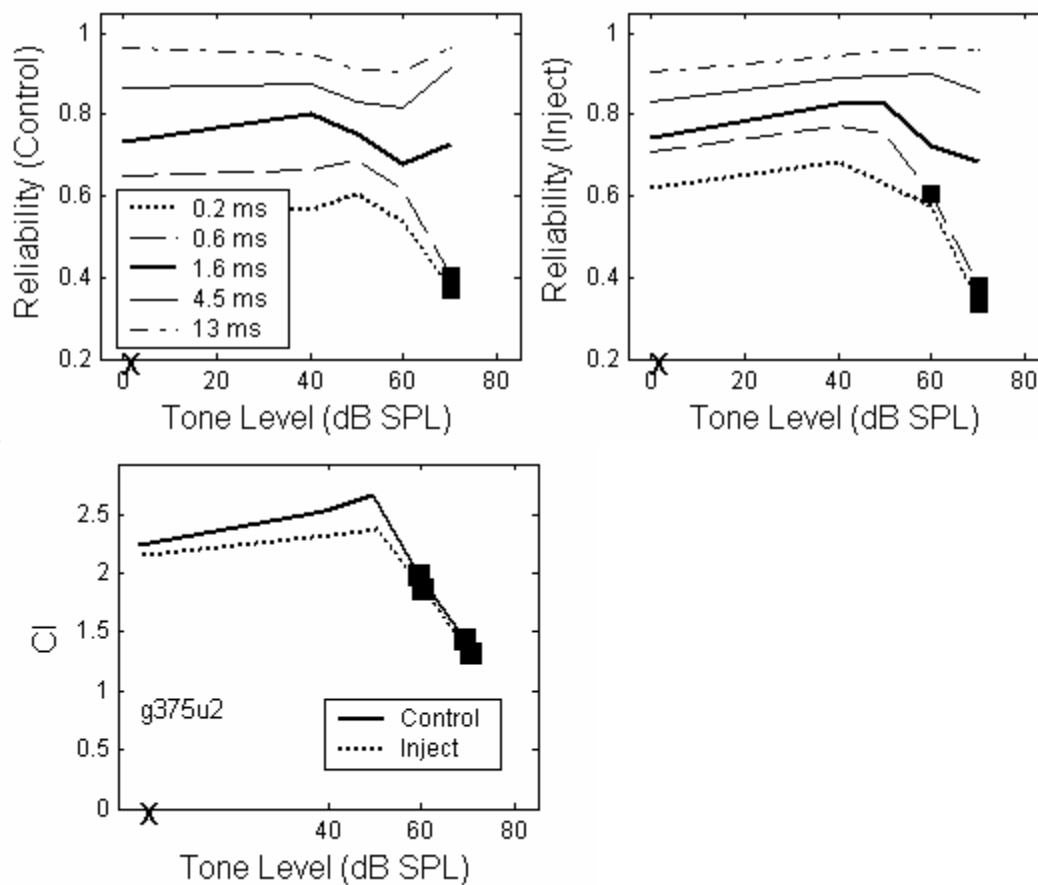
Fig. 5-15 Temporal reliability (top panels) and correlation index (CI, bottom) for a primary-like-with-notch unit before and after blocking glycinergic inhibition. The temporal resolution used for the correlation index was 0.6 msec.

A.
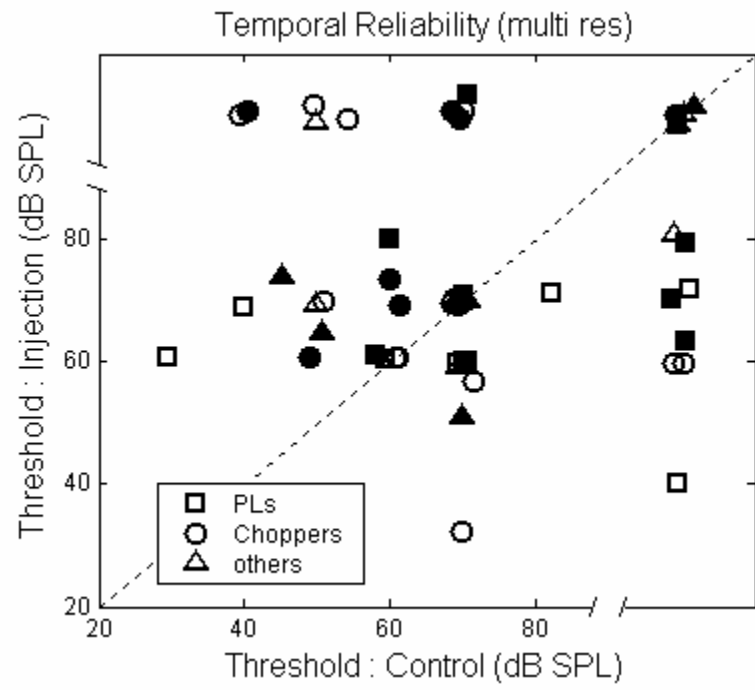
B.
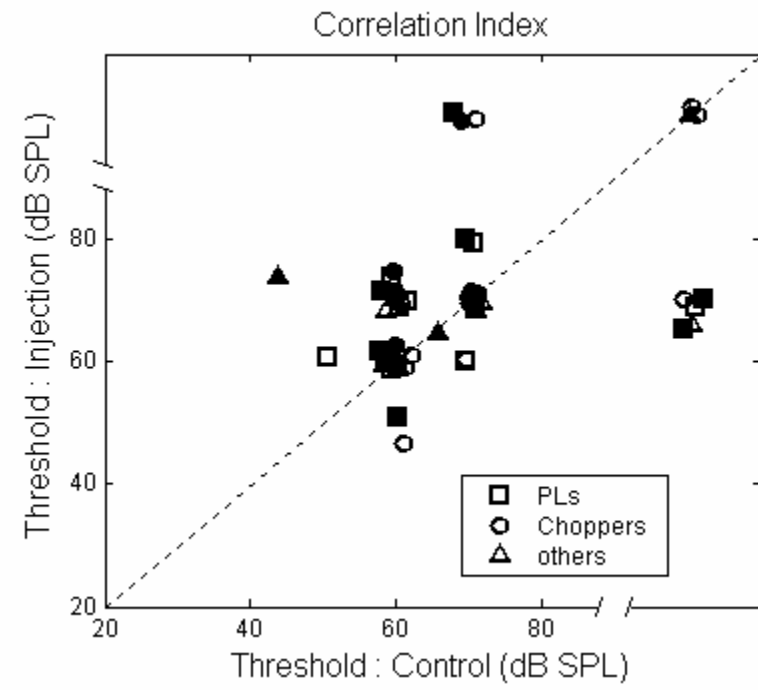
C.
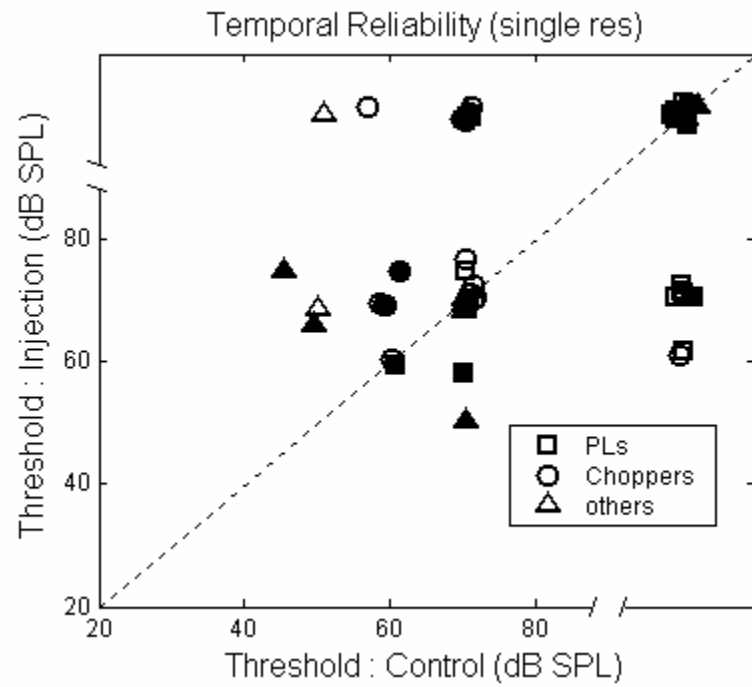
Fig. 5-16 Detection thresholds before and after blocking inhibition based on temporal reliability (*A*, *C*) and correlation index (*B*) in the same format as Fig. 5-11*C*. Detection thresholds plotted in *A* were obtained with multiple temporal resolutions (0.2, 0.6, 1.6, 4.5 and 13 msec). Detection thresholds plotted in *C* were obtained with single temporal resolutions (0.6 msec).

correlation index was always 60 dB SPL. Figure 5-16 *A* and *B* compare the change of

detection thresholds after blocking inhibition based on the two metrics for all units. A

higher percentage of units (66%; all response types) showed threshold changes based on

temporal reliability (*A*) than based on correlation index (*B*, 51%; all response types).

Threshold changes based on the temporal reliability (the mean of the absolute threshold

change was 20 dB, excluding units with unmeasurable thresholds before or after blocking

inhibition) were larger than those based on the correlation index (the mean of the absolute

threshold change was 10 dB, excluding units with unmeasurable thresholds before or

after blocking inhibition). Since the detection threshold based on temporal reliability was

the minimum threshold across 5 temporal resolutions (Chapter II), while the correlation

index was only tested with one resolution (0.6 msec), the temporal reliability analysis

was repeated with only one resolution, 0.6 msec (Fig. 5-16*C*). Changes in the detection

thresholds based on temporal reliability for a single temporal resolution were reduced

(Fig. 5-16*C*; the mean of the absolute threshold change was 13 dB, excluding units with

unmeasurable thresholds before or after blocking inhibition) and became comparable to

the detection thresholds based on correlation index (Fig. 5-16*B*). No obvious difference

was observed with different types of antagonists.

d. Spike distance

Spike distance measures the dissimilarity between two spike trains in terms of

spike timing with respect to stimulus onset (Victor and Purpura, 1996, 1997). The mutual

information based on the spike distance quantifies the efficiency of spike timing in

coding a set of stimuli at different temporal resolutions (Victor and Purpura, 1996, 1997;

Chase and Young, 2006). Figure 5-17 shows three examples of how blocking inhibition affected the spike-timing coding efficiency. Approximately 30% of units (including all major neuron types) showed the largest change with the average-rate coding ($q = 0$), as represented by Fig. 5-17A. The change of mutual information based on average rate did not necessarily indicate threshold change; rather, it measured the separations between tone levels based on the mean and variance of rate. The other 70% of units showed basically no change in the shape of the mutual-information curve, as illustrated by the example in panel B. Exceptions were 3 units (1 PL, 1 chopper, 1 unusual) that showed large increases or decreases of mutual information with $q \neq 0$ after blocking inhibition, as illustrated by the example in panel C. In general, information carried by the spike distance metric was not affected by blocking inhibition.

5.4   Discussion

5.4.1   Synchronization to stimulus envelope

The present study examined the effect of inhibition on the synchronization of neural discharges to stimulus envelope using two types of stimuli, amplitude-modulated stimuli and tones in noise. The amplitude-modulated stimuli included commonly used SAM tones, which had a carrier fixed at CF, and two-tone stimuli. Significantly increased average rate was observed for more than 70% of the units, and different degrees of synchrony reduction were also observed after blocking inhibition. These findings agreed with a previous study in the PVCN and DCN (Backoff et al., 1999). In general, GABAergic inhibition was found to be more effective in enhancing synchrony than glycinergic inhibition. This enhancement was not always caused by a cycle-by-cycle
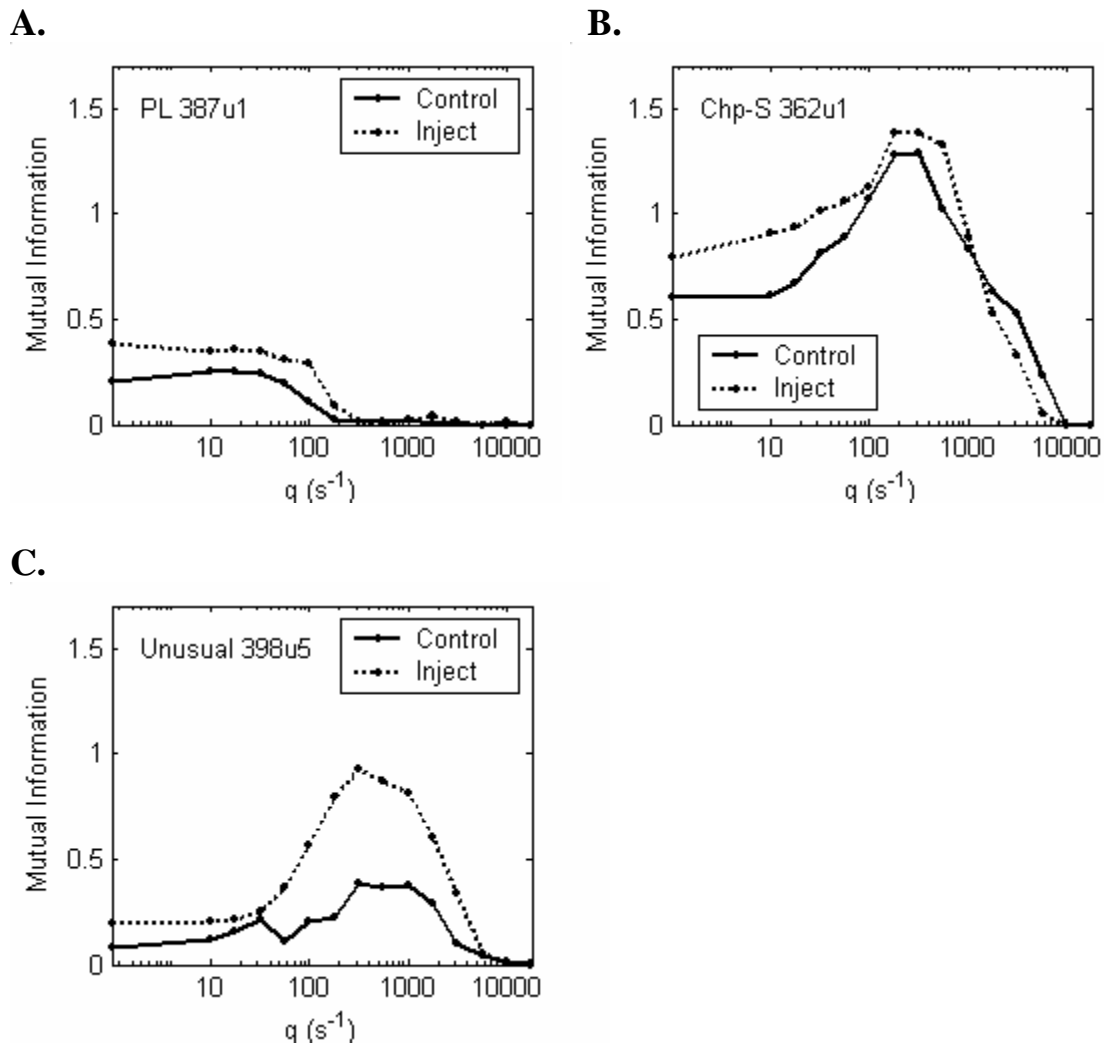
Fig. 5-17 Change in the mutual information based on spike distance by blocking

glycinergic inhibition for a primary-like (*A*) and blocking GABAergic inhibition for a

chopper (*B*) and an unusual unit (*C*).

shaping effect of the inhibition (phasic inhibition), but was also caused by a constant

reduction of activity (tonic inhibition). Although in this study an analysis was used to

separate tonic vs. phasic inhibition, in reality there may not be a clear boundary between

these two inhibitory profiles. In fact, it was hypothesized that most inhibitory

interneurons were synchronized to amplitude modulation, since 85% of AVCN units

showed changes in phase at low modulation frequencies after blocking inhibition.

However, due to the smoothing effect when inhibitory inputs synapsed on the cell

dendrites, the synchrony might be too smoothed to observe, especially at mid and high

modulation frequencies when the smoothing effect was longer than a modulation cycle.

By analyzing changes in phase after blocking inhibition for responses to SAM stimuli

with a low modulation frequency (32 Hz), it was found that the majority of choppers with

positive effects in response to inhibitory receptor blockers showed increased phase after

blocking GABAergic inhibition, which indicated that the inhibition was synchronized to

amplitude modulation and was effectively delayed with respect to excitation (Fig. 5-6).

Interestingly, the enhancement of inhibition for these choppers could be largely predicted

by simulated tonic inhibition (Fig. 5-8). This result suggested that most choppers received

GABAergic inhibition on their dendrites that acted as a source of slowly varying

hyperpolarization, consistent with the conclusions of the previous chapter and of

anatomical studies (Wenthold et al., 1988; Saint Marie et al., 1989).

The observations of SAM-tone and two-tone responses generally agreed with

each other, except that some units that showed large changes of synchrony after blocking

inhibitory receptors with SAM tones showed much smaller changes in synchrony with

two tones. In addition, although the general decrease of PSTH fluctuation in response to

tones in noise after blocking inhibition agreed with the decrease of AM synchrony, no correlation was found between the amounts of the reduction across units. In other words, although a general role of inhibition was to enhance the synchronization to the stimulus envelope, the enhancement was not maintained universally; rather, the observed enhancement was outcomes of the interaction between excitation and inhibition, which was dependent on their own responses to different stimuli.

The PSTH fluctuation was presumably caused by locking to the effective stimulus envelope (Louage et al. 2004; Chapter II). However, other factors may determine the fluctuation too, such as the regularity and smoothness of inhibition. In addition, when given the possibility that the frequency tuning (bandwidth and CF) of the inhibition may differ from that of the excitation, it is hard to define the "effective" stimulus. Therefore, it may not be accurate to state that the inhibition enhanced the locking to the envelope of the effective stimulus, because the inhibition may alter the locking property.

5.4.2   Effect of inhibition on tone-in-noise responses

When comparing responses to noise-alone and tone-alone stimuli, the majority of AVCN units showed larger rate changes in response to noise than in response to tones (Fig. 5-12). Therefore, inhibition seemed to have a stronger effect on noise responses than on tone responses. However, this differential effect was not strong enough to facilitate the detection of tones in noise, because the majority of units showed increases in rate of a similar size for noise alone and noise-plus-tones at different tone levels. Only 5 out of 53 units showed lower detection thresholds in the presence of inhibition compared to the thresholds after blocking inhibition. It should be noted that the present

study used relatively high-level noise and the tone levels were close to psychophysical thresholds. Different conclusions might be drawn with lower-level noise. For example, Ebert and Ostwald (1995a) find that inhibition has a strong suppressive effect on low-level background-noise activity, but a minimal effect on responses to a tone added to the noise.

A similar phenomenon was observed for PSTH fluctuations. Eighty-eight percent units showed more than 10% decrease in the PSTH fluctuation after blocking inhibition, but the change was parallel for responses to noise-alone and tone-in-noise stimuli. There were 42% units that showed changed detection thresholds based on the SFIE model rate. However, it was unclear whether the change in threshold was only due to changes in PSTH fluctuation or a mixture of fluctuation changes and rate changes. Forty-seven and 51% of the units showed changed thresholds based on temporal reliability and correlation index using single temporal resolution, respectively. When different temporal resolutions were used for the temporal reliability, 66% of units showed threshold change and the change was larger. No significant effect of blocking inhibition was found on synchronization to tone frequency or spike-distance metric.

In summary, the presence of inhibition at the level of the AVCN did not greatly affect the detectability of a tone in noise. Although for each metric there were units with changed thresholds, the changes were not consistent in direction, which made it difficult to confirm a general role of the inhibition in terms of detection. We cannot exclude the possibility that information contained in a small group of neurons was critical for the detection task. In that situation, the presence of inhibition might be important for detection, if this group of neurons all showed large threshold changes in the same

direction. It is also possible that the tone-level resolution used here was too low $(10 - 15$ dB step) to observe small changes in detection threshold caused by blocking inhibition.

Although inhibition was not found to consistently affect detection thresholds, this study showed that inhibition can significantly affect certain response features (e.g., PSTH fluctuation) and not other features (e.g., synchronization to tone frequency). These findings may be important for other auditory tasks that involve similar temporal features.

5.4.3   Possible inhibitory neurons

By comparing the effect of inhibition on broadband-noise and pure-tone responses, this study was trying to provide useful information about the identity of the inhibitory neurons that projected to single AVCN neurons. As mentioned before, 47% of units showed stronger responses to noise after blocking inhibition, while only 10% of units showed stronger responses to tones. When glycinergic inhibition was concerned, there were possibly fewer vertical neurons (which responded stronger to tones) than D-stellate neurons (which responded stronger to noise) that projected to the recorded AVCN neurons. However, for the 43% of units that showed similar rate increase for noise-alone and tone-alone stimuli, it was likely that a mixture of inputs from D-stellate and vertical neurons compromised the effect from each other. This could be a challenge for modeling of AVCN neurons.

Chapter VI

General Discussion and Summary

6.1   The importance of temporal responses

An important message of this study was that the temporal responses of AVCN neurons can be important for certain auditory tasks. At first glance, it might seem surprising to try all kinds of analytical approaches on responses at such a low level of the auditory system. However, if information is gradually processed along the ascending auditory pathway, and decisions for certain tasks are made at high levels, it will be appropriate to apply more complex analyses to low levels, and look at more direct or simpler cues at high levels. For example, a group of neurons in the auditory cortex are found to be selective for particular pitches based on their firing rates, even after the fundamental frequency is removed from the stimulus (Bendor and Wang, 2005). No such neurons have been found at lower levels; however, the information has to be present at lower levels, and likely is in some form of temporal features.

Analyzing the change in temporal responses by blocking inhibition was also found to provide more information about the functions and characteristics of the inhibitory inputs than simply studying changes in average rates at or off CF. For neurons in the DCN or the IC, by studying the frequency response area and analyzing the distinct excitatory and inhibitory bands, certain connections between different types of neurons can be inferred (for review, see Davis, 2005). However, this approach is less useful for the study of AVCN neurons, which do not have distinct inhibitory bands in their response

areas. Even with the iontophoresis technique, which shows clearly the inhibitory frequency tuning, the tuning property can be consistent with more than one candidate neurons and is still not clear enough to link to certain types of inhibitory interneurons.

By analyzing changes in temporal responses of AVCN neurons, certain speculations concerning the temporal properties of the inhibitory interneurons can be made. However, further identification of the type of inhibitory neurons will require knowledge of the response characteristics of the candidates. For example, D-stellate cells are known to have different PSTHs compared to vertical cells in response to CF tones, but both of them have low spontaneous activity. The present study and previous studies (Caspary et al., 1979; Ebert and Ostwald, 1995a) found that the spontaneous activity was affected by inhibition more than the sound-evoked activity was, when the variance of spontaneous activity was not considered. However, the present study found that the change in spontaneous activity was in fact insignificant once the variance taken into account. The present study also found units with early inhibition. The mean first-spike latency of these units could decrease by more than 0.8 msec after blocking glycinergic or GABAergic inhibition. It is puzzling that descending inputs can affect the onset response of excitatory inputs from auditory nerve fibers. To solve the puzzle, a better understanding of the sound-evoked responses of the neurons in the SOC that project back to the AVCN is required.

After knowing the temporal responses of all candidates for the inhibitory neurons, modeling simulations may also be necessary to predict the observed change by blocking inhibition with a certain candidate. For example, it was hypothesized that inhibitory neurons with high spontaneous activity had a strong suppressive effect on the

spontaneous activity of the target neuron (see Chapter 4). Whether this was true for both primary-likes and choppers needs to be confirmed with corresponding model simulations.

6.2   Mechanisms for detection of tones in noise

Although monaural detection of a pure tone in broadband noise is a basic auditory task, knowledge about how humans or other mammals perform this task is quite limited. For example, whether sound energy or temporal features are used as cues for detection is still unclear. Physiologically, it is unknown what types of neurons, what auditory levels, and what detection cues are responsible for monaural detection of tones in noise. If these "critical" neurons could be identified, further analysis of what sound features are captured by these neurons would also help to understand what perceptual cues are used by humans or other animals for detection. Presently, since no "critical" neurons have been identified, this study chose to analyze information contained in the AVCN, which sends major projections to many higher levels of the auditory pathway. If neural responses based on particular stimulus features provide useful and reliable information for detection of tones in noise, it is very likely that higher-level neurons will continue to rely on this type of information.

An interesting finding of this study was that temporal features that were not anchored in time seemed to provide more useful information for detection than did absolute spike times. This finding was certain for primary-likes; it was not as certain for choppers and other types of neurons since detection thresholds based on the spike-distance metric cannot be directly compared with those of other metrics. This finding did not indicate that the absolute spike times are unimportant; rather, the message here was

that for the purpose of detecting a tone in noise, the decision can be made based on sound features that are not anchored in time. For example, similar to the PSTH fluctuation applied to neural responses, the envelope slope (Richards, 1992) measures the fluctuation of the sound envelope. Davidson et al. (2006) show that the envelope slope can predict a significant amount of variance observed for human listeners in monaural detection of tones in reproducible noise.

Another focus of this study was the exploration of physiological mechanisms to extract each type of temporal information. This study showed that combinations of excitation and delayed inhibition can represent the PSTH fluctuation, but this study was unable to find neural mechanisms to extract other types of information without using internal clocks to mark the beginning of each tone cycle (Joris et al. 2005; Louage et al. 2004). However, we cannot totally rule out the possibility of internal clocks, since neurons with certain intrinsic timing properties have been observed (for review, see DeWeese et al., 2005). Moreover, it is possible that single types of information are not extracted in reality, but play their roles by means of affecting more complex response patterns.

6.3   Role of inhibition at the level of the AVCN

Contradictory to the lateral inhibition commonly observed in the visual or somatosensory system, the inhibition received by AVCN neurons mainly affects the responses to tones at CF or maximum responses of target neurons (Caspary et al, 1993, 1994). If the role of inhibition is not to improve frequency contrast, what does it do for other aspects of the response? And more interestingly, what is the benefit of receiving

inhibitory inputs? Improvement of the dynamic range of discharge rate was not observed for either pure tones or for tones in noise. In fact, Kopp-Scheinpflug et al. (2002) found that the rate-level functions of some primary-likes with large prepotentials become non-monotonic by receiving inhibition. Improvement of temporal contrast is proposed by Ebert and Ostwald (1995a), since they find that inhibition has a larger suppressive effect on spontaneous and low-level background-noise activity than on tone-evoked activity when a tone is presented alone or added to an ongoing background noise. Using high-level noise, the present study found that for a larger percentage of neurons, responses to noise-alone stimuli were suppressed by inhibition more than responses to tone-alone stimuli; however, when the tone was added to the noise, responses to noise-alone and tone-plus-noise stimuli were suppressed by similar amounts. In other words, the improvement of temporal contrast was only true for tones in quiet or tones in low-level noise (when the tone dominates the response), but not for tones in high-level noise (when the noise dominates the response). In general, the presence of inhibition did not facilitate the detection of tones in noise based on discharge rate or any other temporal metrics. For responses to tones in quiet, findings of this study agreed with previous studies (Caspary et al., 1979; Ebert and Ostwald, 1995a) in that inhibition had a stronger suppressive effect on spontaneous activity than on tone-evoked activity if the variance of spontaneous rate was not considered. The change in spontaneous activity was in fact less significant compared to the change in tone-evoked activity once the variance was included in the measurement.

The enhancement of the synchrony to amplitude modulation or the fluctuation of the PSTH can be thought of as another type of temporal-contrast improvement by

inhibition. For responses to amplitude-modulated stimuli, tonic inhibition enhanced the synchrony since the suppression of a constant response had a larger effect on response valleys than on response peaks; phasic inhibition enhanced the synchrony by suppressing activity at some phases more than at others. It should be noted that neither the enhancement of synchrony nor the enhancement of PSTH fluctuation suggested that information contained in the peaks was more important than information contained in the valleys. It was the dynamic transition between peaks and valleys that provided information, at least for PSTH fluctuation.

Note that both glycinergic and GABAergic inhibition can come from descending inputs, and direct pathways have been found from the IC to the CN via the SOC by inhibitory projections (Schofield and Cant, 1999). Some of the observations by blocking inhibition can reflect possible feedback mechanisms that exist at the level of the AVCN.

6.4 The diversity of AVCN neurons beyond the known categories

AVCN neurons can be categorized based on cellular morphologies (e.g., bushy vs. stellate cells), membrane properties (e.g., type II vs. type I cells), or sound-evoked properties (e.g., primary-likes, primary-like-with-notches, choppers) (Oertel, 1983; Wu and Oertel, 1984; Blackburn and Sachs, 1989; Feng et al., 1994). The present study showed that even within the finest sub-categories proposed to date, such as slowly adapting choppers or transient choppers (Blackburn and Sachs, 1989), neurons within a category can still be quite different from each other. For example, within each sub-category, there were some units with flat rate-level functions and some units with monotonic rate-level functions in response to tones in noise. Within each sub-category,

there were units that showed positive effect and units that showed negative effect after blocking inhibition. Even for units that showed positive effect within a certain category, the change in first-spike latency or frequency response could differ.

The present study concluded that inhibition generally did not affect the detectability of tones in noise based on average rate or any temporal metric. In fact, for each metric, there were a number of units that showed changes in detection threshold. However, since both decreased and increased thresholds were observed after blocking inhibition, and units that did or did not show changes in threshold did not differ in terms of category, it was hard to specify a clear role of inhibition for detection of tones in noise. If further categorization can identify some unique response properties for units that showed changed or unchanged thresholds, the effect of inhibition would be more convincing.

6.5 Implications for AVCN models

Caspary et al. (1993, 1994) provide information about the frequency tuning of inhibitory inputs, which should be taken into account when constructing AVCN models. The present study provided other useful information for modeling of AVCN neurons as stated below.

For simulations of choppers, inhibitory inputs are likely to terminate on the dendrites of the target neurons to provide relatively smoothed hyperpolarizations. Chapter 4 shows that the regularity change of choppers was consistent with a delaying process of temporal summation across a large number of excitatory inputs by smoothed inhibitory inputs. Moreover, for simulations of transient choppers, excitatory inputs are

responsible for creating the transient patterns, since blocking inhibition only affected the transient properties by a small amount. Exceptions were 1 transient chopper that became as regular as a sustained chopper after blocking inhibition, which indicated that inhibitory inputs had the ability to create transient properties alone in some cases. In contrast, for primary-like units that showed phase locking to tone frequency, since no phase change was observed after blocking inhibition, the amount of temporal summation should be minimal[8].

The traditional view of low-spontaneous and delayed inhibition was not always correct. Since most units (approximately 72%) showed decreased first-spike latency after blocking inhibition, inhibition that can affect the onset of excitatory responses must be considered.

It can be a challenge for AVCN models that more than one source of inhibitory interneuron may project to a single target neuron, as indicated by units that showed comparable changes for noise and for tones after blocking glycinergic inhibition (the two major glycinergic neurons, D-stellate and vertical neurons, respond differently to noise and tones. Correspondingly, other response properties of the mixed inhibitory inputs, such as temporal response patterns, can also be complicated to simulate.

6.6   General summary

Average discharge rate and several temporal metrics were applied to tone-in-noise responses of AVCN neurons. Detection thresholds based on average discharge rates of

---

[8] Here the temporal summation refers to the situation that a post-synaptic spike is generated only when more than two EPSPs overlap in time to reach the discharge threshold.

AVCN neurons were generally higher than the psychophysical detection threshold. Temporal approach based on either stimulus fine structure or envelope was then tested. Detection thresholds based on synchronization to tone frequency for some neurons can predict the psychophysical threshold at low and mid frequencies. It was difficult to find a physiological mechanism to extract the information. Detection thresholds based on the SFIE model, which measured the fluctuation of PSTH (presumably caused by fluctuations of stimulus envelope), for some neurons can predict the psychophysical threshold at all frequencies. The SFIE model can be easily realized with physiological mechanisms.

Spike-timing consistency has not been used as a detection cue in previous studies. Detection thresholds based on the temporal reliability and correlation index for some neurons can predict the psychophysical threshold at all frequencies. Although both metrics measured the consistency of spike timing in response to the same stimulus presentation, the two metrics did not always agree on detection thresholds of individual neurons. It was difficult to find a physiological mechanism to extract the information.

Last, detection information based on the absolute spike timing as measured by the spike-distance metric was tested, and found to be less useful for detection of tones in noise compared to other temporal features that were not anchored in time, especially for primary-likes.

Changes in neural responses to pure tones and complex stimuli by blocking inhibition provided some knowledge about the function and properties of inhibitory inputs received by AVCN neurons. For tone-in-quiet responses, most AVCN neurons showed on-CF (or broad) inhibition rather than off-CF inhibition. In response to CF

tones, the shape of rate-level functions was generally invariant, although the average rate increased. Spontaneous activity was more affected by blocking inhibition than tone-evoked activity in terms of percentage of change. However, the larger variance in spontaneous activity made the change insignificant.

Changes in the temporal responses by blocking inhibition were diverse across neuron types. After blocking inhibition, choppers generally showed more chopping cycles at the later part of the response (higher regularity), and the chopping frequency increased. Some slowly adapting choppers and 1 transient chopper became sustained choppers after blocking inhibition. All but one transient choppers only showed slight increase of regularity at the early part of the response. The mean first-spike latency decreased for the majority of AVCN neurons. For a group of primary-likes and unusual neurons, the decrease of latency can be large.

Decreased synchrony to amplitude-modulated stimuli after blocking inhibition was observed for most neurons. Both tonic and phasic inhibition were likely to cause the enhancement of envelope locking. Choppers were more likely to receive tonic inhibition except for very low modulation frequencies. For tone-in-noise responses, no systematic change of detection threshold based on average rates or any temporal metric was observed after blocking inhibition. The synchronization to tone frequency and the spike-distance metric were found to be generally unaffected by inhibition. The average rate increased and the PSTH fluctuation decreased after blocking inhibition, but by similar amounts for noise alone and tone plus noise. Detection thresholds based on the temporal reliability or the correlation index were found to be affected by inhibition most, yet both decreased and increased thresholds were observed, which made it difficult to speculate

the general role of inhibition for detection of tones in noise. However, the effect of

inhibition on the measured temporal properties might be useful for studies of other

auditory tasks involving these temporal properties.

Bibliography

Abel SM, Krever EM and Alberti PW. Auditory detection, discrimination and speech processing in ageing, noise-sensitive and hearing-impaired listeners. *Scand Audiol* 19:43-54, 1990.

Altschuler RA, Betz H, Parakkal MH, Reeks KA, and Wenthold RJ. Identification of glycinergic synapses in the cochlear nucleus through immunocytochemical localization of the postsynaptic receptor. *Brain Res* 369:316-320, 1986.

Arnott RH, Wallace MN, Shackleton TM, and Palmer AR. Onset neurons in the anteroventral cochlear nucleus project to the dorsal cochlear nucleus. *J Assoc Res Otolaryngol* 5:153-170, 2004.

Babalian AL, Jacomme AV, Doucet JR, Ryugo DK, and Rouiller EM. Commissural glycinergic inhibition of bushy and stellate cells in the anteroventral cochlear nucleus. *Neuroreport* 13:555-558, 2002.

Backoff PM, Palombi PS and Caspary DM. γ-aminobutyric acidergic and glycinergic inputs shape coding of amplitude modulation in the chinchilla cochlear nucleus. *Hearing Res* 134:77-88, 1999.

Banks MI and Sachs MB. Regularity analysis in a compartmental model of chopper units in the anteroventral cochlear nucleus. *J Neurophysiol* 65:606-629, 1991.

Bendor D and Wang X. The neuronal representation of pitch in primate auditory cortex. *Nature* 436:1161-1165, 2005.

Blackburn CC and Sachs MB. Classification of unit types in the anteroventral cochlear nucleus: PST histograms and regularity analysis. *J Neurophysiol* 62:1303-1329, 1989.

Blalock HM. *Social statistics*. New York: McCraw-Hill. p. 219-415, 1972.

Breebaart J, van de Par S, and Kohlrausch A. Binaural processing model based on contralateral inhibition. I. Model structure. *J Acoust Soc Am* 110:1074-1088, 2001.

Brown MC. Anatomical and physiological studies of type I and type II spiral ganglion neurons. In: *The mammalian cochlear nuclei: organization and function*, edited by Merchán, M. A., Juiz, J. M., Godfrey, R. A., and Mugnaini, E. New York: Plenum Press, 1993.

Brownell WE, Manis PB, and Ritz LA. Ipsilateral inhibitory responses in the cat lateral superior olive. *Brain Res* 177:189-193, 1979.

Caird D and Klinke R. Processing of binaural stimuli by cat superior olivary complex neurons. *Exp Brain Res* 52:385-399, 1983.

Cant NB. The fine structure of two types of stellate cells in the anterior division of the anteroventral cochlear nucleus of the cat. *Neuroscience* 6:2643-2655, 1981.

Cant NB. Identification of cell types in the anteroventral cochlear nucleus that project to the inferior colliculus. *Neurosci Lett* 32:241-246, 1982.

Cant NB and Morest DK. The bushy cells in the anteroventral cochlear nucleus of the cat. A study with the electron microscope. *Neuroscience* 4:1925-1945, 1979.

Cant NB and Casseday JH. Projections from the anteroventral cochlear nucleus to the lateral and medial superior olivary nuclei. *J Comp Neurol* 247:457-476, 1986.

Cant NB and Hyson RL. Projections from the lateral nucleus of the trapezoid body to the medial superior olivary nucleus in the gerbil. *Hearing Res* 58:26-34, 1992.

Cariani PA and Delgutte B. Neural correlates of the pitch of complex tones. I. Pitch and pitch salience. *J Neurophysiol* 76:1698-1716, 1996.

Carney LH, Heinz MG, Evilsizer ME, Gilkey RH, and Colburn HS. Auditory phase opponency: A temporal model for masked detection at low frequencies. *Acta Acust Acust* 88:334-347, 2002.

Caspary DM, Havey DC, and Faingold CL. Effects of microiontophoretically applied glycine and GABA on neuronal response patterns in the cochlear nuclei. *Brain Res* 172:179-185, 1979.

Caspary DM, Palombi PS, Backoff PM, Helfert RH, and Finlayson PG. GABA and glycine inputs control discharge rate within the excitatory response area of primary-like and phase-locked AVCN neurons. In: *The mammalian cochlear nuclei: organization and function*, edited by Merchán, M. A., Juiz, J. M., Godfrey, R. A., and Mugnaini, E. New York: Plenum Press, 1993.

Caspary DM, Backoff PM, Finlayson PG, and Palombi PS. Inhibitory inputs modulate discharge rate within frequency receptive fields of anteroventral cochlear nucleus neurons. *J Neurophysiol* 72:2124-2133, 1994.

Cedolin L and Delgutte B. Pitch of complex tones: rate-place and interspike interval representations in the auditory nerve. *J Neurophysiol* 94:347-362, 2005.

Chase SM. The coding of sound localization cues in the inferior colliculus. PhD thesis. Biomedical Engineering. Johns Hopkins University. 2007.

Chase SM and Young ED. Spike-timing codes enhance the representation of multiple simultaneous sound-localization cues in the inferior colliculus. *J Neurosci* 26:3889-3898, 2006.

Cook DL, Schwindt PC, Grande LA, and Spain WJ. Synaptic depression in the localization of sound. *Nature* 421:66-70, 2003.

Costalupes JA. Broadband masking noise and behavioral pure tone thresholds in cats. I. Comparison with detection thresholds. *J Acoust Soc Am* 74:758-764, 1983.

Costalupes JA. Representation of tones in noise in the responses of auditory nerve fibers in cats. I. Comparison with detection thresholds. *J Neurosci* 5:3261-3269, 1985.

Dau T, Puschel D, and Kohlrausch A. A quantitative model of the "effective" signal processing in the auditory system. II. Simulations and measurements. *J Acoust Soc Am* 99:3623-3631, 1996.

Davidson SA, Gilkey RH, Colburn HS, and Carney LH. Binaural detection with narrowband and wideband reproducible noise maskers. III. Monaural and diotic detection and model results. *J Acoust Soc Am 119*:2258-2275, 2006.

Davis KA. Spectral processing in the inferior colliculus. *Int Rev Neurobiol* 70:169-205, 2005.

de Cheveigne and Pressnitzer D. The case of the missing delay lines: synthetic delays obtained by cross-channel phase interaction. *J Acoust Soc Am* 119:3908-3918, 2006.

Delgutte B. Physiological models for basic auditory percepts. In: Auditory computation. Hawkins HL, McMullen TA, Popper AN, and Fay RR (ed). Springer: New York, 1995.

DeWeese MR, Hromadka T, and Zador AM. Reliability and representational bandwidth in the auditory cortex. *Neuron* 48:479-488, 2005.

Domnitz RH and Colburn HS. Analysis of binaural detection models for dependence on interaural target parameters. *J Acoust Soc Am* 59:598-601, 1976.

Ebert U and Ostwald J. GABA can improve acoustic contrast in the rat ventral cochlear nucleus. *Exp Brain Res* 104:310-322, 1995a.

Ebert U and Ostwald J. GABA alters the discharge pattern of chopper neurons in the rat ventral cochlear nucleus. *Hear Res* 91:160-166, 1995b.

Evans EF. Place and time coding of frequency in the peripheral auditory system: some physiological pros and cons. *Audiology* 17:369-420, 1978.

Evilsizer ME, Gilkey RH, Mason CR, Colburn HS, and Carney LH. Binaural detection with narrowband and wideband reproducible noise maskers: I. Results for human. *J Acoust Soc Am* 111:336-345, 2002.

Fekete DM, Rouiller EM, Liberman MC, and Ryugo DK. The central projections of intracellularly labeled auditory nerve fibers in cats. *J Comp Neurol* 229:432-450, 1984.

Feng JJ, Kuwada S, Ostapoff EM, Batra R, and Morest DK. A physiological and structural study of neuron types in the cochlear nucleus. I. Intracellular responses to acoustic stimulation and current injection. *J Comp Neurol* 346:1-18, 1994.

Ferragamo MJ, Golding NL, and Oertel D. Synaptic inputs to stellate cells in the ventral cochlear nucleus. *J Neurophysiol* 79:51-63, 1998a.

Ferragamo MJ, Golding NL, and Oertel D. Golgi cells in the superficial granule cell domain overlying the ventral cochlear nucleus: morphology and electrophysiology in slices. *J Comp Neurol* 400:519-528, 1998b.

Frisina RD, Smith RL, and Chamberlain SC. Encoding of amplitude modulation in the gerbil cochlear nucleus: I. A hierarchy of enhancement. *Hearing Res* 44:99-122, 1990.

Gai Y and Carney LH. Temporal measures and neural strategies for detection of tones in noise based on responses in anteroventral cochlear nucleus. *J Neurophysiol* 96:2451-2464, 2006.

Ganz L. Lateral inhibition and the location of visual contours. An analysis of figural after-effects. *Vision Res* 4:465-481, 1964.

Geisler CD and Sinex DG. Responses of primary auditory fibers to combined noise and tonal stimuli. *Hearing Res* 3:317-334, 1980.

Gibson DJ, Young ED, and Costalupes JA. Similarity of dynamic range adjustment in auditory nerve and cochlear nuclei. *J Neurophysiol* 53:940-958, 1985.

Giguere C and Woodland PC. A computational model of the auditory periphery for speech and hearing research. I. Ascending path. *J Acoust Soc Am* 95:331-342, 1994.

Gilkey RH, Robinson DE, and Hanna TE. Effects of masker waveform and signal-to-masker phase relation on diotic and dichotic masking by reproducible noise. *J Acoust Soc Am* 78:1207-1219, 1985.

Gilkey RH and Robinson DE. Models of auditory masking: A molecular psychophysical approach. *J Acoust Soc Am* 79:1499-1510, 1986.

Goldberg JM and Brown PB. Response of binaural neurons of dog superior olivary complex to dichotic tonal stimuli: Some physiological mechanisms of sound localization. *J Neurophysiol* 32:613-636, 1969.

Green DM, Kidd G Jr, and Picardi MC. Successive versus simultaneous comparison in auditory intensity discrimination. J Acoust Soc Am 73:639-643, 1983.

Greenwood DD and Goldberg JM. Response of neurons in the cochlear nuclei to variations in noise bandwidth and to tone-noise combinations. *J Acoust Soc Am* 47:1022-1040, 1970.

Grothe B and Sanes DH. Bilateral inhibition by glycinergic afferents in the medial superior olive. *J Neurophysiol* 69:1192-1196, 1993.

Havey DC and Caspary DM. A simple technique for constructing 'piggy-back' multibarrel microelectrodes. *Electroencephalogr Clin Neurophysiol* 48:249-251, 1980.

Hewitt MJ and Meddis R. Regularity of cochlear nucleus stellate cells: a computational modeling study. *J Acoust Soc Am* 93:3390-3399, 1993.

Isabelle SK and Colburn HS. Detection of tones in reproducible narrow-band noise. *J Acoust Soc Am* 89:352-359, 1991.

Joris PX and Yin TCT. Responses to amplitude-modulated tones in the auditory nerve of the cat. *J Acoust Soc Am* 91:215-232, 1992.

Joris PX, Carney LH, Smith PH, and Yin TC. Enhancement of neural synchronization in the anteroventral cochlear nucleus. I. Responses to tones at the characteristic frequency. *J Neurophysiol* 71:1022-1036, 1994.

Joris PX, Louage DHG, Cardoen L, and van der Heijden M. Correlation index: A new metric to quantify temporal coding. *Hearing Res* 216-217:19-30, 2006.

Kidd G Jr, Mason CR, Brantley MA, and Owen GA. Roving-level tone-in-noise detection. *J Acoust Soc Am* 86:1310-1317, 1989.

Koch C. Synaptic input to a passive tree. In: *Biophysics of computation: Information processing in single neurons*. New York: Oxford, 423-426, 1999.

Kolston J, Osen KK, Hackney CM, Ottersen OP, and Storm-Mathisen J. An atlas of glycine- and GABA-like immunoreactivity and colocalization in the cochlear nuclear complex of the guinea pig. *Anat Embryol (Berl)* 186:443-465, 1992.

Kopp-Scheinpflug C, Dehmel S, Dörrscheidt GJ, and Rübsamen R. Interaction of excitation and inhibition in anteroventral cochlear nucleus neurons that receive large endbulb synaptic endings. *J Neurosci* 22:11004-11018, 2002.

Kurt S, Crook JM, Ohl FW, Scheich H, and Schulze H. Differential effects of iontophoretic in vivo application of the GABA$_A$-antagonists bicuculline and gabazine in sensory cortex. *Hear Res* 212:224-235, 2006.

Kuwada S, Yin TC, and Wickesberg RE. Response of cat inferior colliculus neurons to binaural beat stimuli: possible mechanisms for sound localization. Science 206:586-588, 1979.

Lawson JL and Uhlenbeck GE. *Threshold signals. MIT Radiation Laboratory*. Series, Vol. 24. New York: McGraw-Hill, 1950.

Le Beau FE, Rees A, and Malmierca MS. Contribution of GABA- and glycine-mediated inhibition to the monaural temporal response properties of neurons in the inferior colliculus. *J Neurophysiol* 75:902-919, 1996.

Lenn NJ and Reese TS. The fine structure of nerve endings in the nucleus of the trapezoid body and the ventral cochlear nucleus. *Am J Anat* 118:375-389, 1966.

Lewis ER and Henry KR. Nonlinear effects of noise on phase-locked cochlear-nerve responses to sinusoidal stimuli. *Hearing Res* 92:1-16, 1995.

Liberman MC. Auditory-nerve response from cats raised in a low-noise chamber. *J Acoust Soc Am* 63:442-455, 1978.

Liberman MC. Central projections of auditory-nerve fibers of differing spontaneous rate. I. Anteroventral cochlear nucleus. *J Comp Neurol* 313:240-258, 1991.

Licklider JCR. A duplex theory of pitch perception. *Experimentia* 7:128-134, 1951.

Louage DHG, van der Heijden M, and Joris PX. Temporal properties of responses to broadband noise in the auditory nerve. *J Neurophysiol* 91:2051-2065, 2004.

Louage DHG, van der Heijden M, and Joris PX. Enhanced temporal response properties of anteroventral cochlear nucleus neurons to broadband noise. *J Neurosci* 25:1560-1570, 2005.

MacMillan NA and Creelman CD. *Detection theory: a user's guide.* Mahwah, NJ: Lawrence Erlbaum Associates, p. 57-67, 2005.

Mainen ZF and Sejnowski TJ. Reliability of spike timing in neocortical neurons. *Science* 268:1503-1506, 1995.

Manis PB and Marx SO. Outward currents in isolated ventral cochlear nucleus neurons. *J Neurosci* 11:2865-2880, 1991.

Mardia KV. *Statistics of directional data: Probability and mathematical statistics*. London-New York: Academic Press, 1972.

Martin MR and Dickson JW. Lateral inhibition in the anteroventral cochlear nucleus of the cat: a microiontophoretic study. *Hear Res* 9:35-41, 1983.

Martin EM, West MF, and Bedenbaugh PH. Masking and scrambling in the auditory thalamus of awake rats by Gaussian and modulated noises. *PNAS* 101:14961-14965, 2004.

May BJ and Sachs MB. Dynamic range of neural rate responses in the ventral cochlear nucleus of awake cats. *J Neurophysiol* 68:1589-1602, 1992.

Meddis R and Hewitt MJ. Virtual pitch and phase sensitivity of a computer model of the auditory periphery. I: Pitch identification. *J Acoust Soc Am* 89:2866-2882, 1991.

Miller MI, Barta PE, and Sachs MB. Strategies for the representation of a tone in background noise in the temporal aspects of the discharge patterns of auditory-nerve fibers. *J Acoust Soc Am* 81:665-679, 1987.

Moller AR. Latency of unit responses in cochlear nucleus determined in two different ways. *J Neurophysiol* 38:812-821, 1975.

Moore BC, Peters RW, Glasberg BR. Auditory filter shapes at low center frequencies. *J Acoust Soc Am* 88:132-140, 1990.

Moore DS, McCabe GP, Duckworth WM, and Sclove SL. *The Practice of Business Statistics: Using Data for Decisions.* New York: WH Freeman and Company. *p* 18-4 – 18-65, 2002.

Muller CM. Intracellular Microelectrodes. In: *Practical electrophysiological methods*. Kettenmann H and Grantyn R (ed.) Wiley-Liss: p183-188, 1992.

Nabelek AK, Tampas JW, and Burchfield SB. Comparison of speech perception in background noise with acceptance of background noise in aided and unaided conditions. *J Speech Lang Hear Res* 47:1001-1011, 2004.

Nelson PC and Carney LH. A phenomenological model of peripheral and central neural responses to amplitude-modulated tones. *J Acoust Soc Am* 116:2173-2186, 2004.

Oertel D. Synaptic responses and electrical properties of cells in brain slices of the mouse anteroventral cochlear nucleus. *J Neurosci* 3:2043-2053, 1983.

Oertel D and Wickesberg RE. Glycinergic inhibition in the cochlear nuclei: evidence for tuberculoventral neurons being glycinergic. In: *The mammalian cochlear nuclei:*

organization and function, edited by Merchán, M. A., Juiz, J. M., Godfrey, R. A., and Mugnaini, E. New York: Plenum Press, 1993.

Palombi PS and Caspary DM. GABA$_A$ receptor antagonist bicuculline alters response properties of posteroventral cochlear nucleus neurons. *J Neurophysiol* 67:738-746, 1992.

Palombi PS and Caspary DM. GABA inputs control discharge rate primarily within frequency receptive fields of inferior colliculus neurons. *J Neurophysiol* 75:2211-2219, 1996.

Paolini AG, Clarey JC, Needham K, and Clark GM. Balanced inhibition and excitation underlies spike firing regularity in ventral cochlear nucleus chopper neurons. *Eur J Neurosci* 21:1236-1248, 2005.

Pfafflin SM and Mathews MV. Detection of auditory signals in reproducible noise. *J Acoust Soc Am* 39:340-345, 1966.

Oliver DL. Projections to the inferior colliculus from the anteroventral cochlear nucleus in the cat: possible substrates for binaural interaction. *J Comp Neurol* 264:24-46, 1987.

Ostapoff EM, Benson CG, and Saint Marie RL. GABA- and glycine-immunoreactive projections from the superior olivary complex to the cochlear nucleus in guinea pig. *J Comp Neurol* 381:500-512, 1997.

Ramachandran R, Davis KA, and May BJ. Singe-unit responses in the inferior colliculus of decerebrate cats. I. Classification based on frequency response maps. *J Neurophysiol* 82:152-163, 1999.

Rees A and Palmer AR. Rate-intensity functions and their modification by broadband noise for neurons in the guinea pig inferior colliculus. *J Acoust Soc Am* 83:1488-1498, 1988.

Rhode WS, Geisler CD, and Kennedy DT. Auditory nerve fiber responses to wide-band noise and tone combinations. *J Neurophysiol* 41:692-704, 1978.

Rhode WS, Oertel D, and Smith PH. Physiological response properties of cells labeled intracellularly with horseradish peroxidase in cat ventral cochlear nucleus. *J Comp Neurol* 213:448-463, 1983.

Rhode WS and Greenberg S. Encoding of amplitude modulation in the cochlear nucleus of the cat. *J Neurophysiol* 71:1797-1825, 1994.

Richards VM. The detectability of a tone added to narrow bands of equal-energy noise. *J Acoust Soc Am* 91:3424-3435, 1992.

Robert A and Eriksson JL. A composite model of the auditory periphery for simulating responses to complex sounds. *J Acoust Soc Am 106*:1852-1864, 1999.

Rose JE, Galambos R, and Hughes JR. Microelectrode studies of the cochlear nucleus of the cat. *Bull Johns Hopkins Hospital* 104:211-251, 1959.

Rothman JS, Young ED, and Manis PB. Convergence of auditory nerve fibers onto bushy cells in the ventral cochlear nucleus: implications of a computational model. *J Neurophysiol* 70:2562-2583, 1993.

Rothman JS and Young ED. Enhancement of Neural Synchronization in Computational Models of Ventral Cochlear Nucleus Bushy Cells. *Audit Neurosci* 2:47-62, 1996.

Saint Marie RL, Morest DK, and Brandon CJ. The form and distribution of GABAergic synapses on the principal cell types of the ventral cochlear nucleus of the cat. *Hear Res* 42:97-112, 1989.

Schofield BR and Cant NB. Descending auditory pathways: projections from the inferior colliculus contact superior olivary cells that project bilaterally to the cochlear nuclei. *J Comp Neurol* 409:210-223, 1999.

Shailer MJ, Moore BC, Glasberg BR, Watson N, and Harris S. Auditory filter shapes at 8 and 10 kHz. *J Acoust Soc Am* 88:141-148, 1990.

Smith PH and Rhode WS. Characterization of HRP-labeled globular bushy cells in the cat anteroventral cochlear nucleus. *J Comp Neurol* 266:360-75, 1987.

Smith PH and Rhode WS. Structural and functional properties distinguish two types of stellate cells in the ventral cochlear nucleus. *J Comp Neurol* 282:596-616, 1989.

Smith AJ, Owens S, and Forsythe ID. Characterization of inhibitory and excitatory postsynaptic currents of the rat medial superior olive. *J Physiol* 529.3:681-698, 2000.

Thompson AM and Schofield BR. Afferent projections of the superior olivary complex. *Microsc Res Tech* 51:330-354, 2000.

van Gisbergen JAM, Grashuis JL, Johannesma PIM, and Vendrik AJH. Neurons in the cochlear nucleus investigated with tone and noise stimuli. *Exp Brain Res* 23:387-406, 1975.

van Tasell DJ, Larsen SY, and Fabry DA. Effects of an adaptive filter hearing aid on speech recognition in noise by hearing-impaired subjects. *Ear Hear* 9:15-21, 1988.

Victor JD and Purpura KP. Nature and precision of temporal coding in visual cortex: A metric-space analysis. *J Neurophysiol* 76:1310-1326, 1996.

Victor JD and Purpura KP. Metric-space analysis of spike trains: theory, algorithms and application. *Network: Comput Neural Syst* 8:127-164,1997.

von Békésy G. *Sensory Inhibition*. Princeton University Press, Princeton, NJ. 1967.

Warr WB. Parallel ascending pathways from the cochlear nucleus: neuroanatomical evidence of functional specialization. *Contrib Sens Physiol* 7:1-38, 1982.

Wenthold RJ. Evidence for a glycinergic pathway connecting the two cochlear nuclei: an immunocytochemical and retrograde transport study. *Brain Res* 415:183-187, 1987.

Wenthold RJ, Parakkal MH, Oberdorfer MD, and Altschuler RA. Glycine receptor immunoreactivity in the ventral cochlear nucleus of the guinea pig. *J Comp Neurol* 276:423-435, 1988.

Wickesberg RE and Oertel D. Tonotopic projection from the dorsal to the anteroventral cochlear nucleus of mice. *J Comp Neurol* 268:389-399, 1988.

Wickesberg RE and Oertel D. Delayed, frequency-specific inhibition in the cochlear nuclei of mice: A mechanism for monaural echo suppression. *J Neurosci* 10:1762-1768, 1990.

Wier CC, Green DM, Hafter ER, and Burkhardt S. Detection of a tone burst in continuous- and gated-noise maskers; defects of signal frequency, duration, and masker level. *J Acoust Soc Am* 61:1298-1300, 1977.

Winter IM and Palmer AR. Intensity coding in low-frequency auditory-nerve fibers of the guinea pig. *J Acoust Soc Am* 90:1958-1967, 1991.

Winter IM and Palmer AR. Level dependence of cochlear nucleus onset unit responses and facilitation by second tones or broadband noise. *J. Neurophysiol.* 73:141-159, 1995.

Wu SH and Oertel D. Inhibitory circuitry in the ventral cochlear nucleus is probably mediated by glycine. *J Neurosci* 6:2691-2706, 1986.

Wu SH and Kelly JB. Physiological evidence for ipsilateral inhibition in the lateral superior olive: Synaptic responses in mouse brain slice. *Hearing Res* 73:57-64, 1994.

Wu SH, Ma CL, and Kelly JB. Contribution of AMPA, NMDA, and $GABA_A$ receptors to temporal pattern of postsynaptic responses in the inferior colliculus of the rat. *J Neurosci* 24:4625-4634, 2004.

Young ED and Barta PE. Rate responses of auditory nerve fibers to tones in noise near masked threshold. *J Acoust Soc Am* 79:426-442, 1986.

Young ED, Robert JM, and Shofner WP. Regularity and latency of units in ventral cochlear nucleus: Implications for unit classification and generation of response properties. *J Neurophysiol* 60:1-29, 1988.

Zhang X, Heinz MG, Bruce IC, and Carney LH. A phenomenological model for the responses of auditory-nerve fibers: I. Nonlinear tuning with compression and suppression. *J Acoust Soc Am* 109:648-670, 2001.

Zheng L, Early SJ, Mason CR, Idrobo F, Harrison JM, and Carney LH. Binaural detection with narrowband and wideband reproducible noise maskers: II. Results for rabbit. *J Acoust Soc Am* 111:346-356, 2002.

Zilany MS and Bruce IC. Modeling auditory-nerve responses for high sound pressure levels in the normal and impaired auditory periphery. *J Acoust Soc Am* 120:1446-1466, 2006.

VITA

NAME OF AUTHOR: Yan Gai

PLACE OF BIRTH: Shandong, P. R. China

GRAUDUATE AND UNDERGRADUATE SCHOOLS ATTENDED:

South China University of Technology, P. R. China

DEGREES AWARDED

Master of Science in Bioengineering, 2004, Syracuse University

Master of Engineering in Electrical Engineering, 2002, South China University of

Technology

Bachelor of Science in Electrical Engineering, 1999, South China University of

Technology

PROFESSIONAL EXPERIENCE

Research Assistant, Bioengineering, Syracuse University, 2002-2007